Université Paris Cité

École doctorale Médicament, Toxicologie, Chimie, Imageries (MTCI ED 563)

Laboratoire de Chimie et Biochimie Pharmacologiques et Toxicologiques (LCBPT)
Chemistry & Biology, Modelisation & Immunologie pour la thérapie (CBMIT)

Etude des effets immunorégulateurs des ligands du récepteur à chimiokine CXCR4, avec application thérapeutique pour les maladies auto-immunes et inflammatoires

Par Nassima Bekaddour Benatia

Thèse de doctorat d'immunologie

Dirigée par Dr. Jean-Philippe Herbeuval

Présentée et soutenue publiquement le 14 décembre 2022

Devant un jury composé de :

Marc Dalod, Directeur de Recherche CNRS, Centre d'immunologie de Marseille-Luminy	Rapporteur
Pauline Soulas-Sprauel, PU-PH, Université de Strasbourg	Rapporteur
Amanda Silva Brun, Chargée de Recherche CNRS, Université Paris Cité	Examinateur
Francois Trottein, Directeur de Recherche CNRS, Institut Pasteur Lille	Membre invité
Jean-Philippe Herbeuval, Directeur de Recherche CNRS, Université Paris Cité	Directeur de Thèse

Résumé : Etude des effets immunorégulateurs des ligands du récepteur à chimiokine CXCR4, avec application thérapeutique pour les maladies auto-immunes et inflammatoires

Les interférons (IFN) sont des cytokines qui jouent un rôle central dans la réponse immunitaire aux agents infectieux, notamment dans la lutte contre les virus, et qui contribuent à prévenir le développement de tumeurs. Une production aberrante d'IFN de manière chronique ou aiguë est néfaste pour l'organisme car induit des lésions plus ou moins importantes. Le lupus, maladie qui touche près de cinq millions de personnes dans le monde fait partie de cette catégorie de pathologie. Il a récemment été identifié qu'une protéine présente à la surface des cellules immunitaires, appelée CXCR4 est capable de réguler la production d'IFN en présence de virus. Cette régulation se fait par l'intermédiaire de composés aminés, naturels ou synthétiques, qui se fixent sur la poche mineure de CXCR4. L'IT1t ainsi que l'analogue de l'histamine : le clobenpropit (CB) sont capables de se fixer au niveau de cette poche, induisant une activité anti-IFN. L'IT1t a été testé *in vivo* dans un modèle de lupus chez la souris : l'inflammation systémique et la progression de la maladie ont été considérablement réduites. La molécule s'est aussi avérée efficace sur des cellules de patients atteints de lupus, confirmant ainsi l'immense potentiel de cette nouvelle option thérapeutique dans le traitement de cette maladie. L'objectif de mon travail de thèse a été dans un premier temps de mieux caractériser les effets immunorégulateurs de l'IT1t et du CB. Nous avons ainsi pu identifier que ces composés exercent des effets anti-inflammatoires à large spectre en inhibant notamment la production de cytokines pro-inflammatoires tels que le TNFα, l'IL6 et IL1β par des monocytes activés. Ces cytokines inflammatoires sont incriminées dans un grand nombre de maladies inflammatoires tel que la polyarthrite rhumatoïde qui touche plus de 23 millions de personnes. Le CB a ainsi été testé en *ex vivo* sur des cellules immunitaires de patients atteints d'arthrites, ce qui a permis de réduire drastiquement la production de cytokines pro-inflammatoires. Nous avons démontré que l'effet anti-inflammatoire du CB sur la production de cytokines inflammatoires est strictement dépendant de CXCR4. Enfin, le CB a été testé *in vivo* dans un modèle de souris lupus : l'inflammation systémique et la progression de la maladie ont été considérablement réduites. Mon deuxième objectif a été d'identifier de nouveaux composés avec des effets anti-inflammatoires capables de se fixer sur la poche mineure de CXCR4. Deux composés ont ainsi pu être identifiés avec une meilleure activité anti-inflammatoire que le CB et l'IT1t. Enfin, la dernière partie de mes travaux consiste à décortiquer le mécanisme d'action induit par les ligands de la poche mineure de CXCR4 qui aboutit aux effets anti-inflammatoires et anti-IFN observés.

Mots-clés : CXCR4 ; cytokines, inflammation ; interféron ; monocytes ; pDC ; lupus ; arthrite rhumatoïde ; amine

Abstract: Study of the immunoregulatory effects of CXCR4 chemokine receptor ligands, with therapeutic application in autoimmune and inflammatory diseases

Interferons (IFN) are cytokines playing a central role in the immune response to infectious agents, especially against viruses, and help prevent the development of tumors. Aberrant IFN production, whether chronic or acute, is harmful to the body because it induces significant damage. Lupus, a disease that affects nearly five million people worldwide, falls into this category. It has recently been identified that a protein present on the surface of immune cells, called CXCR4, is able to regulate the production of IFN in the presence of viruses. This regulation is mediated by natural or synthetic amino compounds that bind to the minor pocket of CXCR4. IT1t and the histamine analogue clobenpropit (CB)are able to bind to this pocket, thereby inducing anti-IFN activity. IT1t was tested *in vivo* in a mouse model of lupus: systemic inflammation and disease progression were significantly reduced. The molecule was also shown to be effective on cells from lupus patients, confirming the immense potential of this new therapeutic option in the treatment of this disease. The goal of my phD work was first to better characterize the immunoregulatory effects of IT1t and CB. We were thus able to identify that these compounds exert broad-spectrum anti-inflammatory effects by inhibiting the production of pro-inflammatory cytokines such as TNF, IL6 and IL1 by activated monocytes. These inflammatory cytokines are incriminated in many inflammatory diseases such as rheumatoid arthritis which affects more than 23 million people. CB was tested in ex vivo on immune cells from patients with arthritis, which drastically reduced the production of pro-inflammatory cytokines. We demonstrated that the anti-inflammatory effect of CB on inflammatory cytokine production is strictly dependent on CXCR4. Finally, CB was tested *in vivo* in an lupus mouse model: systemic inflammation and disease progression were significantly reduced. My second goal was to identify new compounds with anti-inflammatory effects able to bind to the minor pocket of CXCR4. Two compounds were identified with better anti-inflammatory activity than CB and IT1t. Finally, the last part of my work consists in identifying the mechanism of action induced by the ligands of the minor pockets of CXCR4 which leads to the anti-inflammatory and anti-IFN effects.

Keywords: CXCR4; cytokines, inflammation; interferon; monocytes; pDC; lupus; rheumatoid arthritis; amine

Remerciements

Avant toute chose, je souhaiterais m'adresser à toutes les personnes qui ont su m'épauler, m'accompagner, me soutenir dans ce projet, et qui ont fait de cette expérience un moment profitable.

Je souhaite tout d'abord m'adresser à Jean-Philippe Herbeuval, mon directeur de thèse, pour avoir dirigé cette thèse avec beaucoup de passion et de bienveillance. Tu as très tôt su me révéler un goût pour la recherche et l'immunologie chose qui n'était pas gagnée d'avance…Grâce à toi, je me retrouve plongé dans cette aventure du doctorat, un des meilleurs choix que j'ai pu faire et pour cela, je ne te remercierai jamais assez. Ses années de thèse ont été très intenses, que soit d'un point de vue technique, scientifique et humain, mais elles resteront inoubliables. J'ai apprécié chacun travaux réalisés avec toi. Un énorme merci aussi pour ton soutien, tes encouragements et ta bonne humeur. C'était un réel plaisir de travailler et d'apprendre avec toi.

Je tiens à remercier sincèrement Pierre olivier Vidalain. Tu m'as toi aussi accordé ta confiance durant mon stage de M1 et M2. Je te dois mon profond attachement à la science. Tu m'as accompagné et soutenu dans tous les moments que pouvait connaître une étudiante et grâce à toi j'ai bénéficié d'une formation complète comme peu ont pu connaître. s. Un énorme merci à toi PO pour ton professionnalisme et ton humanité

Je tiens à remercier tout particulièrement et à témoigner toute ma reconnaissance aux personnes passées et présentes de l'équipe CBMIT, pour l'expérience enrichissante et pleine d'intérêt qu'elles m'ont fait vivre durant ma thèse au sein de l'équipe : Armelle, Mathieu, Birgit et Sabrina, le rayon de soleil du labo ! Je ne peux oublier dans ces remerciements, Nikaïa, qui a beaucoup contribué à ma formation scientifique et qui m'a soutenue, que ce soit dans le cadre professionnel et personnel. Et enfin Simon, mon partenaire de thèse avec qui j'ai partagé le bureau pendant plus de deux ans et qui devenu un ami. Je te remercie d'avoir été là pour moi, tu as su m'épauler et être à l'écoute. Merci pour ta bonne humeur et nos discussions, plus ou moins scientifique….

Je tiens aussi à remercier les différents membres de l'UMR8601, qui m'ont accueillie durant mon stage de M1 et M2 et durant ma thèse, notamment Laurent Micouin et Marie-Agnès Sari. Je tiens aussi à remercier Mandy, Ludo, Abdou, Amit, Kassim...pour vos aides aux quotidiens

Je tiens à m'adresser à Benoît Schneider et toute son équipe, malgré le fait que notre collaboration est assez récente, je te suis reconnaissante de m'avoir accordé ta confiance. Notre collaboration m'a beaucoup apporté et appris, et ce n'est qu'un début…
Un grand merci à Hector et Vincent pour votre soutien, nos pauses café et nos longues discussions passionnantes.

C'est non avec une certaine émotion que je m'adresse désormais à ma famille. Je vous dois mon évolution dans tous domaines confondus, vous m'avez toujours accompagné, encouragé et soutenu. Malgré mes incertitudes lors du choix du chemin à emprunter au départ de mes études, vous m'avez toujours conseillé avec bienveillance en me poussant à exercer seulement un métier qui me comblerait. Même si mes choix pouvaient parfois sembler effrayants, vous avez toujours placé une grande confiance en moi alors je vous adresse ici un grand merci.

Je ne pourrais adresser des remerciements sans celui qui fait partie de mon quotidien depuis 5 ans, mon mari. Grâce à toi, cette vie d'étudiante paraît moins contraignante. Malgré les inconvénients qu'implique cette situation, tu as pu réaliser des concessions et le poids qui ne reposait que sur mes épaules et depuis ces dernières années partagées répartie au sein de notre vie quotidienne alors je te dis merci.

A mes amis, Morgane, Kenza, Emilie, Margaux, Sarah, Cynthia…. sans qui mon quotidien ne serait pas le même !

Je souhaite désormais clôturer tous ces remerciements avec mes amies doctorantes : Alexandre, Alexandra, Sonia, Louis, Yasmina, Juliette, Morgane, Chloé,.. Je souhaite tout d'abord vous remercier d'avoir partagé un bout de route semé d'embuche qu'est celle de doctorants. Nos quotidiens à la fois différents mais similaires nous ont rapprochés, nous ont permis de grandir et d'acquérir de nouvelles connaissances que seule l'expérience de la vie peut nous apporter. Je vous remercie d'avoir été cette équipe soudée pour laquelle j'ai toujours pu compter, une équipe ou l'entraide fut un mot clé. Ensemble nous avons partagé de bons moments, qui désormais restent en mémoire tels des souvenirs de moment de bonne rigolade comme peu d'étudiants chanceux ont pu en bénéficier.

Table des matières

Abstract: Study of the immunoregulatory effects of CXCR4 chemokine receptor ligands, with therapeutic application in autoimmune and inflammatory diseases 3

Remerciements 5

Liste des abréviations 10

Chapitre 1 : Introduction 13

I. L'inflammation 14

1. Introduction à l'immunité 14
2. Les acteurs de la réponse immunitaire innée 15
   - i. Les granulocytes 15
   - ii. Les cellules NK 16
   - iii. Les monocytes/macrophages 17
   - iv. Les cellules dendritiques 17
3. La réponse inflammatoire 18
   - A. Facteurs déclenchant l'inflammation 19
     - i. Signaux de dangers exogènes 19
     - ii. Signaux de dangers endogènes 20
     - iii. Les récepteurs de l'immunité innée 20
       - a. Les TLR 21
       - b. Les NOD-like récepteurs (NLRs) 24
       - c. Les capteurs d'ADN intracellulaire (cGAS) 28
       - d. Les récepteurs aux lectines de type C (CLR) 29
       - e. Les RIG-I-like receptors (RLR) 29
   - B. Médiateurs de l'inflammation 31
     - i. Les interleukines 31
     - ii. Les chimiokines 33
     - iii. Les Interférons 35
       - a. Les interférons de type I 36
       - b. L'interféron de type II 38
       - c. Les interférons de type III 38

II. Les maladies auto-immunes et inflammatoires 39

1. Arthrite juvénile idiopathique 39
   - A. Définition, classification 39

B. Le système immunitaire dans l'AJI 42
C. Traitements 43
2. Le lupus érythémateux disséminé 45
A. Définition, classification 45
B. Le système immunitaire dans le LES 46
C. Traitements 49
III. CXCR4 : nouvelle cible thérapeutique pour des maladies auto-immunes et inflammatoires 50
1. Rôle de CXCR4 dans l'immunité 50
A. Généralité 50
B. Interaction CXCR4-CXCL12 51
C. Physiopathologie associé à CXCR4 52
D. Antagoniste de CXCR4 53
2. Nouvelle propriété de CXCR4 54
Chapitre 2 : Projet de thèse et résultats 55
Partie I : réduction de l'inflammation dans l'arthrite juvénile avec un analogue de l'histamine qui cible le récepteur CXCR4 57
Partie II : Un analogue de l'histamine contrôle la production d'IFN dans le lupus érythémateux systémique 70
Partie III : Identification d'un nouveau composé aux propriétés anti-inflammatoires via son engagement sur le récepteur CXCR4 77
Chapitre 3 : Discussion 84
I. Résultats majeurs 85
II. Modèles utilisés 85
III. Mécanisme cellulaire induit par l'engagement de CXCR4 86
A. Voie de signalisation induit par CXCR4 87
B. Formation d'hétéromères CXCR4 en présences de ses ligands de la poche mineure. 91
IV. Perspectives 93
LISTE DES FIGURES 94
LISTE DES TABLEAUX 95

Article 1 ..... *96*

Article 2 .....*111*

Article 3 .....*124*

Article 4 .....*138*

Article 5 .....*147*

Article 6 .....*161*

REFERENCES BIBLIOGRAPHIQUES.....*174*

Liste des abréviations

A

AAN : anticorps antinucléaires

ACR : the American College of Rheumatology

AINS : arthrite idiopathique juvénile

AJI : arthrite idiopathique juvénile

ALR: AIM-2-Like Receptors

APC: Antigen Presenting Cells

ARN : acide ribonucléique

B

BAFF : B-cell activating factor

C

CARD: caspase activation and recruitment domain

CB : clobenpropit

CCP ; peptides cycliques citrullinés

CD : cluster of differentiation ou antigène de différentiation

CLR : récepteurs aux lectines de type C

CMH : omplexe majeur d'histocompatibilité

COX : Cyclooxygenase

CPA : cellules présentatrice antigène

CSH : cellule souche hématopoïétique

CXCL: C-X-C Ligand

CXCR: C-X-C chemokine receptor

D

DAMP : Damage Associated Molecular Pattern

DC : cellules dendritique

DMARD : Disease Modifying Anti Rheumatic Drug

J

JNK : c-jun N-terminal kinase

H

HMGB1: high mobility group box 1

I

IFN : interféron

IFNAR : The interferon-α/β receptor

IL : interleukine

IRAK : IL-1R-associated kinase

IRF : Interferon regulatory factors

ISG : interferon-stimulated genes

ISRE: IFN-Stimulated Response Element

L

LES : lupus erythemateux systemique

LPS : lipopolysaccharide

LRR : leucine-rich repeat

M

mDC : Myeloid dendritic cells

N

NLR : Nod-like receptor

NF-KB : nuclear factor-κ B

NK : natural killer

NSAID : Non-steroidal anti-inflammatory drugs

P

PAMP : pathogen-associated molecular pattern

PBMC : Peripheral blood mononuclear cells

pDC : Plasmacytoid Dendritic Cell

PR : polyarthrite rhumatoïde

PRR : pattern recognition receptor

PYD: pyrin domain

R

RCPG : Récepteur couplé aux protéines G

RIG-I : retinoic acid-inducible gene I

RLR : RIG-I-like receptors

S

STAT : signal transducer and activator of transcription

T

TIR: Toll IL-1 Receptor

TLR : récepteurs Toll-like

TNF : tumor necrosis factor

V

VIH : virus de l'immunodéficience humaine de type 1

VSV : Vesicular Stomatite Virus

W

WHIM: Warts, Hypogammaglobulinemia, Infections, Myelokathexis

Chapitre 1 : Introduction

I. L'inflammation

1. Introduction à l'immunité

L'immunité est définie comme l'ensemble des mécanismes de défense de l'organisme. Elle a pour rôle de le défendre contre des agents infectieux tels que les virus et les bactéries, mais également capable de reconnaitre et détruire les cellules cancéreuses. L'ensemble des tissus, des cellules et des molécules qui participent à la défense de l'organisme constituent le système immunitaire.

Parmi ces cellules, on retrouve majoritairement des leucocytes (ou globules blancs), qui circulent dans le sang et la lymphe. Il existe plusieurs familles de leucocytes. Chaque membre de cette famille joue un rôle dans la défense de notre organisme.

Chez l'Homme, le système immunitaire comporte deux grands systèmes qui coopèrent étroitement afin de limiter la propagation des agents pathogènes. Il y a d'une part le système immunitaire inné qui est précoce. Cette forme d'immunité est déterminée génétiquement et elle constitue la 1ère ligne de défense vis-à-vis des éléments pathogènes. Les cellules de l'immunité innée comprennent les cellules lymphoïdes innées (ILC pour Innate Lymphoid Cells), les granulocytes et les phagocytes. Ces dernières se caractérisent par leurs capacités à reconnaitre des motifs moléculaires spécifiques des pathogènes, grâce à leurs récepteurs PRR (Pattern Recognition Receptors). Cette reconnaissance déclanche de la part des cellules de l'immunité innée la production et la libération de médiateurs chimiques afin d'attirer et activer d'autres cellules de l'immunité dites adaptatives. Le deuxième pan du système immunitaire est donc le système immunitaire adaptatif qui est plus tardif et cible spécifiquement l'agent pathogène détecté. Les cellules de l'immunité adaptative incluent des lymphocytes B qui participent à l'immunité à médiation humorale et des lymphocytes T qui participent à l'immunité à médiation cellulaire. Dans le cadre de mes travaux, je me suis principalement intéressé au système immunitaire inné, et plus spécifiquement aux monocytes et pDC.

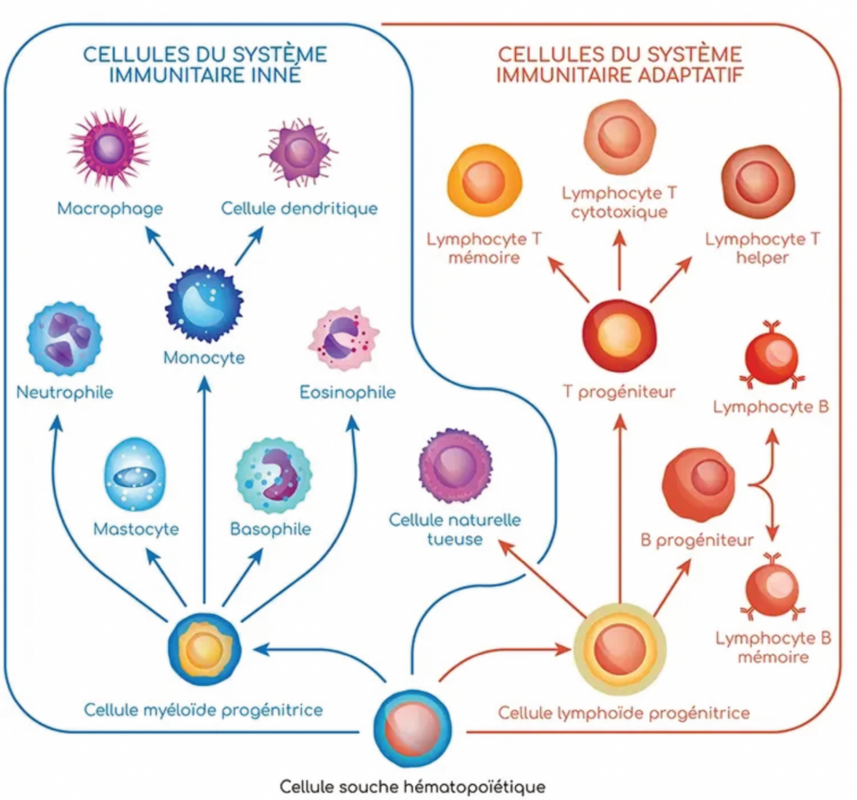

Figure 1: Les acteurs cellulaires de l'immunité innée et adaptative.
(Image tiré du site nutrixeal-info.fr/index/immunite-adaptative)

2. Les acteurs de la réponse immunitaire innée

i. Les granulocytes

Les granulocytes ou polynucléaires sont classés en 3 catégories : les neutrophiles, les éosinophiles et les basophiles. Les granulocytes possèdent un noyau unique qui présente plusieurs lobes de formes diverses. C'est la raison pour laquelle durant un moment, ils ont été considérés à tort comme étant multinucléés, d'où le nom de « polynucléaires ». Ce sont les premières cellules à migrer au niveau de l'inflammation, suivies des monocytes.

Les neutrophiles représentent 60 à 70% des leucocytes. Ils agissent localement au niveau des tissus, afin d'éliminer les agents pathogènes ainsi que les cellules ou molécules devenues anormales. Pour cela, les neutrophiles qui se trouvent initialement au niveau de la circulation sanguine sont capables de se rendre sur le site de l'inflammation par chimiotactisme (Mantovani et al., 2011). C'est grâce à des molécules d'adhésion présentes à leur surface qu'elles sont capables de traverser les parois endothéliales. Les neutrophiles reconnaissent spécifiquement des motifs présents à la surface des micro-organismes (bactéries, virus), ce qui déclenche leur phagocytose. Les neutrophiles libèrent alors des médiateurs cytotoxiques comme les espèces réactives de l'oxygène (ROS) par la NADPH oxydase, des protéines enzymatiques

(myéloperoxydase, élastases, lysosyme, gélatinase) et antimicrobiennes (lactoferrine, BPI: bactericidal/permeability-increasing protein , défensines)(Segal, 2005). Les neutrophiles ont été décrit comme ayant une durée de vie très courte de l'ordre de quelques heures, cependant des travaux recents montrent que ces cellules pourraient avoir une durée de vie plus longue (quelques jours) (Koenderman et al., 2022; Monceaux et al., 2016).

Les éosinophiles ou acidophiles ont une action antiparasitaire et représentent 5% des leucocytes. Ils sont capables de reconnaitre et se fixer sur des parasites, puis de libérer des enzymes contenues dans leurs granules afin de les détruire. Parmi ces enzymes, on peut citer la MBP (protéine basique majeure), l'EPO, l'ECP ou encore l'EDN (peroxydase de l'éosinophile). La MBP possède une activité cytotoxique contre les helminthes mais aussi contre les bactéries. Son action est due à sa capacité de perturber l'intégrité de la membrane cellulaire en modifiant l'équilibre électrostatique de la bicouche de phospholipides permettant d'augmenter sa perméabilité. Ils ont une demi-vie de quelques heures dans la circulation sanguine, puis se retrouvent au niveau des tissus dans lesquels ils persistent quelques jours.

ii. Les cellules NK

Les **cellules NK** ont été découvertes au début des années 1970. D'un point de vue fonctionnel, ces cellules ont deux rôles principaux : lyser les cellules infectées ou tumorales et produire des cytokines et chimiokines afin de signaler aux autres cellules de l'immunité la présence de pathogène (Robertson and Ritz, 1990). Parmi les cytokines produites par les cellules NK, certaines jouent un rôle déterminant dans l'orientation de la réponse immunitaire adaptative. Elles sont issues de cellules souches hématopoïétiques (CSH) CD34+ de la moelle osseuse et leurs différenciations s'achèvent au niveau des ganglions, des amygdales ou encore du thymus. Elles représentent 5 à 15% des lymphocytes au niveau du sang périphérique. Au cours de leur développement, les cellules NK acquièrent un répertoire complexe de récepteurs activateurs et inhibiteurs, ainsi que des récepteurs aux cytokines, chimiokines et d'autres récepteurs tels que les Toll-Like Receptors (TLR). La balance entre les deux signaux inhibiteurs et activateurs est primordiale dans la mise en place de la réponse NK et dans le type de réponse qui est engagée. Lors de leur développement, les cellules NK sont également éduquées afin d'être tolérantes vis-à-vis du Soi à l'état basal. Les cellules NK humaines sont phénotypiquement caractérisées par l'expression de CD56 et l'absence d'expression de CD3.

iii. Les monocytes/macrophages

De grande taille (15 à 20µm), les monocytes représentent 2 à 10% des leucocytes totaux du sang périphérique chez l'homme. Elles sont originaires de la moelle osseuse, plus précisément des cellules souches hématopoïétiques CD34+, et ont une demi-vie de 1 à 3 jours (Gordon and Taylor, 2005). Les monocytes migrent classiquement de la moelle osseuse vers le sang, et éventuellement vers les tissus périphériques en fonction des signaux qu'elles reçoivent. Cette infiltration vers les tissus nécessite l'activation de récepteurs aux chimiokines ainsi que des récepteurs à l'adhésion endothéliale. En fonction des stimuli rencontrés, les monocytes peuvent s'activer, se différencier en cellules dendritiques (Dendritic Cell, ou DC) ou en macrophage (Chow et al., 2017; Ginhoux and Jung, 2014; Jakubzick et al., 2013).
Ces cellules sont des acteurs essentiels dans les réponses immunes innées en jouant un rôle de défense, de réparation tissulaire et dans l'homéostasie. Les monocytes possèdent des propriétés de phagocytose, de présentation d'antigènes, de production de cytokines et de chimiokines. Ces fonctions permettent de lutter contre les infections de type bactériennes, virales ou encore fongiques, et forment un lien essentiel entre l'immunité innée et adaptative (Cros et al., 2010).
La différenciation des monocytes permet une spécialisation des fonctions cellulaires : certaines propriétés sont conservées ou amplifiées, d'autres sont perdues, et de nouvelles fonctions sont acquises suivant le type cellulaire produit.
Les monocytes sont capables de produire en grande quantité des cytokines pro-inflammatoires telles que le TNF-α, IL-6 ou encore l'IL-1β. Des taux élevés de ces cytokines pro-inflammatoire sont retrouvés dans de nombreuses maladies inflammatoires, notamment l'arthrite juvénile idiopathique qui nous intéressera plus particulièrement au cours de cette thèse.

iv. Les cellules dendritiques

Les **cellules dendritiques** (DC) ont été décrites chez l'Homme pour la première fois en 1868 par Paul Langerhans au niveau de la peau humaine. Il a ainsi pu décrire des cellules présentant une morphologie étoilée. Ce n'est qu'en 1970 que les DC ont pu être décrites de façon plus détaillée grâce à des études chez la souris (Steinman and Cohn, 1973, 1974). Leur caractérisation est rendue difficile en raison de leur rareté. Ce n'est qu'en améliorant les protocoles de génération de DC fonctionnelle in vitro à partir de progéniteurs tels que les

cellules souches hématopoïétiques qui ont rendu possibles leurs caractérisations(Balan et al., 2018; Caux et al., 1992; Kirkling et al., 2018; Romani et al., 1994; Sallusto and Lanzavecchia, 1994). Les DC sont dérivées des cellules souches hématopoïétiques et jouent un rôle majeur dans la décision du type de réponse immunitaire à mettre en jeu. Les DC ont pour principales fonctions d'orchestrer l'activation des lymphocytes T spécifiques d'antigène. Parmi les DC, on distingue 2 sous-populations avec des phénotypes bien caractérisés (Dzionek et al., 2000; MacDonald et al., 2002) :

- Les DC myéloïdes (mDC) : elles sont dérivées des monocytes et expriment des marqueurs myéloïdes tels que CD11b et CD33. Chez l'homme, les mDC résident dans le sang périphérique et sont capables de reconnaitre de nombreux signaux de danger grâce à un large panel de récepteur de type PRR. (Pattern recognition receptor). Cette reconnaissance enclenche la production de diverses cytokines. Les mDC font également partie des cellules présentatrices d'antigène (CPA), leur permettant ainsi d'activer efficacement les LT CD8+(Cohn et al., 2013; Jin et al., 2014; Segura et al., 2013) et CD4+ (Sittig et al., 2016)
- Les cellules dendritiques plasmacytoïdes (pDC) : Chez l'homme, elles diffèrent phénotypiquement des mDC grâce à l'expression de certains marqueurs comme CD123, les lectines BDCA-2 (blood DC antigen 2), BDCA-4 et par l'absence de CD11c (Dzionek et al., 2001). Elles expérimentent moins les CMH de classe II que les mDC. Les pDC sont particulièrement actives en réponse à une infection virale en produisant en grande quantité un antiviral puissant : les interférons de type I (IFN), essentiellement l'IFN-α et l'IFN-β., mais egalement des IFN de type III (Yin et al., 2012). Les pDC qui représentent 0,2-0,4% des PBMC, sont capables de produire de 100 à 1000 fois plus d'IFN de type I que tous les autres types cellulaires (Cella et al., 1999; Ito et al., 2006; Siegal et al., 1999). Cette caractéristique leur vaut la qualification de cellules professionnelles de la production d'IFN de type I. Une production excessive d'IFN de type I par les pDC est impliquée dans plusieurs maladies auto-immunes, donc le lupus érythémateux systémique (Huang et al., 2015) qui nous intéressera plus particulièrement dans cette thèse.

3. La réponse inflammatoire

La réponse inflammatoire est une réponse adaptative de l'organisme en réponse à une agression telle une infection ou une agression tissulaire comme une brulure ou une plaie par exemple. Ce processus nécessite une régulation fine qui est généralement bénéfique pour l'organisme afin d'éliminer le pathogène en cause et réparer les tissus lésés. Cependant, la réaction inflammatoire peut aussi être néfaste lorsqu'elle est inadaptée ou incontrôlée et peut engendrer des dommages irréversibles. Une réponse inflammatoire déficiente engendre une immunodéficience pouvant entrainer une infection secondaire ou un cancer. Si au contraire cette réponse est exacerbée, elle augmente la morbidité et la mortalité dans des pathologies comme la polyarthrite rhumatoïde, le lupus, la maladie de Crohn ou encore le diabète. Dans ce cas de figure, le recours aux médicaments, plus particulièrement aux anti-inflammatoires est parfois nécessaire pour traiter l'inflammation. Quand l'inflammation est mal contrôlée, cette dernière peut s'etendre au reste de l'organisme *via* la circulation sanguine et aboutir à des dommages tissulaires irréversibles, parfois à un choc septique entrainant dans les cas les plus sévères le décès (dans Nathan, 2002 ; et dans Tracey, 2002; Revue dans Barton, 2008).

Les cellules du système immunitaire inné possèdent des récepteurs PRR (Pattern Recognition Receptors) et des voies de signalisations hautement conservées afin de détecter et de donner l'alerte face à une infection ou à une lésion. Ces récepteurs permettent de détecter des signaux exogènes, les PAMPs (Pathogen-associated molecular pattern) ou endogènes comme les DAMP (Damage Associated Molecular Patterns) et les alarmines (Revue dans Bianchi, 2007). Cette reconnaissance conduit à l'initiation de la cascade inflammatoire et à l'activation de la réponse immunitaire adaptative (Revue dans Barton, 2008 ; Revue dans Medzhitov, 2008). La réponse inflammatoire est décrite selon quatre étapes : la reconnaissance des signaux de danger, le recrutement de cellules sur le site d'infection, l'élimination du pathogène et la résolution de l'inflammation conduisant à un retour à l'homéostasie et à la cicatrisation du tissu lésé (Revue dans Barton, 2008). En absence de résolution, s'installe une inflammation chronique.

A. Facteurs déclenchant l'inflammation

i. Signaux de dangers exogènes

Le principal mécanisme d'induction de l'inflammation est la reconnaissance d'un pathogène qui exprime des motifs moléculaires particulier : les PAMPs (Pathogen-Associated Molecular

Patterns). Ces PAMPs sont reconnus par les cellules de l'immunité innée via des récepteurs appelés PRR (Pathogen-Associated Molecular Patterns). Cette reconnaissance déclenche l'activation et/ou la maturation des cellules immunitaires qui sécrètent alors des médiateurs de l'inflammation : c'est la réponse inflammatoire.

ii. Signaux de dangers endogènes

Des signaux de dangers endogènes peuvent également être reconnus par les PRR (Matzinger, 1994). Ces signaux ont été définis en 2007 sous le terme alarmine (Oppenheim et al., 2007). Les alarmines sont des molécules endogènes qui sont libérées à la suite d'une dégranulation, d'une lésion ou d'une mort cellulaire ou en réponse à une induction immunitaire (Yang et al., 2017). L'interleukine-IL-1α et de l'IL-33, la protéine S100 ou encore l'acide urique font partie de la famille des alarmines. Elles recrutent les cellules immunitaires exprimant les PRR, notamment des cellules dendritiques ce qui induit par la suite la réponse immunitaire adaptative. Les alarmines participent ainsi au retour à l'homéostasie en promouvant la reconstruction du tissu lésé.

iii. Les récepteurs de l'immunité innée

Il existe six principales classes de PRR :

- Les toll-like receptors (TLR), des protéines transmembranaires à la surface des cellules ou des endosomes. Il s'agit de la famille la plus étudiée,
- Les NOD-like receptors (NLR), localisés dans le cytoplasme,
- Les capteurs d'ADN intracellulaire tels que cGAS
- Les récepteurs aux lectines de type C (CLR), des récepteurs transmembranaires caractérisés par la présence d'un domaine de liaison aux carbohydrates,
- Les RIG-I-like receptors (RLR), des hélicases à ARN qui reconnaissent l'ARN viral,
- La famille des AIM-2-Like Receptors (ALR)

Après reconnaissance d'un ligand, les récepteurs ci-dessus activent des voies de signalisation comme celle du NF-ϰB, des MAP kinases ou des interférons de type I. Ces voies déclenchent l'induction de cytokines pro-inflammatoires et de chimiokines, capables de recruter et d'activer les cellules du système immunitaire. En dehors de ces cinq familles, Il existe également des PRR atypiques comme le récepteur RAGE (receptor for advanced glycation end-products) qui

reconnaît des molécules de danger exclusivement endogènes (DAMP) libérées dans le milieu extracellulaire tel que HMGB1.

a. Les TLR

Les TLR constituent la famille des PRR la plus étudiée dans l'inflammation. La découverte des TLR humains par Jules Hoffman et Bruce Beutler en 1996 a été importante pour la recherche immunologique et leur a valu le prix Nobel de médecine et de physiologie 2011. Jules Hoffmann a fourni la première preuve de l'implication des récepteurs de type Toll dans l'immunité innée chez la drosophile. C'est en 1997 que Charles Janeway et Ruslan Medzhitov identifient un paralogue TLR qu'ils nomment « h-Toll » (identifié plus tard comme TLR4) (Medzhitov et al., 1997). Ils suggèrent que chez les mammifères, h-Toll pourrait « activer l'immunité adaptative ». En 1998, Bruce Beutler précise le rôle du TLR4 en tant que récepteur lipopolysaccharide bactérien (LPS). Chez les mammifères, actuellement, 13 TLRs ont été identifiés : 10 chez l'homme (TLR1-10) et 12 chez la souris (TLR1-9 et TLR11-13). Ce sont des protéines transmembranaires caractérisées par un domaine riche en leucine (LRR), couplé à un domaine intracellulaire proche de celui du récepteur à l'IL-1, nommé TIR. Le domaine LRR est impliqué dans la reconnaissance des ligands, alors que le domaine TIR est impliqué dans la transmission du signal.

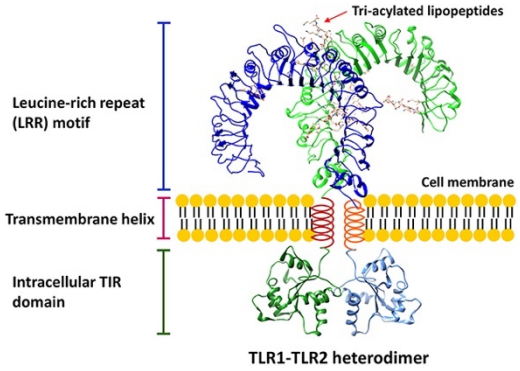

Figure 2: Structure représentative des Toll-Like Receptors.
Les TLR sont sous forme de dimères. Ils se composent de trois composants : (1) motif de répétition riche en leucine (LRR); (2) hélice transmembranaire; (3) domaine TIR intracellulaire. Modifié à partir de (Gao et al., 2017)

Selon la nature des PAMPs reconnus et de leur localisation subcellulaire, deux sous-familles de TLR peuvent être distinguées. D'un côté les TLR1, 2, 4, 5, 6 et 10, exprimés au niveau de la membrane plasmique, reconnaissent des produits bactériens spécifiques (Fore et al., 2022). De l'autre les TLR3, 7, 8 et 9, exprimés au niveau des lysosomes et des endosomes, reconnaissent des acides nucléiques de micro-organismes avec une discrimination du soi et du

non soi apportée en partie par la localisation des ligands (Mogensen, 2009). Les TLR4 peuvent également se localiser au niveau des endosomes suite à leur endocytose (Bonham et al., 2014; Kagan et al., 2008). Les TLR forment majoritairement des homodimères. Cependant ils peuvent aussi former des hétérodimères comme le TLR2 avec TLR1 ou avec TLR6 (Ozinsky et al., 2000). Pour chaque TLRs humain, un ou plusieurs ligands ont pu être identifié (voir tableau 1)

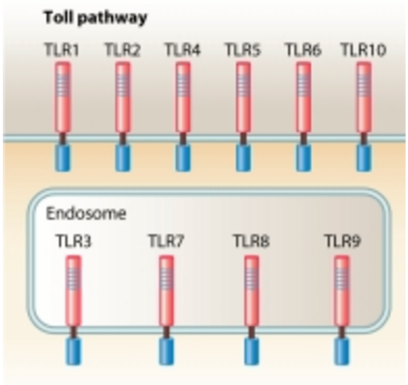

Figure 3: Localisation des Toll-Like Receptors.

(revue dans Mogensen, 2009)

TLR	Location of TLR	PAMPs recognized by TLR	Co-receptor (s)	Signaling adaptor	Transcription factor(s)	Effector cytokines induced
TLR1/2	Plasma membrane (cell surface)	Triacyl lipopeptides (Bacteria and Mycobacteria)	Hetrodimer of TLR1/2 forms a functional receptor	TIRAP, MyD88	NFκB	Inflammatory cytokines (TNF-α, IL-6 etc.)
TLR2	Plasma membrane (cell surface)	Peptidoglycan (Gram-positive bacteria), LAM (Mycobacteria), Hemagglutinin (Measles virus), phospholipomannan (*Candida*), Glycosylphosphophatidyl inositol mucin (*Trypanosoma*)	CD36, RP105	TIRAP, MyD88	NFκB	Inflammatory cytokines (TNF-α, IL-6 etc.)
TLR3	Endosome	ssRNA virus (WNV), dsRNA virus(Reovirus), RSV, MCMV		TRIF	NFκB, IRF3,7	Inflammatory cytokines (TNF-α, IL-6 etc.), type I IFNs
TLR4	Plasma membrane (cell surface)	LPS (Gram-negative bacteria), Mannan (*Candida*), Glycoinositolphospholipids (*Trypanosoma*), Envelope proteins (RSV and MMTV)	MD2, CD14, LBP, RP105	TIRAP, MyD88, TRAM and TRIF	NFκB, IRF3,7	Inflammatory cytokines (TNF-α, IL-6 etc.), type I IFNs
TLR5	Plasma membrane (cell surface)	Flagellin (Flagellated bacteria)		MyD88	NFκB	Inflammatory cytokines (TNF-α, IL-6 etc.)
TLR6/2	Plasma membrane (cell surface)	Diacyl lipopeptides (Mycoplasma), LTA (Streptococcus), Zymosan (*Saccharomyces*)	Hetrodimer of TLR6/2 or dectin-1 forms a functional receptor	TIRAP, MyD88	NFκB	Inflammatory cytokines (TNF-α, IL-6 etc.)
TLR7	Endosome	ssRNA viruses (VSV, Influenza virus)		MyD88	NFκB, IRF7	Inflammatory cytokines (TNF-α, IL-6 etc.), type I IFNs
TLR8[#]	Endosome	ssRNA from RNA virus		MyD88	NFκB, IRF7	Inflammatory cytokines (TNF-α, IL-6 etc.), type I IFNs
TLR9	Endosome	dsDNA viruses (HSV, MCMV), CpG motifs from bacteria and viruses, Hemozoin (Plasmodium)		MyD88	NFκB, IRF7	Inflammatory cytokines (TNF-α, IL-6 etc.), type I IFNs
TLR11[*]	Plasma membrane (cell surface)	Uropathogenic bacteria, profillin-like molecule (*Toxoplasma gndii*)		MyD88	NFκB	Inflammatory cytokines (TNF-α, IL-6 etc.)

LAM, Lipoarabinomannan; WNV, West Nile virus; RSV, Respiratory syncytial virus; MCMV, Murine cytomegalovirus; MMTV, Mouse mammary tumor virus; LTA, Lipoteichoic acid; VSV, Vesicular stomatitis virus; HSV, Herpes simplex virus and CpG, Cytidine-phosphate-guanosine.

[#] Human TLR8.

[*] Expressed in mouse.

Tableau 1: Ligands et localisation des TLR
(Revue dans Kumar *et al.*, 2009)

Dans le cadre de ce travail, nous nous sommes particulièrement intéressés au TLR7 et 8. Ces derniers sont capables de reconnaitre l'ARN simple brin (ARNsb) extracellulaire dès lors que cet ARN est internalisé par la voie endosomale. Le TLR7 est très exprimé dans les cellules dendritiques plasmacytoïdes (pDC) et dans les lymphocytes B (Crozat et al., 2009). Il joue un rôle essentiel dans la production des IFN de type I par les pDC quand ces dernières rencontrent des virus à ARN comme le virus de l'immunodéficience humaine (VIH) (Chang and Altfeld, 2009), le VSV (Vesicular Stomatite Virus) (Lund et al., 2004) ou encore le virus influenza A (Kawai and Akira, 2006). TLR8 est majoritairement exprimé dans les monocytes/macrophages, dans les cellules dendritiques myéloïdes (mDC) et dans les neutrophiles (Crozat et al., 2009). Son activation induit la production des cytokines pro-inflammatoires par la voie NF-κB.

Une fois les TLR activés, plusieurs voies de transduction sont induites. Les TLR recrutent dans un premier temps des molécules dit « adaptatrices ». Ces dernières induisent une signalisation intracellulaire par l'intermédiaire de phosphorylations, d'ubiquitinylations ou d'interactions protéine-protéine. Cette cascade aboutit à la translocation nucléaire de facteurs de transcription régulant l'expression de gènes impliqués dans la réponse inflammatoire, notamment des cytokines. Tout d'abord, les TLR recrutent les molécules adaptatrices MyD88 « Myeloid Differentiation primary-response gene 88 ») ou TRIF (« TIR domain-containing adaptor inducing IFN ») qui jouent un rôle essentiel pour l'expression des gènes de l'immunité innée. Ce recrutement conduit à l'activation des kinases TBK1 (« Tank-Binding Kinase »), IKKε, et IKKα/β (« Inducible IκB kinase »). Ces kinases induisent la phosphorylation des facteurs de transcription IRF3 et IRF7 d'une part et NF-κB (« Nuclear Factor Kappa-light-chain-enhancer of activated B cells ») d'autre part (Tomasello et al., 2014).

Les protéines IRF3 et IRF7 ainsi phosphorylées vont être transloquées dans le noyau et se fixer sur les éléments de réponse IRE (« IRF Response Element ») afin d'induire l'expression des IFN-α/β et différents ISG (interferon-stimulated genes) (Goubau et al., 2013 ; Wu and Chen, 2014). L'expression d'IFN-α repose principalement sur la formation de dimères d'IRF7, alors que l'expression d'IFN-β nécessite le recrutement des dimères d'IRF3, NF-κB et le complexe ATF2/c-Jun au niveau du promoteur du gène (Marié et al., 1998).

La phosphorylation de NF-κB induit par les molécules adaptatrices joue un rôle très important dans l'expression de cytokines pro-inflammatoires. Les différents TLR utilisent des

combinaisons différentes des molécules adaptatrices Myd88 et TRIF pour activer leurs gènes cibles, ce qui explique l'induction de profils de gènes différents.

Ainsi, le récepteur TLR3 utilise l'adaptateur TRIF pour induire la production des IFN-I. Le récepteur TLR4 utilise les adaptateurs TIRAP et TRAM pour recruter à la fois Myd88 et TRIF puis activer NF-κB et IRF3 ce qui permet l'induction des cytokines inflammatoires et des IFN-I (Fitzgerald et al., 2003 ; Yamamoto et al., 2003). Les récepteurs TLR7/8 et 9 quant à eux mobilisent MyD88 pour activer IRF7 et NF-κB, et ainsi induire l'expression des cytokines pro-inflammatoires et la production des interférons type I (Takeuchi and Akira, 2010).

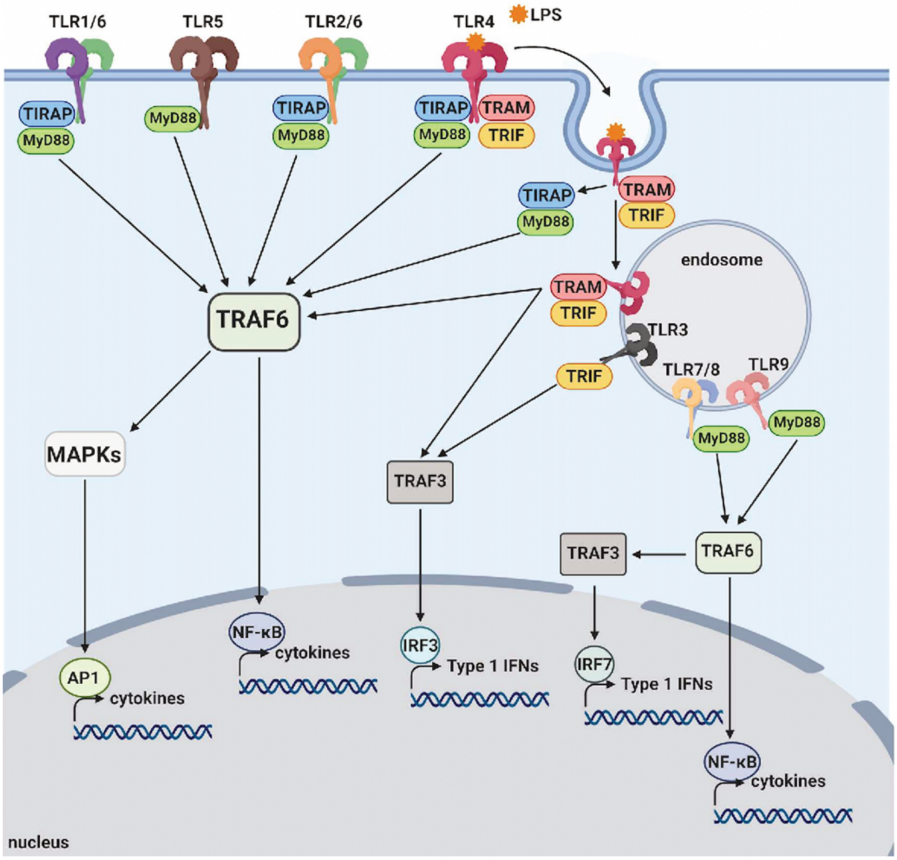

Figure 4: Signalisation par les TLR.
(Yang et al., 2020)

b. Les NOD-like récepteurs (NLRs)

Les NLR sont présents au niveau du cytoplasme des cellules. Ils reconnaissent donc des PAMPs intracellulaires. Chez l'homme, 22 NLRs ont été identifiés et 33 chez la souri. Les NLRs sont majoritairement exprimés dans les cellules immunitaires, cependant ils sont aussi exprimés dans des cellules épithéliales et mésothéliales. Ils reconnaissent des fragments bactériens présents dans le cytoplasme des cellules, notamment le peptidoglycane (PGN) des bactéries

GRAM positifs et la flagelline. Les NLR sont constitués de trois parties. Une partie C-terminale riche en leucine (LRR) qui permet de reconnaitre les PAMPs, un domaine central liantles nucléotides (NBD) nécessaire à la dimérisation de la protéine et donc à la transduction du signal par un domaine N-terminal effecteur (Martinon and Tschopp, 2005). Le NBD est constitué de domaines NACHT (nommé d'après les initiales des premières protéines identifiées le possédant : NAIP, CIIA, HET-E et TP1) et NAD (NACHT associated domain). Le domaine effecteur en N-terminal des protéines NLRs détermine les 5 sous-familles des NLRs. La sous-famille NLR-C présente des domaines de recrutement de caspases (CARD), NLR-P des domaines pyrines (PYD), NLR-A des domaines acides, NLR-B des domaines inhibiteurs de baculovirus (BIRs) (Inohara and Nuñez, 2003) et NLR-X (Tattoli et al., 2008) qui présente des domaines inconnus (Ting et al., 2008).

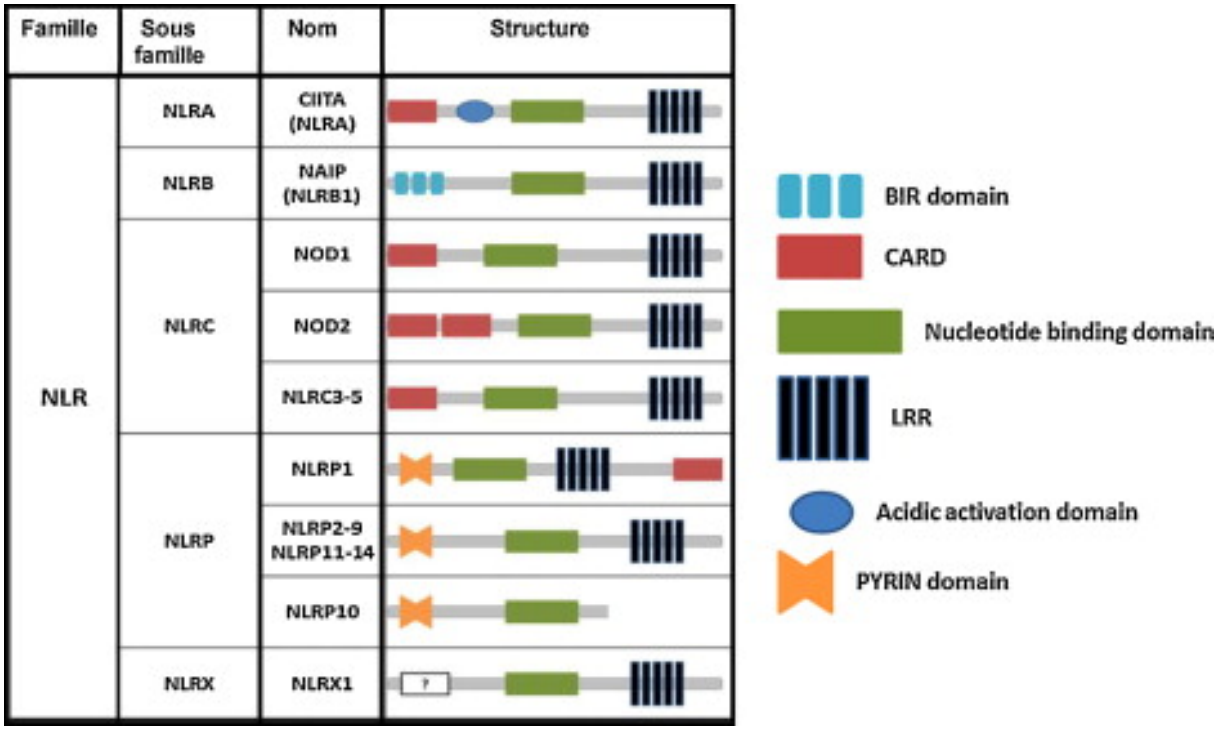

Figure 5: Récepteur de type NOD
(Ait Yahia et al., 2013)

NOD1 et NOD2 sont les premiers récepteurs de la famille des NLR à être découverts, et donc les mieux décrits (Inohara et al., 1999). L'expression de NOD1 est ubiquitaire alors celle de NOD2 est plus restreinte. D'un point de vue immunitaire, NOD2 est exprimé par les macrophages (Ogura et al., 2001) et les cellules dendritiques (Tada et al., 2005).

Transduction du signal par les NLR

La transduction du signal des NLRs est dépendante de sa structure en N-terminal. Ainsi on distingue les NLR ayant un domaine NOD (caspase) de ceux qui ont un domaine NALP (pyrine) qui aboutissent respectivement à l'activation de la voie NF-κB ou caspase-1

- Transduction du signal des NOD

Le domaine LRR des récepteurs NOD change de conformation en présence d'un PAMP bactérien (peptidoglycane) au niveau du cytoplasme. Ce changement de conformation induit une oligomérisation de la molécule reconnue grâce au domaine NACHT. Par la suite, la sérine-thréonine kinase RIP2 (RICK) et la caspase-9 sont recrutées (Inohara et al., 2000). Pour NOD1, il est nécessaire d'avoir deux récepteurs NOD1 pour la reconnaissance d'un PAMP alors qu'un seul suffit pour NOD2. Le complexe CARD-RIP2 permet d'ubiquitiner les IKKγ (I-kappa B kinase-gamma) ou NEMO. Les IKK ubiquitinées induisent la phosphorylation des sous-unités inhibitrices IκB qui sont liés au NF-κB en les maintenant inactifs. Le changement de conformation des IκB libèrent alors les sous-unités actives du NF-κB qui peuvent alors transloquer vers le noyau (Franchi et al., 2009). Ils vont pouvoir activer la transcription et la traduction de gènes codant des cytokines pro- et anti-inflammatoires. A noter que RIP2 peut aussi interagir avec TAK1 et ainsi activer les MAP kinases. Les voies stimulées par les NOD sont liées aux voies de signalisation des TLR, ce qui amplifie la réponse (Martinon and Tschopp, 2005).

- Transduction du signal des NALP

La sous-famille des NALP a un domaine pyrine au niveau N-terminal. Ainsi, l'activation des NALP aboutit à l'activation de la caspase 1 qui est une enzyme de maturation pour l'IL1β. Parmi les NALP, NLRP3 (ou NALP3 ou cryopyrine) est la mieux décrite. Lors d'une infection, l'activation des TLRs permet la translocation de NF-κB dans le noyau ce qui induit la production de pro-IL-1β cytoplasmique. Cette forme pro-IL-1β est inactive. Afin d'induire ce phénomène dit de « priming », les cellules immunitaires cultivées *in vitro* sont généralement stimulés avec du LPS, le ligand de TLR4 (Bauernfeind et al., 2009). La maturation du pro-IL-1β en IL-1β se fait grâce à un second stimulus qui induit la formation d'un complexe protéique : l'inflammasome (Martinon et al., 2002). Ce complexe est formé de la protéine ASC (Apoptosis associated Speck-like protein containing a CARD), de la pro-caspase-1 (forme inactive de la caspase-1), et de NLRP3. La formation de ce complexe induit l'activation de la caspase-1 qui est capable de cliver la pro-IL-1β accumulée dans le cytoplasme, afin d'aboutir à la sécrétion de l'IL-1β mature. L'oligomérisation de l'inflammasome est induite suite à la reconnaissance

de nombreux signaux par NLRP3. 3 modèles d'activations ont été identifiés : l'effet d'ions potassium (K+) la rupture lysosomale et la génération de ROS (Reactive Oxygen Species)

On peut citer l'ATP extracellulaire qui est détecté par le récepteur membranaire purinergique P2X7 (Ferrari et al., 2006). L'activation de ce dernier aboutit à un efflux d'ions potassium hors de la cellule. La diminution de la concentration intracellulaire en potassium induit un changement conformationnel de NLRP3 et l'activation de l'inflammasome NLRP3 (Pétrilli et al., 2007). Certaines toxines bactériennes comme la nigéricine induisent la formation de pores membranaires conduisant également en un flux d'ion potassium.

Les cristaux et certaines particules peuvent entraîner une rupture des lysosomes ou des phagolysosomes comme les cristaux de silice, les sels d'aluminium (Hornung et al., 2008), les cristaux d'acide urique (MSU) (Martinon et al., 2006). Cette rupture est associée à un relargage du contenu de ces organites dans le cytosol, notamment les cathepsines B (protéases lysosomales). Cette dernière a la capacité de se lier directement au récepteur NLRP3 induisant son oligomérisation et son l'activation de l'inflammasome (Bruchard et al., 2013).

Le principal générateur de ROS dans le cytosol des cellules est lié aux stress des mitochondries. Ces ROS activent NLRP3, et donc l'inflammasome, en modifiant la thiorédoxine, une protéine sensible aux ROS, en libérant son partenaire d'interaction TXNIP (thioredoxin-interacting protein) (Zhou et al., 2010). Les ROS, ainsi que d'autres signaux de stress cellulaires, conduisent à la lyse mitochondriale ce qui libère de l'ADN mitochondrial oxydé dans le cytosol. Ce dernier se fixe sur NLRP3 et active l'inflammasome (Shimada et al., 2012).

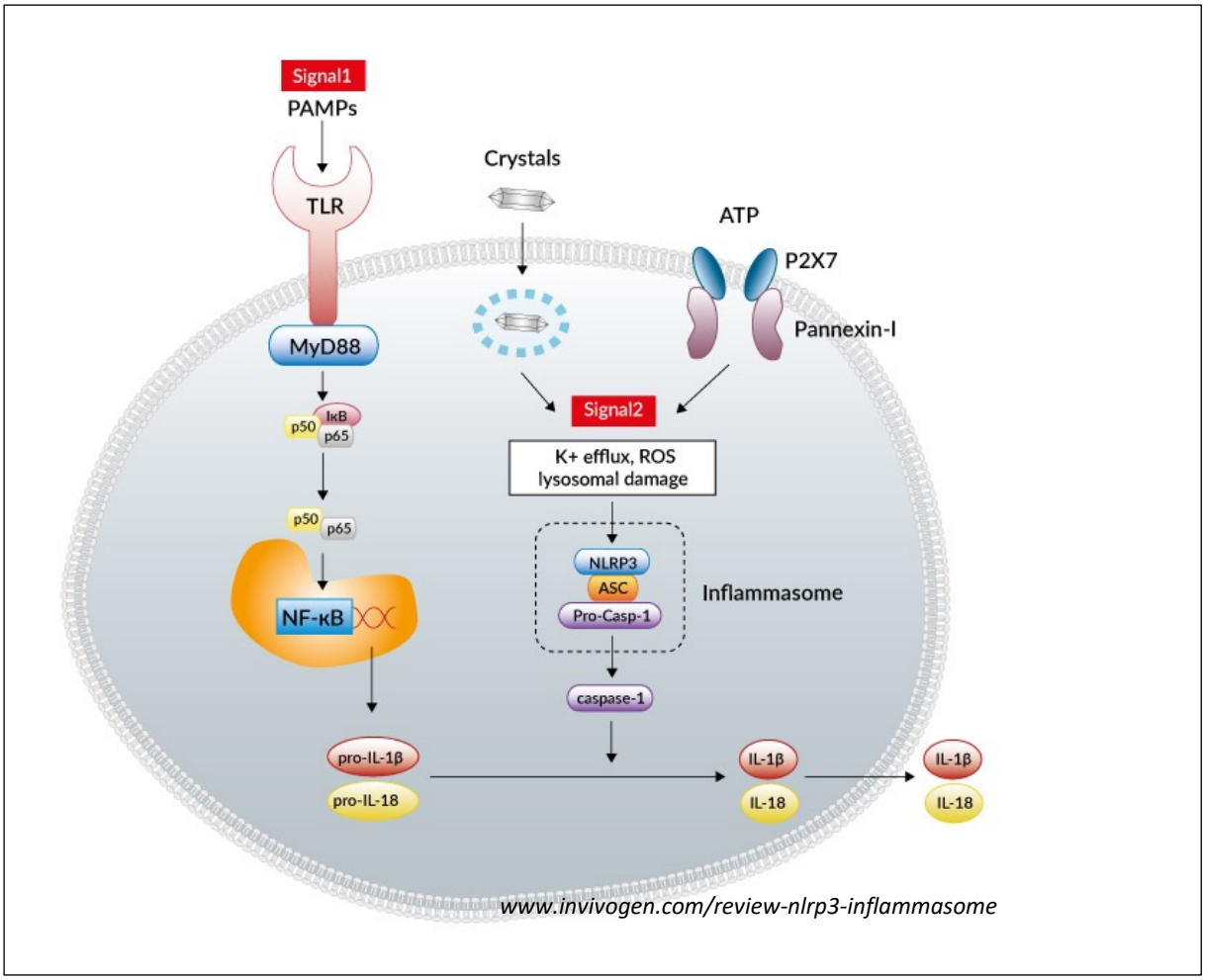

Figure 6: Activation of the NLRP3 Inflammasome
("Activation of the NLRP3 Inflammasome," 2017)

c. Les capteurs d'ADN intracellulaire (cGAS)

La voie cGAS-STING est un élément du système immunitaire inné capable à détecter la présence d'ADN bicaténaire au niveau du cytoplasme des cellules. Une fois induite, cette voie active l'expression de gènes inflammatoire. L'ADN est naturellement absent du cytosol des cellules car il situé au niveau du noyau et certains organites (mitochondries, chloroplastes). La présence d'ADN dans le cytosol présume donc d'une anomalie, et est associée à la cancérogenèse, à l'infection par des virus ou à l'invasion par des bactéries. Ainsi, la voie cGAS-STING à pour but de détecter de l'ADN cytosolique et d'induire une réponse immunitaire en conséquence. En présence d'ADN, la synthase de GMP-AMP cyclique (cGAS) induit la formation d'un messager cellulaire, le GMP-AMP cyclique (cGAMP), qui se lie à STING (de l'anglais Stimulator of Interferon Genes), une protéine adaptatrice. L'engagement de STING

induit la production de cytokines et d'interférons de type I, jouant un rôle majeur dans l'élimination du pathogène. Pour cela, STING induit la phosphorylation des facteurs de transcription STAT6 et IRF3 par l'intermédiaire de la kinase TBK1 (TANK-binding kinase 1). Le facteur IRF3 induit l'expression des gènes codant les interférons de type I (IFN-I) et des cytokines inflammatoires. Ces derniers contribuent à l'induction d'une réponse immunitaire contre le pathogène détecté. Le facteur STAT6 active des chimiokines telles que CCL2 et CCL20.

d. Les récepteurs aux lectines de type C (CLR)

Les récepteurs aux lectines de type C sont des récepteurs membranaires spécialisés dans la reconnaissance des hydrates de carbone. Ces dernières sont un des composants de la paroi des champignons, des virus et des mycobactéries (Geijtenbeek and Gringhuis, 2009). Parmi les plus connus on retrouve les Dectin-1 et Dectin-2. Ils sont respectivement les récepteurs spécifiques du béta-glucane (Brown et al., 2002) et de l'alpha-mannose (McGreal et al., 2006). La reconnaissance d'un pathogène par un CLR induit son internalisation par endocytose puis sa dégradation. Cela a pour conséquence d'activer le système immunitaire adaptatif via la présentation d'antigène. Dectin-1 et Dectin-2 sont également capables d'activer NLRP3, et donc l'inflammasome avec la sécrétion de l'IL-1b (Kankkunen et al., 2010).

e. Les RIG-I-like receptors (RLR)

Les membres de la famille des « RIG-Like Receptors » (RLR) sont cytoplasmiques et spécialisés dans la détection des ARN viraux cytoplasmique. Cette famille compte trois membres : RIG-I (« Retinoic acid-Inducible Gene I, ou DDX58 »), MDA-5 également nommé IFIH1(« Melanoma Differentiation-Associated protein 5 »), et LGP2 (« Laboratory of Genetics and Physiology 2 »).

RIG-I détecte les ARN 5'-tri et biphosphates bicaténaires alors que MDA5 reconnait les ARN bicaténaires de grande taille. Cette différence a pour conséquence que MDA5 et RIG-I sont impliqués dans la réponse à des virus différents. RIG-I et MDA5 présentent deux domaines CARD (« caspase recruiting domain ») N-terminaux, un domaine hélicase centrale DExD/H-box, et un domaine régulateur C-terminale (CTD). LGP2 ne contient pas de domaine CARD à son extrémité N-terminale. En l'absence d'ARNdb, RIG-I présente une conformation fermée qui est inactive. La liaison de l'ARN aux domaines hélicase et CTD libère les domaines CARD

de RIG-I qui se regroupe sous forme de filaments. Dans le cas de MDA5, c'est la multimérisation le long d'ARN bicaténaires qui permet l'oligomérisation des domaines CARD. Ceux-ci se lient alors à un facteur mitochondrial ayant également un domaine CARD : la protéine MAVS (« Mitochondrial Antiviral Signaling Protein ») également nommées CARDIF, VISA ou IPS1 (Meylan et al. 2005 ; Reikine, Nguyen, and Modis 2014 ; Xu et al. 2005). Il a été montré que l'interaction de RIG-I ou MDA5 à MAVS induit la multimérisation de ce dernier à la membrane mitochondriale externe. Ce phénomène permet de recruter des kinases IKKε et TBK1 afin d'induire l'expression des IFN.

Tout comme la signalisation des TLR, ces kinases activent IRF3 et IRF7. En parallèle, MAVS peut également induire l'activation de la voie NF-κB.

LGP2 n'ayant pas de CARD, il ne peut s'associer au MAVS. Il jouerait plutôt un rôle de régulation d'activité de RIG-I et MDA5 en s'associant à eux.

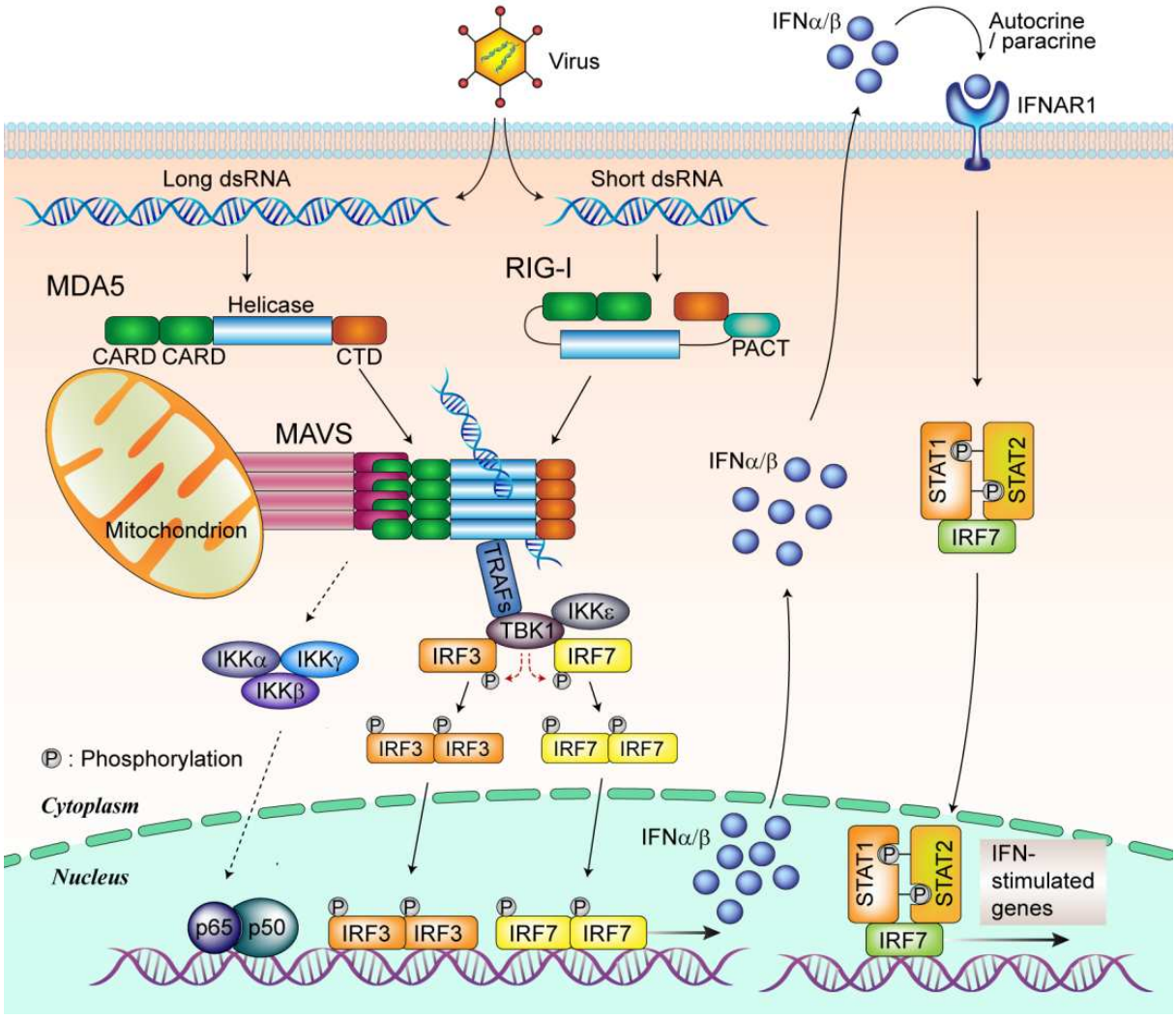

Figure 7: Voie de signalisation des RLR
(Jin et al. 2017)

B. Médiateurs de l'inflammation

L'inflammation est induite par des dommages tissulaires ou de l'intrusion de particules ou de pathogène dans l'organisme. Ce processus inflammatoire fait intervenir des médiateurs pro inflammatoires. Ces médiateurs sont d'origine cellulaire ou dérivée de protéines plasmatiques. Les médiateurs auxquels nous nous intéresserons sont les cytokines. Ce sont des glycoprotéines comparables aux hormones, qui peuvent être membranaires, ou sécrétées suite à une stimulation. Elles sont une centaine et classées par classes suivant l'homologie de structures. Parmi elles, on trouve le TNF-α, les interleukines, les chimiokines et les interférons. Chaque cytokine peut être synthétisée par plusieurs types cellulaires et agir sur un grand nombre de cellules cibles sur lesquelles elle aura des actions diverses et variées. Les cytokines agissent selon différents modes d'action : autocrine, juxtacrine, paracrine et endocrine.

i. Les interleukines

Les interleukines régulent la croissance, la différenciation et la motilité des cellules. Elles sont particulièrement importantes dans la stimulation des réponses immunitaires, dont l'inflammation. Les premières interleukines ont été identifiées dans les années 1970 ("Revised nomenclature for antigen-nonspecific T cell proliferation and helper factors," 1979). Au départ, les chercheurs pensaient que les interleukines étaient fabriquées principalement par les leucocytes pour agir principalement sur d'autres leucocytes. C'est pour cette raison qu'ils ont été nommés interleukines, ce qui signifie "entre les leucocytes". Les leucocytes étant impliqués dans l'élaboration des réponses immunitaires, on pensait que les interleukines avaient uniquement un rôle de modulateur des fonctions immunitaires. Bien qu'il s'agisse d'une fonction importante des interleukines, on sait aujourd'hui que les interleukines sont également produites par de nombreux types cellulaires qui ne participent pas à l'immunité et interagissent avec elles, et qu'elles sont impliquées dans de nombreuses autres fonctions physiologiques. Ainsi, le rôle que jouent les interleukines dans l'organisme est beaucoup plus large que ce qui a été initialement décrit.

Le génome humain compte plus de 50 gènes codant les interleukines (Brocker et al., 2010). Sont présentées ici les principales interleukines étudiées durant ce travail de thèse.

- la famille de **l'interleukine 1** (IL-1) est produite majoritairement par les macrophages/monocytes mais aussi par d'autres types cellulaires : les lymphocytes B, lymphocytes T et cellules endothéliales. Initialement, la famille des IL-1 ne comprenait que deux membres : l'IL-1α et l'IL-1β. Cette famille comprend désormais 11 membres qui ont une structure génétique similaire : IL-1α, IL-1β, IL-1RA, IL- 18, IL-33, IL-36α, IL-36β, IL-36γ, IL-36RA, IL-37 et IL-38 (Dinarello et al., 2010). Les IL-1α et IL-1β, produits par les macrophages et les monocytes activés, sont l'un des acteurs clés de la réponse immunitaire innée. Ils jouent un rôle important dans la coordination de l'inflammation locale et systémique en provoquant une inflammation et en induisant l'expression d'autres gènes pro-inflammatoires comme la COX de type II, la synthase d'oxyde nitrique inductible et d'autres cytokines ou chimiokines. L'IL-1β est le pyrogène endogène le plus puissant connu et a été impliqué dans les dommages tissulaires et les symptômes systémiques de la septicémie et de plusieurs maladies inflammatoires. C'est pourquoi l'IL-1 (interleukine 1) a été une cible précoce dans la thérapie d'un certain nombre de maladies.

- La famille de l'**interleukine 6** (IL-6) est un groupe de cytokines comprenant l'IL-6, l'IL-11, le facteur neurotrophique ciliaire (CNTF), le facteur inhibiteur de la leucémie (LIF), l'oncostatine M (OSM), la cardiotrophine 1 (CT-1) et la cytokine analogue à la cardiotrophine (CLC) (Rose-John, 2018). Nous nous intéresserons ici plus particulièrement à IL-6, produite rapidement et transitoirement en réponse aux infections et aux lésions tissulaires. Elle est principalement produite par les macrophages, monocytes, les cellules dendritiques, mais également les lymphocytes T, les lymphocytes B, les cellules mésangiales, les fibroblastes, les cellules endothéliales, les kératinocytes et diverses cellules tumorales. Elle se lie au récepteur de l'IL-6 (IL-6R), existant sous formes soluble ou membranaire. L'IL-6 joue un rôle important dans la transition entre l'inflammation aiguë et l'inflammation chronique. Les taux d'IL-6 sont élevés dans un grand nombre de maladies inflammatoires chez l'homme. L'expression de l'IL-6 est accrue au niveau site de l'inflammation, et le blocage de l'IL-6 et de la signalisation de l'IL-6 est efficace pour la prévention et le traitement dans des modèles de maladies inflammatoires, comme l'arthrite. Dans la polyarthrite rhumatoïde (PR), elle est, entre autres, responsable de la prolifération et de l'hypertrophie synoviale (Lipsky, 2006).

- La famille de l'**interleukine 10** (IL-10) comprend l'IL-10, l'IL-19, l'IL-20, l'IL-22, l'IL-24 et l'IL-26 (Wei et al., 2019). L'IL-10 est la cytokine la plus importante pour supprimer les réponses pro-inflammatoires dans toutes sortes de maladies auto-immunes et limiter les réponses

immunitaires excessives. Elle est ainsi capable de bloquer la synthèse des cytokines pro-inflammatoires (IL-1, IL-6, IFN-γ et TNF-α) dans les cellules T, les monocytes et les macrophages, et en inhibant l'expression des molécules de surface cellulaire impliquées dans la présentation des antigènes.

- La famille de l'**interleukine 12** (IL-12) comprend IL-12, IL-23, IL-27 et IL-35 (Sun et al., 2015). L'IL-12, l'IL-23 et l'IL-27 sont sécrétés par les cellules présentatrices d'antigènes (CPA) activées pendant la présentation de l'antigène aux cellules T naïves, tandis que l'IL-35 est un produit des cellules T et B régulatrices (Collison et al., 2007; Shen et al., 2014; Wang et al., 2014). Ils assurent la liaison entre les systèmes immunitaires innés et adaptatifs en polarisant la différenciation des cellules T CD4+ naïves en sous-ensembles T auxiliaires producteurs de cytokines et en cellules T mémoires (Steinman, 2006). L'IL-12 est produit par les macrophages, les cellules dendritiques et les lymphocytes B. L'IL-12 permet la stimulation de la production des interféron-gamma (IFN-γ) et du TNF-α par les cellules NK, NKT et les ILC1s. L'IL-23 est essentielle à la différenciation, l'expansion et la survie des Th17 et des ILC3s en se liant à son récepteur. De nombreuses études ont révélé que la voie IL-23/Th17 est impliquée dans la physiopathologie de diverses maladies auto-immunes, telles que l'arthrite auto-immune, et les maladies inflammatoires de l'intestin.

ii. Les chimiokines

Les chimiokines sont de toutes petites cytokines de 8-14 kDa, dont la plupart sont produites lors d'une réponse inflammatoire et qui ont pour rôle d'activer les cellules immunitaires, ainsi que de les recruter au niveau du site de l'inflammation. Les chimiokines agissent par l'intermédiaire de leurs récepteurs qui comptent sept domaines transmembranaires couplés à la protéine G (GPCR). Les chimiokines comptent actuellement près de 50 membres chez les mammifères. Bien que les chimiokines aient un faible homologie d séquence, elles présentent une structure tridimensionnell hautement conservée. Cette structure commune comprend trois feuillets plissés β et une partie carboxy-terminale en hélice α (Baggiolini et al., 1997; Mackay, 1997). Au cours de l'année 2000, une nouvelle classification des chimiokines a été instaurée qui a permis de classer les 50 membres de cette famille en quatre groupes (Zlotnik and Yoshie, 2000). Il a ainsi été défini les sous-familles : les CXC, les CC, les et les CX3C chimiokines (Fig. 8).

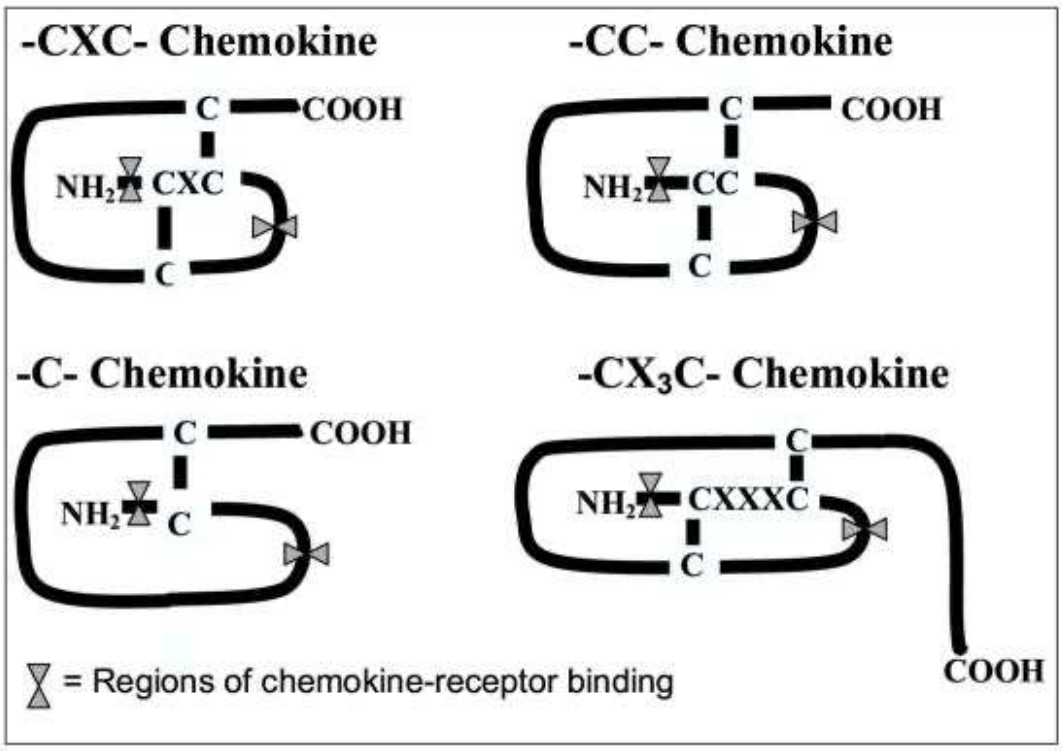

Figure 8: Les quatre sous-familles de chimiokines classées selon leur structure
(Townson and Liptak, 2003)

- **Les CXC chimiokines ou CXC ligands (CXCL)** comptent 16 membres subdivisés en deux sous-groupes selon la présence ou non d'un motif ELR (Glutamine-Leucine-Arginine). La majorité des gènes *CXCL* se situent sur le chromosome 4, à l'exception de *CXCL12, CXCL14* et *CXCL16* qui sont localisés sur le chromosome 10.

8 chimiokines possèdent le motif ELR+ : CXCL1, CXCL2, CXCL3, CXCL5, CXCL6, CXCL7, CXCL8 et CXCL15. Ces chimiokines attirent principalement les polynucléaires neutrophiles. Elles peuvent être produites par différentes cellules en réponse à des stimuli cytokiniques pro-inflammatoires, essentiellement l'IL-1 et le TNF-α. Ces chimiokines favorisent l'adhésion des neutrophiles aux cellules épithéliales et la migration à travers l'endothélium. De plus, elles possèdent un pouvoir chimioattractant pour les cellules endothéliales (Strieter et al., 1995).

8 chimiokines possèdent le motif ELR- : CXCL4, CXCL9, CXCL10, CXCL11, CXCL12, CXCL13, CXCL14 et CXCL16. Contrairement aux chimiokines ELR+, les ELR- ont une

activité anti-angiogénique. Elles attirent principalement les monocytes et les lymphocytes (Cole et al., 1998; Sleeman et al., 2000).

- **Les CC chimiokines ou CC** comptent 28 membres. La majorité des gènes codant ces CC-chimiokines sont localisés au niveau du chromosome 17, sauf CCL19 qui se situ sur le chromosome 9 et CCL24 et CCL26 qui sont sur le chromosome 7. Les cellules mononuclées sont les premières cibles de ces chimiokines. Certaines d'entre elles jouent un rôle dans l'homéostasie cellulaire pour lequel leurs expressions sont constitutives : CCL19, CCL20 et CCL2 (Inngjerdingen et al., 2000; Luster and Rothenberg, 1997). Les lymphocytes T et les cellules dendritiques sont guidés avec ces trois chimiokines vers des sites spécifiques au travers du tissu lymphoïde (von Andrian and Mempel, 2003). D'autres chimiokines sont impliquées dans l'inflammation et les allergies, où cette fois-ci leurs expressions sont inductibles : CCL1, CCL2, CCL7, CCL8, CCL11, CCL13, CCL17, CCL22, CCL24 et CCL26. Les C chimiokines impliquées dans le développement sont CCL17 et CCL25 (Imai et al., 1996; Vicari et al., 1997).

- **Les C chimiokines ou CL** compren 2 membres : XCL1 et XCL2. XCL1 stimule la chimiotaxie des leucocytes CD4+ et CD8+, et des cellules NK (Zavala-Flores et al., 2009). XCL1 a également un effet suppressif et cytotoxique contre des tumeurs et des cellules T effectrices (Huang and Xiang, 2004).

- **Les CX3C chimiokines ou CX3CL** comptent comme membre CX3CL1 qui existe sous deux formes : soluble et membranaire. La forme soluble a une activité chimiotactique sur les lymphocytes T et les monocytes. La forme membranaire est principalement exprimée sur les cellules endothéliales activées et les cellules épithéliales bronchiques. Cette forme favorise l'adhésion ferme des lymphocytes (Bazan et al., 1997). CX3CL est fortement présente dans le sang et le LBA (Lavage bronchiolo-alvéolaire) (Rimaniol et al., 2003).

iii. Les Interférons

C'est en 1957 que Alick Isaacs et Jean Lindenmann ont découvert pour la première fois les interférons (IFN). Ils ont montré qu'à la suite d'une exposition au virus de la grippe inactivée, les cellules en culture sécrètent des peptides solubles capables de protéger les cellules naïves

d'une infection virale. Ces peptides ont été nommés « interférons » en raison de leur capacité à interférer avec les infections virales (Isaacs and Lindenmann, 1957).
Actuellement, trois grandes familles d'IFN ont été décrites : les IFN de type I, II et III. Ces peptides ont été catégorisés selon leur localisation chromosomique, leurs séquences nucléotidiques et leurs récepteurs membranaires spécifiques.

a. Les interférons de type I

A ce jour, il existe huit sous-types IFN de type I (IFN-I) toutes espèces confondues : IFNα, IFNβ, IFNε, IFNω, IFNτ, IFNκ, IFNδ et IFNζ. L'homme compte IFNα, IFNβ, IFNε, IFNω et IFNκ. Les deux IFN-I les mieux caractérisés sont l'IFN-α et l'IFN-β car ils sont les plus exprimés. L'IFNω, IFNκ, IFNε ont été décrits mais sont présents en faible quantité (Pestka et al., 2004). En plus de leurs propriétés antivirales, les IFN-I possèdent également de fortes propriétés antiprolifératives, ils interagissent avec un grand nombre de cellules immunitaires et jouent un rôle dans l'embryogenèse et dans l'inhibition de l'angiogenèse. Tous les IFN-I se lient au même récepteur qui, une fois activé, forme un hétérodimère formé des protéines transmembranaires IFNAR1 et IFNAR2. Ces récepteurs induisent une voie de signalisation qui stimule l'expression de plusieurs centaines de gènes : les ISG pour « Interféron-Stimulated Genes » (Fig. 9). Ces ISG provoquent un état antiviral et aident à la mise en place des réponses immunitaires innées et adaptatives (Capobianchi et al., 2015; Pestka et al., 2004).

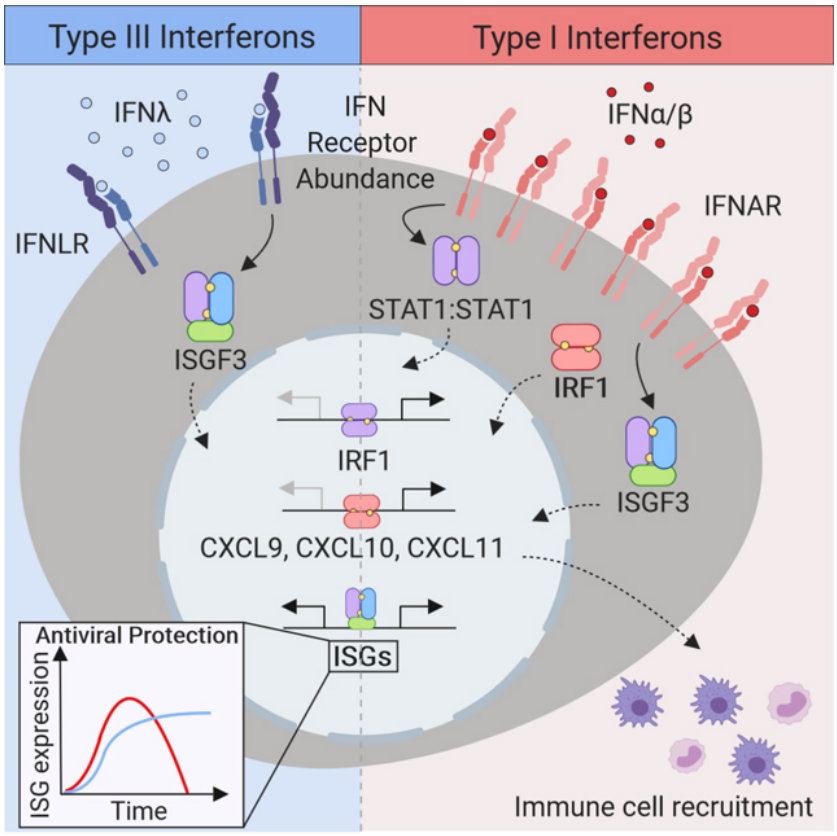

Figure 9: Transcription des ISG activée par les IFN I et III: voie de signalisation des IFNAR (Forero et al., 2019)

- **Les interférons α** comptent chez l'homme 13 sous-types d'IFN : IFN-α1, α2, α4, α5, α6, α7, α8, α10, α13, α14, α16, α17 et α21. Ces IFN sont codés par treize gènes différents situés sur le chromosome 9 et partagent une identité de séquence de l'ordre de 70–80%. Malgré cette forte homologie entre les différents sous-types, les propriétés antivirales et antiprolifératives sont très variables d'un sous-type à un autre (Evinger et al., 1981). Les IFN-α et l'IFN-β que nous décrirons ci-dessous, sont exprimés par la quasi-totalité des cellules de l'organisme en réponse à une infection virale et certains stress cellulaire. Cependant, les pDC, peuvent produire en réponse à une infection virale jusqu'à 10 000 fois plus d'IFN-α que les autres types cellulaires. Pour cette raison, elles sont également nommées IPC pour « interferon producing cells ». Les pDC peuvent produire de grandes quantités de tous les types d'IFNα, à l'exception de IFNα6 et IFNα8 qui sont produits en faible quantité, et IFNα7 qui n'est pas induit (Hillyer et al., 2012).

Les IFN-α2, 6, 7, 8, 10 et 14 sont particulièrement efficaces pour l'induction des protéines dépendantes de l'IFN possédant des répétitions tétratricopeptides de type 1 (IFIT1), mais aussi des cytokines telles que CXCL10, CXCL11, ISG15 et CCL8 (Gibbert et al., 2013).

-**L'interféron β** est codé que par un seul gène et ne partage que 35% d'identité de séquence avec les IFN-α. Le gène de l'IFN-β est toujours localisé à proximité des gènes de l'IFNα (Fujisawa et al., 1978).

-**Les interférons ε, IFN-ω, et IFN-κ** possèdent des activités antivirales mais les différences fonctionnelles peuvent être importantes d'un sous-type à l'autre. L'IFN-ε et IFN-κ sont exprimés par diverses muqueuses et dans la peau, notamment l'appareil génital féminin et les kératinocytes (Fung et al., 2013; Hardy et al., 2004; LaFleur et al., 2001). L'IFN-ε est également capable d'induire des facteurs de restriction qui limitent l'infection par le VIH-1 (Garcia-Minambres et al., 2017; Tasker et al., 2016) alors que l'IFN-κ ne présente qu'une faible activité antivirale. L'IFN-ω est similaire à d'autres IFN dans le sens où il est produit par les cellules en réponse à une infection virale et est principalement produit dans les leucocytes (Li et al., 2017).

b. L'interféron de type II

La famille de l'IFN de type II est composée d'un seul membre produit d'un seul gène, l'IFN-γ. Il est principalement produit par les lymphocytes T et les cellules NK, mais a parfois été également proposé être secrété par d'autres cellules comme les lymphocytes B et les cellules présentatrices d'antigène (CPA), notamment les macrophages (Bach et al., 1997; Frucht et al., 2001). L'IFN-ɣ se lie à un récepteur spécifique, un tétramère formé de deux sous-unités IFNGR1 et deux sous-unités IFNGR2 (Crisafulli et al., 2008). L'IFN-ɣ est un inhibiteur de la réplication virale et joue également un rôle immunomodulateur entre cellules immunitaires pour la mise en place des réponses innées et adaptatives. Il active les cellules dendritiques et les macrophages en augmentant la phagocytose et en stimulant l'expression des molécules de CMH de classe I et II pour la présentation antigénique (Bach et al., 1997; Wheelock, 1965).

c. Les interférons de type III

La famille de l'IFN de type III comprend l'IFN-λ1, IFN-λ2 et IFN-λ3, aussi connu respectivement sous les noms de IL-29, IL-28A et IL-28B. Ils sont produits par la plupart des cellules mais l'expression de leur récepteur est principalement restreinte aux muqueuses (Syedbasha and Egli, 2017). Le récepteur de cette famille est un hétérodimère constitué de IFNLR1 et de IL10R2. Ces IFN jouent un rôle important au niveau des tissus les plus exposés aux infections virales.

II. Les maladies auto-immunes et inflammatoires

Le système immunitaire défend l'organisme des agressions extérieures, comme les bactéries ou les virus, et tolère habituellement ses propres constituants. Dans certains cas, cette tolérance du soi est défaillante ce qui est source de maladie. Typiquement, des « anticorps » habituellement produits par les plasmocytes pour neutraliser des pathogènes en se fixant à certaines de leurs molécules (antigènes) peuvent aussi apparaître et viser des éléments de notre propre organisme. On parle alors d'auto-anticorps. Dans le diabète de type 1 par exemple, des auto-anticorps ciblent les cellules du pancréas sécrétrices d'insuline. Dans le lupus érythémateux disséminé, les auto-anticorps sont dirigés contre des molécules exprimées par de nombreuses cellules du corps, conduisant à des lésions tissulaires (peau, articulations, reins, cœur…).

Dans certains cas, on ne trouve pas d'auto-anticorps. C'est un disfonctionnement des cellules immunitaires innées (neutrophiles, macrophages, monocytes, cellules NK, pDC…) qui déclenche une inflammation chronique ; on parle alors de maladies auto-inflammatoires. Ce disfonctionnement correspond en grande majorité à des productions anormales de cytokines conduisant à la destruction de certains tissus : la peau dans le psoriasis, certaines articulations dans la spondylarthrite rhumatoïde (voir plus loin), le tube digestif dans la maladie de Crohn, le système nerveux dans la sclérose en plaques. Entre 5 à 8% de la population mondiale est touché par une maladie auto-immune ou inflammatoire.

Dans le cadre de cette thèse, nous nous sommes plus particulièrement intéressés à l'arthrite juvénile idiopathique (AJI) et le lupus érythémateux disséminé.

1. Arthrite juvénile idiopathique

A. Définition, classification

L'AJI (l'arthrite juvénile idiopathique) est une maladie qui regroupe des formes hétérogènes de rhumatismes inflammatoires chroniques de l'enfant d'origine inconnue. Il s'agit de la forme d'arthrite la plus répandue chez les enfants de moins de 16 ans (Prakken et al., 2011). L'AJI est une maladie rare avec une incidence annuelle de 2 à 20 cas pour 100 000 habitants dans les pays à revenus élevés et une prévalence de 16 à 150 individus pour 100 000 habitants. Les études effectuées sur l'AJI montrent que cette maladie est en partie causé par des dérèglements de mécanismes impliqués dans la régulation de la réponse immunitaire. L'analyse de la

physiopathologie de l'AJI montre un rôle des cellules de l'immunité innée et adaptative (Macaubas et al., 2009).
En 2001, la « International League of Associations for Rheumatology » (ILAR) a établi une classification de 7 sous−types d'AJI en fonction de critères spécifiques avec comme point commun une inflammation chronique au niveau de la membrane synoviale (Petty et al., 2004). Les patients atteints d'AJI ont un gonflement persistant des articulations touchées associé à des douleurs. En cas d'atteinte sévère et prolongée, la persistance de l'inflammation augmente le risque de développer des lésions ostéo−cartilagineuses.

-L'**AJI oligoarticulaire** est une arthrite qui touche 1 à 4 articulations pendant les 6 premiers mois de la maladie. Ce sous−type est le plus répandu dans les pays occidentaux avec une incidence comprise entre 50 et 60% (Oen and Cheang, 1996). Elle touche principalement les jeunes enfants de sexe féminin. Les premières cibles sont souvent le genoux et la cheville, et est souvent associée à la présence d'anticorps antinucléaires (AAN) et à une uvéite. Certaines cytokines inflammatoires tels que l'IL−1β, l'IL−2, l'IL−6, les IFN et le TNF−α ont été détectées dans les liquides et tissus oculaires, et semblent être impliquées dans la présence des uvéites (Ooi et al., 2006).

-L'**AJI polyaticulaire à facteur rhumatoïde positif** (FR+) est une arthrite qui touche 5 articulations pendant les 6 premiers mois de la maladie (Petty et al., 2004). Le FR est associé à la présence d'anticorps dirigés contre la portion Fc des immunoglobulines (Ig)G. Elle est également associée à la présence d'anticorps dirigés contre les peptides cycliques citrullinés (anti−CCP) qui prédisent les formes plus graves (Nielen et al., 2004).
Parmi les AJI, cette forme représente 5% des cas en Europe, principalement des enfants de sexe féminin. Les premiers symptômes apparaissent généralement en début de l'adolescence, avec majoritairement des atteintes au niveau des poignets, des petites articulations des pieds et des mains. Cette forme d'AJI est assimilable et comparable à la PR (polyarthrite rhumatoïde) chez les adultes. Toutes deux partagent des facteurs de risque comme les allèles HLA−DR1, HLA−DR4 et HLA−DR14 (Gorman and Criswell, 2002). Parmi les patients AJI, ceux présentant une forme polyarticulaire FR positive ont le taux de rémission la plus faible, près de 5% en excluant l'AJI systémique (Wallace et al., 2005).

- **L'AJI polyaticulaire à facteur rhumatoïde négatif** (FR-) est une arthrite qui touche plus de 5 articulations durant les 6 premiers mois de la maladie, sans qu'il n'y ait de FR (Petty et al.,

2004). Ce sous– type d'AJI est très hétérogène : il est associé à des signes cliniques très divers et variés. En Europe, la prévalence de ce sous– type d'AJI est de l'ordre de 10-25%. Généralement, les poignets et les chevilles sont les articulations les plus atteintes.
Trois profils se distinguent au sein de ce groupe d'AJI. Le premier est caractérisé par une atteinte symétrique des articulations, un début des symptômes à un âge scolaire, l'absence d'anticorps antinucléaires et une évolution variable de la maladie. Le deuxième phénotype est comparable à une oligoarthrite avec des anticorps antinucléaires, une apparition en bas âge, une arthrite asymétrique, apparition possible d'uvéite et une association avec l'allèle HLA–DRB1*08. C. Le troisième phénotype est également nommé « synovite sèche » à cause d'hypertrophie synoviale.

-L'**AJI associée au psoriasis** est définie comme une association entre une inflammation des articulations et à une éruption psoriasique. S'il n'y a pas d'éruption psoriatique, cette forme d'AJI doit être associée à une dactylite, des ongles de la couturière ou une onycholyse, ou encore des antécédents familiaux de psoriasis (Petty et al., 2004). Dans la moitié des cas d'AJI psoriasique, les atteintes de la peau ne surviennent pas immédiatement, mais plutôt plusieurs années après les manifestations articulaires. Cette forme représente 5 à 10% des AJI présents dans les pays occidentaux (Berntson et al., 2001). Elle touche généralement des jeunes enfants âgés de 2−3 ans ou entrant dans l'adolescence. L'AJI psoriasique regroupe un ensemble hétérogène de manifestations arthritiques et présente de nombreux traits communs avec les autres sous−types.

-L'AJI liée à l'enthèse est une arthrite associée à une enthésite. Cette forme d'AJI est généralement associée à des antécédents familiaux d'arthrites, à la présence de l'allèle HLA–B27 ou d'une uvéite (Petty et al., 2004). Durant les premiers stades de la maladie, les membres inférieurs sont principalement atteints de façon asymétrique. Elle peut ensuite évoluer vers le squelette axial. L'AJI liée à l'enthèse représente 8 à 16% des AJI dans les pays du nord. Ce sont majoritairement des enfants âgés de 10 et 13 ans qui en sont atteints (Prutki et al., 2008). Les hommes sont plus atteints que les femmes (Weiss et al., 2012). Cette maladie induit des incapacités physiques associées à d'importantes douleurs, particulièrement pour les formes positives à l'allèle HLA–B27. Un âge élevé lors du diagnostic est également lié à un mauvais pronostic.

-L'**AJI systémique** est une arthrite qui touche une ou plusieurs articulations. Elle est associée à une fièvre d'au moins 3 jours consécutives, qui peut durer 2 semaines ou plus. Ces symptômes peuvent être accompagnés d'éruption érythémateuse, de gonflement des ganglions lymphatiques, d'hépatomégalie et/ou splénomégalie et/ou de sérite (Petty et al., 2004). De plus, cette forme d'AJI présente des atteintes au niveau des organes pouvant affecter le pronostic vital du patient (Vannucci et al., 2013). L'AJI systémique représente environ 5 à 15 % des cas d'AJI. Ce sous–type présente des différences importantes par rapport aux autres formes d'AJI autant au niveau de la pathogenèse, du profil clinique qu'au niveau des choix de traitement. Cette forme d'AJI est catégorisée comme une maladie auto–inflammatoire avec des taux importants de cytokines pro-inflammatoires telles que l'IL–1 et l'IL–6 (Prakken et al., 2011).

- **L'AJI non différenciée** inclut les cas qui ne rentrent pas dans les autres sous–types d'AJI ou qui répondent aux critères de plusieurs catégories (Petty et al., 2004). Cette forme d'AJI représente environ 15% des enfants atteints AJI.

B. Le système immunitaire dans l'AJI

L'AJI est une maladie complexe qui est principalement la conséquence de dérèglements liés à la régulation de la réponse immunitaire. Les études physiopathologiques ont montré le rôle central des cellules de l'immunité adaptative et innée dans l'AJI (Macaubas et al., 2009).

-**Les monocytes** : une augmentation du nombre de monocytes intermédiaires dans le sang de patients atteints de maladies auto–immunes comparé au sang de donneurs sains. Parmi ces maladies, on peut citer le lupus et des cas d'AJI liée à l'enthèse (Gaur et al., 2017; Smiljanovic et al., 2018). L'étude du profil cytokinique des monocytes issus de sang de patients atteints d'AJI oligoarticulaire, polyarticullaire ou systémique révèle une augmentation des concentrations des cytokines l'IL–1, l'IL–1Ra, l'IL–6 et l'IL–18 par rapport à des monocytes de sang de donneurs sains (Lotito et al., 2007). Les concentrations d'IL–6 et d'IL–18 sont plus élevées dans l'AJI systémique par rapport aux autres formes d'arthrite. De plus, des niveaux plus importants de TNFα ont été détectés dans le sérum d'enfants atteints d'AJI polyarticulaire par rapport aux individus sains (Mangge et al., 1995). L'ensemble de ces cytokines pro-inflammatoires libérées entretient l'inflammation en activant et recrutant d'autres cellules immunitaires qui vont sécréter à leur tour davantage de médiateurs de l'inflammation.

-Les **cellules dendritiques** jouent également un rôle dans la physiopathologie de l'AJI. Une accumulation des différents sous–types de DCs au niveau des articulations a été observée chez des patients atteints d'AJI systémique, oligoarticulaire et polyarticulaire (Smolewska et al., 2008) alors que leur nombre diminue dans la circulation en comparaison à des individus sains. Tout comme pour la PR chez l'adulte, les DCs semblent être recrutées depuis le sang vers les articulations via l'action de chimiokines telles que CXCL–10, CXCL–11 et CXCL–12 (Lande et al., 2004). Des études ont montré une expression plus élevée des récepteurs HLA–DR au niveau des articulations de patients AJI par rapport aux contrôles (Tabarkiewicz et al., 2011). Les concentrations importantes de DCs activées dans le liquide synovial des patients AJI sont associées à des taux de cytokines pro–inflammatoires plus élevés, dont le TNFα et l'IFNα (Gattorno et al., 2007).

-Les **lymphocytes T** activés sont présents en grandes quantités dans les articulations touchées et la circulation des patients atteints d'AJI par rapport au sang de donneurs sains (Macaubas et al., 2009, 2009; Murray et al., 1996). Des chimiokines comme le CCL21 sont retrouvées en grande quantité dans le liquide synovial de ces patients (Gattorno et al., 2005). Les articulations sont enrichies en Th17, cellules productrices d'IL–17 pouvant induire la production d'IL–6, IL–8 et de MMP–1 et 3 qui sont des protéines exerçant une action destructrice sur les structures articulaires (Agarwal et al., 2008; Nistala et al., 2008). Des données ont montré une auto–réactivité importante des cellules T, dirigée notamment contre des protéines articulaires comme les aggréganes et la fibrilline (Kamphuis et al., 2006). Plusieurs protéines de type HSP représentent également de potentiels autoantigènes, tel que HSP60 qui induit une activation des T circulants de patients AJI et non de T contrôles (Sedlackova et al., 2006).

Peu d'études ont été réalisées sur les **lymphocytes B**. Cependant une étude récente a montré que les niveaux de cellules B $CD24^{hi}CD38^{hi}$ étaient plus faibles dans le sang et les articulations des patients atteints d'AJI par rapport aux donneurs sains (Zhao and Jung, 2018). Ces concentrations de cellules B régulatrices seraient associée à un faible taux d'IL–10, une cytokine anti-inflammatoire, et ainsi à l'incapacité d'inhiber la réaction inflammatoire.

C. Traitements

- Les **anti-inflammatoires non stéroïdiens** (NSAID), administrable par voie orale, sont utilisés pour l'ensemble des formes d'AJI. Il s'agit généralement du tout premier traitement que

les enfants atteints d'AJI reçoivent. Les NSAID ont des propriétés analgésiques et anti−inflammatoires par le biais de l'inhibition des cyclooxygénases (COX)−1 et −2, qui bloquent la production des prostaglandines (Beukelman et al., 2011). Le naproxène, le méloxicam, l'ibuprofène et l'indométacine sont les NSAID les plus courants. Des complications gastrointestinales peuvent être associées à ces traitements.

- Les **glucocorticoïdes** stéroidiens, administrable par voie locale, peuvent être utilisés en association avec les NSAID pour augmenter les chances de rémission. Des injections intra−articulaires de glucocorticoïdes permettent d'éviter les contractures musculaires et des malformations telles que le valgus du genou. Le triamcinolone hexacetonide est un des traitements les plus utilisés car plus efficace que d'autres stéroïdes sur du long terme (Zulian et al., 2004). Un des effets secondaires les plus marquants est l'atrophie sous−cutanée ou cutanée, ou une décoloration de la peau. Les patients qui ne répondent pas aux injections intra−articulaires reçoivent des glucocorticoïdes de façon systémique. Ces traitements sont administrés sur une longue période et induisent d'effets secondaires importants. Ils ne peuvent pas être associés aux NSAID. Un traitement en systémique des glucocorticoïdes sur du très long terme peut provoquer une réduction de la croissance, une ostéoporose, des troubles d'humeur, une cataracte, une hypertension ainsi que des effets métaboliques (Harris et al., 2013). En raison de ces graves effets secondaires, ces traitements systémiques sont principalement utilisés pour les d'AJI systémique, maladie nécessitant des traitements agressifs, ou encore pour des enfants atteints d'AJI polyarticulaire.

-Les **Médicaments antirhumatismaux non biologiques** (DMARD : Disease-modifying antirheumatic drugs) sont utilisés comme traitement de deuxième intention. Le plus connus est le méthotrexate qui est recommandé pour les formes d'arthrites persistantes. Il est assez bien toléré avec une efficacité au bout de 1 à 3 mois de traitement (Ruperto et al., 2004). Le méthotrexate est un analogue de l'acide folique qui inhibe l'action de la dihydrofalate réductase. Cette dernière réduit la synthèse des purines et la production d'acide désoxyribonucléique (ADN). De plus elle augmente le taux d'adénosine ce qui induit un processus anti−inflammatoire indirect en bloquant la division cellulaire (Harris et al., 2013). Le méthotrexate est très utilisé en cancérologie et pour le traitement des maladies auto-immunes. Ses effets secondaires notables sont des nausées, des douleurs abdominales, des plaies dans la bouche ou encore une toxicité hépatique. Du fait de son action immunosuppressive, ce traitement peut induire une augmentation des risques d'infection (Ravelli et al., 1999). Le

léflunomide est un autre DMARD non biologique utilisé en cas de non-réponse au méthotrexate qui inhibe la synthèse de pyrimidine, diminuant ainsi la prolifération lymphocytaire (Giancane et al., 2016).

-Les **DMARD biologiques** sont utilisés dès lors que les patients ne tolèrent pas ou ne répondent pas aux traitements antirhumatismaux conventionnels. Les DMARD biologiques utilisés dans le cadre de l'AJI sont des biothérapies, principalement des anticorps ciblant des cytokines ou les récepteurs. Parmi eux, les inhibiteurs du récepteur du TNF, comme l'étanercept. Le TNF–α est une cytokine pro–inflammatoire à action pléiotropique, dont l'implication est décrite dans de nombreuses maladies autoimmunes (Alonso-Ruiz et al., 2008; Shenoi and Wallace, 2010). Les inhibiteurs de TNF sont généralement utilisés en deuxième voire troisième intention, dans le cas où le traitement avec le méthotrexate ne permet pas de réduire les signes cliniques, et après une persistance de plus de 3 mois de ces manifestations articulaires. Le traitement par les anti–TNF compte de nombreux effets secondaires liés à leurs propriétés immunosuppressives : risque d'infection, de vascularite leucocytoclasique, de maladie démyélinisante et de lupus (Harris et al., 2013). D'autres biothérapies sont utilisées dans l'AJI tel que les inhibiteurs du récepteur de l'IL–1 comme l'anakinra, les inhibiteurs de l'IL–1β comme le canakinumab, ou encore les inhibiteurs du récepteur de l'IL–6 comme le tocilizumab.

2. Le lupus érythémateux disséminé

A. Définition, classification

Le Lupus Erythémateux Disséminé ou systémique (LES) est une maladie auto-immune, inflammatoire et chronique qui affecte la peau, les articulations, les reins, les poumons, le système nerveux, les séreuses et/ou d'autres organes. Cette affection multi-système conduit à des expressions cliniques différentes d'un sujet à un autre avec comme point commun
Des poussées entrecoupées par des périodes de rémission. La cause du LES est encore inconnue, mais cette pathologi est caractérisée par un déséquilibre du syst immunitaire, provoquant une production d'auto-anticorps dirigés contre l'ADN natif (Hung et al., 2011; Li et al., 2015). Cela a pour conséquence des phases alternés de poussées plus ou moins sévères voire invalidantes, puis de rémissions. Le LES touche 9 femmes pour 1 homme. Les traitements médicamenteux actuellement empêchent l'apparitiondes poussées et de leurs complications, augmentant ainsi l'espérance de vie des patients.

Le diagnostic repose sur un ensemble d'arguments clinico-biologiques. Les manifestations cliniques et biologiques ont permis d'établir des critères conçus pour la classification des patients proposés par l'ACR (the American College of Rheumatology) (Aringer et al., 2019). Ces critères sont souvent utilisés pour le diagnostic. La présence d'au moins 10 critères parmi les 21 critères proposés permettent le diagnostic de LED avec une sensibilité de 96% et une spécificité de 93%.

- Fièvre
- Leucopénie
- Thrombopénie
- Hémolyse d'origine auto-immune
- Délire
- Psychose
- Convulsion
- Alopécie non cicatricielle
- Erosion buccale
- Lésions cutanées de lupus discoïde ou subaigu
- Lésions cutanées de lupus aigu
- Epanchement pleural ou péricardique
- Péricardite aigue
- Atteinte articulaire
- Protéinurie > 0,5 g/24h
- Glomérulonéphrite lupique de classe II ou V
- Glomérulonéphrite lupique de classe III ou IV
- Anticardiolipine ou anti-beta2GP1 ou anticoagulant circulant
- C3 OU C4 bas
- C3 ET C4 bas
- Anti-ADNnatif ou anti-Sm

B. Le système immunitaire dans le LES

Dans le LES, l'interaction entre des prédispositions génétiques et les facteurs environnementaux est responsable d'une activation aberrante des cellules du système

immunitaire inné et adaptatif. La caractéristique majeure de cette dérégulation est la perte de tolérance face aux antigènes nucléaires du soi, aboutissant à la production d'auto-anticorps dits ANA (Anti-nuclear antibody). On peut ainsi distinguer les anti-dsDNA (anti-double stranded DNA), et les anticorps anti-antigènes nucléaires solubles : anti-Sm (anti-Smith), anti-RNP (anti-ribonucleoprotein), anti-SSA/Ro (anti-Sjögren syndrom A), Anti-SSB/La (anti-Sjögren syndrom B). De plus, un rôle important a été décrit pour les interférons de type I (IFN-I), principalement l'IFN-α dans la pathogenèse du SLE.

Le lien entre LES et IFN a était fait pour la première fois en 197 suite à la découverte de taux élevés d'IFN, dans le sérum de patients LES (Hooks et al., 1979). A ce moment-là, l'IFNγ été incriminé dans le LES C'est en 1982 que cet IFN a été identifié comme étant l'IFNα (Ytterberg and Schnitzer, 1982). Depuis, plusieurs études ont montréque le concentrations d'IFN-αsont directement corrélées à l'activité de la maladie (Bengtsson et al., 2000). Des taux élevés de la 2'-5' oligoadenylate synthetase et la MxA, ont également été trouvés chez la plupart des patients LES (Preble et al., 1983; von Wussow et al., 1989). Ces dernières sont directement induites par l'IFN-α, ce qui démontre bien son rôle central dans cette pathologie.

Bien que la majorité des cellules soient capables de produire de l'IFNαen petite quantité, les principales productrices de ces IFN--α sont le pDC. L'IFNα va par la suite activer les récepteurs de l'IFN (Interferon-a/b receptor – IFNAR) exprimés de façon ubiquitaire. L'activation de cette voie induit la production d'Interferon Stimulated Genes (ISGs) qui sont responsables du phénotype inflammatoire observé chez les patients LES. Chez les patients LES, un nombre élevé de pDC est retrouvé au niveau des ganglions lymphatiques (Rönnblom and Alm, 2002), de la peau (Farkas et al., 2001) et du tissu rénal (Tucci et al., 2008). En parallèle, leur nombre diminue dans le sang périphérique suggérant ainsi un recrutement des pDC circulantes vers les tissus suite à leur activation (Cederblad et al., 1998).

L'IFN-α produit en excès dans le LES occupe une place centrale dans le développement de la maladie à travers l'activation du système immunitair inn et adaptatif. Cette production excessive d'IFN-α induit plusieurs effets sur les différents types cellulaires du système immunitaire.

Au niveau des **monocytes**, l'IFN-α induit leurs différenciations en cellules myeloides (mDC) (Blanco et al., 2001)

Au niveau des **mDC**, l'IFN-α induit :
- une augmentation de l'expression de molécules du CMH-II (complexe majeur d'histocompatibilité), des molécules de co-stimulation CD80 et CD86 et de la molécule de maturation CD83 (Kirou et al., 2007)
- une augmentation de la survie
- la différenciation des lymphocytes T CD8+ cytotoxiques effecteurs (Blanco et al., 2005)
- la production des cytokines BAFF (B-cell activating factor) et APRIL (a proliferation inducing ligand) favorisant la survie des lymphocytes B, leur différenciation en plasmocytes et le changement isotypique des IgM en IgG.

Au niveau des cellules **Natural Killer**, l'IFN-α induit l'augmentation de la cytotoxicité via l'expression du FasL (Fas ligand) aboutissant à une élévation du taux d'apoptose et le relargage d'auto-antigènes (Kirou et al., 2000).

Au niveau des **lymphocytes B**, l'IFN-α induit une augmentation de leur survie et de la différentiation des LB auto-réactifs favorisant la production d'auto-anticorps (Kirou et al., 2007; Le Bon et al., 2006)

Au niveau des **lymphocytes T CD4**, l'IFN-α induit l'orientation de la réponse immune vers la voie Th1 et la stimulation de la génération de LTfh (LT-follicular helper) impliqués dans l'activation des LB et la production d'anticorps (Cucak et al., 2009).

Au niveau des **lymphocytes T régulateurs**, l'IFNα induit l'altération des fonctions immuno-suppressives des LTreg favorisant une dérégulation de la réponse inflammatoire et ledéveloppement des réponses auto-réactives (Yan et al., 2008).

Au niveau des **lymphocytes T CD8**, l'IFN-α induit l'augmentation de la cytotoxicité via l'expression de la perforine et du granzyme B favorisant le relargage de nucléosomes solubles et d'auto-antigènes (Blanco et al., 2005)

C. Traitements

Même si aujourd'hui, on ne guérit pas définitivement d'un lupus, les traitements existants soignent poussées et complications, et préviennent leur apparition.

- Les **Anti-inflammatoires non stéroïdiens** (AINS) tels que l'ibuprofène, peuvent être utilisés pour traiter la douleur, les gonflements et la fièvre associés au lupus. Des AINS plus puissants sont disponibles sur ordonnance. Les effets secondaires des AINS peuvent inclure des saignements d'estomac, des problèmes rénaux et un risque accru de problèmes cardiaques.

-**Médicaments antipaludéens** couramment utilisés pour traiter le paludisme, comme l'hydroxychloroquine (Plaquenil), affectent le système immunitaire et peuvent contribuer à diminuer le risque de poussées de lupus. Les effets secondaires peuvent inclure des maux d'estomac et, plus rarement, des lésions de la rétine de l'œil. Des examens réguliers de la vue sont recommandés lors de la prise de ces médicaments.

- Les **corticostéroïdes** comme la prednisone et d'autres types de corticostéroïdes peuvent contrer l'inflammation du lupus. De fortes doses de stéroïdes, comme le méthylprednisolone, sont souvent utilisées pour contrôler des formes graves qui touchent les reins et le cerveau. Les effets secondaires comprennent la prise de poids, les ecchymoses faciles, l'amincissement des os, l'hypertension artérielle, le diabète et un risque accru d'infection.

- Les autres **immunosuppresseurs** peuvent être utiles dans les formes graves du lupus. Par exemple l'azathioprine, le mycophénolate, le méthotrexate, la cyclosporine et le léflunomide. Les effets secondaires potentiels peuvent inclure un risque accru d'infection, des lésions hépatiques, une diminution de la fertilité et un risque accru de cancer

- Les **biothérapies** comme le bélimumab (anti-BAFF) est administré par voie intraveineuse, peuvent réduit les symptômes du lupus chez certaines personnes. Les effets secondaires comprennent les nausées, la diarrhée et les infections. Dans de rares cas, une aggravation de la dépression peut survenir. Le rituximab (anti-CD20) peut être bénéfique pour certains patients chez qui les autres médicaments n'ont pas marché.

III. CXCR4 : nouvelle cible thérapeutique pour des maladies auto-immunes et inflammatoires

Précédemment, l'équipe du CBMIT dans laquelle j'ai réalisé mes travaux de thèse a découvert que la liaison de petits composés aminés naturels et synthétiques au récepteur de chimiokine CXCR4 entraîne une inhibition de l'activation des pDC humaines (Smith et al., 2017). L'équipe a ainsi pu démontrer qu'un ligand de la poche mineure de CXCR4, le composé IT1t, a une forte activité immunosuppressive sur les pDCs activées par TLR7, ce qui en fait une cible thérapeutique pour le traitement du LES (Smith et al., 2019). Cette partie est donc consacrée à la caractérisation du récepteur CXCR4 et à son rôle immunosuppresseur dans les pDC.

1. Rôle de CXCR4 dans l'immunité

A. Généralité

Le récepteur CXCR4 a été découvert en 1996 en tant que cofacteur permettant la fusion du virus de l'immunodéficience humaine de type 1 (VIH-1) avec ses cellules cibles (Berger et al., 1999). Il s'agit d'un récepteur membranaire appartenant à la famille des récepteurs transmembranaires couplés aux protéines G (RCPG) qui possèdent 7 domaines. L'identification du ligand de CXCR4, la chimiokine CXCL12 (SDF1), a permis de classer le récepteur CXCR4 parmi les récepteurs de chimiokines (Deng et al., 1996; Oberlin et al., 1996). Les chimiokines sont responsables de la migration cellulaire, et plus particulièrement la migration des leucocytes, vers les tissus cibles. Elles interviennent également dans l'inflammation et la maturation du système immunitaire. On compte aujourd'hui 19 chimiokines et une cinquantaine de ligands a été décrit (Murphy et al., 2000). Le récepteur CXCR4 est exprimé très tôt durant le développement embryonnaire. La suppression du gène de CXCR4 dans des modèles murins mène à la mort périnatale des souriceaux causés par de multiples défauts d'organogenèse au niveau cérébral, cardiaque, vasculaire et immunitaire (Murphy et al., 2000).

CXCR4 possède sept domaines transmembranaires qui sont liés à une protéine G existant sous forme d'hétérotrimère (Gα, Gβ, and Gγ) (fig. 10). La transduction du signal par un RCPG se produit lorsqu'une molécule de signalisation extracellulaire active le récepteur au niveau de la surface cellulaire. Cela induit un changement de conformation qui conduit à la dissociation de l'hétérotrimère. Cette dissociation expose des sites des sous-unités qui peuvent interagir avec d'autres molécules. Le mécanisme particulier de l'interaction SDF-1-CXCR4 a été bien caractérisé.

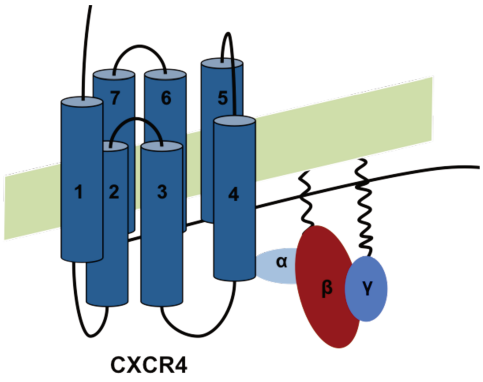

Figure 10: Chemokine receptor CXCR4
(Liang, 2008)

CXCR4 est exprimé dans les tissus hématopoïétiques mais également au niveau des tussus du poumon, du cœur et du cerveau. CXCR4 est exprimé par un spectre de cellules hématopoïétiques qui comprend les neutrophiles, les monocytes, les lymphocytes B et T, les macrophages et les cellules dendritiques. De nombreux types cellulaires exprimant CXCR4 ont été identifiés au niveau des sites stratégiques de passage de VIH : les muqueuses génitales et digestives, les glandes salivaires, le placenta et le SNC (système nerveux central). Le récepteur CXCR4 est également exprimé sur les cellules dendritiques immatures, les progéniteurs des cellules B de la moelle osseuse et le cerveau embryonnaire.

B. Interaction CXCR4-CXCL12

L'activation de CXCR4 par le SDF-1 peut conduire à différentes voies de signalisation en aval qui entraînent une variété de réponses physiologiques, telles que le chimiotactisme, la survie et la prolifération cellulaire, le flux calcique intracellulaire et la transcription des gènes (Ganju et al., 1998). Le terme « sélectivité fonctionnelle » décrit le fait que certains ligands activent pleinement une partie de ces voies de signalisation et n'ont aucun effet sur d'autres. Cela suggère qu'il n'existerait pas qu'une seule conformation pleinement active du récepteur. Différentes conformations de récepteur transmettraient ainsi différentes activités. La figure 10 représent les principales voies de signalisation qui peuvent être impliquées dans la transduction du signal CXCR4 (Teicher and Fricker, 2010).

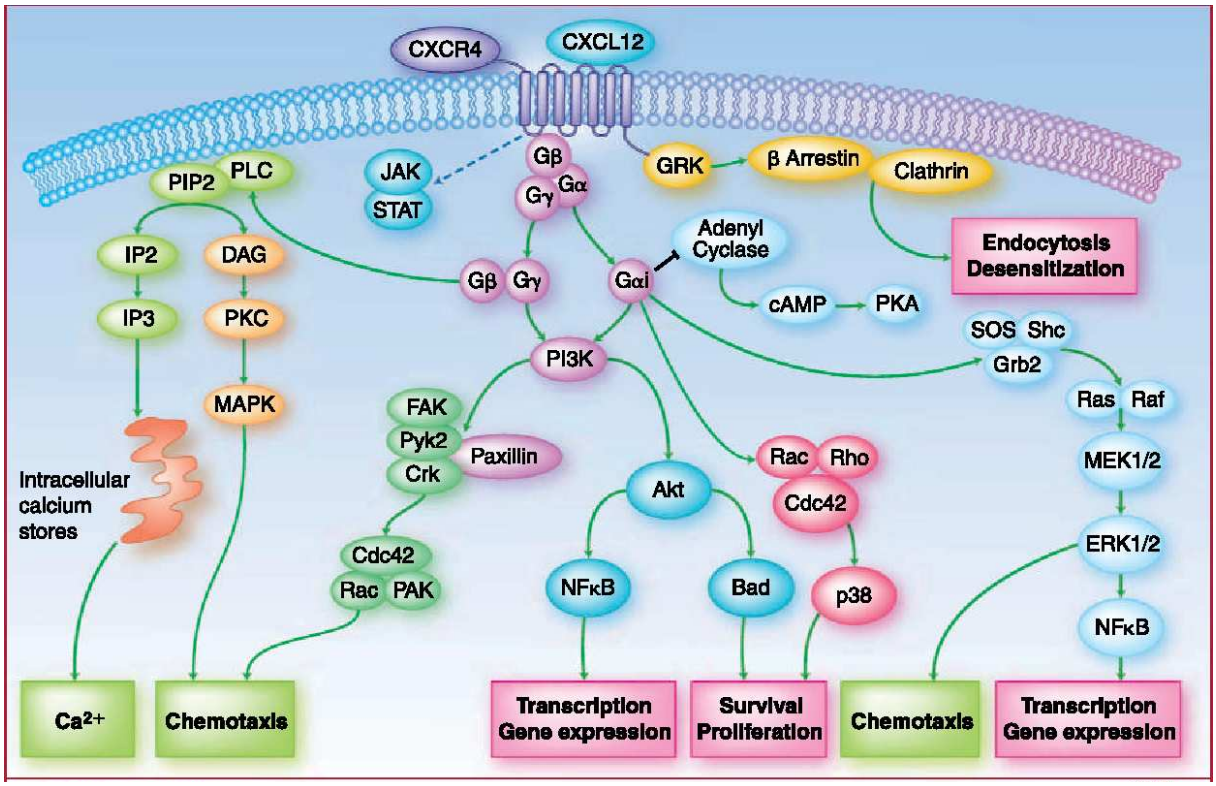

Figure 11: voies de la signalisation intracellulaire du couple SDF-1/CXCR4
(Teicher and Fricker 2010)

C. Physiopathologie associé à CXCR4

Chez l'homme, des mutations de CXCR4 ont été identifiés comme induisant une hyper-activation de l'axe SDF-1/CXCR4. Ces mutations sont associées à une neutropénie avec myélokathexis : c'est le syndrome de WHIM (Warts Hypogammaglobulinemia Infections and Myelokathexis) (Gulino et al., 2004; Rimaniol et al., 2003). Cette neutropénie est caractérisée par une rétention anormale de neutrophiles matures dans la moelle osseuse (Hernandez et al., 2003). De plus, l'expression de CXCR4 sur des cellules cancéreuses permet leur migration vers des sites distants de la tumeur primaire, où elles forment des métastases. Cela concerne en particulier la formation de métastases dans la moelle osseuse, les poumons et le foie, qui sont les sites les plus importants de production de CXCL12 (Murphy, 2001). Il a été mis également en évidence que la production de CXCL12 dans la moelle osseuse est responsable de la domiciliation et de la rétention de cellules souches qui assurent le développement et le renouvellement du système hématopoïétique (Lapidot, 2001). De plus, l'inhibition pharmacologique de CXCR4 dans des modèles de maladies inflammatoires, tels que l'asthme et l'arthrite rhumatoïde, entraîne une amélioration symptomatique, suggérant l'implication de

CXCR4 dans la migration des leucocytes effecteurs comme les neutrophiles et les cellules T vers le site affecté.

CXCR4 a été détecté dans 23 différents types de cancer, y compris la leucémie, le cancer du sein, le cancer d'ovaire et récemment détecté dans le cancer de la prostate (Furusato et al., 2010)

D. Antagoniste de CXCR4

L'importance de CXCR4 dans de nombreuses maladies a favorisé le développement de molécules antagonistes de CXCR4. Ainsi la première molécule antagoniste qui a été développée est l'AMD3100 (Plerixafor ou Mozobil) (De Clercq, 2015) (Fig. 12), une molécule composée de deux squelettes cyclam connectés avec un lien restrictif.

L'AMD3100 est un inhibiteur de CXCR4 : il bloque uniquement la voie de signalisation de CXCR4 et empêche la fixation de CXCL12 (Hatse et al., 2002). Broxmeyer et al., sont les premiers à avoir montré que l'AMD3100 a la capacité de mobiliser les cellules souches hématopoïétiques (HSC) et les cellules progénitrices (Broxmeyer et al., 2005).

En effet, CXCR4 est normalement le récepteur de CXCL12. Ce dernier est responsable du maintien des HSC dans la moelle osseuse. En présence de l'AMD3100, CXCL12 ne peut plus se fixer à CXCR4 et les HSC ne sont plus retenues dans la moelle osseuse. Elles peuvent alors migrer en direction d'autres chimiokines et entrer dans la circulation périphérique. L'AMD3100 permet de récupérer un grand nombre de HSC initialement retenue dans la moelle osseuse, technique utilisée dans les transplantations et autogreffes.

Cependant, les applications cliniques de l'AMD3100 et de ses dérivées sont limitées en raison de leur manque de biodisponibilité orale, liée à leur charge positive élevée. Afin d'améliorer l'absorption orale, des composés analogues tels que des dérivés de monocyclame (AMD3465, AMD3529) ont été développés (Lam et al., 2011). Plus récemment, une nouvelle série d'analogues hétérocycliques a été mise au point, contenant différents motifs telles que l'imidazole, le benzimidazole, la pyridine ou la guanidine (AMD11070, KRH1636, GSK812397) (Choi et al., 2012). Parmi eux, AMD11070 est la première petite molécule CXCR4 biodisponible par voie orale.

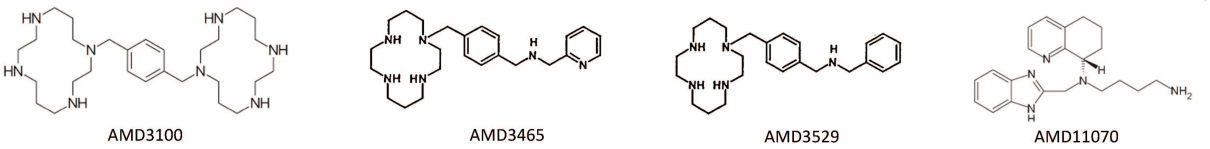

Figure 12: Antagonistes de CXCR4

2. Nouvelle propriété de CXCR4

Récemment, les dernières études de l'équipe ont permis de découvrir une nouvelle fonction biologique de CXCR4 (Smith et al., 2017). En effet, la liaison des monoamines à une région spécifique (poche mineure) de CXCR4 entraîne un puissant signal anti-IFN-I sur des pDCs activées par les récepteurs de type Toll (TLR). Cette poche agoniste est située plus profondément dans le domaine extracellulaire de CXCR4 que la poche antagoniste ciblée par l'AMD3100 (Plerixafor), même si ces deux poches partagent certains acides aminés communs (Fig.13). Plusieurs agonistes à poche mineure de CXCR4 ont été identifié tels que l'IT1t. Le potentiel thérapeutique de cette molécule anti-IFN a été testé dans le lupus érythémateux systémique (LES), une maladie auto-immune complexe caractérisée par la production d'auto-anticorps pathogènes, la production chronique d'IFN-I et l'inflammation. L'IT1t contrôle la sécrétion d'IFN-I dans les pDCs primaires activées par TLR-7, et réduit drastiquement la progression de la maladie dans un modèle de souris lupique induit par le pristane. De plus l'IT1t inhibe la production spontanée d'IFN-I à partir des cellules de patients atteints de lupus (Smith et al., 2019). De manière intéressante, l'IT1t a également présenté une activité anti-inflammatoire en réduisant de manière significative la production d'IL1, d'IL-17 et de TRAIL chez des souris atteintes de lupus (Smith et al., 2019, 2017). A noter que le traitement par l'IT1t chez les souris atteintes de lupus a entraîné une réduction significative des anticorps anti-ADNdn circulants (Smith et al., 2019), ce qui suggère un effet sur l'immunité adaptative. D'autres composés aminés sont également capables de se loger dans la poche mineure de CXCR4 tels que l'histamine, et son analogue synthétique : le clobenpropit (Smith et al., 2017). Ce dernier a initialement été développé comme antagoniste des récepteurs de l'histamine H3.

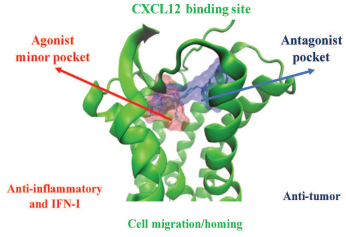

Figure 13: Modélisation in silico de CXCR4. Représentation des sites de liaison de CXCR4 et des propriétés biologiques des agonistes des poches mineures (IT1t), de l'antagoniste AMD3100 et du CXCL12.

Chapitre 2 : Projet de thèse et résultats

Projet de thèse

Il a récemment été mis en évidence que de petits composés aminés pouvaient se fixer au niveau de la poche mineure de CXCR4 est induire une réponse anti-IFN-I sur des pDC activés par des virus (grippe, HIV), par des agonistes synthétiques de TLR7, ou encore des pDC auto-inflammatoires issus de patients souffrant de LED. Plusieurs composés aminés : naturelle et synthétique ont été identifiés comme ayant une activité anti-IFN-I via leur engagement sur CXCR4 : l'histamine, le clobenprobite (CB) ou encore l'IT1t. L'objective de mes travaux de thèse est de mieux caractériser les effets de ces différents composés sur les cellules du système immunitaire, notamment en étudiant leurs effets dans différents contextes inflammatoires, tout en étudiant une multitude de facteurs inflammatoires en plus des intéreférons. Un autre objectif de ma thèse était d'identifier de nouveaux composés capables de se fixer au niveau de la poche mineure de CXCR4 avec une meilleure affinité et une meilleure activité anti-IFN que les composés de référence IT1t et CB.

Partie I : réduction de l'inflammation dans l'arthrite juvénile avec un analogue de l'histamine qui cible le récepteur CXCR4

Parmi les cellules immunitaires, les monocytes activés jouent un rôle néfaste dans les pathologies inflammatoires chroniques. L'activation incontrôlée des monocytes et la production excessive de facteurs inflammatoires endommagent les articulations, les os et le cartilage dans l'arthrite idiopathique juvénile (AJI), une maladie infantile de la polyarthrite rhumatoïde (PR). Notre objectif ici est d'étudier les effets des ligands de la poche mineure de CXCR4 sur l'activation des monocytes via le dosage d'une multitude de cytokines inflammatoires. Nous montrons ici que le ciblage de CXCR4 avec de petits composés aminés tels que l'analogue de l'histamine : le clobenpropit (CB), inhibe la production spontanée et induite d'un ensemble de cytokines inflammatoires par des monocytes isolés du sang et des fluides synoviaux de patients atteints d'AJI. De plus, le traitement quotidien intrapéritonéal par du CB chez des souris arthritiques entraîne une diminution significative des niveaux de cytokines inflammatoires circulantes, des infiltrats de cellules immunitaires, de l'érosion des articulations et de la résorption osseuse, ce qui réduit la progression de la maladie.

CB inhibe la production de TNF-α, IL-1β et IL-6 des monocytes activés par TLR-7/8

Afin d'évaluer les potentielles propriétés anti-inflammatoires de l'histamine et de l'analogue de l'histamine CB, la lignée cellulaire rapporteuse de THP-1-Dual a été utilisée. Cette lignée est un modèle de monocytes humain. Elle permet d'étudier la voie NF-κB en réponse à certains agonistes des TLRs. Lors de l'activation du TLR7/8 par le R848, le gène rapporteur SEAP (Secreted embryonic alkaline phosphatase) est induit par l'activation de la voie de signalisation NF-κB. Nous avons donc mesuré la production de SEAP par les cellules THP-1 activées avec le R848, en présence ou en l'absence de concentration croissante d'histamine (Fig. 14A) ou de CB (Fig. 14B) allant de 1 à 100 µM. Nous avons ainsi montré que le CB, et dans une moindre mesure l'histamine, réduisait de manière dose-dépendante l'activation de NF-κB dans les cellules THP-1, sans toxicité. De plus, le traitement avec le CB (20 µM) a empêché la transcription des gènes codant pour le TNF-α, l'IL-1β et l'IL-6 dans les cellules THP-1 activées par le R848 (Fig. 14C).

Afin d'étendre nos résultats obtenus avec la lignée cellulaire THP-1, nous avons ensuite testé la capacité du CB à contrôler la production de cytokines dans des cellules mononuclées sanguines

humaines (PBMC) stimulées par le R848 et issues de donneurs sains (HD). Pour ce faire, nous avons dosé une multitude de cytokines (i.e. IL-1β, -6, -8, -10, TNF-α..), chimiokines (i.e. CCL2, CCL3, CCL4, CCL5...), facteurs de croissance et d'interférons (IFNα/β/γ) dans les surnageants des cultures cellulaires des PBMCs stimulées avec le R848 en présence ou en l'absence de CB à 20 μM (n=5) (Fig. 14D). Ces dosages ont été réalisés par luminex. Le CB a inhibé la production de chimiokines, de facteurs de croissance, de sous-types d'IFN et de toutes les cytokines pro-inflammatoires induites par le R848, y compris le TNF-α, l'IL-1β et l'IL-6 (Fig. 14D et 14E). L'analyse par cytométrie de masse (CyTOF) a révélé qu'au sein des PBMCs, les monocytes représentaient les principaux producteurs de TNF-α, IL-1β et IL-6 lors de la stimulation de TLR7/8 par le R848. Le traitement par CB a réduit de manière drastique la production de ces facteurs inflammatoires par les monocytes activés avec le R848 (Fig. 14F, G) (n=4). Pour mieux évaluer l'effet du CB sur les cytokines pro-inflammatoires, nous avons purifié des monocytes à partir du sang de donneurs sains (HD). Ces monocytes ont été traités avec du CB puis activés avec l'agoniste des TLR7/8. Un dosage multiplex à base de billes (Legendplex) au niveau des surnageants de culture (Fig. 14H) et le marquage intracellulaire du TNF-α et de l'IL-1β par cytométrie en flux, montrent que dans les monocytes purifiés de donneurs sains, le CB inhibe la production de TNF-α et d'IL-1β (avec respectivement des IC50 de 2,8 μM et 8 μM) sans toxicité observée (Fig. 14I).

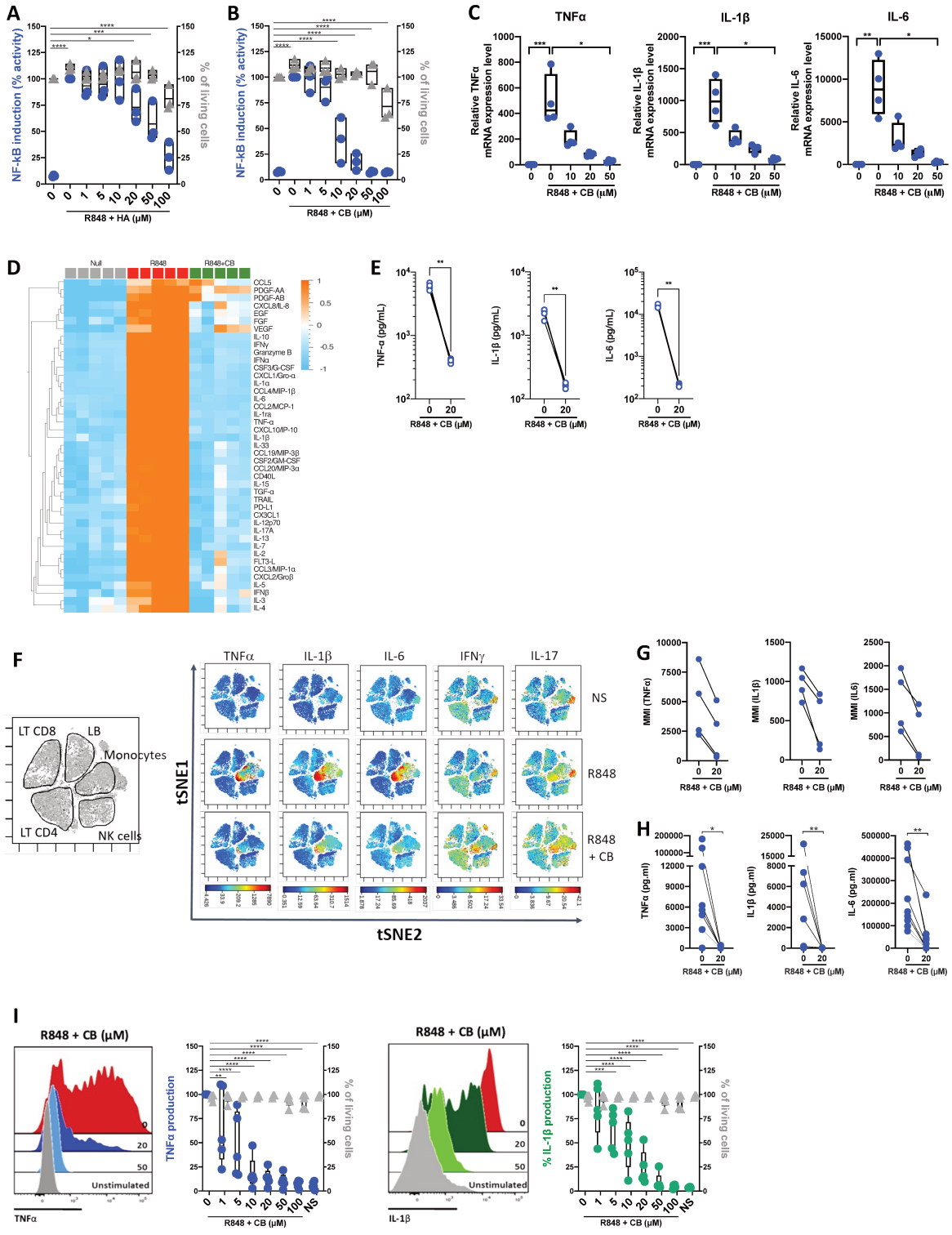

Figure 14: CB inhibe la production de TNF-α, IL-1β et IL-6 médiée par TLR-7/8 des monocytes humains. (**A-B**) Les cellules THP1-Dual rapporteuses de NF-κB ont été traités avec une concentration croissante d'Histamine (**A**) ou de CB (**B**) allant de 1 à 100 µM puis stimulées avec du R848 (5 µg/ml) pendant 24 heures. L'activité du rapporteur NF-κB a été mesurée en utilisant le QUANTI-Blue, un réactif de détection SEAP (bleu) ainsi que la viabilité cellulaire (gris). (**C**) Les niveaux d'ARNm de TNF-α, IL-1β et IL-6 de THP1-dual pré-incubés avec des doses croissantes de CB et stimulés pendant la nuit avec R848 (5 µg/ml), ont été mesurés par RT-qPCR et normalisés par rapport à RPL13A. Kruskal-Wallis avec test de comparaisons multiples de Dunn. (**D-G**) Les PBMC de donneurs sains (HD) ont été préincubés avec du CB (20 µM) puis stimulés avec du R848 (5 µg/mL) pendant la nuit. (**D-E**) La production de cytokines a été mesurée dans le surnageant à l'aide d'un système d'immunodosage multiplexé à base de billes Luminex. (**D**) Représentation sous forme de carte thermique des

cytokines statistiquement différentes (P<0,05) entre les différentes conditions (Null, R848, R848+CB), classées par regroupement hiérarchique. Les cytokines régulées vers le haut sont représentées en orange, et celles régulées vers le bas en bleu. Les valeurs P ont été déterminées par le test de Kruskal-Wallis. (**E**) Les cytokines du Luminex sont représentées de manière individuelles. Test de Mann-Whitney. (**F**) Les PBMCs ont été analysées par cytométrie de masse (CyTOF) et l'analyse tSNE a été réalisée en utilisant les marqueurs CD56, CD3, CD11c, BDCA4, CD14, HLADR, CD123, CD4, CD8 et CD19. Les niveaux intracellulaires de TNF-α, IL-1β, IL-6, IFNγ et IL-17 ont été évalués. (**G**) L'intensité métallique moyenne (MMI) du TNF-α, de l'IL-1β et de l'IL-6 a été évaluée sur la population de monocytes issus des quatre donneurs. (**H**) La production de cytokines a été mesurée dans les surnageants des monocytes purifiés de neuf donneurs sains (HD) à l'aide d'un dosage multiplex à base de billes : LEGENDplex. Test de Mann-Whitney. (**I**) Les monocytes purifiés de cinq donneurs sains (HD) ont été préincubés avec des doses croissantes de CB puis stimulés avec du R848 pendant 5 h. Les niveaux intracellulaires de TNF-α et IL-1β ainsi que la viabilité ont été évalué par cytométrie de flux. 2-way ANOVA. All data are presented as median ± écart-type. ****P < 0,0001, ***P < 0,001, **P < 0,01, *P < 0,05.

Le CB contrôle l'activation des monocytes via son engament sur le récepteur CXCR4

Nous avons ensuite vérifié si les propriétés anti-inflammatoires de CB dépendent de CXCR4. Nous avons d'abord utilisé l'antagoniste bien connu de CXCR4, AMD3100, pour moduler les effets anti-inflammatoires du CB sur les PBMC activées. Les cellules ont été cultivées avec des concentrations croissantes d'AMD3100 en présence de CB (20M), puis activé avec le R848 pendant 24h. Les surnageants ont été transférés sur les cellules rapporteuses THP1-Dual permettant la quantification simultanée de l'activité des promoteurs IRF et NF-κB. Nous avons ainsi montré que le CB réduit l'activation de l'IRF et du NF-κB et que l'AMD3100 bloque de manière dose dépendante l'activité anti-inflammatoire du CB (Fig. 15A-B).

Nous avons ensuite mesuré les productions de TNF-α, IL-1β et IL-6 par les monocytes primaires purifiés de donneurs sains et stimulés avec le R848 en présence de CB (20 μM) et de concentrations croissantes d'AMD3100 (jusqu'à 50 μM) en utilisant la cytométrie de flux. Comme prévu, l'AMD3100 a bloqué de manière dose-dépendante la capacité du CB à réduire les niveaux intracellulaires de TNF-α, IL-1β et IL-6 dans les monocytes, sans toxicité notable (Fig. 15C-D).

Pour établir fermement que l'activité immunorégulatrice du CB est liée à CXCR4, l'expression de CXCR4 a été réduite dans les monocytes primaires à l'aide d'un petit ARN interférent (siARN) ciblant l'ARN messager codant pour CXCR4. Alors que la transfection d'un siARN control (siControl) n'a pas eu d'impact sur l'inhibition de la production des cytokines pro-inflammatoires induite par CB, ce dernier a perdu sa capacité à inhiber les productions intracellulaires de TNF-α, IL-1 et IL-6 dans les monocytes humains traités avec le siARN ciblant CXCR4 (siCXCR4) (Fig. 15E-F). En tenant compte de l'efficacité de transfection de 95% dans les monocytes, nous avons vérifié que l'expression de CXCR4 était fortement réduite

dans les monocytes transfectés par le siARN CXCR4 par rapport à siControl (Fig. 15G-H). Ces données globales montrent que les effets immunorégulateurs de CB dépendent strictement de l'engagement de CXCR4.

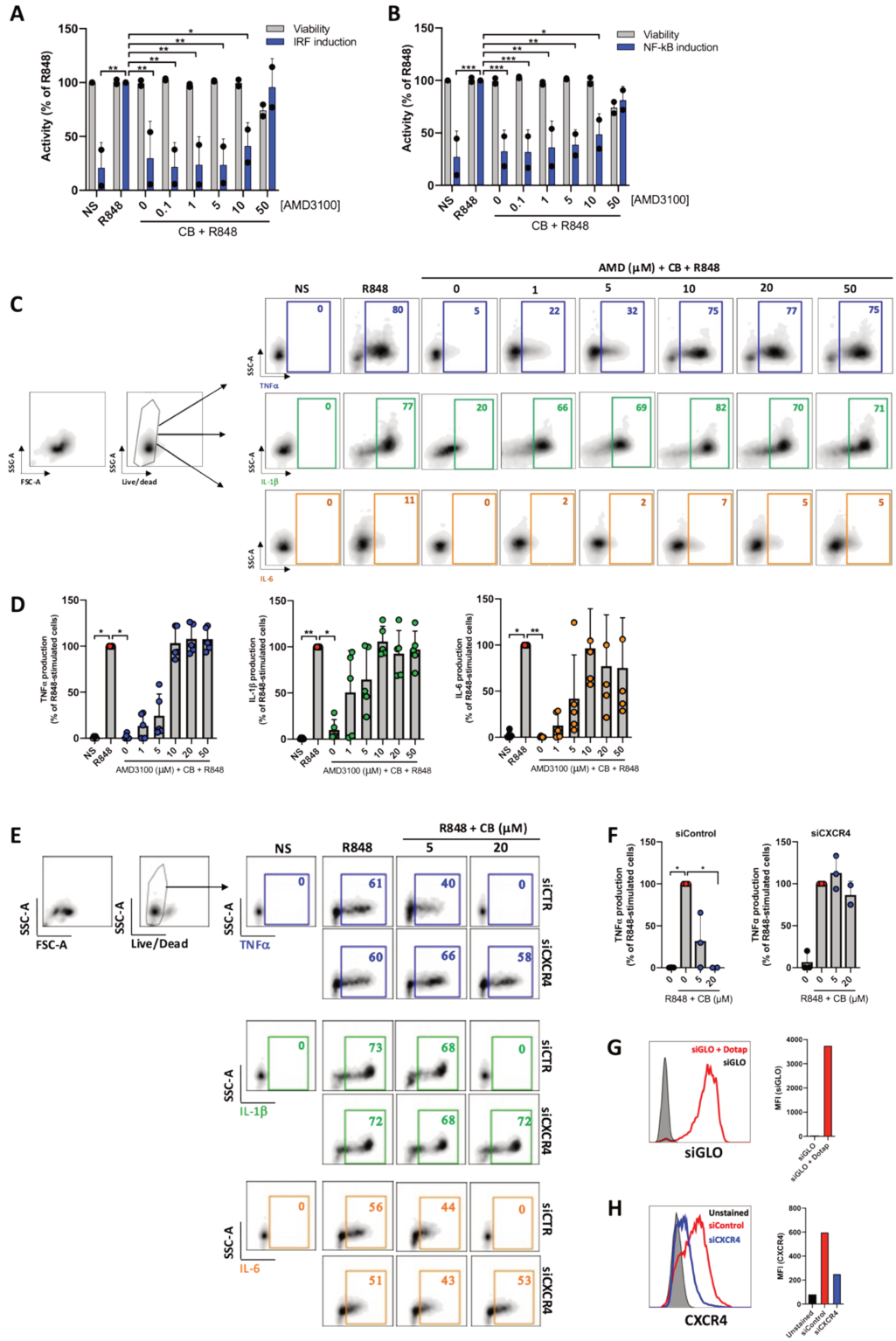

Figure 15: L'activité immunorégulatrice du CB sur les monocytes primaires est dépendant de CXCR4.

(**A**) et (**B**) Les PBMC de deux donneurs sains ont été mis en culture en présence de concentrations croissantes d'AMD3100, puis traités avec du CB (20 µM) et activés avec du R848 (5 µg/mL) pendant 24 heures. Le taux (**A**) d'interférons et (**B**) de cytokines inflammatoires dans les surnageants de culture a été mesuré à l'aide de la lignée

cellulaire rapporteur THP1-dual. 2-way ANOVA avec le test de comparaisons multiples de Dunnett. (**C**) et (**D**) Des monocytes isolés provenant de cinq donneurs sains ont été mis en culture en présence de concentrations croissantes d'AMD3100, puis traités par du CB (20 µM) et activés par du R848 (1 µg/mL) pendant 6 heures. Les niveaux intracellulaires de TNF-α, IL-1β et IL-6 ont été évalués par cytométrie de flux, (**C**) représentation en dot plot d'un donneur et (**D**) représentation en histogramme de 5 donneurs. Friedman avec test de comparaisons multiples de Dunn. (**E-F**) Les monocytes ont été traités pendant 24 heures avec le siRNA CXCR4 (siCXCR4) ou le siRNA contrôle (siControl) à 160 nM. Les cellules ont ensuite été pré-incubées avec du CB (20 µM) et stimulées avec du R848 (1µg/mL) pendant 6 heures. Les niveaux intracellulaires de TNF-α, IL-1β et IL-6 ont été évalués par cytométrie en flux : (**E**) représentation en dot plot d'un donneur et (**F**) représentation en histogramme de 3 donneurs. Les données sont représentées par la médiane +/- écart-type. Krustal-Wallis avec le test de comparaisons multiples de Dunn. (**G**) l'efficacité de la transfection avec le dotap sur les monocytes a été évaluée avec le siRNA GLO en cytométrie de flux. (**H**) L'expression de CXCR4 sur les monocytes traités avec le siControl et le siCXCR4 a été évaluée par cytométrie en flux. **P < 0,01, *P < 0,05. NS, non stimulé.

Le CB inhibe la production spontanée de cytokines pro-inflammatoires dans les monocytes de patients atteints d'AJI

Nous avons ensuite étudié la capacité du CB à exercer un effet anti-inflammatoire sur des cellules immunitaires isolées de patients atteints d'AJI. L'inflammation spontanée est une caractéristique bien connue de l'AJI. Alors que des niveaux élevés d'IL-6 sont facilement mesurables dans le plasma des patients atteints de PR (Gualtierotti et al., 2016), la détection du TNF-α circulant chez ces patients reste un défi. Ainsi, pour capturer le TNF-α dans le plasma, nous avons développé un ELISA digital du TNF-α (Simoa) qui détecte de faible concentration de TNF-α, de l'odre de 1 fg/mL. Grâce à cette technologie, nous avons pu détecter du TNF-α dans le plasma des patients et trouvé une concentration plus élevée de TNF-α dans le plasma sanguin des patients atteints d'AJI que dans celui des donneurs sains (HD) (médiane des patients atteints d'AJI = 3,4 pg/mL contre médiane des HD = 1,07 pg/mL) (Fig. 16A). Afin de mieux détecter l'inflammation spontanée chez les patients atteints d'AJI, nous avons réalisé un tableau d'expression génique de 579 marqueurs inflammatoires sur des monocytes purifiés de PBMC provenant de donneurs sains (HD) et de patients atteints d'AJI. Par rapport aux HD, l'expression de 51 gènes inflammatoires a significativement augmenté et 16 ont diminué chez les patients atteints d'AJI (Fig. 16B). L'analyse en composantes principales (ACP) a montré que les monocytes de chaque groupe se regroupaient (Fig.16C). L'analyse des voies à l'aide de DAVID (Huang et al., 2009a, 2009b) a montré un enrichissement dans la voie de la polyarthrite rhumatoïde (Fig. 16D). L'AJI étant principalement une maladie inflammatoire liée aux articulations (de Jager et al., 2007), cela nous a incités à examiner le statut inflammatoire des fluides synoviaux. À l'aide de la technologie Simoa, nous avons mesuré des concentrations de TNF-α comprises entre 3 et 26 pg/mL (médiane = 10,8 pg/mL) dans le liquide synovial (SF) de dix-huit genoux de patients atteints d'AJI présentant une arthrite active (Fig. 16E). En

comparant les niveaux circulants de TNF-α dans le plasma et le SF de six patients appariés, des niveaux plus élevés de TNF-α ont été systématiquement mesurés dans le SF par rapport au plasma sanguin (Fig. 16F).

Nous avons ensuite évalué l'impact du traitement avec le CB sur la production spontanée de TNF-α par les monocytes humains isolés des PBMC (Fig. 16G) et des cellules mononuclées du liquide synovial (SFMC) (Fig. 16H) de patients atteints d'AJI. Le traitement par CB a significativement diminué les niveaux de TNF-α dans le milieu de culture des monocytes SFMCs et PBMCs. Nous avons également montré que le CB exerçait un effet anti-inflammatoire de manière dose-dépendante sur les monocytes purifiés provenant des SF d'un patient sans aucune toxicité significative (Fig. 16I).

Dans l'ensemble, ces données fournissent la preuve que le CB inhibe la production spontanée de cytokines inflammatoires par les monocytes humains sanguins et synoviaux dans un contexte arthritique.

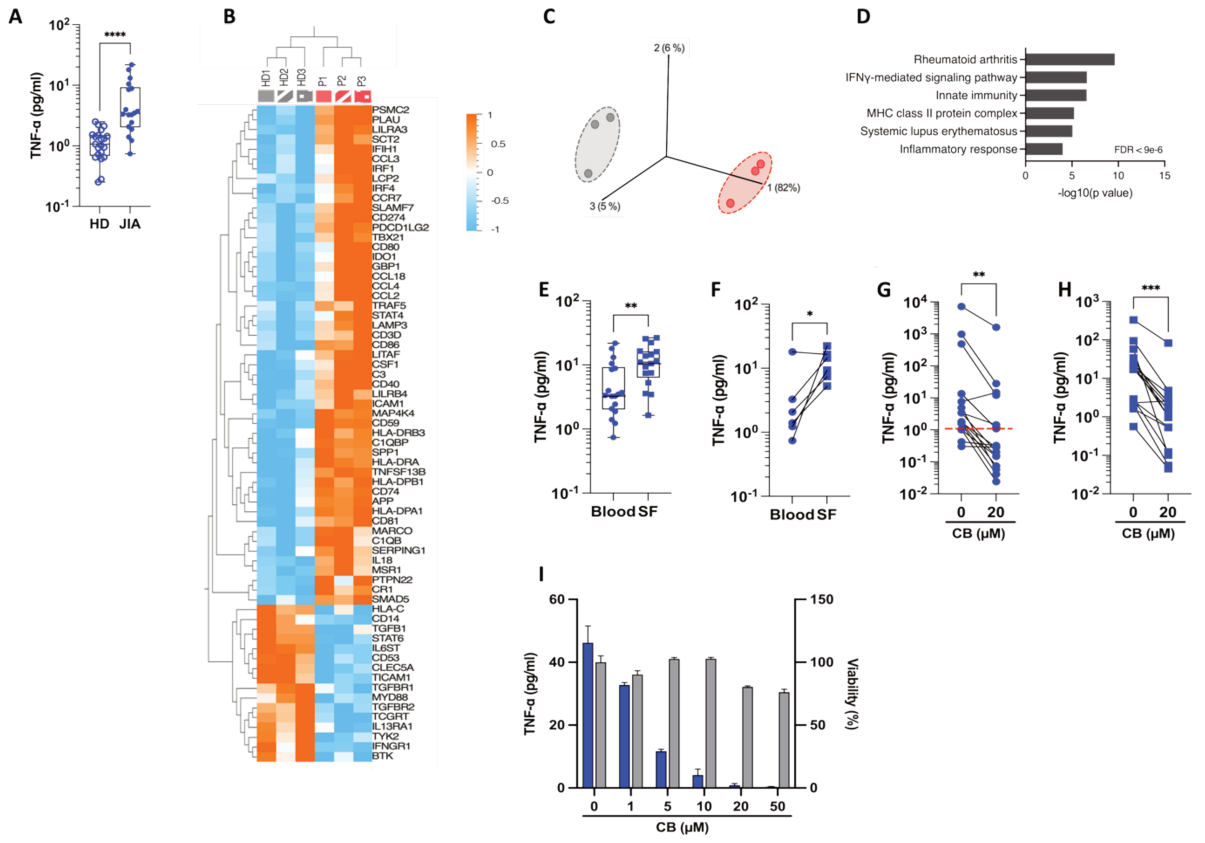

Figure 16: Le CB contrôle l'inflammation spontanée des cellules de patients atteints d'AJI.
(**A**) Le TNF-α a été mesuré dans le plasma du sang de donneurs sains (HD) et de patients AJI par ELISA digital (Simoa). Graphiques en boîte et moustaches avec médiane et écart-type. Test de Mann-Whitney. (**B**) Les monocytes du sang de donneurs sains (HD) et de patients atteints d'AJI ont été isolés et l'ARN total des cellules a été isolé et analysé à l'aide du NanoString nCounter. La Heat map représente l'augmentation des niveaux d'ARNm des gènes significativement différents entre les deux groupes ($P < 0,05$, fold change > 1,5). (**C**) Une ACP a été réalisée sur la base des gènes de la matrice différentielle exprimés entre les patients HD (en gris) et les patients JIA (en rouge). ($P < 0,05$, fold change > 1,5). (**D**) L'analyse David a été utilisée pour l'analyse de l'enrichissement des voies des gènes régulés différemment chez les patients atteints d'AJI par rapport aux HD. (**E**) Le TNF-α a été

dosé dans le plasma du sang ou des fluides synoviaux (FS) des patients atteints d'AJI par Simoa. Test de Mann-Whitney. (**F**) Les niveaux de TNF-α dans le plasma et le SF appariés de six donneurs différents ont été dosés par Simoa. Test de Wilcoxon. Le TNF-α a été mesuré dans le surnageant de monocytes par ELISA digital (Simoa) purifiés à partir de PBMCs (**G**) ou de SFMCs (**H**) de patients atteints d'AJI. La ligne de base moyenne des donneurs sains (HD) est représentée par la ligne pointillée rouge. Test de Mann-Whitney. (**I**) Les monocytes d'un patient atteint d'AJI ont été traités avec différentes concentrations de CB pendant 16h et le TNF-α a été mesuré dans le surnageant par ELISA digital (Simoa).

Le CB inhibe la production de cytokines induite par le R848 dans les cellules de patients atteints d'AJI

Nous avons ensuite évalué si le CB pouvait également inhiber la production de cytokines par les cellules immunitaires stimulées de patients atteints d'AJI. Pour cela, nous avons d'abord comparé la production de cytokines par les PBMCs de donneurs sains (HD) et de patients atteints d'AJI en utilisant le dosage par Luminex à 45 billes. Nous avons montré que les PBMCs de trois patients atteints d'AJI sur cinq sécrétaient plus de cytokines que celles de HD (Fig. 17A). Ce résultat confirme que les cellules des patients atteints d'AJI sont hyperréactives à la stimulation TLR-7/8. De plus, le CB a inhibé la production de cytokines inflammatoires induite par le R848 des PBMC de donneurs sains ainsi que l'hypersécrétion de cytokines inflammatoires par les cellules de patients AJI (Fig. 17B). Les monocytes étant les principaux producteurs de cytokines pro-inflammatoires, nous avons purifié les monocytes de patients souffrant d'AJI oligo-articulaire (n=20), polyarticulaire (n=8) ou systémique (n=5), ou d'arthrite liée à l'enthésite (ERA) (n=3). Pour tous ces sous-types d'AJI, le traitement par le CB a réduit de façon drastique les niveaux d'IL-1β, d'IL-6 et de TNF-α dans les surnageants de culture des monocytes des patients activés par le R848 (Fig. 17C).

Enfin, en utilisant des SFMCs purifiées de patients atteints d'AJI, nous avons montré que le CB inhibait la production des 40 facteurs solubles induits par l'activation du R848 (Fig. 17D). Ces données globales indiquent que le CB pourrait réduire l'hyper sécrétion de cytokines inflammatoires observée chez les patients atteints d'AJI pendant les poussées.

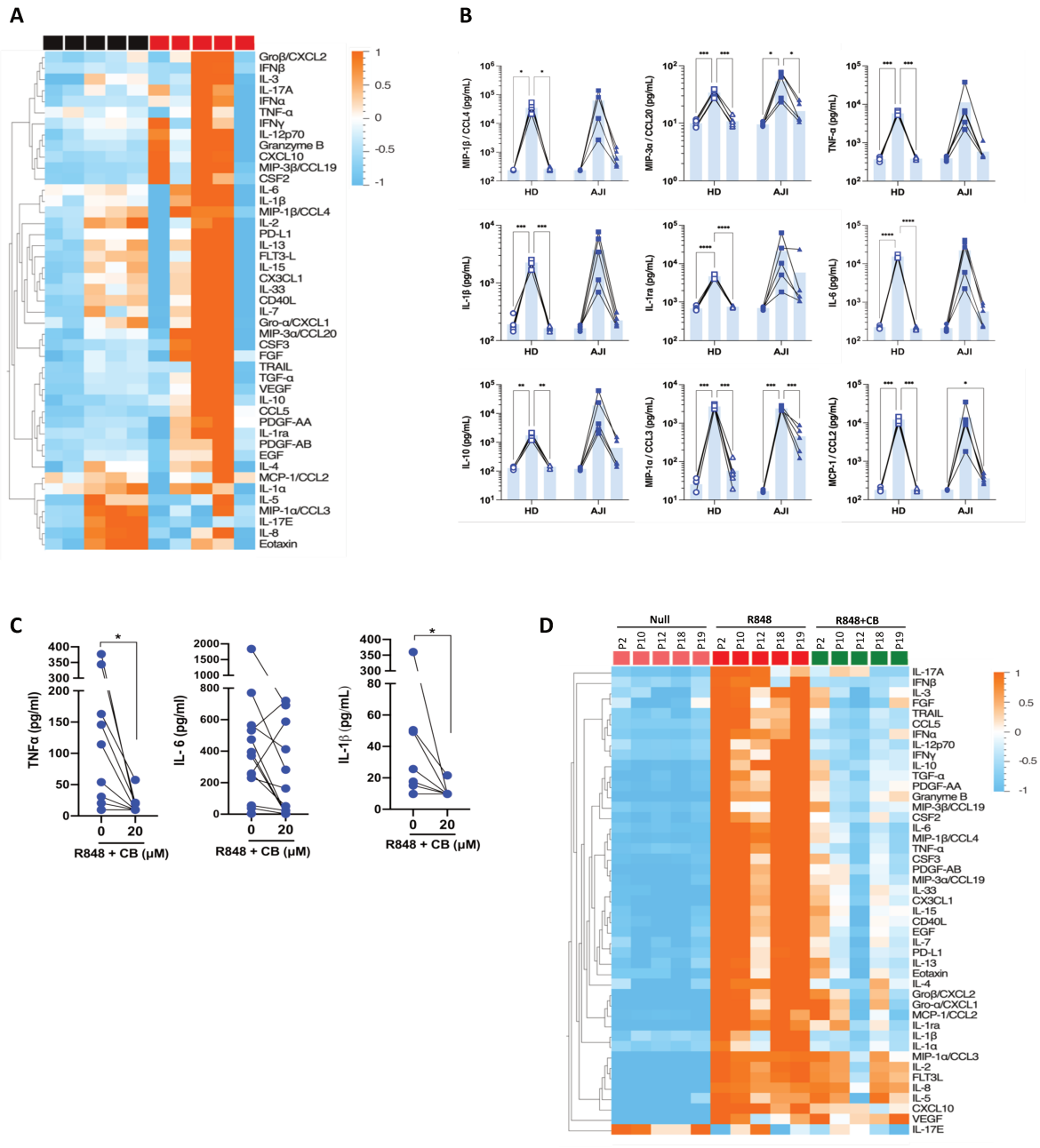

Figure 17: Le CB contrôle l'inflammation induite par les TLR7/8 dans les cellules de patients atteints d'AJI

(A) et (**B**) Les PBMCs des donneurs sains (HD) et patients atteints d'AJI ont été pré-incubés avec du CB à 20 µM puis stimulés avec R848 (5 µg/mL) pendant 16h. La production de cytokines a été mesurée dans le surnageant à l'aide d'un Luminex sur des billes. (**A**) Représentation sous forme de Heat map des cytokines statistiquement différentes (P<0,05) dans le surnageant des PBMCs lors de la stimulation par le R848 entre les donneurs sains HD et les patients AJI, classées par regroupement hiérarchique. Test de Mann-Whitney. (**B**) Les cytokines sont représentés de manière individuelle. Two-way RM ANOVA with Tukey post hoc correction. (**C**) Les monocytes de patients atteints d'AJI ont été pré-incubés avec du CB à 20 µM puis stimilés avec du R848 (5 µg/mL) pendant 16h. La production d'IL-6, d'IL-1β et de TNF-α a été mesurée dans le surnageant avec un multiplex à base de billes : LEGENDplex. Test de Mann-Whitney. (**D**) Les SFMCs ont été pré-incubées avec du CB à 20 µM et ensuite stimulées avec du R848 (5 µg/mL) pendant 16h. La production de cytokines a été mesurée dans le surnageant avec un Luminex basé sur des billes.

Le CB inhibe les cytokines inflammatoires et réduit la progression de la maladie dans un modèle de souris d'arthrite induite par le collagène.

Les propriétés anti-inflammatoires du CB dans les PBMCs, les SFMCs et les monocytes purifiés de patients atteints d'AJI, suggèrent que le CB représente une option thérapeutique prometteuse pour l'arthrite. Nous avons donc testé l'effet thérapeutique potentiel du CB dans un modèle de souris présentant une pathologie semblable à l'arthrite, les souris DBA/1J (Km et al., 2015) atteintes d'arthrite induite par le collagène (CIA). Les souris CIA partagent de nombreuses caractéristiques cliniques, histologiques et immunologiques avec la PR humaine (Hegen et al., 2008). Elles présentent notamment une atteinte symétrique des articulations, une synovite, des érosions du cartilage et des os. Plusieurs études ont signalé un rôle majeur de l'IL-1β dans le développement de la maladie dans le modèle de souris CIA (Williams et al., 2000), ainsi qu'un rôle pathologique de l'IL-6 dans la phase effectrice de l'arthrite auto-immune en favorisant la destruction osseuse (Lipsky, 2006).

Les souris CIA ont reçu une injection intrapéritonéale quotidienne de CB (à 3 mg/kg (mpK), 10 mpK et 30 mpK) sur une période de deux semaines. Le corticostéroïde prednisolone (15 mpK) a également été injecté aux souris CIA comme traitement contrôle. Le traitement par le CB n'a exercé aucun effet sur le poids corporel des souris, quelle que soit la dose testée (Fig. 18A), ce qui indique l'absence de toxicité majeure du CB chez les souris traitées. Alors que les souris CIA présentaient des taux élevés d'IL-1β et d'IL-6 circulants deux semaines après l'apparition de la maladie (Fig. 18B), le traitement par le CB a entraîné une profonde inhibition de ces deux cytokines (Fig. 18B). Il convient de noter que la dose la plus élevée de CB (30 mpK) était aussi efficace que le corticostéroïde de référence, la prednisolone.

Nous avons également étudié l'effet du traitement par le CB sur la progression de la maladie. L'injection quotidienne de CB a atténué la progression de la maladie pendant les 14 jours de traitement (Fig. 18C). Les souris traitées avec du CB avaient des pattes plus fines que les souris traitées avec du PBS (Fig. 18D). Chez les souris arthritiques, l'analyse histologique des lésions tissulaires a révélé des lésions graves du cartilage (flèche jaune), du remodelage osseux (flèche noire) et une infiltration tissulaire par des cellules immunitaires (flèche verte) (Fig. 18E). Le traitement quotidien avec du CB a atténué tous ces marqueurs pathologiques (Fig. 18E). Pour mieux caractériser l'effet du traitement par CB, les pattes ont été noté individuellement pour donner des scores afin de refléter la gravité de la maladie. Le traitement par le CB a considérablement réduit le score terminal des pattes (Fig. 18F), ce qui a été associé à une

réduction de l'inflammation, des dommages au cartilage, du remodelage osseux sur les membres et du pannus (Fig. 18G et 18H).

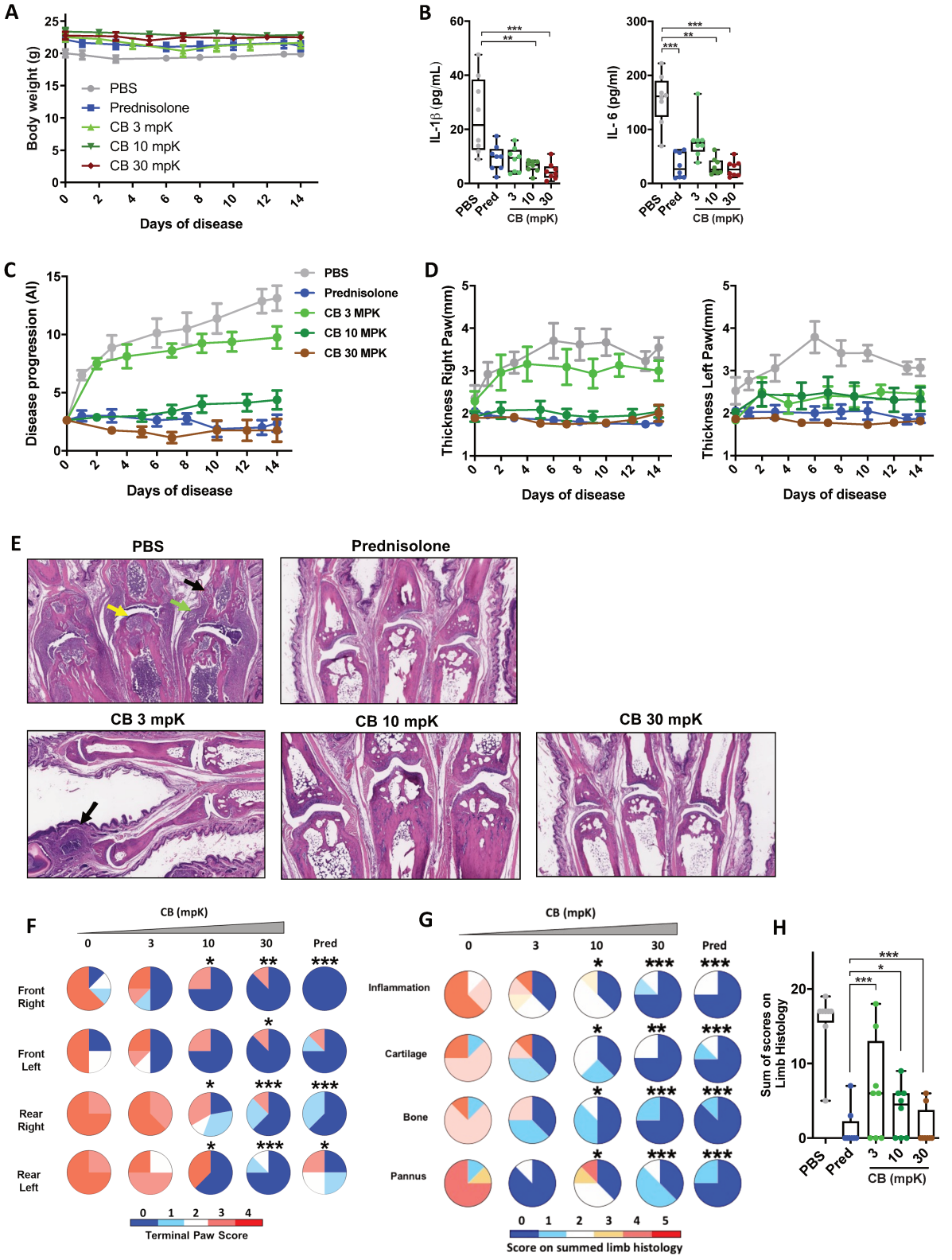

Figure 18: Le CB contrôle l'inflammation et l'apparition de la maladie chez les souris arthritiques induites par le collagène.

(**A**) Le poids corporel des souris arthritiques induites par le collagène traité avec de la prednisolone (Pred, 15 mpK) ou 3, 10, ou 30 mpK de CB a été mesuré tous les deux jours. (**B**) IL-1β et IL-6 ont été mesurés par ELISA dans le sérum après 2 semaines de traitement. Test de Kruskal-Wallis avec correction post hoc de Dunn. (**C**) la progression de la maladie a été évaluée selon plusieurs marqueurs au niveau des pattes. (**D**) L'épaisseur des pattes a été mesurée. (**E**) Coloration à l'hématoxyline et à l'éosine de coupe de pattes de souris arthritiques induites par du collagène et traitées avec du prednisolone (Pred, 15 mpK) ou 3, 10 ou 30 mpK de CB : articulations avec pannus et inflammation (flèche verte), perte de cartilage articulaire (flèche jaune) et remodelage osseux (flèche noire). (**F**) L'impact du traitement a été évalué avec un score au niveau des pattes selon une échelle de 0 à 4 de gravité croissante, après 2 semaines de traitements. (**G**) Effets du traitement sur le score de l'inflammation, des lésions cartilagineuses, du remodelage osseux et du pannus après 2 semaines de traitement. (**H**) Score combiné de la maladie après 2 semaines de traitement. Test de Kruskal-Wallis avec correction post hoc de Dunn. Toutes les données sont présentées sous forme de médiane ± intervalle, ***P < 0,001, **P < 0,01, *P < 0,05. n = 8 souris par groupe.

Le CB atténue la production spontanée de cytokines dans le sang total des patients COVID-19

Les monocytes sont également soupçonnés de jouer un rôle délétère au cours de l'inflammation aiguë lors de l'infection par le SARS-CoV-2 responsable de la maladie à coronavirus 2019 (COVID-19). En effet, le SARS-CoV2 infecte les voies respiratoires supérieures et inférieures et provoque un syndrome respiratoire léger ou très aigu avec une libération conséquente de cytokines pro-inflammatoires par des monocytes hyper-activés (Conti et al., 2020; Hadjadj et al., n.d.). Récemment, nous avons mesuré une surproduction de cytokines pro-inflammatoires chez des patients atteints du COVID-19, provoquant un orage de cytokines dans les poumons (Hadjadj et al., 2020). En outre, les niveaux élevés d'IL-6 et de TNF- dans le lavage broncho-alvéolaire et le plasma de ces patients sont en corrélation avec la gravité de la pathologie. Cette pandémie de SARS-CoV2 a poussé les communautés scientifiques et cliniques à développer de toute urgence de nouvelles stratégies anti-inflammatoires. Dans ce contexte de maladie inflammatoire chronique et aiguë, le récepteur des chimiokines CXCR4 pourrait devenir une cible thérapeutique potentielle.

Chez les patients sévères atteints de COVID-19, les monocytes infiltrés dans les poumons produisent des niveaux élevés de cytokines inflammatoires telles que l'IL-1β, l'IL-6 et le TNF-α, ce qui entraîne une inflammation incontrôlée (Blanco-Melo et al., 2020), une « tempête cytokinique » et de la fièvre (Merad and Martin, 2020). De plus, les patients COVID-19 nécessitant des soins intensifs dans les hôpitaux, présentent des taux plasmatiques de cytokines pro-inflammatoires (Hadjadj et al., n.d.), comme l'IL-1β, l'IL-6, l'IL-10 et le TNF-α plus élevés que ceux des donneurs sains (HD) (Fig. 19A). Ainsi, cibler les cytokines proinflammatoires et/ou les monocytes représenterait une stratégie thérapeutique pour le traitement des cas graves

de COVID-19. Ici, nous faisant la preuve de concept que le ciblage de CXCR4 avec le CB pourrait représenter une nouvelle approche thérapeutique pour les patients hospitalisés COVID-19. Selon l'ELISA digital (Simoa), le traitement du sang total des patients COVID-19 avec du CB à 20M pendant 16h a diminué la production spontanée de IL-1β, TNF-α, IL-6 et IL-10. (Fig. 19B).

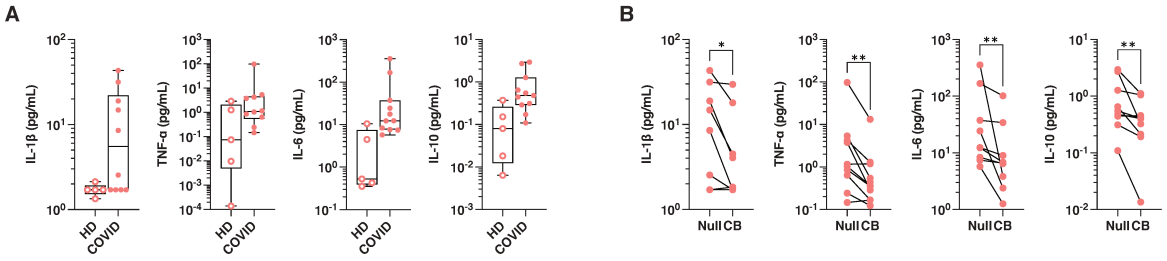

Figure 19: Le CB contrôle l'inflammation dans le sang total des patients COVID-19.
(**A**) IL-1β, TNF-α, IL-6 et IL-10 ont été mesurés après 16h de culture à 37° dans le plasma de sang total de donneurs sains (HD) et de patients COVID-19 par ELISA digital (Simoa) (**B**) Le sang total des donneurs HD et COVID-19 a été traité avec du CB à 20 µM pendant 16h et les cytokines IL-1β, TNF-α, IL-6 et IL-10 ont été mesurées dans le surnageant par ELISA digital (Simoa). Graphiques en boîte à moustaches avec médiane et écart-type. Test de Mann-Whitney. **P < 0,01, *P < 0,05

Conclusion

Dans cette étude, nous révélons une activité anti-inflammatoire à large spectre de l'analogue de l'histamine CB. Nous démontrons que CB réduit significativement la production spontanée et induite des principales cytokines inflammatoires par les monocytes du sang et des fluides synoviaux de patients atteints d'AJI. Cette activité immuno-modulatrice du CB dépend de l'engagement du récepteur de chimiokine CXCR4. De plus, *in vivo*, le CB montre une grande efficacité de réduction de l'inflammation et des dommages tissulaires chez les souris arthritiques, ce qui conduit à une réduction de la progression de la maladie. Nous apportons également la preuve que le ciblage de CXCR4 avec le CB calme l'hyper inflammation associée au COVID-19 sévère. En conclusion, la très faible cytotoxicité de CB, son activité inhibitrice à large spectre sur la production de cytokines inflammatoires et son activité thérapeutique *in vivo*, suggèrent que le ciblage de CXCR4 avec des molécules de type CB pourrait représenter une nouvelle stratégie thérapeutique prometteuse pour les maladies inflammatoires chroniques telles que la polyarthrite rhumatoïde et potentiellement pour l'inflammation aiguë à médiation virale telle que la maladie COVID-19.

Partie II : Un analogue de l'histamine contrôle la production d'IFN dans le lupus érythémateux systémique

Il a récemment été identifié une petite molécule IT1t, un ligand de CXCR4 précédemment décrit, comme un inhibiteur très puissant de l'inflammation médiée par le récepteur TLR7. IT1t inhibe l'inflammation induit par le TLR7 dans les cellules dendritiques plasmacytoïdes humaines purifiées provenant du sang et des amygdales humaines (Smith et al., 2019). Dans un modèle de souris lupus induit par le collagène, le traitement *in vivo* de souris avec IT1t entraîne une réduction drastique de l'inflammation systémique et des auto-anticorps anti-ADN double brin et prévient la glomérulonéphrite. En outre, IT1t contrôle l'inflammation, y compris la sécrétion d'interféron α, dans les cellules non stimulées et stimulées de patients atteints de lupus érythémateux systémique (Smith et al., 2019). L'objectif de cette partie est de déterminer si un autre ligand de la poche mineure de CXCR4, l'analogue de l'histamine CB, peut avoir des effets comparables à ceux de l'IT1t sur l'inflammation induit par le TLR7 dans les cellules dendritiques plasmacytoïdes humaines et le modèle de souris lupus induit par le collagène. A noter que contrairement à l'IT1t, le CB n'empêche pas la fixation du ligand naturel de CXCR4 : le CXCL12, de se fixer sur son récepteur. Cela permet de conserver les propretés physiologiques de CXCL12.

Le CB inhibe l'inflammation médiée par TLR7/8 dans les amygdales et les PBMCs humains

Nous avons précédemment démontré que l'engagement de CXCR4 par les amines naturelles et l'analogue synthétique de l'histamine (clobenpropit) inhibe fortement la production d'interféron de type I induite par des virus dans les pDCs humaines primaires (Smith et al., 2017). Afin d'évaluer les propriétés immunorégulatrices du CB dans un modèle plus complexe et physiologique, des amygdales de donneurs sains riches en cellules mononuclées (TMC) ont été utilisées. Les TMC de sept donneurs ont été stimulées avec du R848 en présence ou en l'absence de CB. Les cytokines ont été mesurés dans les surnageants de cultures. Ainsi, le CB inhibe la production d'IFN de type I et de type II et les cytokines pro-inflammatoires IL-1β, TNFα, IL-6, IL-10, IL12p70, IL-8, IP-10, GM-CSF et la chimiokine CXCL-10 dans les TMCs des sept donneurs (Fig. 20 B et D) sans aucune toxicité (Fig. 20 C). Afin d'étendre nos résultats obtenus avec les TMCs, nous avons ensuite testé la capacité du CB à contrôler la production d'IFN de type I dans les surnageants de cellules mononuclées sanguines humaines (PBMCs) stimulées

par le R848 de trois donneurs sains (Fig. 20E et F). De manière dose-dépendante, le CB contrôle la sécrétion d'IFN de type I, sans toxicité associée. Par conséquent, le CB contrôle l'IFN de type I et un large spectre de production de cytokines inflammatoires dans les populations de cellules complexes (TMCs) et les PBMCs.

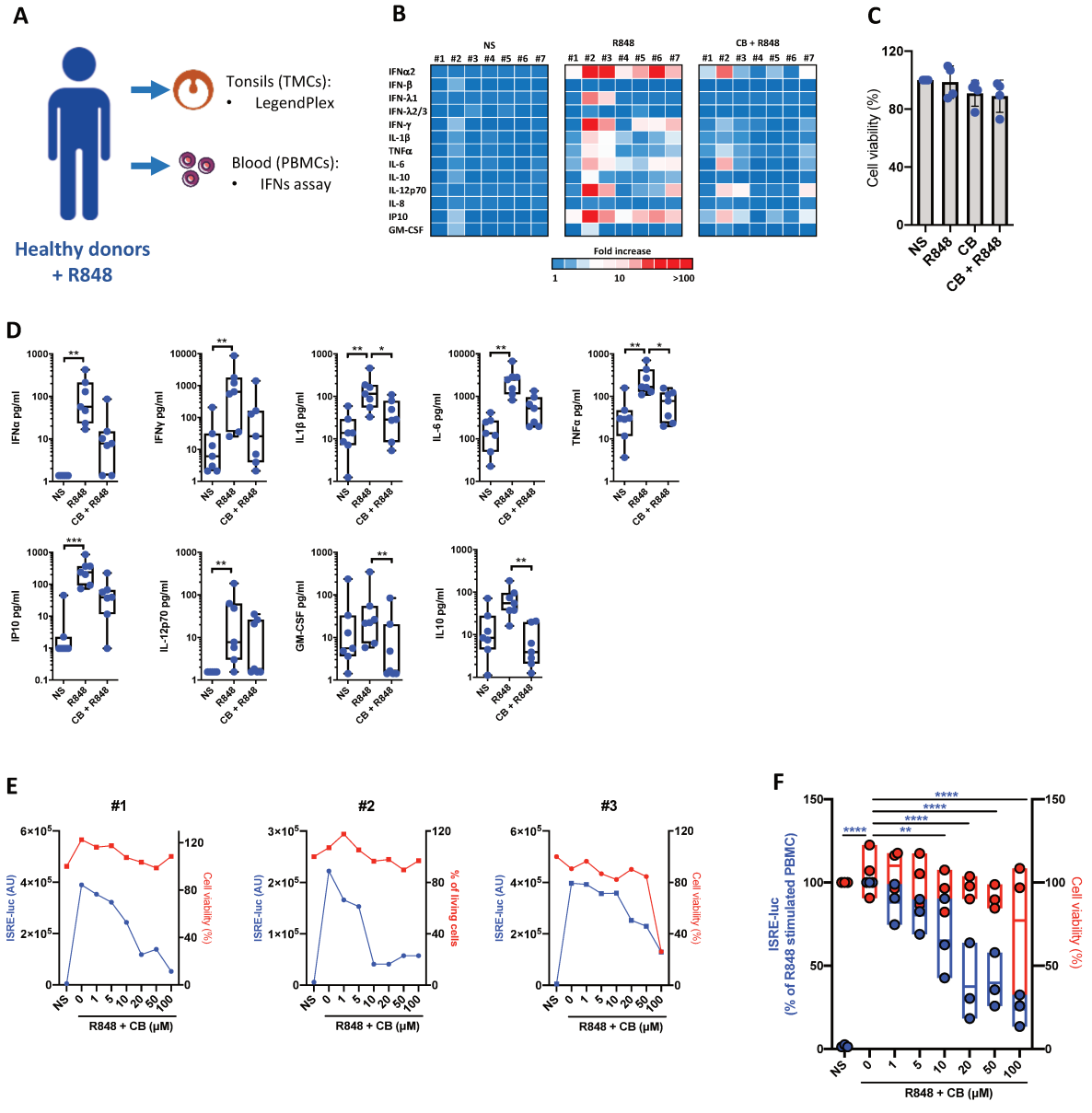

Figure 20: Le CB inhibe l'inflammation médiée par TLR7/8 dans les amygdales et les PBMC de donneurs sains.
(A) Déroulement des expériences (B-D) L'effet du CB sur les TMC stimulées par le R848 a été évalué en dosant la sécrétion de cytokines dans les surnageants de culture de sept individus sains à l'aide d'un LEGENDplex. (B) La Heat map représente l'augmentation de la sécrétion de cytokines par rapport à la condition non stimulé. (C) La viabilité cellulaire a été évalué par Cell-Titer Glo. (D) Les graphiques représentent la concentration en picogrammes par millilitre de chaque cytokine mesurée. Box and whisker plots with median ± minimum to maximum. Friedman test with Dunn's post hoc correction. (E) L'effet sur chacun individu et (F) sur les trois donneurs du CB sur les PBMC stimulées par le R848 a été évalué dans le surnageant des cultures en utilisant la

lignée cellulaire rapporteuse STING-37. La viabilité cellulaire a été mesurée par Cell-Titer Glo. 2 way ANOVA RM avec correction post hoc de Dunn. ****P < 0,0001, ***P < 0,001, **P < 0,01, *P < 0,05. NS, non stimulé.

CB contrôle l'inflammation induite et spontanée des cellules immunitaires d'un patient atteint de LES.

Après avoir découvert que le CB était un puissant inhibiteur de la production d'IFN, nous avons ensuite cherché à évaluer si cette modulation immunitaire par le CB pouvait avoir un impact sur la progression de maladies inflammatoires telles que les interféronopathies. Il a précédemment été démontré que les niveaux circulants d'IFNα sont plus élevés chez les patients atteints de LES dont l'activité de la maladie est plus importante (Rodero et al., 2017). Le rôle central de la production d'IFN de type I induite par TLR7 dans la physiopathologie du LES étant bien établi, nous avons étudié la capacité du CB à inhiber la sécrétion d'IFN de type I par des pDC isolées à partir de PBMC de donneurs sains activées par l'agoniste TLR7 : R848. Les effets du traitement par le CB ont été comparés à ceux du traitement par hydroxychloroquine (HCQ), le traitement classique du LES. (Fig. 21B). Le CB a contrôlé la production d'IFN dans les cellules activées par le R848 avec une meilleure efficacité que HCQ (Fig. 21B).

Par conséquent, nous avons évalué si le traitement par CB réduit la production d'IFN-α médiée par TLR7 chez les patients atteints de LES. Afin de mieux caractériser les effets immunitaires du CB sur les cellules de patients atteints de LES, des cellules immunitaires de moelle osseuse ont été prélevées dans le sternum d'un patient atteint de LES aiguë. Les cellules immunitaires de la moelle osseuse ont été stimulées avec du R848 en présence ou en l'absence de CB et d'hydroxychloroquine (HCQ) à 20 µM. Un dosage de l'IFN-α a été effectué sur les surnageants de culture cellulaire (Fig. 21C). Le CB et le HCQ inhibent drastiquement la production d'IFN-α médiée par les R848, avec une meilleure efficacité pour le CB par rapport au HCQ (Fig. 21C). Aucune toxicité n'a été observée sur les cellules immunitaires de la moelle osseuse traitées par CB et HCQ (Fig. 21D). Nous avons ensuite cherché à caractériser plus en détail cette réponse des cellules immunitaires de la moelle osseuse. Pour cela, un phénotypage des cellules immunitaires de la moelle osseuse a été réalisé. Ainsi, 5% sont des monocytes CD14+, 5% des lymphocytes B CD19+, 2% des cellules NK CD56+, 6% des lymphocytes T CD3+ et 0,3% des cellules pDC CD123+ BDCA4+ (Fig. 21E). En réponse à une stimulation médiée par le R848, les pDCs directement isolées de la moelle osseuse produisent de l'IFNα et du TNFα. Cette production est inhibée par le traitement par CB et HCQ (Fig. 21F). Enfin, un niveau basal d'activation des cellules immunitaires dans la moelle osseuse d'un patient atteint de LES a pu

être détecté, illustré par la production spontanée de TNFα. Cette production a été contrôlée par le traitement par CB et HCQ (Fig. 21G). L'ensemble de ces résultats montre que le CB est capable de contrôler la production d'IFNα et de TNFα dans des conditions d'inflammation médiée par le R848, mais aussi la production spontanée de TNFα chez les patients atteints de LES.

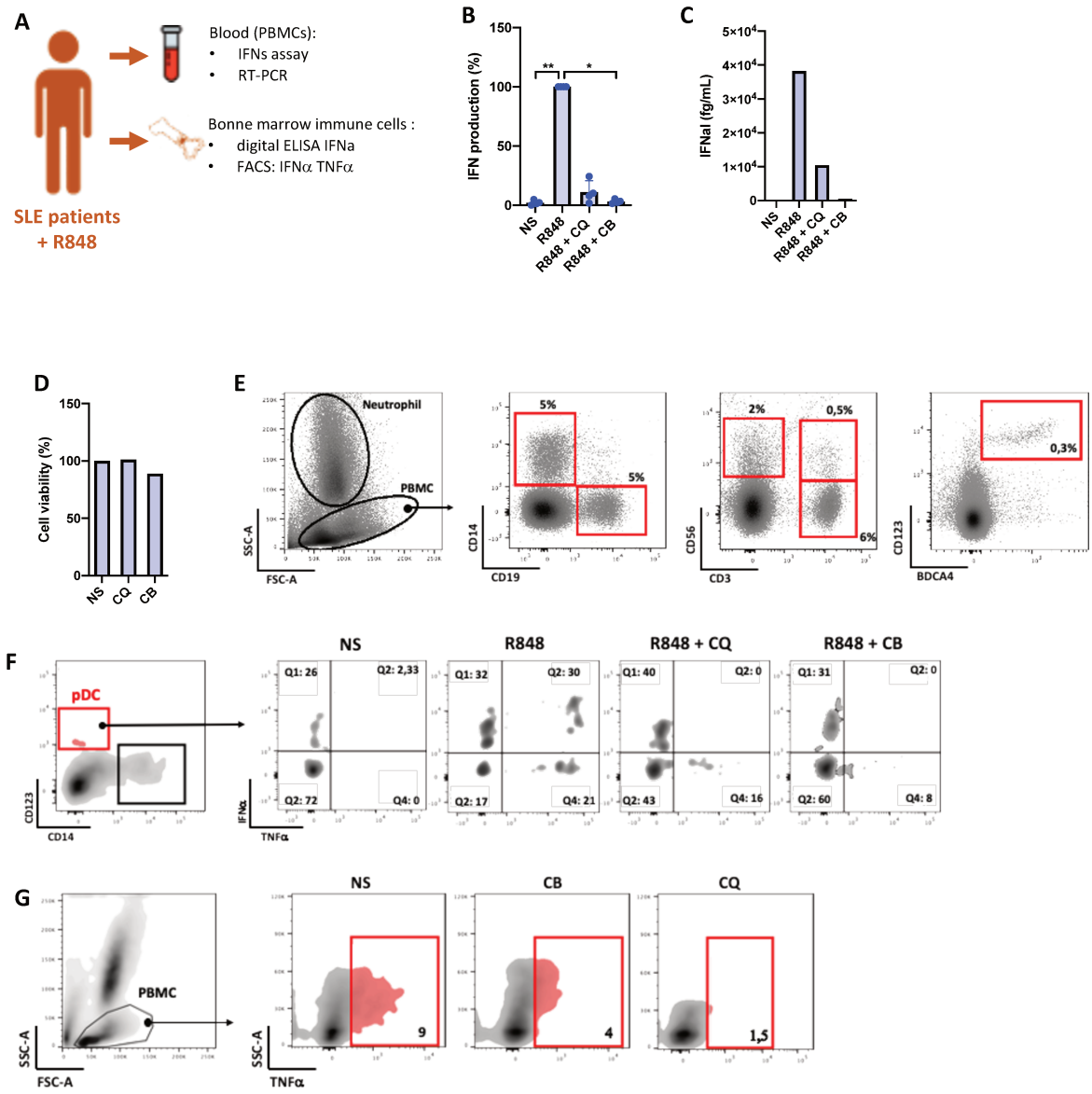

Figure 21: Le CB contrôle l'inflammation induite et spontanée des cellules immunitaires de la moelle osseuse d'un patient atteint de LES.
(**A**) Déroulement de l'expérience. (**B**) L'effet du CB sur les pDC stimulées par le R848 a été évalué par le dosage de l'IFN dans le surnageant de trois individus sains en utilisant la lignée cellulaire rapporteur STING-37. (**C-G**) L'effet de CB a été évalué *in vitro* sur les cellules immunitaires de la moelle osseuse d'un patient atteint de LES. (**C**) Les cellules immunitaires de la moelle osseuse ont été mis en cultire avec du R848 (5 µg/ml) en présence ou en l'absence de CB (20 µM) et de chloroquine (20 µM). La sécrétion d'IFN-α a été mesurée par Simoa. (**D**) La viabilité cellulaire a été mesurée par Cell-Titer Glo. (**E**) Le phénotype des cellules immunitaires de la moelle osseuse d'un patient atteint de LES a été réalisé par cytométrie de flux en utilisant les anticorps CD14, CD19, CD56, CD3, CD123 et BDCA4. (**F**) Les cellules immunitaires de la moelle osseuse ont été cultivées avec du R848

(5 µg/ml) en présence ou en l'absence de CB (20 µM) et de chloroquine (20 µM). Les pDCs IFN+ TNF + ont été identifiées et quantifiées par cytométrie de flux. (**G**) Les cellules immunitaires de la moelle osseuse ont été mis en culture en présence ou en absence de CB (20 µM) ou de chloroquine (20 µM). Les PBMCs TNF + ont été identifiées et quantifiées par cytométrie de flux. **P < 0,01, *P < 0,05. NS, non stimulé.

Le CB inhibe la production de cytokines inflammatoires et la progression de la maladie dans un modèle de souris LES

Nous évaluons si le CB pourrait représenter un composé thérapeutique *in vivo* dans un modèle murin de LES induit par le pristane. Le lupus érythémateux systémique (LES) représente l'une des interféronopathies les plus courantes (Kaul et al., 2016). TLR7 et la signalisation IFN médiée par TLR7 sont bien documentés comme étant un acteur majeur du développement de la maladie du LES et de la réponse au traitement (Alonso-Ruiz et al., 2008; Banchereau et al., 2016; Garcia-Romo et al., 2011; Lande et al., 2011; Nehar-Belaid et al., 2020). Plusieurs modèles de souris ont permis de mieux comprendre le rôle de l'IFN de type I dans la pathogenèse de la maladie lupique. Le LES induit par le pristane répond à la plupart des critères de la Systemic Lupus Collaborating Clinic (SLICC) utilisés pour la classification du lupus humain, avec la présence d'une signature IFN et d'anticorps anti ADNdb (Zhuang et al., 2015). Le pristane induit la production d'IFN de type I principalement par la voie TLR7/MyD88 (Savarese et al., 2008). En effet, la déficience en TLR7 non seulement abolit la production d'IFN de type I induite par le pristane mais prévient également la production d'auto-anticorps et la maladie rénale, indiquant un rôle clé de la voie TLR7/MyD88/IFN de type I dans ce modèle (Chen et al., 2016; Savarese et al., 2008). Compte tenu des vastes propriétés immunorégulatrices du CB sous la stimulation de TRL7/8, notamment l'inhibition des IFN de type I et III, de la production de TNF α et de la protéine IL-6, nous avons évalué le potentiel du CB comme approche thérapeutique pour le LES. Le LES a été induit chez des souris Balb/c par co-injection intrapéritonéale quotidienne de pristane (0,5 ml par souris) avec un véhicule ou avec différentes doses de CB (3, 10 et 30 mg/kg ou mpK) pendant 10 semaines. Comme traitement de référence, des souris atteintes de LES ont été traitées quotidiennement avec le corticostéroïde prednisolone à 15 mpK. Les souris traitées par CB n'ont montré aucun signe de stress ou de perte de poids par rapport au véhicule, indiquant la bonne tolérance du traitement par les animaux (Fig. 22B).

Les cytokines IL-17, IL-1β TNFα et TRAIL ont été dosés à partir du sérum aux semaines 4 et 10. Il convient de noter que l'IFN-α n'était pas détectable dans le sérum des souris traitées au pristane. Cependant, nous avons pu détecter des niveaux accrus de la protéine TRAIL induite

par l'interféron et de cytokines inflammatoires. Le traitement à la prednisolone a été utilisé comme contrôle thérapeutique positif et a réduit toutes les cytokines mesurées (Fig. 22, C à F). Le CB, comme la prednisolone, a fortement réduit l'ensemble de ces cytokines de manière dose dépendante (Fig. 22. C à F). Ensemble, ces résultats soulignent que l'injection intrapéritonéale de CB réduit les phénotypes associés au LES.

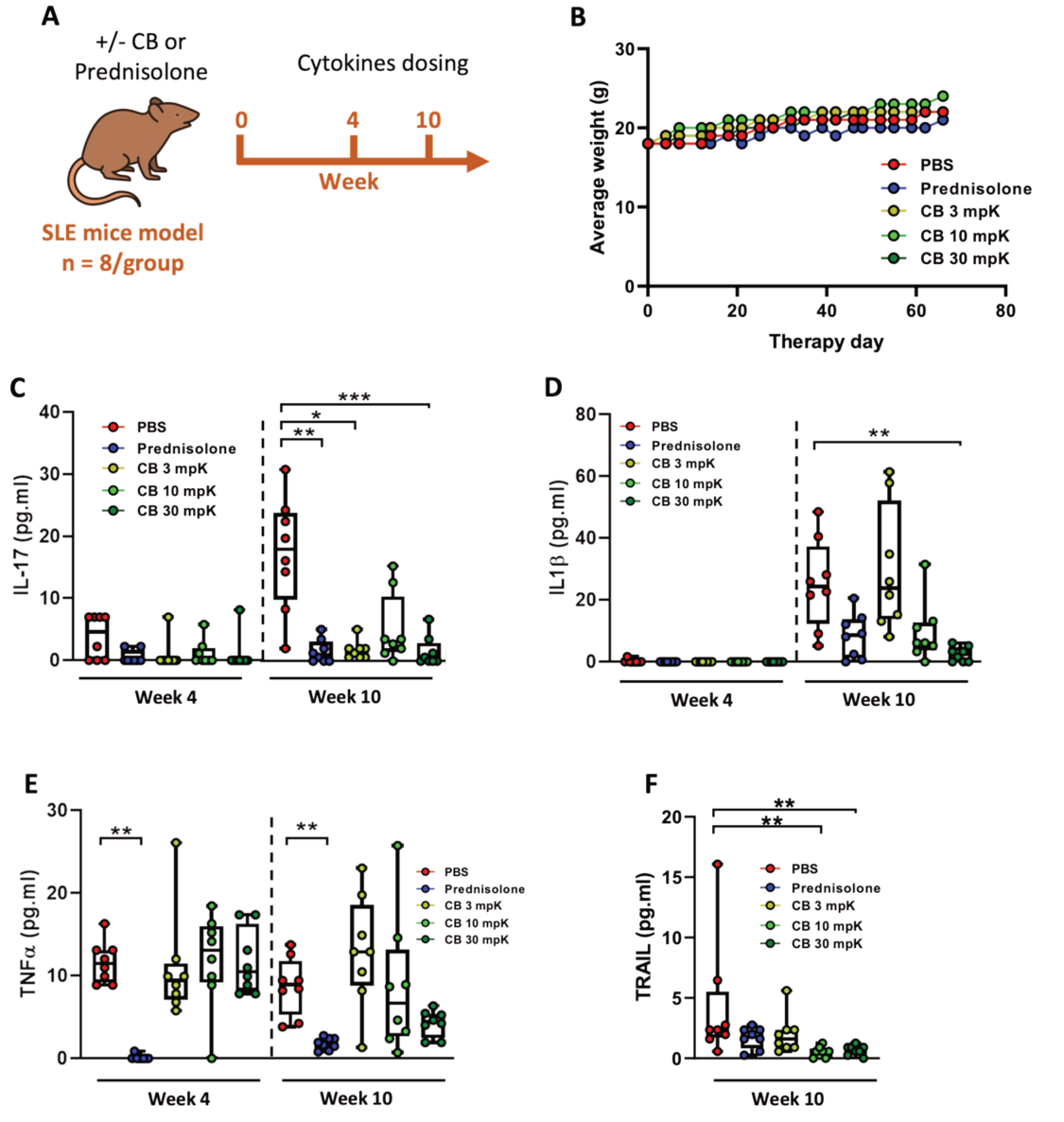

Figure 22: Le CB contrôle l'inflammation et le développement de la maladie chez les souris atteintes de LES.

(**A**) Plan expérimental (**B-F**) Les souris ont reçu une injection intrapéritonéale quotidienne de 0,5 ml de pristane pour induire la maladie et un traitement avec de la prednisolone (15 mg/kg) ou 3, 10 ou 30 mpK de CB pendant 10 semaines. (**A**) Le poids corporel a été mesuré. (**C-F**) L'état inflammatoire a été évalué dans le sérum des souris par le dosage des protéines de IL-17 (C), IL-1β (D), TNF-α (E) et TRAIL (F). Test de Krustal Wallis avec correction post hoc de Dunn. ***P < 0,001, **P < 0,01, *P < 0,05

Conclusion

Dans cette étude, nous montrons que le CB, a une forte activité immunosuppressive sur les pDCs activées par TLR7. De plus, le traitement par le CB a permis de contrôler l'inflammation dans un modèle de souris lupique, et de contrôler la production et la signalisation de l'IFN de type I dans des cellules isolées de patients atteints de lupus. Cibler le récepteur CXCR4 en utilisant de petits composés aminés tels que le CB représente donc une stratégie thérapeutique innovante dans les interféronopathies.

Partie III : Identification d'un nouveau composé aux propriétés anti-inflammatoires via son engagement sur le récepteur CXCR4

Au cours de ma thèse, j'ai eu l'occasion de tester différents ligands de CXCR4 qui se fixent au niveau de la poche mineure du récepteur, induisant une réponse anti-inflammatoire : des amines naturelles comme l'histamine, mais également synthétique comme le CB et l'IT1t. Dans le cadre de ce projet, un des objectifs était d'identifier de nouveaux composés qui se fixent dans la même poche mineure de CXCR4, avec une affinité plus importante, dénoués de toxicité et surtout avec des activités anti-inflammatoires plus puissantes. En se basant sur les sites d'interactions du CB, de l'IT1t et de l'histamine avec la poche mineure de CXCR4, des nouveaux composés ont été synthétisé (Fig.23A). Ces derniers ont fait l'objet d'un test d'activité anti-inflammatoire sur des PBMC de 3 donneurs sains (Fig.23B). Brièvement, des gammes de doses des composés ont été incubé avec les PBMC, puis stimulé avec un agoniste de TLR7/8 : le R848. Un dosage des IFN a été réalisé dans les surnageants de culture, et un test de viabilité a été réalisé sur les PBMC. Ce test permet de calculer les IC50 de l'activité anti-IFN des composés (voir tableau 2). Ainsi, deux composésprésentent une activité anti-IFN intéressante : le composé 2003 avec un IC50=10,3 µM et 1411 avec une IC50=0,9 µM. A titre de comparaisons, les molécules de références IT1t et CB ont respectivement des IC50 de 8 et 11 µM. Nous nous sommes plus particulièrement intéressés au composé 1411.

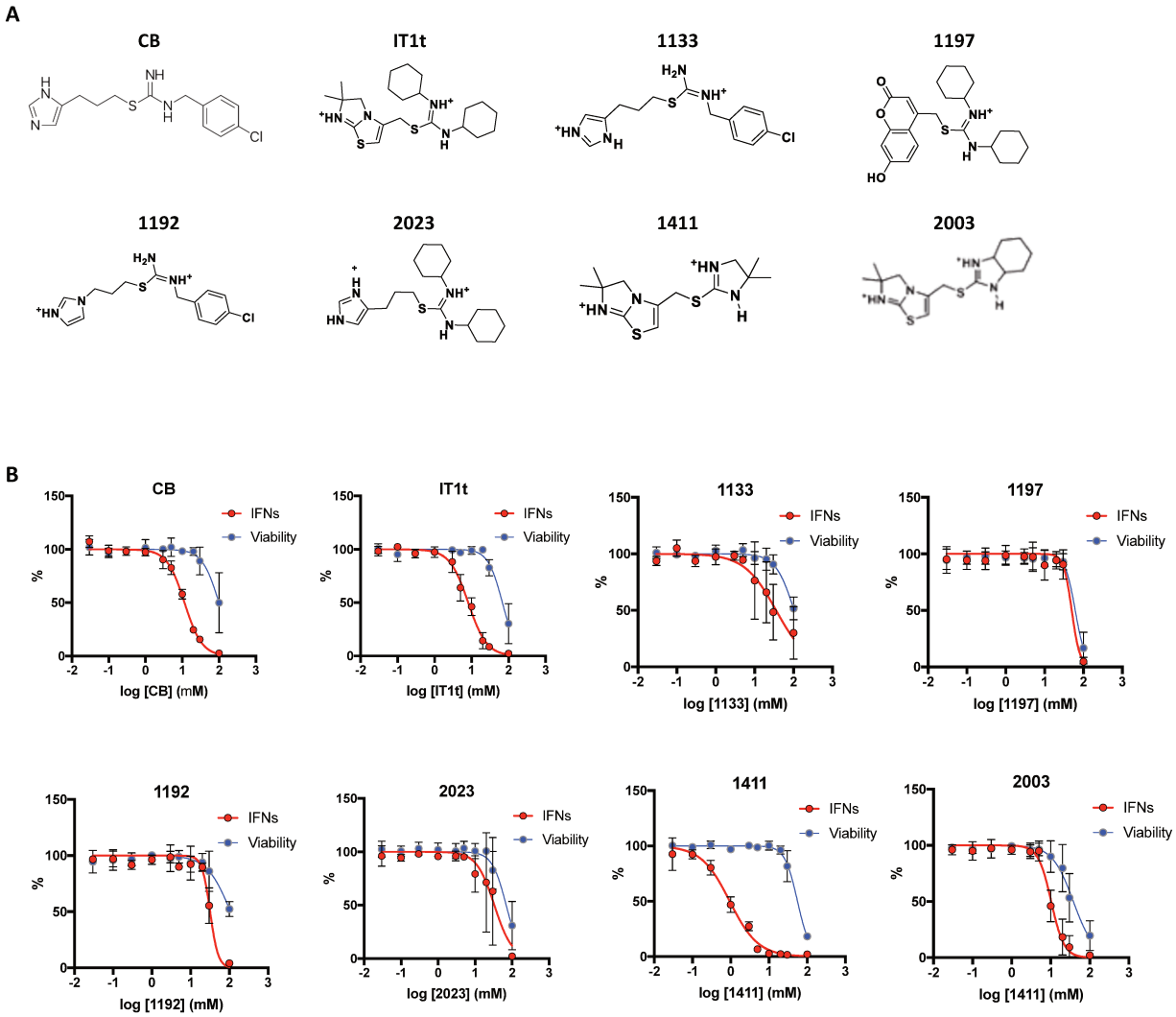

Figure 23: Nouvelles molécules anti-IFN ciblant le récepteur CXCR4.
(A) liste des composés candidats pour une activité anti-IFN dépendant de CXCR4. (**B**) Les composés ont été incubé avec des PBMC de trois donneurs sains selon une gamme doses de 1 à 100 µM, puis stimulé avec du R848 à 5µg.ml^{-1}. Le dosage des IFNs dans les surageants a été réalisé avec la lignée rapportrice STING-37. La viabilité cellulaire a été mesuré avec le Cell Titer Glo.

	IC_{50} IFNs (µM)	IC_{50} viability (µM)
CB	11,53	99,64
IT1t	8,116	68,21
1133	35,59	103,8
1197	50,12	61,64
1192	31,84	107,4
2023	33,22	69,41
1411	0,9425	55,76
2003	10,29	37,99

Tableau 2: IC50 des activités anti-IFNs et de la viabilité des différents composés

Caractérisation des effets anti-inflammatoire du composé 1411

Dans le but de bien caractériser et étudier les effets anti-inflammatoires du composé 1411, un dosage de 13 cytokines (IL1β, IFNα, IFNγ, TNFα, IL6,…) a été réalisé sur des surnageants des PBMC de 6 donneurs traités avec du 1411à 5 µM ou de l'HCQ à 20 µM, puis stimulé avec du R848 (fig 24. A et B). Le composé 1411 a permis d'inhiber, de manière plus efficace que l'HCQ, l'ensemble des cytokines inflammatoires induites par la stimulation R848, démontrant ainsi une forte activité anti-inflammatoire à large spectre du composé. La même expérience a été réalisé avec des monocytes isolés issus de sang de 4 donneurs sains (fig 24. C et D). Le composé 1411 à encore une fois montré une forte activité anti-inflammatoire en inhibant l'ensemble des cytokines induites par la stimulation R848. L'activation des monocytes par d'autres TLRs que le TLR8 a également été testé en présence ou pas du composé 1411(fig 24. E et F). Nous avons ainsi traité les monocytes avec du 1411 à 1 ou 5 µM, puis stimulé les cellules avec soit un agoniste de TLR7 : R848, de TLR4 : LPS (lipopolysaccharides) ou TLR2 : LTA (acide lipotéichoïque). Un dosage intracellulaire du TNFα a été réalisé par cytométrie en flux. Ainsi, quel que soit le TLR activé, le composé 1411 à une forte activité anti-inflammatoire illustré ici par l'inhibition de la production du TNFα (fig 24. E et F).

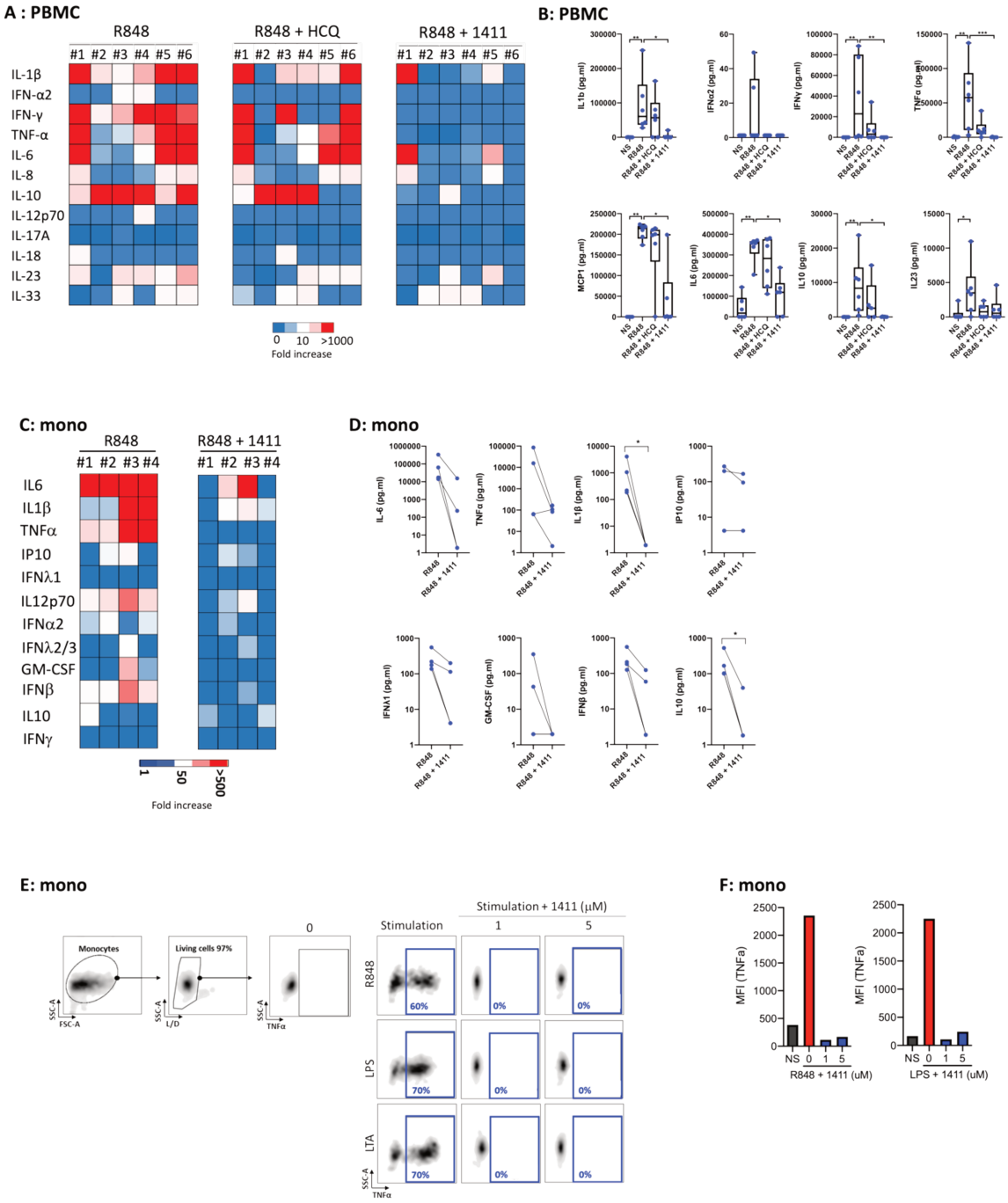

Figure 24: Caractérisation des effets anti-inflammatoires du composé 1411 sur des cellules immunitaires. (**A-B**) Des PBMC de 6 donneurs sains ont été traités avec le composé 1411 à 5µM ou avec de l'HCQ à 20µM, puis stimulés avec les R848 (5µg.ml^{-1}). Un dosage de 13 cytokines inflammatoires a été réalisé au niveau des surnageants de cultures avec un LegendPlex. (**A**) Représentation en heat map des niveaux de productions de cytokines comparés à la condition non stimulé. (**B**) représentation en histogramme des concentrations de cytokines en pg.ml des dosages LegendPlex. (**C-D**) Des monocytes isolés à partir de PBMC de 4 donneurs sains ont été traités avec le composé 1411 à 5µM, puis stimulés avec les R848 (5µg.ml^{-1}). Un dosage de 13 cytokines inflammatoires a été réalisé au niveau des surnageants de cultures avec un LegendPlex. (**C**) Représentation en heat map des niveaux de productions de cytokines comparés à la condition non stimulé. (**D**) représentation en histogramme des concentrations de cytokines en pg.ml des dosages LegendPlex. (**E-F**) Des monocytes isolés à partir de PBMC ont été traités avec le composé 1411 à 1 et 5 µM, puis stimulés avec du R848 (5µg.ml^{-1}), ou du LPS (100ng.ml^{-1}) ou du LTA (1µg.ml^{-1}). La production intracellulaire de TNFα a été mesuré par cytométrie en

flux. (**E**) Représentation en dot plot (**F**) représentation en histogramme de la MFI (TNFα) de la production de TNFα

Validation de la cible CXCR4 du composé 1411

Nous avons ensuite vérifié si les propriétés anti-inflammatoires de composé 1411 dépendent de son engagement via CXCR4. Nous avons d'abord utilisé l'antagoniste bien connu de CXCR4, AMD3100, pour moduler les effets anti-inflammatoires du 1411 sur des monocytes isolés à partir de PBMC. Les cellules ont été cultivées en présence ou en absence d'AMD3100 à 20µM, puis traités avec le composé 1411 à 1µM et stimulé avec le R848. La production intracellulaire de TNFα, d'IL1β et d'IL6 a été mesuré en cytométrie en flux. L'AMD3100 a ainsi pu bloquer l'effet anti-inflammatoire du composé 1411, comme l'illustre la récupération de la production de TNFα d'IL1β et d'IL6 en présence d'AMD3100 (Fig.25 A, B).

Pour établir fermement que l'activité immunorégulatrice du composé 1411 est liée à CXCR4, l'expression de CXCR4 a été réduite dans les monocytes primaires à l'aide d'un petit ARN interférent (siARN) ciblant l'ARN messager codant pour CXCR4. Alors que la transfection d'un siARN control (siControl) n'a pas eu d'impact sur l'inhibition de la production des cytokines pro-inflammatoires induite par le composé 1411, ce dernier a perdu sa capacité à inhiber la production intracellulaire de TNF-α dans les monocytes humains traités avec le siARN ciblant CXCR4 (siCXCR4) (Fig. 24. C, D). L'ensemble de ces données montrent que les effets immunorégulateurs du composé 1411 est dépendant de l'engagement de CXCR4.

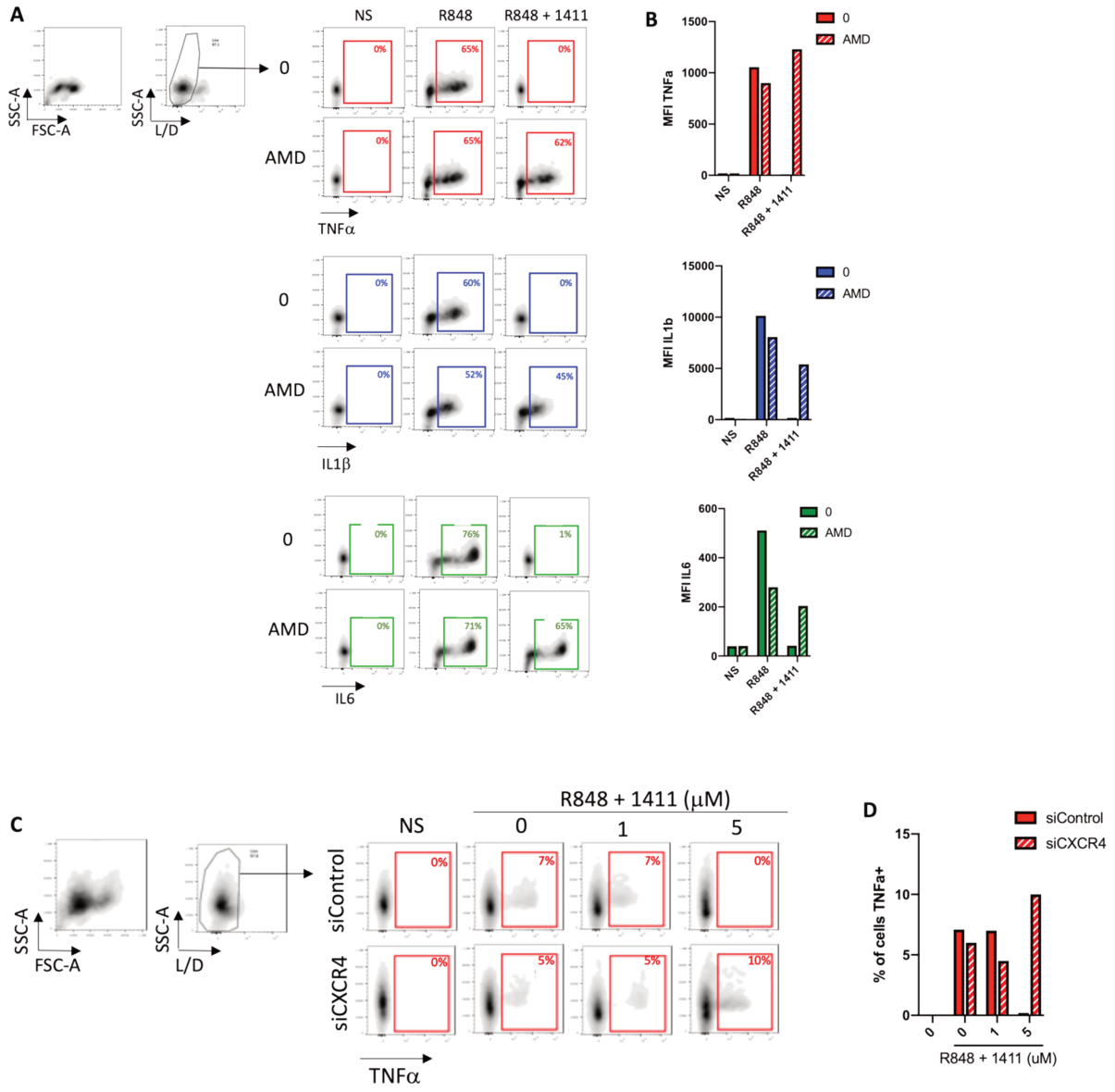

Figure 25: L'activité immunorégulatrice du composé 1411 sur les monocytes primaires est dépendante de CXCR4.
(**A-B**) Des monocytes isolés provenant d'un donneur sain ont été mis en culture en présence d'AMD3100 (20 µM), puis traités par du composé 1411 (1 µM) et activés par du R848 (1 µg/mL) pendant 6 heures. Les niveaux intracellulaires de TNF-α, IL-1β et IL-6 ont été évalué par cytométrie de flux, (**A**) représentation en dot plot d'un donneur et (**B**) représentation en histogramme des MFI (**C-D**) Les monocytes ont été traités pendant 24 heures avec le siRNA CXCR4 (siCXCR4) ou le siRNA contrôle (siControl) à 160 nM. Les cellules ont ensuite été pré-incubées avec le composé 1411 (1 µM) et stimulées avec du R848 (1µg/mL) pendant 6 heures. Les niveaux intracellulaires de TNF-α a été évalués par cytométrie en flux : (**C**) représentation en dot plot d'un donneur et (**D**) représentation en histogramme de la MFI. NS, non stimulé.

Conclusion

Dans cette étude, nous avons identifié un nouveau composé ayant une puissante activité anti-inflammatoire qui dépend de l'engagement dans CXCR4. Ce composé, nommé 1411 à une activité anti-inflammatoire plus forte que les molécules de références IT1t et CB. Ce composé

de présente pas de toxicité particulière, et a une activité anti-inflammatoire à large spectre, c'est-à-dire inhibent tout un panel de cytokines inflammatoire et les interférons. Ce composé est donc un très bon candidat pour des applications cliniques, notamment les maladies inflammatoires et auto-immune.

Chapitre 3 : Discussion

I. Résultats majeurs

Nos travaux nous ont permis de mieux caractériser les effets des composés aminé CB et IT1t sur les cellules immunitaires et plus particulièrement sur les PBMC et monocytes primaires. Nous avons ainsi pu démontrer que non seulement ces molécules avaient une activité anti-IFN-I puissante sur les pDC activés par des ligands naturels ou synthétiques de TLR7 via leur engagement sur CXCR4, mais également un effet anti-inflammatoire à large spectre sur PBMC et monocytes primaires. Ces effets anti-inflammatoires sont strictement dépendant de leurs engagements au niveau du récepteur CXCR4.

Ces nouvelles propriétés anti-inflammatoires à large spectre des composés IT1t et CB ont permis d'envisager de nouvelles applications cliniques afin de proposer ces composés comme traitements potentiels. Nous avons ainsi ciblé des maladies inflammatoires chroniques et aigües, mais également auto-immune tels que l'arthrite juvénile, le COVID-19 et le LED.

Enfin, grâce aux différents outils mis au point au laboratoire, nous avons pu identifier de nouveaux composés se fixant sur CXCR4 ayant des activités anti-inflammatoires et anti-IFN. Nous avons ainsi pu sélectionner deux molécules : le composé 2003 et 1411 dont les IC50 anti-IFN sont plus intéressantes que les molécules de références IT1t et CB.

II. Modèles utilisés

Les études sur cellule immunitaires primaires issues de donneurs sont très complexes. Ce sont des cellules très fragiles et sensibles avec une durée de vie courte. Dans le cadre de ces travaux, nous avons été amenés à isoler différents types cellulaires issues de tissus différents :

- à partir du sang de donneurs sains, nous avons été amenés à travailler sur des PBMC, mais également sur des pDC isolées (environ 0,4% des PBMC), et sur des monocytes isolés (5-15% des PBMC).
- à partir du sang de patients atteints d'AJI, nous avons été amenés à travailler sur des PBMC et sur des monocytes isolés (5-15% des PBMC).
- à partir du liquide synovial issues de patients atteints d'AJI, nous avons été amenés à travailler sur des SFMC (Synovial fluid mononuclear cells) et sur des monocytes isolés (5-15% des PBMC).

- à partir des amygdales issues d'amygdalectomie, nous avons été amenés à travailler sur les TMC (cellules mononuclées des amygdales)

Chacunes des populations cellulaires citées demandent des conditions de cultures et d'activations spécifiques.

Nous avons également été amené à utiliser des lignées cellulaires. Notre choix c'est porté sur la lignée cellulaire THP-1 qui est largement utilisée dans l'étude des fonctions des monocytes et des macrophages. Bien qu'elles ne répondent pas aussi à la stimulation des TLR8 et TLR4 que les monocytes, elles restent un bon modèle cellulaire pour nos travaux, d'autant plus qu'elles expriment le récepteur CXCR4.

Deux modèles murins ont été utilisés afin de tester le potentiel thérapeutique du CB. Nous avons ainsi utilisé le modèle de souris LES induit par le pristane qui répond à la plupart des critères de la Systemic Lupus Collaborating Clinic (SLICC) utilisés pour la classification du lupus humain, avec la présence d'une signature IFN et d'anticorps anti ADNdb. Le deuxième modèle que nous avons utilisé est un modèle de souris présentant une pathologie semblable à l'arthrite, les souris DBA/1J atteintes d'arthrite induite par le collagène (CIA). Les souris CIA partagent de nombreuses caractéristiques cliniques, histologiques et immunologiques avec la PR humaine. Elles présentent notamment une atteinte symétrique des articulations, une synovite, des érosions du cartilage et des os.

III. Mécanisme cellulaire induit par l'engagement de CXCR4

Dans le cadre de ce projet, un axe important qui reste à identifier est de déterminer les mécanismes cellulaires induits par les ligands de la poche mineure de CXCR4 qui permettent d'inhiber l'activation des cellules immunitaires médiée par les TLRs. Deux hypothèses sont envisageables :

- Les ligands de type CB et IT1t qui se fixent sur la poche mineure de CXCR4 induisent une voie de signalisation qui aboutit à l'inhibition des voies TLRs. (fig.26. A).
- Les ligands de type CB et IT1t qui se fixent sur la poche mineure de CXCR4 induisent un changement de conformation qui permet de recruter un partenaire. Ce serait donc la signalisation de ce nouvel hétérodimère avec CXCR4 qui aboutirait à l'inhibition des voies TLRs, et donc à une activité anti-inflammatoire et anti-IFN-I (fig.26. B).

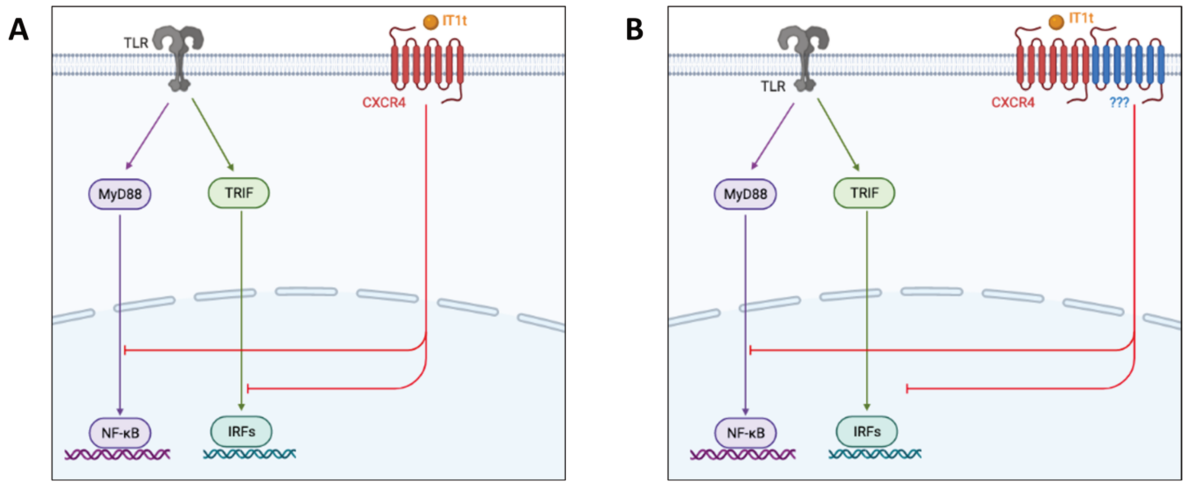

Figure 26: Hypothèse sur le mécanisme d'action induit par les ligands de la poche mineure de CXCR4. (**A**) Induction d'une voie de signalisation dépendant directement de CXCR4 qui inhibe la voie des TLRs. (**B**) Induction de la formation d'un hétérodimère avec CXCR4 qui aboutit à l'activation d'une voie de signalisation inhibant la voie des TLRs

A. Voie de signalisation induit par CXCR4

Comme vu dans l'introduction, de nombreuses voies de signalisations dépendantes de CXCR4 ont été décrites. L'objectif est de déterminer quelle(s) voie(s) est/sont induite(s) par les composés aminés de type CB via CXCR4, qui est forcément différent des voies induites par son ligand naturel CXCL12. Gomariz et al. ont décrit une voie de signalisation induites par la fixation de neuropeptides sur des GPCR. Cette signalisation qui recrute la β-arretine permet de bloquer les voies des TLR sur plusieurs niveaux : inhibition de l'ubiquitination de TRAF6, inhibition de la phosphorylation de p38 et inhibition de la phosphorylation de NF-kB. L'ensemble ces inhibitions permet d'aboutir à un effet anti-inflammatoire (Gomariz et al., 2010) (Fig.27). L'idée ici est de voir si les ligands de type CB induisent la même signalisation via CXCR4.

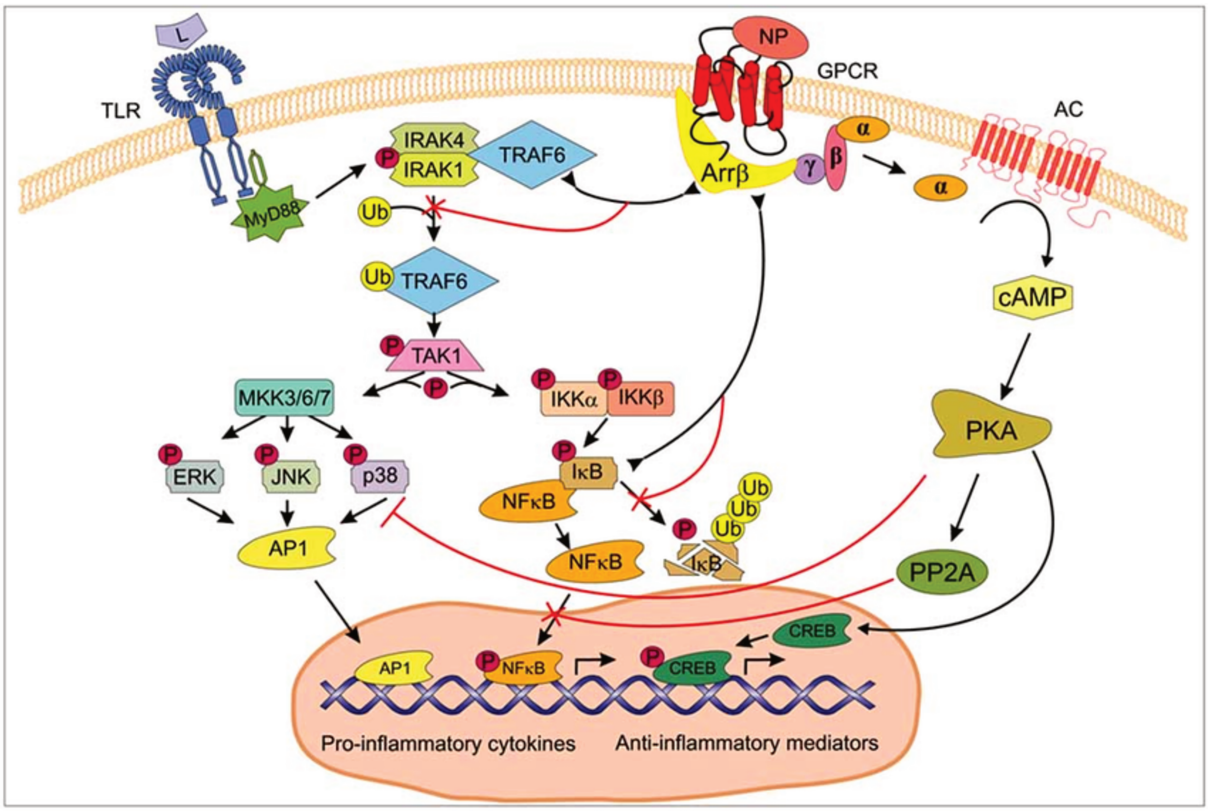

Figure 27: Voie de signalisation induite par la fixation de neuropeptide sur des GPCR qui régule négativement la voie des TLRs.
(Gomariz et al., 2010)

Inhibition de la phosphorylation de p38 par les ligands de CXCR4

Dans un premier temps, nous avons regardé si l'IT1t est capable de bloquer la phosphorylation de la protéine p38 induite par l'activation des TLR7/8 avec le R848. Pour cela, des monocytes ont été traités avec de l'IT1t ou de l'AMD3100, puis activés avec du R848. Après 15, 30 et 60 min d'activation, nous avons essayé de détecter la phosphorylation de p38 avec un anticorps spécifique pour la cytométrie en flux (Fig. 28). En conditions stimulé avec le R848, la forme phosphorylée de p38 est détectée ce qui n'est pas le cas dans les conditions non stimulés (NS). Le traitement par l'lT1t permet de bloquer cette phosphorylation de p38, ce que ne fait pas le cas du traitement AMD3100. Ceci démontre bien une réponse spécifique induite par les ligands de la poche mineure de CXCR4.

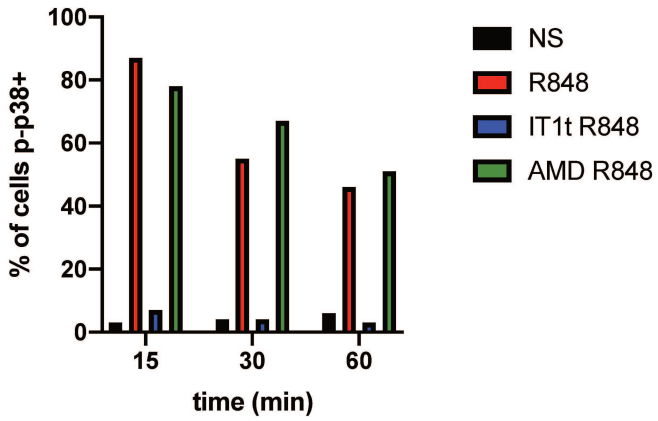

Figure 28: Détection de la phospho-p38 dans des monocytes activés par du R848 et traités avec des ligands de CXCR4.
Les monocytes ont été traités avec de l'IT1t (20µM) ou de l'AMD3100 (20µM), puis stimulés avec du R848. La protéine phospho-p38 a été détectée par cytométrie en flux.

Inhibition de la phosphorylation de pERK par les ligands de CXCR4

Dans un premier temps, nous avons regardé si l'IT1t est capable de bloquer la phosphorylation de la protéine ERK induite par l'activation des TLR7/8 avec le R848. Pour cela, des monocytes ont été traités avec de l'IT1t ou de CXCL12 (SDF1), puis activés avec du R848. Après 5, 10 et 20 min d'activation, nous avons essayé de détecter la phosphorylation de ERK avec un anticorps spécifique pour le western blot (Fig. 29). Après 10 min de stimulation, la forme phosphorylée de ERK est détectée dans les monocytes activés ce qui n'est pas le cas dans les conditions non stimulés (NS). Le traitement par l'lT1t permet de bloquer cette phosphorylation de p38, ce que ne fait pas le traitement CXCL12. Ceci démontre bien une rinduction spécifique des ligands de la poche mineure de CXCR4.

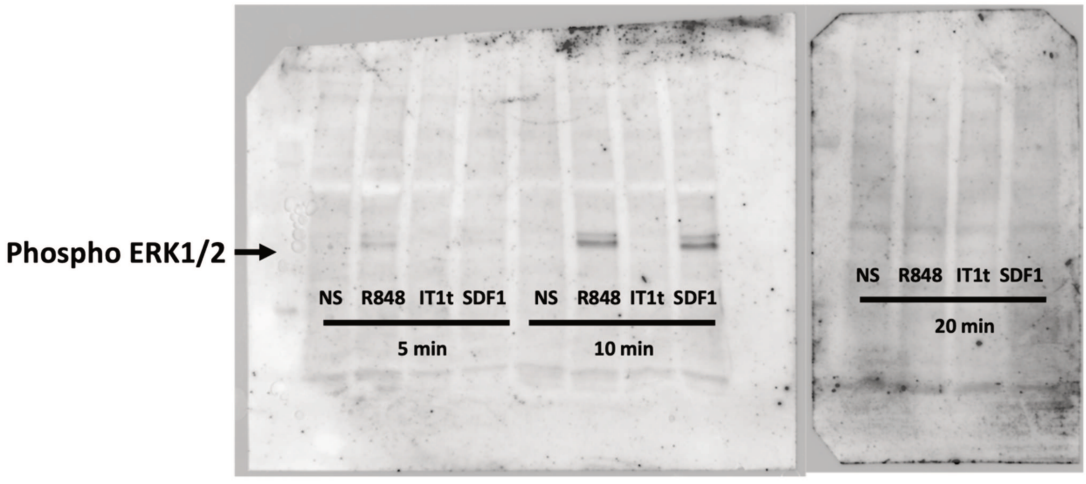

Figure 29: Détection de la phospho-ERK dans des monocytes activés par du R848 et traités avec des ligands de CXCR4.
Les monocytes ont été traités avec de l'IT1t (20µM) ou du SDF1, puis stimulés avec du R848. La protéine phospho-ERK a été détectée par western blot.

Le rôle de la B-arrestin dans l'activité anti-inflammatoire des ligands de la poche mineure de CXCR4

Les travaux de Gomariz et al. montrent un rôle centrale de la B-arrestin pour expliquer les propriétés anti-inflammatoires des neuropeptides via leur fixation sur les GPCRs (Gomariz et al., 2010). Nous avons donc voulu voir si la B-arrestin était aussi centrale dans l'activité anti-inflammatoires des composés de type IT1t et CB. Pour établir si l'activité immunorégulatrice des composés de type CB et IT1t est liée à B-arrestin, l'expression de cette dernière a été réduite dans les monocytes primaires à l'aide d'un petit ARN interférent (siARN) ciblant l'ARN messager codant pour la B-arrestin. Alors que la transfection d'un siARN control (siControl) n'a pas eu d'impact sur l'inhibition de la production des cytokines pro-inflammatoires induite par l'IT1t, ce dernier a perdu sa capacité à inhiber les productions intracellulaires de TNF-α dans les monocytes humains traités avec le siARN ciblant la B-arrestin (si B-arrestin). Ces données montrent que la B-arrestin est essentielle à l'activité immunorégulateurs de l'IT1t (Fig. 30.)

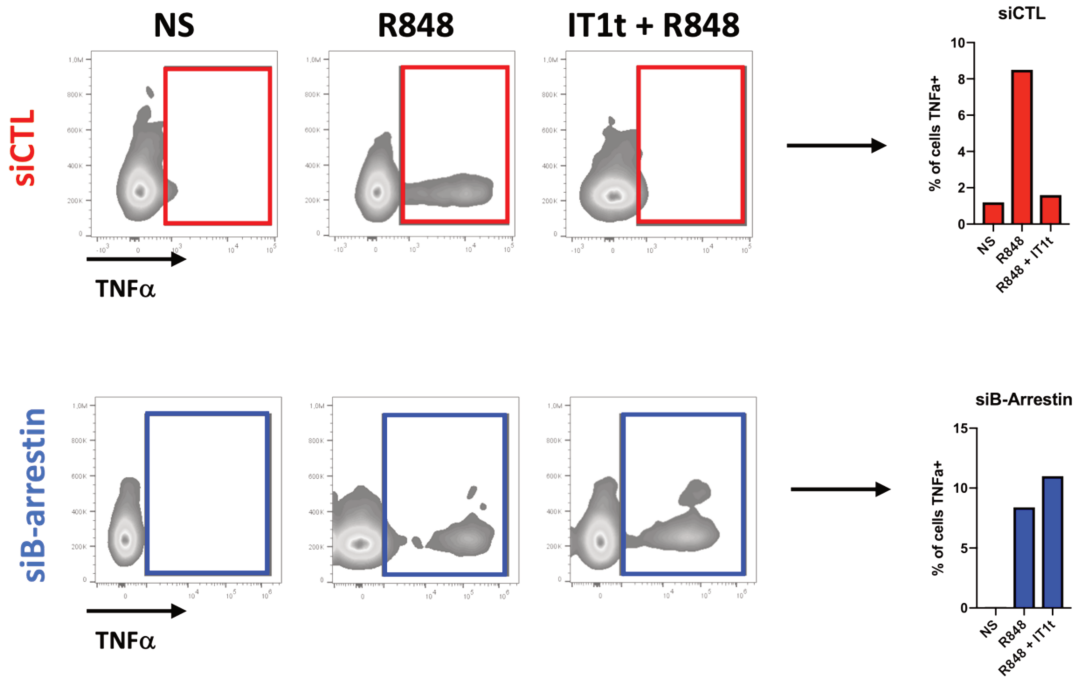

Figure 30: Role de la B-arrestin dans l'activité anti-inflammatoire de l'IT1t.

Les monocytes ont été traités pendant 24 heures avec le siARN B-arrestin (siB-arrestin) ou le siARN contrôle (siCTL) à 160 nM. Les cellules ont ensuite été pré-incubées avec de l'IT1t (20 µM) et stimulés avec du R848 (1μg/mL) pendant 6 heures. Les niveaux intracellulaires de TNF-α, a été évalués par cytométrie en flux.

B. Formation d'hétéromères CXCR4 en présences de ses ligands de la poche mineure.

De manière physiologique, CXCR4 est sous forme d'homodimère (Pawig et al., 2015). La fixation de l'IT1t sur CXCR4 empêche la formation homodimère de CXCR4. On peut ainsi émettre l'hypothèse que le récepteur CXCR4 qui se retrouve seul recrute un autre récepteur pour former un hétérodimère, et induire une signalisation qui aboutit aux propriétés anti-inflammatoires de l'IT1t. Plusieurs hétérodimères avec CXCR4 ont été décrit. Ils impliquent des récepteurs à chémokines : CXCR7, CCR5, CCR2…(Salanga et al., 2009) ou encore le récepteur α1-adrenergic (Albee et al., 2017).

Hétérodimère CXCR4/CXCR7

L'hétérodimère CXCR4/CXCR7 est l'un des plus décrit dans la littérature. Afin de déterminer si l'activité immunorégulatrice des composés de type CB et IT1t est liée au recrutement du récepteur CXCR7, l'expression de ce dernier a été réduite dans les monocytes primaires à l'aide d'un petit ARN interférent (siARN) ciblant l'ARN messager codant pour le récepteur CXCR7. La transfection d'un siARN control (siControl) n'a pas eu d'impact sur l'inhibition de la production des cytokines pro-inflammatoires induite par l'IT1t (Fig.31 A). Il en est de même avec la transfection du siARN CXCR7 (siCXCR7) ce qui implique que ce récepteur n'est pas impliqué dans la signalisation de l'IT1t qui aboutit à une activité immunorégulatrice (Fig.30 C). En parallèle du siCXCR7, nous avions réalisé des siARN ciblant CXCR4. Dans cette condition, l'IT1t perd son activité immunorégulateur ce qui confirme que CXCR4 est essentiel pour cette activité (Fig.31 B). L'expression du récepteur CXCR7 a été mesuré grâce au marquage membranaire du recepteur CXCR7 avec un anticorps anti-CXCR7 par cytométrie en flux (fig. 31.D). Ainsi, le siARN CXCR7 a bien permis de réduire l'expression du récepteur CXCR7 en comparaison aux monocytes ayant été traités avec le siARN control.

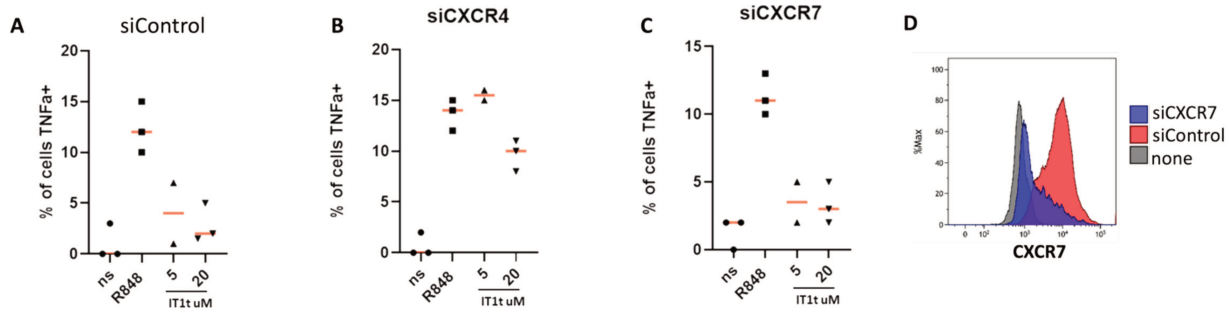

Figure 31: Implication du récepteur CXCR7 dans l'activité anti-inflammatoire de l'IT1t.
Les monocytes ont été traités pendant 24 heures avec le (A) siARN Contrôle (siControl) ou le (B) siARN CXCR4 (siCXCR4) ou le (C) siARN CXCR7 (siCXCR7) à 160 nM. Les cellules ont ensuite été pré-incubées avec de l'IT1t (5 et 20 µM) et stimulés avec du R848 (1µg/mL) pendant 6 heures. Les niveaux intracellulaires de TNF-α, a été évalués par cytométrie en flux. (D) l'expression de CXCR7 a été évalué par cytométrie en flux

Hétérodimère CXCR4/CCR2

De la même manière qu'a été testé l'hétérodimère CXCR4/CXCR7, nous avons testé l'hétérodimère CXCR4/CCR2 via la technologie de siARN ciblant cette fois-ci le récepteur CCR2 (fig.32). La transfection d'un siARN control (siCTL) n'a pas eu d'impact sur l'inhibition de la production des cytokines pro-inflammatoires induite par l'IT1t (Fig.32 A). Il en est de même avec la transfection du siARN CXCR2 (siCXCR2) ce qui implique que ce récepteur n'est pas impliqué dans la signalisation de l'IT1t qui aboutit à une activité immunorégulatrice (Fig.30 C). En parallèle, l'expression du récepteur CCR2 a été mesuré grâce au marquage membranaire du recepteur CCR2 avec un anticorps anti-CCR2 par cytométrie en flux (fig. 32.B). Ainsi, le siARN CCR2 a bien permis de réduire l'expression du récepteur CCR2 en comparaison aux monocytes ayant été traités avec le siARN control.

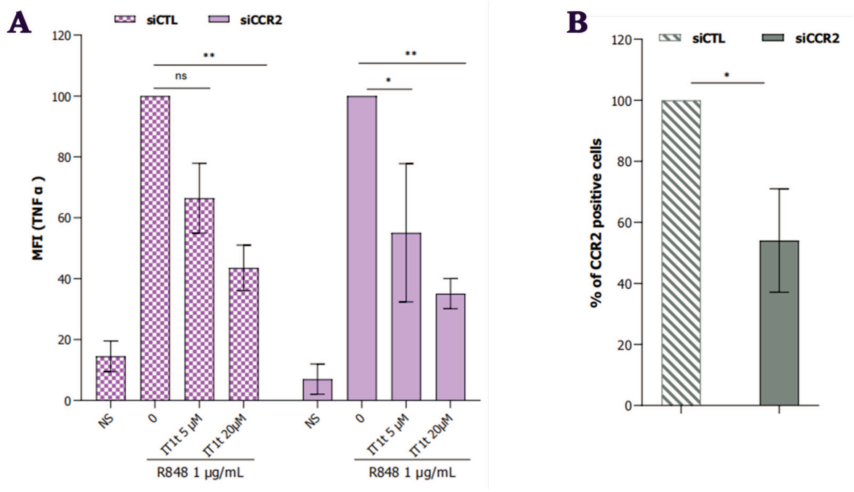

Figure 32: Implication du récepteur CCR2 dans l'activité anti-inflammatoire de l'IT1t.
Les monocytes ont été traités pendant 24 heures avec le siARN Contrôle (siCTL) ou le siARN CCR2 (siCCR2) à 160 nM. Les cellules ont ensuite été pré-incubées avec de l'IT1t (5 et 20 µM) et stimulés avec du R848 (1µg/mL) pendant 6 heures. (**A**) Les niveaux intracellulaires de TNF-α, a été évalués par cytométrie en flux. (**B**) l'expression de CCR2 a été évalué par cytométrie en flux

Les autres candidats pour les hétérodimères CXCR4 n'ont pas encore été testés.

IV. Perspectives

Ces travaux ont permis de mettre la B-arrestin au centre de notre attention. Bien qu'elle semble être essentielle à la signalisation médiée car les ligands de CXCR4, il faut maintenant établir le lien avec les voies des TLRs. La prochaine étape serait donc de voir si la B-arrestin permet de bloquer la poly-ubiquitination de TRAF6. Pour ce faire, il est prévu de faire une immunoprécipitation sur TRAF6, puis de vérifier la présence d'ubiquitine sur TRAF6 par western blot.

Une autre approche envisagée est l'utilisation de la cytométrie de masse (Cytof) afin d'étudier le profil de plusieurs phosphoprotéines d'intérêts au sein des différentes populations des PBMC. La Cytof permet de regarder simultanément plus de 40 marqueurs. Il sera ainsi possible de vérifier l'état de phosphorylation de plusieurs protéines, dont IRAK1 et 4, JNK ; NF-kB, CREB, ERK, p38…dans chaque sous-type cellulaire des PBMC grâce à des marqueurs de phénotypage.

D'autres candidats de la formation d'un hétérodimère avec CXCR4 en présence des ligands de sa poche mineure restent à vérifier avec la technologie siARN. Les prochains sur la liste sont les récepteurs CCR5 et le α1-adrenergique. En raison d'un grand nombre de candidats potentiels, nous allons réaliser en parallèles de la Co-IP sur CXCR4 couplé à de la spectrométrie de masse afin de déterminer quelle protéine est recrutée par CXCR4, en présence et en absence d'IT1t.

Enfin, il serait également intéressant de caractériser les effets des ligands de type CB, IT1t et 1411 sur les cellules de l'immunité adaptative.

LISTE DES FIGURES

Figure 1: Les acteurs cellulaires de l'immunité innée et adaptative. 15
Figure 2: Structure représentative des Toll-Like Receptors. 21
Figure 3: Localisation des Toll-Like Receptors. 22
Figure 4: Signalisation par les TLR. 24
Figure 5: Récepteur de type NOD 25
Figure 6: Activation of the NLRP3 Inflammasome 28
Figure 7: Voie de signalisation des RLR 30
Figure 8: Les quatre sous-familles de chimiokines classées selon leur structure 34
Figure 9: Transcription des ISG activée par les IFN I et III: voie de signalisation des IFNAR (Forero et al., 2019) 37
Figure 10: Chemokine receptor CXCR4 51
Figure 11: voies de la signalisation intracellulaire du couple SDF-1/CXCR4 52
Figure 12: Antagonistes de CXCR4 54
Figure 13: Modélisation in silico de CXCR4. 54
Figure 14: CB inhibe la production de TNF-α, IL-1β et IL-6 médiée par TLR-7/8 des monocytes humains. 59
Figure 15: L'activité immunorégulatrice du CB sur les monocytes primaires est dépendant de CXCR4. 61
Figure 16: Le CB contrôle l'inflammation spontanée des cellules de patients atteints d'AJI. 63
Figure 17: Le CB contrôle l'inflammation induite par les TLR7/8 dans les cellules de patients atteints d'AJI 65
Figure 18: Le CB contrôle l'inflammation et l'apparition de la maladie chez les souris arthritiques induites par le collagène. 67
Figure 19: Le CB contrôle l'inflammation dans le sang total des patients COVID-19 69
Figure 20: Le CB inhibe l'inflammation médiée par TLR7/8 dans les amygdales et les PBMC de donneurs sains. 71
Figure 21: Le CB contrôle l'inflammation induite et spontanée des cellules immunitaires de la moelle osseuse d'un patient atteint de LES. 73
Figure 22: Le CB contrôle l'inflammation et le développement de la maladie chez les souris atteintes de LES. 75
Figure 23: Nouvelles molécules anti-IFN ciblant le récepteur CXCR4. 78

Figure 24: Caractérisation des effets anti-inflammatoires du composé 1411 sur des cellules immunitaires. 80
Figure 25: L'activité immunorégulatrice du composé 1411 sur les monocytes primaires est dépendante de CXCR4. 82
Figure 26: Hypothèse sur le mécanisme d'action induit par les ligands de la poche mineure de CXCR4. 87
Figure 27: Voie de signalisation induite par la fixation de neuropeptide sur des GPCR qui régule négativement la voie des TLRs. 88
Figure 28: Détection de la phospho-p38 dans des monocytes activés par du R848 et traités avec des ligands de CXCR4. 89
Figure 29: Détection de la phospho-ERK dans des monocytes activés par du R848 et traités avec des ligands de CXCR4. 90
Figure 30: Role de la B-arrestin dans l'activité anti-inflammatoire de l'IT1t. 90
Figure 31: Implication du récepteur CXCR7 dans l'activité anti-inflammatoire de l'IT1t. 92
Figure 32: Implication du récepteur CCR2 dans l'activité anti-inflammatoire de l'IT1t. 93

LISTE DES TABLEAUX

Tableau 1: Ligands et localisation des TLR 22
Tableau 2: IC50 des activités anti-IFNs et de la viabilité des différents composés 78

Article 1

IMMUNOLOGY

Control of TLR7-mediated type I IFN signaling in pDCs through CXCR4 engagement—A new target for lupus treatment

Nikaïa Smith[1,2,3,4]*, Mathieu P. Rodero[1,2,3], Nassima Bekaddour[1,2,3], Vincent Bondet[5,6], Yasser B. Ruiz-Blanco[7], Mirja Harms[4], Benjamin Mayer[8], Brigitte Bader-Meunier[3,9,10,11], Pierre Quartier[3,9,10], Christine Bodemer[3,9,12], Véronique Baudouin[13], Yannick Dieudonné[14,15,16], Frank Kirchhoff[4], Elsa Sanchez Garcia[7], Bruno Charbit[17], Nicolas Leboulanger[3,18], Bernd Jahrsdörfer[19], Yolande Richard[3,20,21], Anne-Sophie Korganow[14,15,16], Jan Münch[4], Sébastien Nisole[22], Darragh Duffy[5,6,17], Jean-Philippe Herbeuval[1,2,3]*

Copyright © 2019 The Authors, some rights reserved; exclusive licensee American Association for the Advancement of Science. No claim to original U.S. Government Works. Distributed under a Creative Commons Attribution NonCommercial License 4.0 (CC BY-NC).

Type I interferons are highly potent cytokines essential for self-protection against tumors and infections. Deregulations of type I interferon signaling are associated with multiple diseases that require novel therapeutic options. Here, we identified the small molecule, IT1t, a previously described CXCR4 ligand, as a highly potent inhibitor of Toll-like receptor 7 (TLR7)–mediated inflammation. IT1t inhibits chemical (R848) and natural (HIV) TLR7-mediated inflammation in purified human plasmacytoid dendritic cells from blood and human tonsils. In a TLR7-dependent lupus-like model, in vivo treatment of mice with IT1t drives drastic reduction of both systemic inflammation and anti–double-stranded DNA autoantibodies and prevents glomerulonephritis. Furthermore, IT1t controls inflammation, including interferon α secretion, in resting and stimulated cells from patients with systemic lupus erythematosus. Our findings highlight a groundbreaking immunoregulatory property of CXCR4 signaling that opens new therapeutic perspectives in inflammatory settings and autoimmune diseases.

INTRODUCTION

Type I interferons (IFNs) are key immune response mediators and, in humans, are composed of 13 IFN-α subtypes as well as IFN-β, IFN-ε, IFN-κ, and IFN-ω. Type I IFNs signal through a ubiquitously expressed common receptor (IFNAR) formed by two transmembrane proteins, IFNAR1 and IFNAR2. IFNAR engagement results in activation of the cytoplasmic kinases Janus kinase 1 (JAK1) and tyrosine kinase 2 (TYK2), leading to the formation of the transcription factor complex IFN-stimulated gene factor 3 (ISGF3). This complex translocates to the nucleus to promote transcription of IFN-stimulated genes (ISGs) (*1*). Type I IFNs exert antiproliferative and immunomodulatory effects, essential to control viral infection and spread. However, sustained overproduction of type I IFN can be deleterious for the host in various infection settings (*2*) and in a class of disorders collectively termed type I interferonopathies (*3*) composed of rare monogenic diseases and complex inflammatory/autoimmune diseases such as systemic lupus erythematosus (SLE).

The recurrent development of lupus-like symptoms in patients receiving recombinant type I IFN for treatment of hepatitis or hematological disorders highlights the frequent pathogenic effects of these molecules in individuals with susceptibility to autoimmune disorders. SLE is a heterogeneous disease at the clinical and molecular level, with at least seven subtypes identified by blood transcriptome profile in pediatric SLE (*4*). However, all subtypes present the common feature of increased IFN signaling. Moreover, we previously demonstrated that increased IFN-α levels in the serum of patients with SLE correlate with both disease activity [SLE disease activity index (SLEDAI)] and the expression of prognostic markers such as anti–double-stranded DNA (dsDNA) antibodies and complement activity (*5*).

Plasmacytoid dendritic cells (pDCs) are specialized in rapid and massive secretion of type I IFN (*6*–*8*). pDCs are activated after recognition of pathogen nucleic acids by sensors such as Toll-like receptors (TLRs). pDCs express TLR7 and TLR9 (*9*, *10*), which respond to single-stranded RNA (ssRNA) and imidazoquinolines (R848) (*11*, *12*) or DNA and CpG-containing oligonucleotides (*13*), respectively. TLR activation triggers production of type I IFN and proinflammatory cytokines through MyD88-mediated IRF7 signaling (*14*). Many studies have highlighted a central implication of pDCs in the development of SLE, making these cells paramount targets for innovative therapies (*15*). This is further supported by an up-regulation of TLR7-mediated IFN-α production by pDCs in patients with SLE (*16*). Despite evaluations of multiple therapeutic strategies including

[1]CNRS UMR-8601, CICB, 45 rue des Saints-Pères, 75006 Paris, France. [2]Team Chemistry & Biology, Modeling & Immunology for Therapy, CBMIT, Paris, France. [3]Université Paris Descartes, Sorbonne Paris Cité, Paris, France. [4]Institute of Molecular Virology, Ulm University Medical Center, Ulm 89081, Germany. [5]Immunobiology of Dendritic Cells, Institut Pasteur, Paris, France. [6]INSERM U1223, Paris, France. [7]Computational Biochemistry and Center of Medical Biotechnology, University of Duisburg-Essen, 45141 Essen, Germany. [8]Institute for Epidemiology and Medical Biometry, Ulm University, Ulm, Germany. [9]Imagine Institute, Paris, France. [10]Paediatric Haematology-Immunology and Rheumatology Department, Hôpital Universitaire Necker, Assistance Publique-Hôpitaux de Paris, Paris, France. [11]INSERM UMR 1163, Laboratory of Immunogenetics of Paediatric Autoimmunity, Paris, France. [12]Department of Paediatric Dermatology, Reference Centre for Rare Skin Disorders (MAGEC), Hôpital Universitaire Necker-Enfants Malades, Assistance Publique-Hôpitaux de Paris, 75015 Paris, France. [13]Hôpital Universitaire Robert Debré, Néphrologie pédiatrique, Paris, France. [14]CNRS UPR 3572 "Immunopathology and Therapeutic Chemistry"/Laboratory of Excellence Médalis, Institute of Molecular and Cellular Biology (IBMC), Strasbourg, France. [15]Department of Clinical Immunology and Internal Medicine, National Reference Center for Rare Autoimmune Diseases, University Hospital, Strasbourg, France. [16]UFR Medicine, University of Strasbourg, Strasbourg, France. [17]Centre for Translational Research, Institut Pasteur, Paris, France. [18]Pediatric Otolaryngology Department, Hôpital Necker-Enfants Malades, Assistance Publique Hôpitaux de Paris, Paris, France. [19]Institute of Transfusion Medicine and Immunogenetics (IKT) Ulm, Helmholtzstr. 10, 89081 Ulm, Germany. [20]INSERM U1016, Institut Cochin, Paris, France. [21]CNRS UMR 8104, Paris, France. [22]IRIM, Université de Montpellier, CNRS UMR, 9004 Montpellier, France.
*Corresponding author. Email: jean-philippe.herbeuval@parisdescartes.fr (J.-P.H.); nikaiafjsmith@gmail.com (N.S.)

anti-IFN and anti-IFNAR antibodies, a drug specifically targeting the type I IFN pathway in SLE fails to demonstrate efficacy. Molecular heterogeneity of SLE may provide an explanation for the failure of clinical trials based only on clinical diagnosis (*1*).

Previous studies have proposed the chemokine receptor CXCR4 as a promising drug target to reduce SLE symptoms in severe pathology through inhibition of inflammatory cell recruitment (*17*, *18*). Consistently, we recently discovered that binding of small natural and synthetic amino compounds to CXCR4 drives a profound immunosuppressive signaling in human pDCs (*19*). However, none of these amino compounds were highly specific for CXCR4. Therefore, we aimed to assess two specific ligands with high affinity for CXCR4: the small amino compound named IT1t that was identified as a potential candidate as it is the only small molecule that cocrystalized with CXCR4 (*20*) and the AMD3100 (Plerixafor), a Food and Drug Administration (FDA)–approved CXCR4 blocker used for $CD34^+$ bone marrow–derived progenitor cell collection before hematopoietic stem cell transplantation (*21*). IT1t and AMD3100 bind differently to CXCR4 into the major or the minor subpocket of CXCR4, respectively (*20*, *22*), which are also different from CXCL12 (CXCR4 natural ligand) binding sites.

We examined the effects of IT1t and AMD3100 on pDC activation and IFN production. Notably, we found that IT1t, but not AMD3100, strongly inhibits TLR7–type I IFN signaling in human pDCs from blood and tonsils. Moreover, IT1t controls inflammation in cells of patients with lupus and drastically reduced inflammation and levels of dsDNA antibodies, a pathogenesis marker, in a pristane-induced SLE mouse model. Our study identifies the IT1t binding site on CXCR4 as a potential modulator of pDC activity and places this pocket as a promising novel therapeutic target in autoimmune diseases.

RESULTS

IT1t controls TLR7-mediated type I IFN signaling in human pDCs in a CXCR4-dependent manner

We previously demonstrated that engagement of CXCR4 by natural amines and the synthetic mimic of histamine (clobenpropit) strongly inhibits viral-induced inflammation of human primary pDCs (*19*). To identify synthetic compounds with similar properties, we searched for known CXCR4 ligands with similar structures. The first cocrystalized structure of CXCR4 was achieved with a small compound called IT1t showing a strong structural homology with clobenpropit (fig. S1, A to C) (*20*). IT1t binds to an allosteric deep pocket that appears to be distinct from the FDA-approved CXCR4 antagonist AMD3100 binding site (fig. S1, D and E) (*23*, *24*). These pockets were called major pocket for the AMD3100 binding site (fig. S1F) and minor subpocket for the IT1t binding site (fig. S1G) (*20*, *22*), opening the possibility for distinct biological activity. Furthermore, IT1t K_i was evaluated previously and had a value of 0.41 ± 0.07 nM (*19*).

Given the central role of TLR7-driven type I IFN production in the pathophysiology of SLE, we investigated the ability of IT1t to control secretion of type I IFN by pDCs activated by distinct TLR7 agonists (R848 and HIV-1). A dose range from 0 to 50 μM AMD3100 and IT1t was added to pDCs in vitro in the presence or absence of R848 overnight. We first tested the potential cytotoxicity of both molecules on purified human pDCs (fig. S1H) activated by the TLR7/TLR8 synthetic stimulator R848 by flow cytometry and showed that neither IT1t nor AMD3100 induced toxicity up to 50 μM (fig. S1, I to M). R848 induced a massive increase of intracellular IFN-α production in purified pDCs (Fig. 1A). This increase was blocked in a dose-dependent manner by IT1t starting from 5 μM. In contrast, AMD3100 did not display any inhibitory activity as we previously reported (*19*). To verify the efficacy of AMD3100, we tested it on HIV-1 infection, and we confirmed that both AMD3100 and IT1t were able to block HIV-1 X4 tropism infection but not HIV-1 R5 tropism as previously demonstrated (fig. S1, N and O) (*25*, *26*). IT1t-specific inhibition of R848-induced IFN-α production in pDCs was confirmed with cells derived from six individual donors (Fig. 1, B and C). In agreement with a reduced intracellular expression of IFN, IT1t treatment also resulted in greatly reduced IFN-α/β protein concentrations in supernatants of R848-stimulated pDCs (Fig. 1D). To confirm the ability of IT1t to control TLR7-induced IFN-α, we evaluated its efficacy after HIV-1 stimulation, also known to be a strong TLR7 activator (*12*). As previously published (*19*), we did not observe any inhibitory activity of AMD3100. However, IT1t significantly reduced virus-induced IFN-α production at concentrations ≥5 μM (fig. S2, A to E). To further address the mechanism associated with IT1t inhibition of type I IFN in primary pDCs, we performed intracellular IFN-α and pIRF7 staining on R848-stimulated cells in the presence or absence of IT1t (Fig. 1, E and F). As expected, R848 treatment is associated with a strong increase of $pIRF7^+$ pDCs. Furthermore, 50% of the $pIRF7^+$ cells coexpressed IFN-α. Under IT1t treatment, pDCs failed to phosphorylate IRF7 and, consequently, did not express IFN-α. Furthermore, we showed by confocal microscopy that pIRF7 translocates into the nucleus of cells upon R848 activation (Fig. 1G), which was in turn inhibited by IT1t treatment (Fig. 1H). We validated the latest results by real-time quantitative polymerase chain reaction (RT-qPCR) and showed reduced levels of total IRF7 messenger RNA (mRNA) (Fig. 1G).

To definitively demonstrate that the IT1t immunoregulatory effect is dependent on CXCR4, we silenced CXCR4 expression using a previously established small interfering RNA (siRNA) protocol in human pDCs (*27*). We first confirmed the efficiency of our silencing by measuring CXCR4 mRNA expression by RT-qPCR (Fig. S3A). TLR7 stimulation by HIV particles strongly induced type I IFN and ISG (TRAIL or TNF-related apoptosis-inducing ligand) transcriptions, which were potently inhibited by IT1t. As expected, IT1t inhibitory effect on TLR7-mediated type I IFN and ISG transcription was almost abrogated in siCXCR4 but not in control siRNA cyclophilin B (siCTR)–treated cells (fig. S3, B and C).

To obtain more comprehensive insights into the effect of IT1t on pDC activation, we performed a gene expression array of 579 inflammatory markers in R848-stimulated pDCs from three donors treated or not with IT1t. Principal components analysis (PCA) showed that cells from each donor clustered together depending on treatment (Fig. 2A). Of the 579 genes analyzed, 136 significantly increased (n = 68) or decreased (n = 70) under R848 stimulation (Fig. 2B). Expectedly, 53% of the 68 genes up-regulated are IFN genes (n = 3) and ISGs (n = 32) (Fig. 2C). In comparison, pDCs stimulated with R848 and treated with IT1t display significant up-regulation of merely 18 genes (8 ISGs, 10 IFN). We further confirmed our results on selected genes by RT-qPCR on two different donors and showed that type I IFN, TRAIL, and MxA were inhibited in R848-stimulated pDCs by IT1t (Fig. 2D). Note that genes up-regulated by R848 treatment do not reflect the proportion of the different class of genes in the array. Notably, ISGs increased from 24% in the whole array to 48% in the R848-induced gene list, supporting the impact of this stimulation on type I IFN signaling (fig. S4).

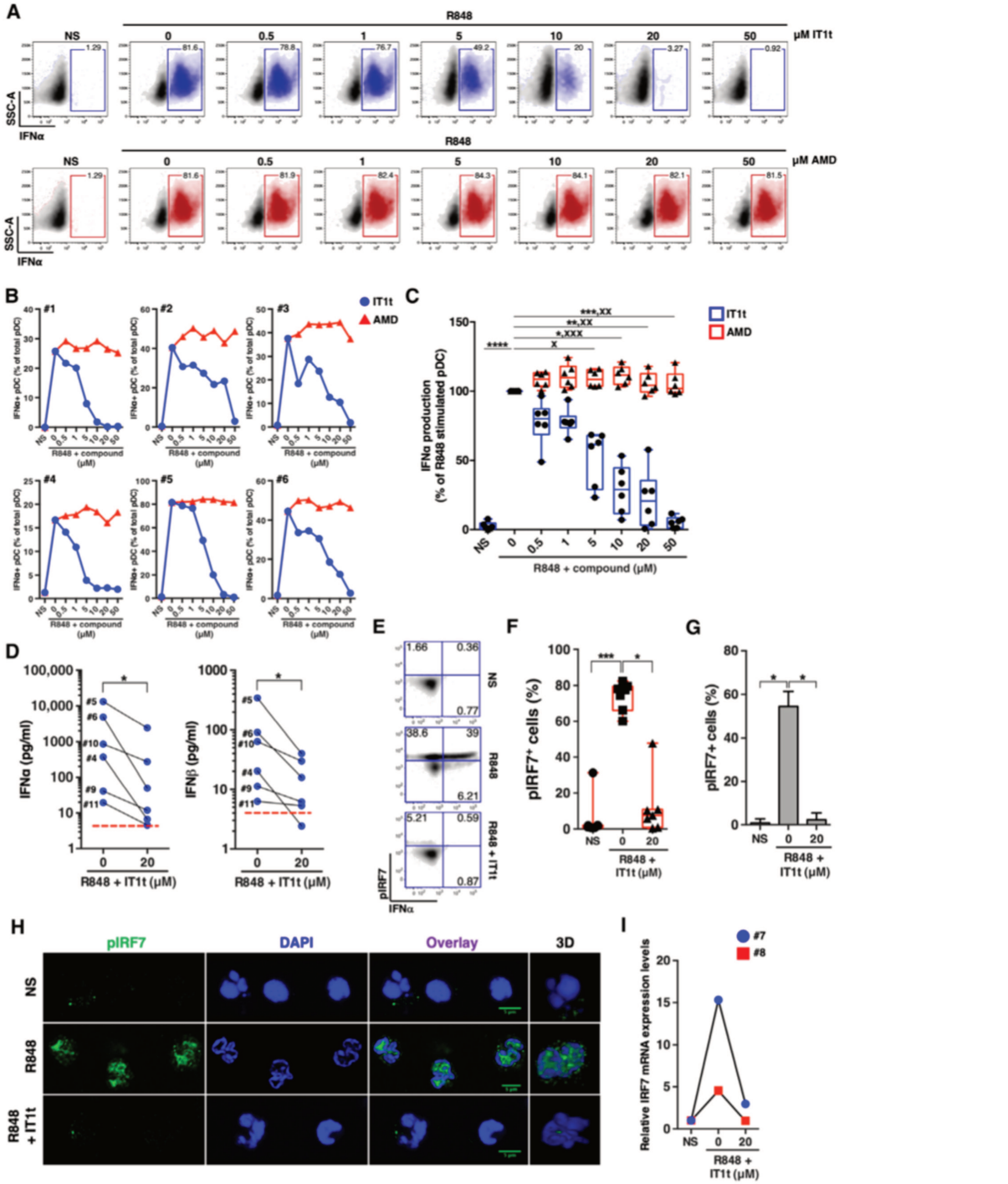

Fig. 1. IT1t suppresses TLR7-mediated IFN-α production in pDCs. Isolated human pDCs were preincubated with IT1t or AMD3100 and then stimulated with R848 overnight (5 μg/ml). (**A**) pDCs were cultured with R848 in the presence of increased dose of AMD3100 or IT1t. Intracellular levels of IFN-α were evaluated by flow cytometry. SSC-A, side scatter. (**B**) Individual and (**C**) combined representation of the effect of AMD3100 and IT1t on the IFN-α production of R848-stimulated pDCs from six healthy donors. Box and whisker plots with median ± minimum to maximum. Friedman test with Dunn's post hoc correction. "*" represents the statistical analysis comparing IT1t to the control R848 alone. "X" represents the statistical analysis comparing each concentration of IT1t to AMD3100. (**D**) Cytokine production was measured in the supernatant of the cells from six healthy donors using the multiplex bead-based immunoassay LEGENDplex. Average baseline of the nonstimulated condition is represented by the red dashed line. Wilcoxon test. (**E**) Intracellular levels of phosphorylated IRF7 and IFN-α were evaluated by flow cytometry. (**F**) Quantification of pIRF7 from seven individuals obtained by flow cytometry. Box and whisker plots with median ± minimum to maximum. Kruskal-Wallis with Dunn's post hoc correction. (**G**) Quantification by microscopy of the number of pIRF7$^+$ pDCs out of 130 cells per condition in average. Friedman test with Dunn's post hoc correction. (**H**) Confocal microscopy of purified pDCs showing pIRF7 (green) and nucleus [DAPI (4′,6-diamidino-2-phenylindole), blue]. Scale bars, 5 μm. 3D was reconstructed with ImageJ using, on average, 30 stacks. (**I**) mRNA levels of IRF7 were quantified by RT-qPCR. ****$P < 0.0001$, ***$P < 0.001$, **$P < 0.01$, *$P < 0.05$. NS, nonstimulated.

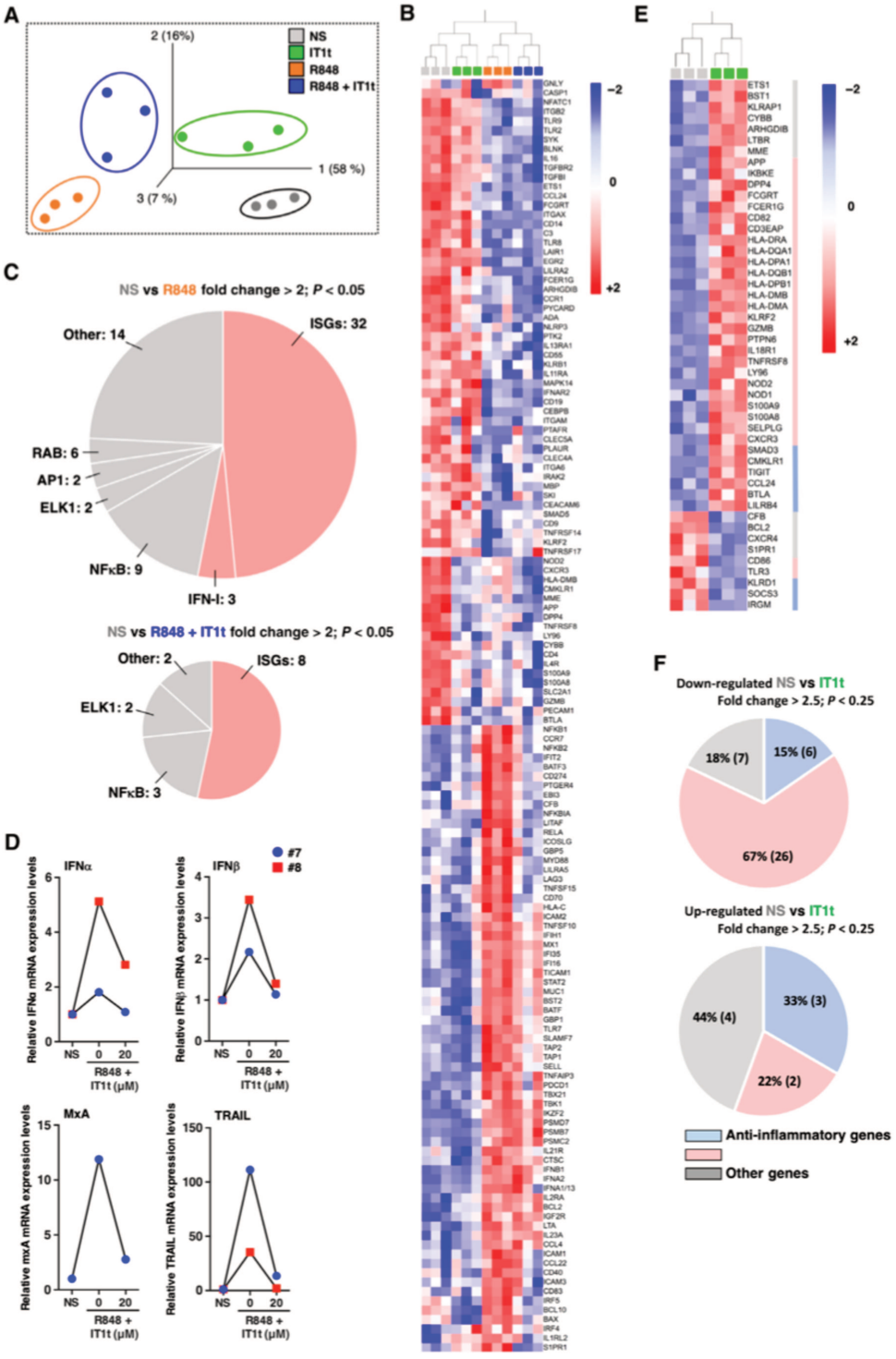

Fig. 2. IT1t prevents TLR7-mediated inflammation in pDCs. Isolated human pDCs were cultured with R848 (5 μg/ml) in the presence or absence of IT1t (20 μM). Total RNA from the cells was isolated and analyzed using the NanoString nCounter. (**A**) PCA was performed on the basis of 136 genes from the array differentially expressed between the NS (gray) and the R848 (orange) conditions. ($P < 0.05$, fold change > 2). (**B**) Heat map represents mRNA fold increase of the 136 genes significantly differently expressed between the NS and the R848 condition ($P < 0.05$, fold change > 2). (**C**) Pie chart representation of the promoters associated with genes significantly up-regulated between the NS and the stimulated (R848) condition and between the NS and the R848 + IT1t condition ($P < 0.05$, fold change > 2). The red parts represent ISGs (ISGF3 promoter) and the type I IFN (IRF7 promoter). Areas of the pie slices are representative of the number of genes. (**D**) mRNA levels of various genes were quantified by RT-qPCR for confirmation in two healthy donors. (**E**) Heat map represents the mRNA fold increase of 85 genes differently expressed between the NS (gray) and the IT1t (green) condition ($P < 0.05$, fold change > 2.5). (**F**) Pie chart represents the impact on inflammation of differently expressed genes between NS and IT1t. NS, nonstimulated.

The comparison of gene expression levels between the nonstimulated and the IT1t groups reveals that IT1t modulates gene transcription in the absence of stimulation (Fig. 2E). We identified 23 up-regulated and 62 down-regulated genes in pDCs treated with IT1t compared to the nonstimulated condition (fold change > 2.5; $P < 0.05$). IT1t treatment alone induced an enrichment of proinflammatory genes in the most down-regulated genes and an enrichment of anti-inflammatory genes, including SOCS1, SOCS3, and IRF4 in the most up-regulated genes (Fig. 2F). Together, these results demonstrate that IT1t treatment controls TLR7-induced type I IFN signaling in human pDCs at the transcriptomic and proteomic level in a CXCR4-dependent manner.

IT1t controls TLR7-mediated type I IFN and inflammation in mixed cell populations

As pDCs represent a very small fraction of immune cells in circulation (0.1 to 0.8%), we aimed to address whether we could target this rare population in the peripheral blood mononuclear cells (PBMCs). First, we assessed which leukocyte subsets in PBMCs could produce IFN-α upon R848 stimulation. R848 did not induce IFN-α production in $CD3^+$ T cells, $CD56^+$ NK (natural killer) cells, $CD3^+CD56^+$ NK T cells, $CD19^+$ B cells, or $CD14^+$ monocytes (Fig. 3A). However, a strong increase of IFN-α^+ pDCs was observed after stimulation. Overall, more than 90% of the IFN-α–producing cells were $CD123^+BDCA4^+$ pDCs (Fig. 3, B and C). Furthermore, treatment of PBMCs with IT1t reduced IFN-α production by pDCs in a dose-dependent manner (Fig. 3, D and E).

Human tonsils represent an integrative and physiological ex vivo model to study innate immune responses at the mucosal interface (Fig. 4A) (*28*, *29*). We thus tested IT1t biological activity on tonsil mononuclear cell suspensions (TMCs), which mimic the role of a secondary lymphoid organ. We first characterized the immune profile of cells present in the culture and quantified the number of pDCs, which represents about 5% of the lineage-negative HLA-DR–positive (Lin^-DR^+) immune cells (Fig. 4, B and C). Stimulation of TMCs overnight with R848 increased the frequency of IFN-α^+ pDCs about 10-fold, and treatment with IT1t (20 μM) resulted in a 67% reduction of this induction (Fig. 4D). We thus took advantage of the cellular diversity of the TMC model to evaluate the impact of IT1t on a broader set of inflammatory molecules. TMCs from seven donors were stimulated with R848 in the presence or absence of IT1t. IT1t reduced type I and type II IFN, proinflammatory cytokines [IL-6 (interleukin-6), TNF-α (tumor necrosis factor–α), IL-1β, IL-12p70, and GM-CSF (granulocyte-macrophage colony-stimulating factor)],

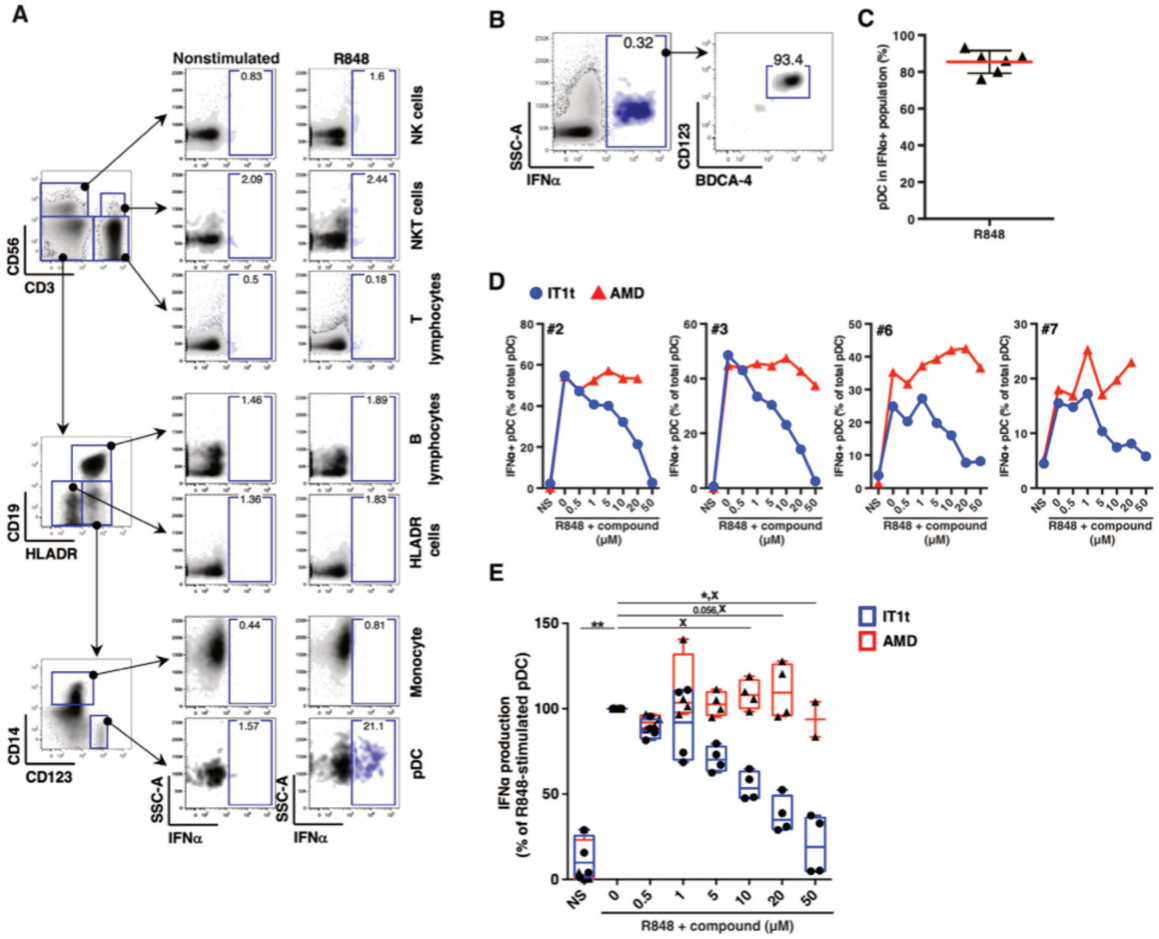

Fig. 3. IT1t blocks TLR7-mediated IFN production of circulating pDCs in PBMC cultures. (**A** and **B**) PBMCs from healthy individuals were cultured with R848 (5 μg/ml). IFN-producing cells were identified by flow cytometry. (**C**) Percentage of pDCs within the IFN-α^+ PBMCs after R848 stimulation from six different donors. (**D**) Individual and (**E**) combined representation of the effects of AMD3100 and IT1t on R848-induced IFN-α production in the pDC fraction from PBMCs from four healthy donors. Box and whisker plots with median ± minimum to maximum. Friedman test with Dunn's post hoc correction. "*" represents the statistical analysis comparing IT1t to the control R848 alone. "X" represents the statistical analysis comparing each concentration of IT1t to AMD3100. $^{**}P < 0.01$, $^{*}P < 0.05$. NS, nonstimulated.

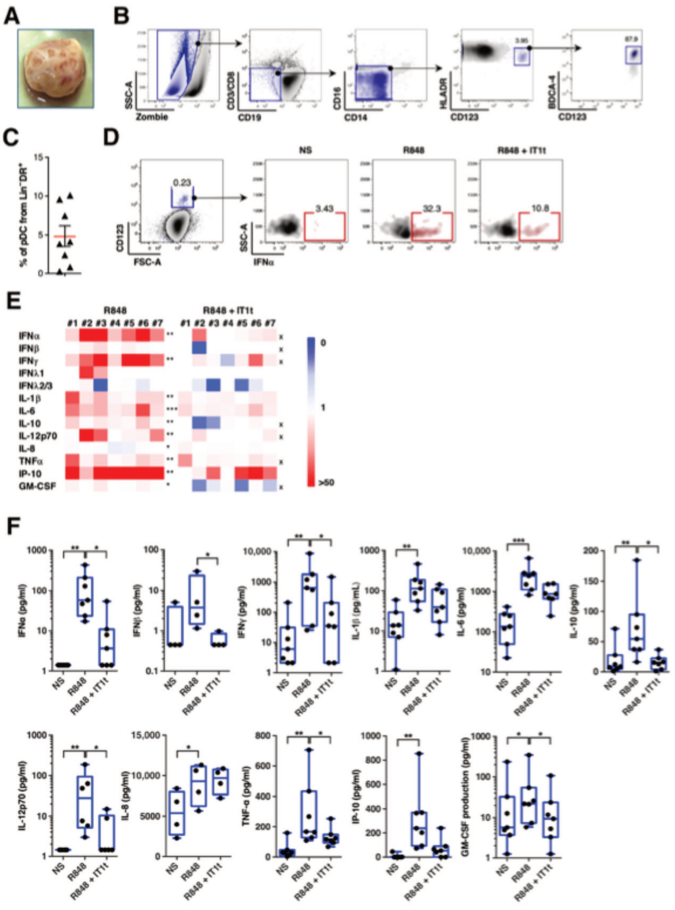

Fig. 4. IT1t suppresses TLR7-mediated inflammation in tonsil resident pDCs. (**A**) Picture of human tonsil after surgical removal. (**B**) pDCs from tonsils were identified as CD8-CD3-CD16-CD14-CD123 + HLADR$^+$BDCA-4$^+$. (**C**) Percentage of pDCs within the Lin$^-$DR$^+$ cells from eight human tonsils. (**D**) TMCs of healthy individuals were cultured with R848 (5 μg/ml) in the presence or absence of IT1t (20 μM). IFN$^+$ pDCs were identified and quantified by flow cytometry. (**E** and **F**) Effect of IT1t on R848-stimualted TMCs was evaluated in the supernatant of seven healthy individuals using LEGENDplex. (E) Heat map represents the fold increase in cytokine secretion compared to NS. "*" represents the statistical analysis comparing the R848 to the NS condition. "X" represents the statistical analysis comparing the R848 to the R848 + IT1t condition. (F) Graphs represent the concentration in picograms per milliliter of each measured cytokine. Box and whisker plots with median ± minimum to maximum. Friedman test with Dunn's post hoc correction. *** or $^{XXX}P < 0.001$, ** or $^{XX}P < 0.01$, * or $^{X}P < 0.05$. (Photo credit: N. Smith, CNRS UMR-8601, CBMIT, Université Paris Descartes, Paris, France, and Institute of Molecular Virology, Ulm University Medical Center, Ulm, Germany.) NS, nonstimulated.

and chemokine (CXCL-10) protein production in cells from all seven donors (Fig. 4, E and F). Therefore, IT1t controls type I IFN and a large spectrum of inflammatory cytokine production in isolated pDCs, as well as in complex cell populations.

IT1t suppresses inflammation and disease progression in an SLE mouse model

We next aimed to evaluate whether IT1t-mediated immune modulation could have an impact in inflammatory disease progression. SLE represents one of the most common interferonopathies (*30*). TLR7 and TLR7-mediated IFN signaling are well documented as a major player of SLE disease development (*16*, *31*–*33*) and response to treatment (*34*). Several mouse models have led to a clearer understanding of the role of type I IFN in the pathogenesis of lupus-like disease. Nevertheless, pristane-induced SLE meets most of the Systemic Lupus Erythematosus International Collaborating Clinics (SLICC) criteria used for human lupus classification, with the presence of an IFN signature and anti-dsDNA antibodies (*35*). Pristane induces type I IFN production mainly through the TLR7/MyD88 pathway (*36*). TLR7 deficiency not only abolishes pristane-induced type I IFN production but also prevents autoantibody production and renal disease, indicating a key role of TLR7/MyD88/type I IFN pathway in this model (*36*, *37*). Given the broad immunoregulatory properties of IT1t under TRL7 stimulation, including inhibition of type I and type III IFNs, TNF-α, and IL-6 protein production, we evaluated the effect of IT1t as a valuable therapeutic approach for SLE.

First, by using either a system of reporter cell line measuring all types of IFN (STING-37 cells) (*38*) or a specific IFN-α bead assay (LEGENDplex), we showed that in ex vivo tonsil cultures, pristane induced IFN-α production, which was significantly reduced by IT1t treatment (Fig. 5, A and B). Then, SLE was induced in BALB/c mice by daily intraperitoneal coinjection of pristane (0.5 ml per mouse) with vehicle or with different IT1t doses (3, 10, and 30 mg/kg or mpK) for 10 weeks. As a reference treatment, SLE mice were treated daily with the corticosteroid prednisolone at 15 mpK (Fig. 5C). IT1t-treated mice did not demonstrate any sign of stress or weight loss as compared to vehicle, indicating the good tolerance of the treatment by the animals (Fig. 5D).

Cytokines IFN-α, IL-1β, IL-17, TNF-α, and TRAIL were quantified as markers for SLE from serum at weeks 4 and 10. It should be noted that IFN-α was not detectable in serum of pristane-treated mice. However, we could detect increased levels of the IFN-induced protein TRAIL and of inflammatory cytokines. Prednisolone treatment was used as a positive therapeutic control and reduced all cytokines measured (Fig. 5, E to H). IT1t, similarly to prednisolone, strongly reduced production of IL-1β, IL-17, and TRAIL in a dose-dependent manner (Fig. 5, E to H). The production of TNF-α at week 10 was totally inhibited by prednisolone in contrast to IT1t treatments (Fig. 5G). Thus, these results suggest a distinct pattern of immunosuppressive activity of prednisolone and IT1t in SLE mice. The severity of SLE pathogenesis was also estimated by measuring levels of dsDNA antibodies. The high dose of IT1t significantly decreased anti-dsDNA levels during the whole treatment as early as week 4, in contrast to prednisolone, which only significantly reduced antibodies levels at week 8 (Fig. 5I). In line with this observation, we observed a reduced proportion of mice developing glomerulonephritis in the groups treated with 10 and 30 mpK of IT1t compared to vehicle (Fig. 5J). Together, these results highlight that intraperitoneal injection of IT1t reduces SLE-associated phenotypes faster than the reference corticosteroid treatment and with a greater selectivity on cytokine production.

IT1t controls type I IFN in vitro in cells from patients with SLE

SLE is a chronic disease characterized by periods of low disease activity and periods of high disease activity termed "flares," where patients experience an inflammatory storm associated with fever and skin rash (*39*). We recently demonstrated that circulating levels of IFN-α are higher in SLE patients with greater disease activity (*5*). Therefore, we evaluated whether IT1t treatment reduces TLR7-mediated IFN-α production in these patients. PBMCs from healthy controls and patients with lupus were stimulated with R848 to mimic an inflammatory burst with a strong type I IFN signature (Fig. 6A).

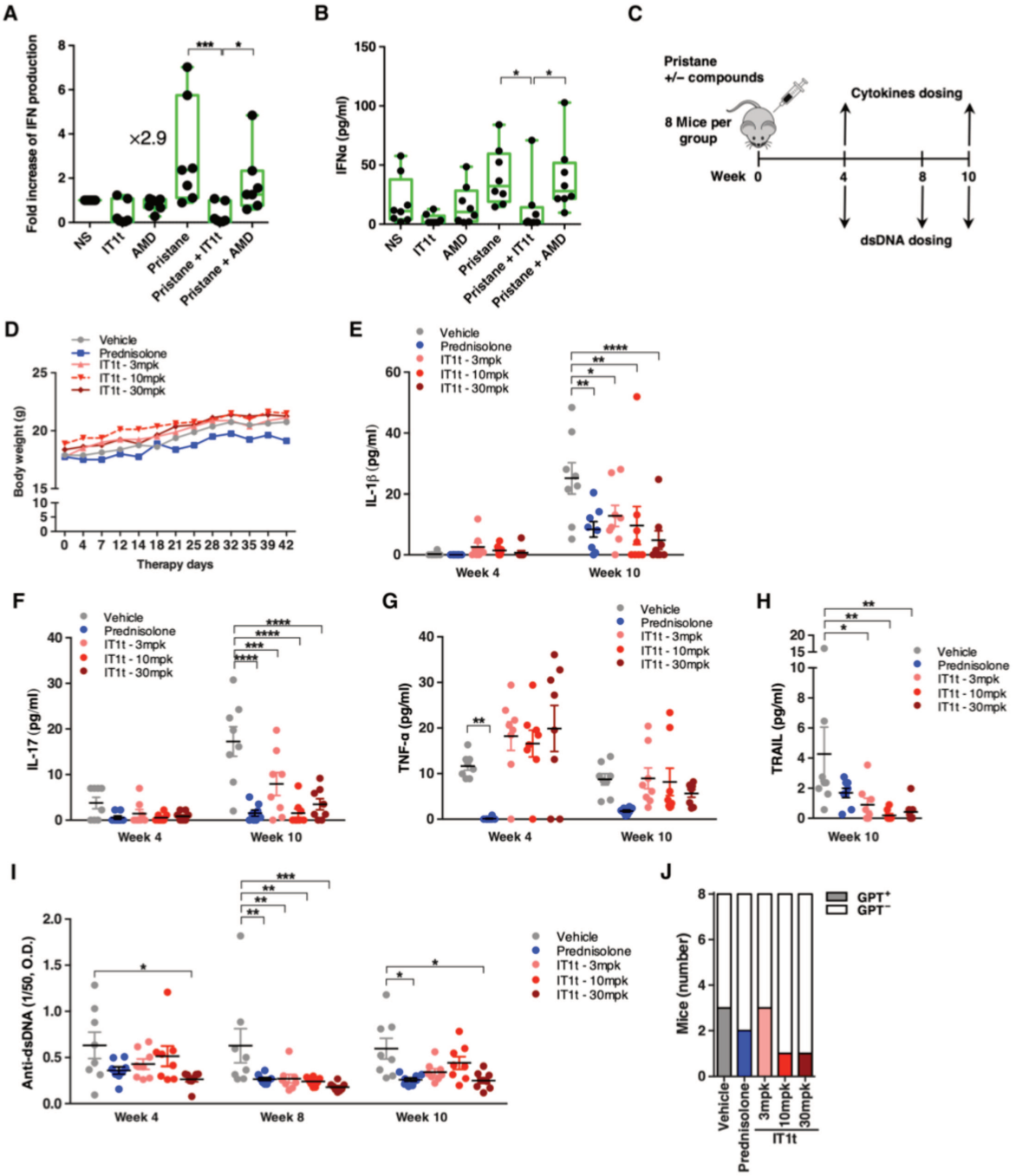

Fig. 5. IT1t reduces TLR7-mediated inflammation and markers of disease progression in SLE mice. Human TMCs were preincubated with IT1t or AMD3100 (20 μM) and stimulated overnight with pristane (200 μg/ml). IFN production was measured in supernatants using (**A**) the STING-37 reporter cell line or (**B**) the multiplex bead-based immunoassay LEGENDplex. Box and whisker plots with median ± minimum to maximum. Kruskal-Wallis test with Dunn's post hoc correction. (**C**) Mice were injected intraperitoneally daily with 0.5 ml of pristane to induce disease and with treatment consisting of prednisolone (15 mg/kg) or 3, 10, or 30 mpK of IT1t for 10 weeks. (**D**) Body weight was measured. (**E** to **H**) Inflammatory status was evaluated in the serum of mice by protein dosage of IL-1β (E), IL-17 (F), TNF-α (G), and TRAIL (H). Two-way repeated-measures analysis of variance (RM ANOVA) with Bonferroni post hoc correction. One-way ANOVA for TRAIL. (**I**) Anti-dsDNA antibody titers were measured on weeks 4, 8, and 10. Two-way RM ANOVA with Bonferroni post hoc correction. (**J**) Relative proportion of mice that develop glomerulonephritis in each group compared to the vehicle was assessed. All data are presented as mean ± SEM. ****$P < 0.0001$, ***$P < 0.001$, **$P < 0.01$, *$P < 0.05$. $n = 8$ mice per group. NS, nonstimulated.

IT1t treatment controlled IFN production in patients' and controls' PBMCs (Fig. 6B). Intracellular flow cytometry analysis reveals that R848-induced IFN production by patient and control PBMCs was mainly restricted to pDCs, which is in line with our previous observations. Furthermore, this IFN production by pDCs was abrogated by IT1t treatment (Fig. 6, C and D).

In humans, SLE is known to be a very heterogeneous disease with a large phenotypic and inflammatory spectrum (*40*). This heterogeneity

was observed in cultured PBMCs from patients, with some demonstrating a measurable spontaneous inflammation (SpI patients), while being undetectable in others. To assess the capacity of IT1t to control human lupus–driven spontaneous inflammation, we cultured PBMCs of four patients and monitored IFN-α secretion by digital ELISA (enzyme-linked immunosorbent assay), STAT1 (signal transducer and activator of transcription 1) and STAT3 phosphorylation status by flow cytometry, and inflammatory transcript levels by RT-PCR (Fig. 6E). For all patients with constitutive in vitro secretion of IFN-α, we observed a strong inhibition with IT1t treatment (Fig. 6F). Similarly, in cells from patients with spontaneous up-regulation of pSTAT1 and pSTAT3, IT1t treatment was associated with a reduction of STAT1 and STAT3 phosphorylation to a level similar to cells from healthy individuals (Fig. 6, G to J). Despite heterogeneous inflammatory profiles, treatment with IT1t consistently normalized the level of inflammatory gene transcripts in cells from patients with lupus (Fig. 6K), suggesting that targeting of CXCR4 by IT1t constitutes a promising strategy for controlling human inflammation.

DISCUSSION

New strategies to block the type I IFN pathway in SLE pathology are of great interest. In this study, we show that IT1t, a CXCR4 minor pocket ligand, has a strong immunosuppressive activity on TLR7-activated pDCs. Furthermore, IT1t treatment controlled inflammation, reduced dsDNA antibody titers in a lupus mouse model, and controlled type I IFN production and signaling in cells isolated from patients with lupus. We propose to consider targeting CXCR4 using small amino compounds such as IT1t as a potential innovative therapeutic strategy in interferonopathies.

pDCs are specialized in rapid and massive secretion of type I IFN in response to innate immune sensor stimulation from the TLR family (*8*, *10*, *41*, *42*). There is supporting evidence that overproduction of type I IFN by pDCs is central in development and progression of numerous inflammatory diseases (*43*, *44*). Thus, we aimed to specifically target pDC activation. We previously showed that clobenpropit (CB), an antihistamine, modulates pDC activation by engagement of CXCR4 (*19*). Therefore, as pDCs express high levels of CXCR4, we hypothesized that pDC activation could be specifically targeted with small amino compounds interacting with this chemokine receptor. However, given the large expression profile of histamine receptors, it is challenging to predict the mechanism of action in a mixed cell population or in a small animal model. We identified IT1t as a compound with similar immunoregulatory properties to histamine and with a high specificity toward CXCR4. We demonstrated that IT1t but not AMD3100, a clinically used CXCR4 antagonist, exhibits strong inhibitory activity on type I IFN production by TLR7-activated primary pDCs. Notably, both synthetic ligand (R848) and viral (HIV) activation of pDCs were strongly inhibited by IT1t but not by AMD3100. This raises the ability of amino compounds targeting CXCR4 to be considered as therapeutic strategies in both inflammatory and chronic infectious diseases, where sustained production of type I IFN is thought to impair the immune response (*45*–*47*).

It is clear that IT1t inhibitory activity on isolated primary pDCs was fully dependent on CXCR4 engagement as demonstrated by the loss of the IT1t effect in CXCR4 siRNA-treated cells. The IFN-α produced following R848 stimulation in human TMCs and PBMCs from healthy controls and patients with SLE was mostly due to pDCs. Together, our in vitro data validate IT1t as a potent inhibitor of type I IFN production by activated pDCs.

Targeting type I IFN production and proinflammatory cytokines in chronic diseases is the predominant therapeutic option in SLE (*48*). However, despite the identification of the up-regulation of IFN signaling in SLE decades ago (*49*, *50*), anti-IFN therapies have developed slowly owing to the heterogeneity of SLE disease progression (*48*) and have yet to reach routine clinical practice. Antibody-based IFN therapies have not yet progressed beyond phase 2 development, while the more promising anti-IFNAR approach (*51*) recently failed to achieve the primary end point in a phase 3 clinical study. Specific targeting of pDCs has provided promising results (*52*), leading to clinical trials based on anti-BDCA2 and anti-CD123 antibodies in phase 2 and phase 1 trials, respectively (*51*). Small molecule–based approaches to control IFN in SLE remain largely unexplored. TBK1 inhibition has demonstrated promising results in mice (*53*), but no inhibitor of IFN secretion has yet entered clinical trials. An alternative strategy that consists of blocking IFNAR signaling with several JAK2 inhibitors is currently evaluated in phase 2 clinical studies (*51*). In this context, we evaluated the effect of chronic IT1t intraperitoneal injection in an SLE pristane-induced mouse model. Several mouse models have led to a clearer understanding of the role of type I IFN in the pathogenesis of lupus-like disease. Pristane-induced SLE meets many SLE features including an IFN signature and anti-dsDNA and anti-RNA antibodies, and reaches a score of 8 in the SLE criteria (*35*). In pristane-induced murine lupus, TLR7 is specifically required for the production of RNA-reactive autoantibodies and the development of glomerulonephritis (*36*). TLR7 deficiency not only abolishes pristane-induced type I IFN production but also eliminates autoantibody production and renal disease, indicating a key role of the TLR7/MyD88/type I IFN pathway in this model (*35*, *54*, *55*). We demonstrate here that IT1t treatment by targeting the TLR7 pathway inhibits the systemic production of IL-1β, IL-17, and the IFN-induced protein TRAIL similarly to prednisolone in pristane-induced SLE mice. Furthermore, IT1t exhibited a better reduction of dsDNA antibodies, which serve as a diagnostic and prognostic marker, than prednisolone. To sum up, IT1t provides a new therapeutic alternative to corticosteroids for IFN-triggered SLE pathogenesis.

In view of the promising effect of IT1t in healthy donors and the SLE mouse model, we tested IT1t on cells isolated from patients with lupus. Patients with SLE experience periods of low disease activity and also periods of "flares," where they undergo an inflammatory storm (*39*). Flares are also associated with a massive increase in the IFN signature in patients' blood. To mimic "flares" in vitro, we stimulated patient's cells with R848. Using pan–IFN-α ultrasensitive digital ELISA (*5*), we demonstrate that IT1t treatment controls IFN-α secretion in activated PBMCs from patients with lupus, acting preferentially through diminution of IFN-α^+ pDCs. In our hands, spontaneous secretion of IFN-α by frozen PBMCs of adult patients with SLE is almost never detectable. However, using digital ELISA, we detected IFN secretion on several occasions from fresh ex vivo unstimulated cultures of PBMCs from juvenile SLE. We identified four patients with clear, albeit distinct, spontaneous inflammatory profiles. For all patients' cells, and irrespective of their specific inflammatory profile, IT1t treatment was associated with a reduction of IFN-α secretion, pSTAT1, and pSTAT3 levels, as well as ISG and cytokine transcription. These promising results with patients' cells, using a small CXCR4

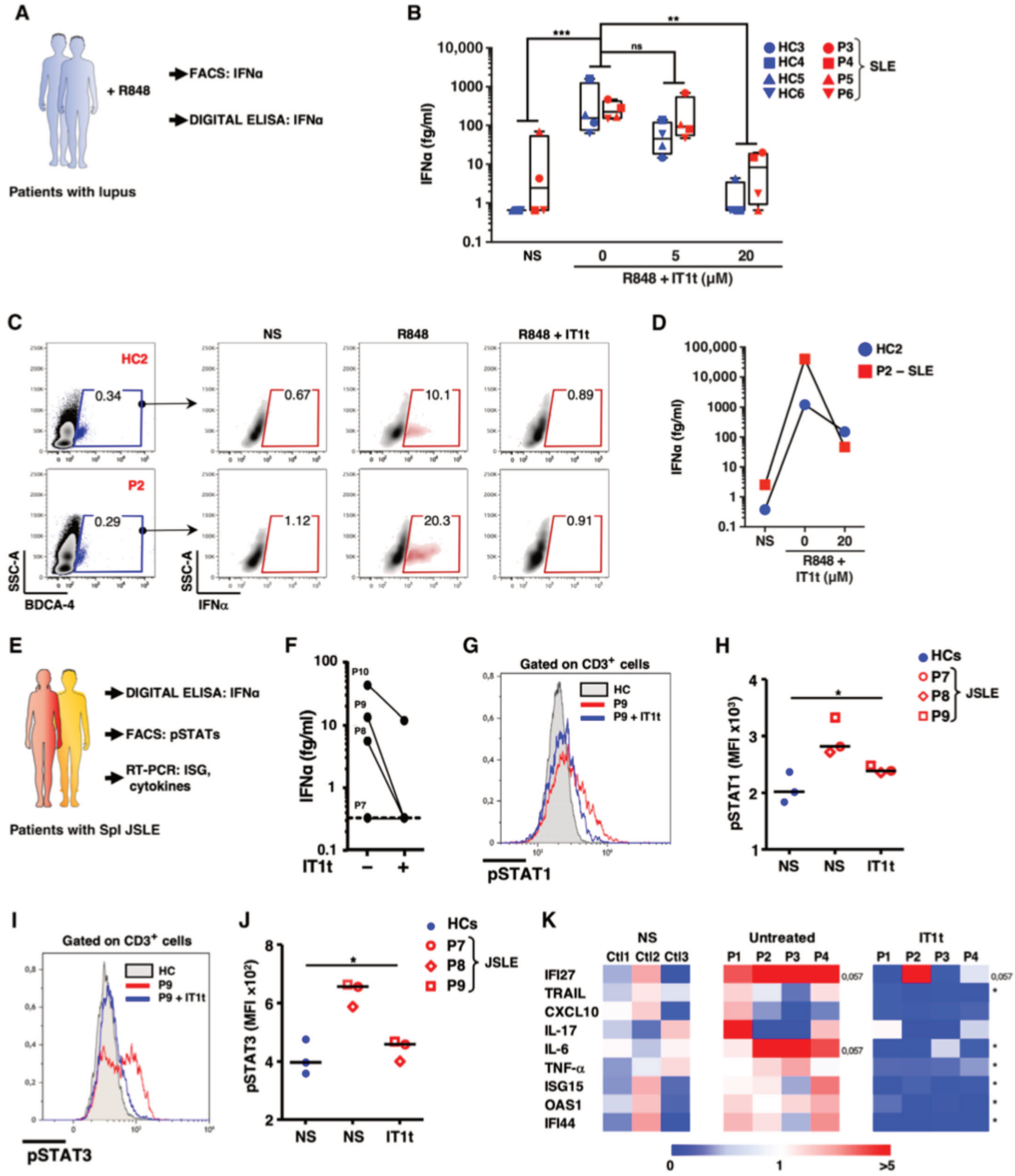

Fig. 6. IT1t controls induced and spontaneous inflammation in vitro in cells from patients with SLE. (**A**) PBMCs from healthy controls (HC) and patients with lupus (P) were stimulated with R848 to recapitulate disease flares and treated or not with IT1t (20 μM). Effect of IT1t was evaluated by IFN-α dosage in cell supernatants by digital ELISA (Simoa) or by intracellular IFN-α expression by flow cytometry. (**B**) Effect of IT1t on IFN-α secretion from TLR7-stimulated cells from patients (P3, P4, P5, and P6) was measured by Simoa. Box and whisker plots with median ± SEM showing minimum to maximum. Friedman test with Dunnett post hoc correction. (**C**) Intracellular IFN-α expression was assessed by flow cytometry and (**D**) IFN-α was dosed in the supernatant of cells from P1 stimulated with R848 (5 μg/ml) and treated with IT1t. (**E**) Effect of IT1t on cells from patients with spontaneous inflammation (Spl) juvenile SLE (JSLE) was evaluated on IFN-α production by (**F**) Simoa in the cell supernatant, by flow cytometry to measure pSTAT1 (**G** and **H**) and pSTAT3 (**I** and **J**), and by RT-qPCR (**K**) to quantify mRNA levels in PBMCs from four different patients with JSLE. (H and J) Friedman test. ***$P < 0.001$, **$P < 0.01$, *$P < 0.05$. NS, nonstimulated.

agonist with previously unappreciated immunoregulatory properties, open new perspectives for the treatment of lupus.

Numerous CXCR4 ligands have been described, including pyridines, quinolones, peptides, or polyazamacrocycle with a large range of affinities (*56*). The excellent control of TLR7-mediated pDCs inflammation by IT1t brings a new level of complexity to CXCR4 signaling and associated functions. Initially characterized by crystallography in 2010, the IT1t binding site has since been further studied. A

combination of structure- and ligand-based virtual screening of the "IT1t pocket" (*57*) identified a set of small molecules with agonist or antagonist properties toward CXCL12, demonstrating the functionality of this pocket. In a previous study, we demonstrated that another thiourea CXCR4 ligand (CB) showed similar biological inhibitory properties to IT1t in vivo (*19*). This highlights the complexity of CXCR4 engagement and validates the IT1t CXCR4 minor pocket as a promising pharmacological target for chronic diseases in contrast to the CXCR4 major pocket of AMD3100 (*20*, *23*). We acknowledge that we have not yet resolved the molecular mechanism linking CXCR4 engagement to TLR7 signaling inhibition. Furthermore, we also found that TLR4/TLR8/TLR9 response in pDCs and monocytes is also drastically inhibited by IT1t, suggesting a broader effect on immune modulation. Thus, understanding the molecular pathway will be the next step to fully characterize the role of CXCR4 in control of innate immunity. However, we can still speculate on some hypothesis. One could be that IT1t binding on CXCR4 blocks TLR pathway by affecting the intracellular vesicular trafficking (*58*). This hypothesis can be supported by the observation that chloroquine, which is known to impair many lysosomal functions, is also a strong inhibitor of IFN production by TLR-stimulated pDC and is used in the clinic to treat patients with lupus.

In conclusion, this study demonstrates that the CXCR4 cocrystalized ligand IT1t controls TLR7-mediated inflammation in human pDCs, controls inflammation and autoantibody formation in mice with lupus, and alleviates induced or spontaneous inflammation from cells of patients with SLE. Thus, IT1t and, by extension, the CXCR4 minor subpocket represent a novel promising axis for therapeutic options in chronic inflammation and autoimmune diseases.

METHODS

Study design

The aim of the study was to evaluate the effect of known antagonists (IT1t and AMD3100) of the chemokine receptor CXCR4 on the modulation of the innate immune response in pDCs and its potential usage as a new therapy in lupus. The sample sizes (healthy donors or patients with lupus) for this exploratory study were designed to ensure robust statistical results, while adhering to experimental feasibility and minimization of donors. Sample size for mice data was designed to maximize statistical power, whereas no randomization or blinding was implemented. Details on sampling and experimental replicates are provided in each figure legend.

Human samples

The study was approved by the Comité de Protection des Personnes (ID-RCB/EUDRACT: 2014-A01017-40) and AC-2014-2289. Investigations were undertaken with written informed consent.

Blood samples, isolation, and culture of blood leukocytes

The blood from healthy donors was obtained from two sources, either from "Etablissement Français du Sang" (convention # 07/CABANEL/106; Paris, France) or from the Apheresis and Blood Donation Unit at the Institute of Clinical Transfusion Medicine and Immunogenetics (Ulm, Germany), after being approved by the Institutional Review Board at Ulm University. For material of patients with lupus, the study was approved by the Comité de Protection des Personnes (ID-RCB/EUDRACT: 2014-A01017-40 and 2018-A01358-47) in France. Experimental procedures with human blood have been approved by the Necker Hospital Ethical Committees for human research and were done according to the European Union guidelines and the Declaration of Helsinki, and informed consent was obtained from all donors (healthy and patients). The clinical data of patients with lupus are summarized in table S1. In vitro experiments were performed using human PBMCs isolated by density centrifugation from peripheral blood leukocyte separation medium (Cambrex, Gaithersburg, MD). Human pDCs were purified by negative selection with the EasySep Human Plasmacytoid DC enrichment kit (STEMCELL Technologies). After purification, we obtained purity higher than 91% for pDCs quantified by flow cytometry. PBMCs and pDCs were cultured in RPMI 1640 (Invitrogen, Gaithersburg, MD) (R10) containing 10% heat-inactivated fetal bovine serum, penicillin (100 U/ml), streptomycin (100 μg/ml; 1% pen-strep), and 1 mM glutamine (HyClone, Logan, UT). Frozen PBMCs from controls and patients with lupus were cultured in RPMI 1640 (Invitrogen, Gaithersburg, MD) (R5) containing 5% heat-inactivated human serum AB (Sigma-Aldrich, MO, USA). The healthy donors were identified from #1 to #11 (Figs. 1 to 3) or HC3 to HC6 (Fig. 6) and P1 to P10 for patients with SLE and JSLE.

TMCs isolation from tonsils

Collection of tonsils was approved by the Comité de Protection des Personnes (ID-RCB/EUDRACT: 2018-A01358-47). Obstructive tonsils from healthy children with sleep apnea were removed after a partial tonsillectomy. The tissue was kept in phosphate-buffered saline (PBS) 1× no longer than 2 hours, cut into small pieces, and disrupted using a glass pestle onto a 60-mesh steel grid. The TMCs were filtered on a 70-μm filter and washed in PBS. Ficoll separation was further performed to remove the rest of the epithelial tissue and debris. TMCs were cultured in R10. The donors were identified from #1 to #7.

CXCR4 knockout experiments

pDCs were seeded at 10^5 cells/100 μl in 96-well plates and incubated at 37°C. Cyclophilin B (control) and CXCR4 siRNA (SMARTPool, Dharmarcon) were diluted in DOTAP (1,2-dioleoyl-3-trimethylammonium-propane; Roche Applied Sciences). The mix was gently mixed and incubated at room temperature for 15 min. After incubation, the mix was added to cells in culture at a final concentration of 160 nM. Last, cells were incubated at 37°C for 24 hours before adding the stimulation for 16 hours.

Cell stimulation

PBMCs and TMCs were seeded at 2×10^6/ml, and purified pDCs were seeded at 5×10^4/100 μl. Cells were then stimulated with the TLR7/TLR8 agonist Resiquimod (R848; Invivogen) at 5 μg/ml or inactivated AT-2 HIV-1_{MN} (X4 tropism) and HIV-1_{ADA} (R5 tropism) at 60 ng/ml $p24^{CA}$ equivalent [provided by J. D. Lifson (SAIC-NCI, Frederick, MD)] or pristane at 200 μg/ml (Sigma-Aldrich). Purified pDCs were pretreated with the IT1t (Tocris Bioscience) or AMD3100 (Sigma-Aldrich) at 20 μM (or other if specified for 1 hour before 16 hours of stimulation or as indicated). Cells were then collected for RT-qPCR, and supernatants were collected for cytokine detection. For intracellular IFN-α staining, brefeldin A was added to the cells at the same time as the stimulus. Cells were then collected and stained for flow cytometry analysis.

Cell infection

TZM-bl cells were seeded in flat-bottomed 96-well dishes, cultured overnight, and incubated with various concentrations of AMD3100

or IT1t for 1 hour before they were infected with virus containing 20 ng of p24 antigen in a total volume of 100 ml of medium. Three days after infection, the cells were lysed, and infection rates were determined using the one-step Tropix Gal-Screen Kit as recommended by the manufacturer.

Flow cytometry

Cells were washed in PBS and then incubated with a viability stain (Zombie-Aqua, BioLegend) for 30 min at 4°C. After washing, the cells were resuspended in PBS containing 2% fetal calf serum and 2 mM EDTA and stained with the extracellular mix using APC (allophycocyanin) anti-BDCA4 (clone 12C2), fluorescein isothiocyanate anti-CD123 (clone 6H6), PerCP.cy5.5 anti-CD56 (clone 5.1H11), BV421 anti-HLADR (human leukocyte antigen–DR isotype) (clone L243), PE.cy7 anti-CD19 (clone 4G7), and APC-cy.7 anti-CD14 (clone M5E2) all from BioLegend and used at 1:200 and V500 anti-CD3 (clone SP34-2, 1:200; BD Bioscience). For IFN-α intracellular staining, a Fixation/Permeabilization Solution Kit (BD Cytofix/Cytoperm) was used according to the manufacturer's protocol. Briefly, the cells were fixed for 10 min at 4°C with 100 μl of the Fixation/Permeabilization solution and then washed and stained in 100 μl of the BD Perm/Wash Buffer containing PE (phycoerythrin) anti–IFN-α (clone REA1013, 1:50; Miltenyi Biotec) antibody for 1 hour at 4°C. For pIRF7 staining, following the extracellular staining, the cells were fixed in 2% paraformaldehyde for 10 min at 4°C and then washed and permeabilized with 90% ice-cold methanol for 20 min at 4°C. The cells were stained with Alexa Fluor 488-IRF7 pS477/pS479 (K47-671, 1:25; BD Biosciences) and PE anti–IFN-α antibodies for 1 hour at 4°C. Data acquisition was performed on a FACSCanto II flow cytometer using FACSDiva software (BD Biosciences, San Jose, CA). FlowJo software (Treestar, Ashland, OR) was used to analyze data.

Confocal microscopy

Purified pDCs were pretreated or not with IT1t at 20 μM and then stimulated with R848 overnight, in the presence of brefeldin A. Cells were washed in ice-cold PBS–bovine serum albumin (BSA; 0.2%) and then were plated on poly-D-lysine–coated slides and fixed with 4% paraformaldehyde. Cells were permeabilized with 90% ice-cold methanol for 20 min at 4°C and, after washing, were incubated with Alexa Fluor 488–IRF7 pS477/pS479 antibody in 0.5% saturation buffer PBS-BSA. Last, slides were washed in PBS and mounted in Fluoromount-G with DAPI (4′,6-diamidino-2-phenylindole) medium (Thermo Fisher Scientific). Images were digitally acquired with a Zeiss LSM 710 confocal microscope using 63× PL APO O.N. 1.4 per oil objective. All analyses were performed using the ImageJ software (National Institutes of Health, Bethesda, MD, USA). The plugin 3D Viewer was used to create three-dimensional images.

All types of IFN detection

To quantify the secretion of functional IFN in TMCs, we used a biological assay based on a stable cell line where luciferase reporter gene is controlled by five IFN-stimulated response elements (STING37 cell line). First, TMCs supernatants were harvested after 24 hours of stimulation and frozen at −20°C for storage. Then, TMCs supernatants were dispensed in culture wells of a 96-well plate containing 35×10^3 STING37 cells per well. After 24 hours of culture, luciferase activity was determined by adding 50 μl of Bright-Glo reagents (Promega) to culture wells and measuring bioluminescence with a luminometer.

STAT phosphorylation assay

PBMCs were treated or not with IT1t (20 μM) overnight. Cells were fixed using Beckman Coulter PerFix EXPOSE Fixation Buffer (10 min at room temperature) and then permeabilized using Beckman Coulter PerFix EXPOSE Permeabilizing Buffer (5 min at 37°C). Cells were stained with PE anti-STAT1 pY701 (clone 4a, 1:5; BD Bioscience) or Alexa Fluor 488 anti-STAT3 pY705 (clone 4/p-STAT3, 1:5; BD Bioscience) and cell surface markers APC-CD3 (clone REA613, 1:30; Miltenyi Biotec) and APC–Alexa Fluor 750–CD14 (clone RM052, 1:30; Beckman Coulter) for 1 hour at room temperature protected from light. Flow cytometry analysis was performed on a Gallios Beckman Coulter flow cytometer. Results were analyzed using Kaluza software v1.3.

Cytokine detection

pDC and tonsil supernatants were tested for multiple cytokine production using the bead assay LEGENDplex Antivirus Human panel (PBL Assay Science, NJ, USA) according to the manufacturer's instructions.

IFN-α in serum and supernatant

As previously reported (*5*), Simoa digital ELISA specific for IFN-α was developed using a Quanterix Homebrew Assay, and two autoantibodies specific for IFN-α were isolated and cloned from two APS1/APECED patients (*59*). The 8H1 antibody clone was used as a capture antibody after coating paramagnetic beads (0.3 mg/ml), and the 12H5 was biotinylated (biotin/Ab ratio = 30:1) and used as the detector. Recombinant IFN-α17/αI (PBL Assay Science) was used as a standard curve after cross-reactivity testing. The limit of detection was calculated by the mean value of all blank runs ± 3 SDs and was 0.23 fg/ml.

RT-qPCR analyses

Total RNA was extracted using the RNeasy Micro kit and was submitted to deoxyribonuclease treatment (Qiagen), following the manufacturer's instructions. RNA concentration and purity were evaluated by spectrophotometry (NanoDrop 2000c, Thermo Fisher Scientific). RNA (500 ng) was reverse-transcribed using the PrimeScript RT Reagent Kit (Perfect Real Time, Takara Bio) in a 10-μl reaction. Real-time PCR reactions were performed in duplicate using Takyon ROX SYBR MasterMix blue deoxythymidine triphosphate (Eurogentec) on an Applied Biosystems QuantStudio 5. Transcripts were quantified using the following program: 3 min at 95°C followed by 35 cycles of 15 s at 95°C, 20 s at 60°C, and 20 s at 72°C. Values for each transcript were normalized to expression levels of RPL13A (60*S* ribosomal protein L13a) using the $2^{-\Delta\Delta Ct}$ method. Primers used for quantification of transcripts by real time quantitative PCR are indicated below:

RPL13A: forward primer, 5′-AACAGCTCATGAGGCTACGG-3′; reverse primer, 5′-TGGGTCTTGAGGACCTCTGT-3′

TRAIL: forward primer, 5′-GCTGAAGCAGATGCAGGACAA-3′; reverse primer, 5′-TGACGGAGTTGCCACTTGACT-3′

IFNα1: forward primer, 5′-CCAGTTCCAGAAGGCTCCAG-3′; reverse primer, 5′-TCCTCCTGCATCACACAGGC-3′

IFNα4: forward primer, 5′-CCCACAGCCTGGGTAATAGGA-3′; reverse primer, 5′-CAGCAGATGAGTCCTCTGTGC-3′

IFNβ: forward primer, 5′-TGCTCTCCTGTTGTGCTTCTC-3′; reverse primer, 5′-CAAGCCTCCCATTCAATTGCC-3′

IFNλ1: forward primer, 5′-GGACGCCTTGGAAGAGTCAC-3′; reverse primer, 5′-CTGGTCTAGGACGTCCTCCA-3′

IFNλ2/3: forward primer, 5′-GGGCCTGTATCCAGCCTCAG-3′; reverse primer, 5′-GAGGAGGCGGAAGAGGTTGA-3′

IFNγ: forward primer, 5′-GGCAGCCAACCTAAGCAAGAT-3′; reverse primer, 5′-CAGGGTCACCTGACACATTCA-3′

IRF7: forward primer, 5'-CAGATCCAGTCCCAACCAAG-3′; reverse primer, 5′-GTCTCTACTGCCCACCCGTA-3′

MxA: forward primer, 5′-AAGCTGATCCGCCTCCACTT-3′; reverse primer, 5′-TGCAATGCACCCCTGTATACC-3′

TNF-α: forward primer, 5′-GGCGTGGAGCTGAGAGATAAC-3′; reverse primer, 5′-GGTGTGGGTGAGGAGCACAT-3′

CXCL10: forward primer, 5′-CGCTGTACCTGCATCAGCAT-3′; reverse primer, 5′-GCAATGATCTCAACACGTGGAC-3′

IFN stimulated gene RNA expression in PBMCs from patients with lupus

mRNA from treated and nontreated cultured cells were quantified by RT-qPCR using TaqMan probes for *IFI27* (Hs01086370_m1), *IFI44L* (Hs00199115_m1), *ISG15* (Hs00192713_m1), *OAS1* (Hs00973637_m1), *CXCL10* (Hs01124251_m1), *TNFa* (Hs01113624_g1), *IL-6* (Hs00985639_m1), and *IL-17* (Hs00174383_m1); the relative abundance of each target transcript was normalized to the expression level of *HPRT1* (Hs03929096_g1) and assessed with the Applied Biosystems StepOne Software v2.1.

Computational details

An initial structure for AMD3100 was obtained from the ZINC15 database (*60*). The receptor structure was obtained from PDB (Protein Data Bank) ID: 3ODU (chain A) (*20*). The program LeDock (*61*) was used for docking. A cubic box with 40 Å of edge, containing the whole extracellular extreme of the CXCR4 receptor, was used to perform the initial docking screening. We conducted 50 runs of docking simulations, keeping the final pose in each of them. Subsequently, the 50 resulting poses are clustered with a root mean square deviation cutoff of 1 Å. The clusters are ordered according to the binding energy values given by the program force field. The best pose was selected from the most populated cluster among the top 10 scored ones. This structure was further optimized with a simulated annealing procedure. The simulations were performed with NAMD 2.12 (*62*), using the CHARMM36m force field (*63*). Parameters and topologies for the ligands were obtained from SwissParam (*64*). The complexes were placed in a box of explicit solvent with 15 Å of padding in the three dimensions around the complex structures. The model TIP3P was used for the water molecules (*65*). Counter ions were added for neutralization in each system. Long-range electrostatics were evaluated using the PME (particle mesh Ewald) method (*66*). The solvent was initially equilibrated to the box dimensions along 150 ps of NVT simulation at 300 K with the complex structure fixed in its initial geometry. Next, 1 ns of NPT simulation was performed with harmonic constraints on the protein and ligand's atoms. Langevin dynamics (*67*) was used to control the temperature and pressure of the system at 300 K and 1 atm, respectively. Then, a local optimization was performed with short cycles of a simulated annealing (SA) procedure. The SA protocol was composed of five cycles, involving a heating ramp between 300 and 350 K for 1 ns, then a cooling ramp back to 300 K for 1 ns, and, afterward, 1 ns of re-equilibration at 300 K. In total, the protocol involved 15 ns of optimization. The last step involved the equilibration at 300 K. The receptor's backbone was kept fixed during the simulation using a harmonic restraint. Side chains, ligand, and solvent were allowed to move freely.

In vivo treatment of mice

Animal experiments were performed blindly by Washington Biotechnology, Inc. The animals were housed in a temperature- and humidity-controlled room with 12-hour light/dark cycles with food and water ad libitum. The Washington Biotechnology, Inc. Animal Care and Use Committee reviewed and approved all mouse experiments (IACUC no. 17-006). Animal welfare and experimental protocols strictly complied with the *Guide for the Care and Use of Laboratory Animals* and the ethics and regulations. For pristane injection, each mouse in all groups was intraperitoneally injected with 0.5 ml of pristane (cat no. P9622, Sigma-Aldrich, BioReagent). Prednisolone (4.5 mg; P4153, Sigma-Aldrich) was dissolved in 3 ml of PBS to prepare a solution (1.5 mg/ml). All mice in group 2 were treated daily with prednisolone (15 mg/ml oral gavage). IT1t was dissolved in PBS and intraperitoneally injected daily at 3 mg/kg (mpK), 10, or 30 mpK (groups 3 to 5). ELISA was performed using the following kit according to the manufacturer's recommendation: TNF-α ELISA kit (cat no. MTA00B, R&D Systems), IL-1β ELISA kit (cat no. MLB00C, R&D Systems), IL-17 ELISA kit (cat no. M1700, R&D Systems), TRAIL ELISA kit (cat. no. ELM-TRAIL-1, RayBiotech), and dsDNA (IgM) ELISA Kit (cat. no. 5120, Alpha Diagnostic). For histology, formalin-fixed samples of each kidney from mice were received by HistoTox Labs and processed routinely. One slide per block was sectioned and stained with hematoxylin and eosin. Glass slides were evaluated by a board-certified veterinary pathologist, using light microscopy. Glomerulonephritis was characterized by slight thickening of mesangial matrix or mesangial hypercellularity (>3 nuclei per segment).

Nanostring gene expression analysis

Total RNA was extracted from isolated pDCs of controls and patients and was diluted with ribonuclease-free water at 20 ng/μl, and 100 ng (5 μl) of each sample was analyzed using the Human Immunology kit v2 and Nanostring Counter. Each sample was analyzed in a separate multiplexed reaction including, in each, eight negative probes and six serial concentrations of positive control probes. Data were imported into nSolver analysis software (version 2.5) for quality checking and normalization of data according to NanoString analysis guidelines, using positive probes and housekeeping genes. For analysis, mRNA expression levels were log-transformed and mean-centered per donor (when applicable) before hierarchical clustering (Qlucore Omics Explorer version 3.1). Up-regulated genes from the heat map shown in Fig. 2B were classified with respect to their known link to IFN signaling or functional promoter. Identification of ISGs was made using the database from Shaw *et al.* (*68*) (http://isg.data.cvr.ac.uk/). Promoters of the remaining genes were identified on the basis of the "Molecular Signatures Database v6.2" C3 from the Broad Institute (http://software.broadinstitute.org/gsea/msigdb/index.jsp) (*69*, *70*). When multiple transcription factors were identified for the same gene, the one in common with other genes was chosen in priority for the graphical representation.

Statistical analysis

Cellular data are shown as median and min/max. Datasets were analyzed by Kruskal-Wallis test with Dunn's post hoc correction. Univariate distributions of flow cytometry data were performed by probability

binning in 300 bins using FlowJo software. Animal data are shown as mean ± SEM. Datasets were analyzed using two-way analysis of variance (ANOVA) with Bonferroni post hoc comparison (cytokine concentration in time course). GraphPad Prism 5 (GraphPad Software, San Diego, CA) was used for data analysis and preparation of all graphs. *P* values less than 0.05 were considered to be statistically significant.

SUPPLEMENTARY MATERIALS

Supplementary material for this article is available at http://advances.sciencemag.org/cgi/content/full/5/7/eaav9019/DC1

Fig. S1. AMD3100 and IT1t bind to CXCR4 and are not toxic.
Fig. S2. IT1t controls TLR7-mediated inflammation in HIV-stimulated pDCs.
Fig. S3. IT1t inhibits pDC activation through CXCR4 engagement.
Fig. S4. Genes from the R848 stimulated group are significantly enrich in ISG.
Table S1. Clinical information of recruited patients.

REFERENCES AND NOTES

1. L. B. Ivashkiv, L. T. Donlin, Regulation of type I interferon responses. *Nat. Rev. Immunol.* **14**, 36–49 (2014).
2. X. Dagenais-Lussier, H. Loucif, A. Murira, X. Laulhé, S. Stäger, A. Lamarre, J. van Grevenynghe, Seustained IFN-I expression during established persistent viral infection: A "bad seed" for protective immunity. *Viruses* **10**, 12 (2017).
3. M. P. Rodero, Y. J. Crow, Type I interferon-mediated monogenic autoinflammation: The type I interferonopathies, a conceptual overview. *J. Exp. Med.* **213**, 2527–2538 (2016).
4. R. Banchereau, S. Hong, B. Cantarel, N. Baldwin, J. Baisch, M. Edens, A.-M. Cepika, P. Acs, J. Turner, E. Anguiano, P. Vinod, S. Khan, G. Obermoser, D. Blankenship, E. Wakeland, L. Nassi, A. Gotte, M. Punaro, Y.-J. Liu, J. Banchereau, J. Rossello-Urgell, T. Wright, V. Pascual, Personalized immunomonitoring uncovers molecular networks that stratify lupus patients. *Cell* **165**, 551–565 (2016).
5. M. P. Rodero, J. Decalf, V. Bondet, D. Hunt, G. I. Rice, S. Werneke, S. L. McGlasson, M.-A. Alyanakian, B. Bader-Meunier, C. Barnerias, N. Bellon, A. Belot, C. Bodemer, T. A. Briggs, I. Desguerre, M.-L. Frémond, M. Hully, A. M. J. M. van den Maagdenberg, I. Melki, I. Meyts, L. Musset, N. Pelzer, P. Quartier, G. M. Terwindt, J. Wardlaw, S. Wiseman, F. Rieux-Laucat, Y. Rose, B. Neven, C. Hertel, A. Hayday, M. L. Albert, F. Rozenberg, Y. J. Crow, D. Duffy, Detection of interferon alpha protein reveals differential levels and cellular sources in disease. *J. Exp. Med.* **214**, 1547–1555 (2017).
6. G. Grouard, M.-C. Rissoan, L. Filgueira, I. Durand, J. Banchereau, Y.-J. Liu, The enigmatic plasmacytoid T cells develop into dendritic cells with interleukin (IL)-3 and CD40-ligand. *J. Exp. Med.* **185**, 1101–1111 (1997).
7. M. Colonna, M. Cella, Crosspresentation: Plasmacytoid dendritic cells are in the business. *Immunity* **27**, 419–421 (2007).
8. F. P. Siegal, N. Kadowaki, M. Shodell, P. A. Fitzgerald-Bocarsly, K. Shah, S. Ho, S. Antonenko, Y.-J. Liu, The nature of the principal type I interferon-producing cells in human blood. *Science* **284**, 1835–1837 (1999).
9. D. Jarrossay, G. Napolitani, M. Colonna, F. Sallusto, A. Lanzavecchia, Specialization and complementarity in microbial molecule recognition by human myeloid and plasmacytoid dendritic cells. *Eur. J. Immunol.* **31**, 3388–3393 (2001).
10. N. Kadowaki, Y.-J. Liu, Natural type I interferon-producing cells as a link between innate and adaptive immunity. *Hum. Immunol.* **63**, 1126–1132 (2002).
11. M. Gandini, C. Gras, E. L. Azeredo, L. M. de Oliveira Pinto, N. Smith, P. Despres, R. V. da Cunha, L. J. de Souza, C. F. Kubelka, J.-P. Herbeuval, Dengue virus activates membrane TRAIL relocalization and IFN-α production by human plasmacytoid dendritic cells in vitro and in vivo. *PLOS Negl. Trop. Dis.* **7**, e2257 (2013).
12. A. W. Hardy, D. R. Graham, G. M. Shearer, J. P. Herbeuval, HIV turns plasmacytoid dendritic cells (pDC) into TRAIL-expressing killer pDC and down-regulates HIV coreceptors by Toll-like receptor 7-induced IFN-alpha. *Proc. Natl. Acad. Sci. U.S.A.* **104**, 17453–17458 (2007).
13. H. Hemmi, O. Takeuchi, T. Kawai, T. Kaisho, S. Sato, H. Sanjo, M. Matsumoto, K. Hoshino, H. Wagner, K. Takeda, S. Akira, A Toll-like receptor recognizes bacterial DNA. *Nature* **408**, 740–745 (2000).
14. M. Swiecki, M. Colonna, The multifaceted biology of plasmacytoid dendritic cells. *Nat. Rev. Immunol.* **15**, 471–485 (2015).
15. L. Rönnblom, V. Pascual, The innate immune system in SLE: Type I interferons and dendritic cells. *Lupus* **17**, 394–399 (2008).
16. K. Sakata, S. Nakayamada, Y. Miyazaki, S. Kubo, A. Ishii, K. Nakano, Y. Tanaka, Up-regulation of TLR7-mediated IFN-α production by plasmacytoid dendritic cells in patients with systemic lupus erythematosus. *Front. Immunol.* **9**, 1957 (2018).
17. B. F. Chong, C. Mohan, Targeting the CXCR4/CXCL12 axis in systemic lupus erythematosus. *Expert Opin. Ther. Targets* **13**, 1147–1153 (2009).
18. A. Wang, A.-M. Fairhurst, K. Tus, S. Subramanian, Y. Liu, F. Lin, P. Igarashi, X. J. Zhou, F. Batteux, D. Wong, E. K. Wakeland, C. Mohan, CXCR4/CXCL12 hyperexpression plays a pivotal role in the pathogenesis of lupus. *J. Immunol.* **182**, 4448–4458 (2009).
19. N. Smith, N. Pietrancosta, S. Davidson, J. Dutrieux, L. Chauveau, P. Cutolo, M. Dy, D. Scott-Algara, B. Manoury, O. Zirafi, I. McCort-Tranchepain, T. Durroux, F. Bachelerie, O. Schwartz, J. Münch, A. Wack, S. Nisole, J.-P. Herbeuval, Natural amines inhibit activation of human plasmacytoid dendritic cells through CXCR4 engagement. *Nat. Commun.* **8**, 14253 (2017).
20. B. Wu, E. Y. T. Chien, C. D. Mol, G. Fenalti, W. Liu, V. Katritch, R. Abagyan, A. Brooun, P. Wells, F. C. Bi, D. J. Hamel, P. Kuhn, T. M. Handel, V. Cherezov, R. C. Stevens, Structures of the CXCR4 chemokine GPCR with small-molecule and cyclic peptide antagonists. *Science* **330**, 1066–1071 (2010).
21. J. F. Dipersio, I. N. Micallef, P. J. Stiff, B. J. Bolwell, R. T. Maziarz, E. Jacobsen, A. Nademanee, J. McCarty, G. Bridger, G. Calandra, Phase III prospective randomized double-blind placebo-controlled trial of plerixafor plus granulocyte colony-stimulating factor compared with placebo plus granulocyte colony-stimulating factor for autologous stem-cell mobilization and transplantation for patients with non-hodgkin's lymphoma. *J. Clin. Oncol.* **27**, 4767–4773 (2009).
22. D. J. Scholten, M. Canals, D. Maussang, L. Roumen, M. J. Smit, M. Wijtmans, C. de Graaf, H. F. Vischer, R. Leurs, Pharmacological modulation of chemokine receptor function. *Br. J. Pharmacol.* **165**, 1617–1643 (2012).
23. M. M. Rosenkilde, L.-O. Gerlach, S. Hatse, R. T. Skerlj, D. Schols, G. J. Bridger, T. W. Schwartz, Molecular mechanism of action of monocyclam versus bicyclam non-peptide antagonists in the CXCR4 chemokine receptor. *J. Biol. Chem.* **282**, 27354–27365 (2007).
24. M. M. Rosenkilde, L.-O. Gerlach, J. S. Jakobsen, R. T. Skerlj, G. J. Bridger, T. W. Schwartz, Molecular mechanism of AMD3100 antagonism in the CXCR4 receptor: Transfer of binding site to the CXCR3 receptor. *J. Biol. Chem.* **279**, 3033–3041 (2004).
25. G. A. Donzella, D. Schols, S. W. Lin, J. A. Esté, K. A. Nagashima, P. J. Maddon, G. P. Allaway, T. P. Sakmar, G. Henson, E. DeClercq, J. P. Moore, AMD3100, a small molecule inhibitor of HIV-1 entry via the CXCR4 co-receptor. *Nat. Med.* **4**, 72–77 (1998).
26. G. Thoma, M. B. Streiff, J. Kovarik, F. Glickman, T. Wagner, C. Beerli, H.-G. Zerwes, Orally bioavailable isothioureas block function of the chemokine receptor CXCR4 in vitro and in vivo. *J. Med. Chem.* **51**, 7915–7920 (2008).
27. N. Smith, P. O. Vidalain, S. Nisole, J. P. Herbeuval, An efficient method for gene silencing in human primary plasmacytoid dendritic cells: Silencing of the TLR7/IRF-7 pathway as a proof of concept. *Sci. Rep.* **6**, 29891 (2016).
28. J. P. Herbeuval, J. Nilsson, A. Boasso, A. W. Hardy, M. J. Kruhlak, S. A. Anderson, M. J. Dolan, M. Dy, J. Andersson, G. M. Shearer, Differential expression of IFN-alpha and TRAIL/DR5 in lymphoid tissue of progressor versus nonprogressor HIV-1-infected patients. *Proc. Natl. Acad. Sci. U.S.A.* **103**, 7000–7005 (2006).
29. J.-P. Herbeuval, A. Boasso, J.-C. Grivel, A. W. Hardy, S. A. Anderson, M. J. Dolan, C. Chougnet, J. D. Lifson, G. M. Shearer, TNF-related apoptosis-inducing ligand (TRAIL) in HIV-1-infected patients and its in vitro production by antigen-presenting cells. *Blood* **105**, 2458–2464 (2005).
30. A. Kaul, C. Gordon, M. K. Crow, Z. Touma, M. B. Urowitz, R. van Vollenhoven, G. Ruiz-Irastorza, G. Hughes, Systemic lupus erythematosus. *Nat. Rev. Dis. Primers* **2**, 16039 (2016).
31. V. Salvi, V. Gianello, S. Busatto, P. Bergese, L. Andreoli, U. D'Oro, A. Zingoni, A. Tincani, S. Sozzani, D. Bosisio, Exosome-delivered microRNAs promote IFN-alpha secretion by human plasmacytoid DCs via TLR7. *JCI Insight* **3**, 98204 (2018).
32. G. Murayama, N. Furusawa, A. Chiba, K. Yamaji, N. Tamura, S. Miyake, Enhanced IFN-alpha production is associated with increased TLR7 retention in the lysosomes of palasmacytoid dendritic cells in systemic lupus erythematosus. *Arthritis Res. Ther.* **19**, 234 (2017).
33. V. Sisirak, D. Ganguly, K. L. Lewis, C. Couillault, L. Tanaka, S. Bolland, V. D'Agati, K. B. Elkon, B. Reizis, Genetic evidence for the role of plasmacytoid dendritic cells in systemic lupus erythematosus. *J. Exp. Med.* **211**, 1969–1976 (2014).
34. C. Guiducci, M. Gong, Z. Xu, M. Gill, D. Chaussabel, T. Meeker, J. H. Chan, T. Wright, M. Punaro, S. Bolland, V. Soumelis, J. Banchereau, R. L. Coffman, V. Pascual, F. J. Barrat, TLR recognition of self nucleic acids hampers glucocorticoid activity in lupus. *Nature* **465**, 937–941 (2010).
35. H. Zhuang, C. Szeto, S. Han, L. Yang, W. H. Reeves, Animal models of interferon signature positive lupus. *Front. Immunol.* **6**, 291 (2015).
36. E. Savarese, C. Steinberg, R. D. Pawar, W. Reindl, S. Akira, H.-J. Anders, A. Krug, Requirement of Toll-like receptor 7 for pristane-induced production of autoantibodies and development of murine lupus nephritis. *Arthritis Rheum.* **58**, 1107–1115 (2008).
37. X. Chen, R. Cui, R. Li, H. Lin, Z. Huang, L. Lin, Development of pristane induced mice model for lupus with atherosclerosis and analysis of TLR expression. *Clin. Exp. Rheumatol.* **34**, 600–608 (2016).
38. M. Lucas-Hourani, D. Dauzonne, P. Jorda, G. Cousin, A. Lupan, O. Helynck, G. Caignard, G. Janvier, G. André-Leroux, S. Khiar, N. Escriou, P. Desprès, Y. Jacob, H. Munier-Lehmann, F. Tangy, P.-O. Vidalain, Inhibition of pyrimidine biosynthesis pathway suppresses viral growth through innate immunity. *PLOS Pathog.* **9**, e1003678 (2013).

39. M. J. Mirzayan, R. E. Schmidt, T. Witte, Prognostic parameters for flare in systemic lupus erythematosus. *Rheumatology* **39**, 1316–1319 (2000).
40. S. Caielli, S. Athale, B. Domic, E. Murat, M. Chandra, R. Banchereau, J. Baisch, K. Phelps, S. Clayton, M. Gong, T. Wright, M. Punaro, K. Palucka, C. Guiducci, J. Banchereau, V. Pascual, Oxidized mitochondrial nucleoids released by neutrophils drive type I interferon production in human lupus. *J. Exp. Med.* **213**, 697–713 (2016).
41. S. S. Diebold, T. Kaisho, H. Hemmi, S. Akira, C. Reis e Sousa, Innate antiviral responses by means of TLR7-mediated recognition of single-stranded RNA. *Science* **303**, 1529–1531 (2004).
42. S. S. Diebold, M. Montoya, H. Unger, L. Alexopoulou, P. Roy, L. E. Haswell, A. Al-Shamkhani, R. Flavell, P. Borrow, C. Reis e Sousa, Viral infection switches non-plasmacytoid dendritic cells into high interferon producers. *Nature* **424**, 324–328 (2003).
43. J. Banchereau, V. Pascual, Type I interferon in systemic lupus erythematosus and other autoimmune diseases. *Immunity* **25**, 383–392 (2006).
44. T. B. Niewold, Type I interferon in human autoimmunity. *Front. Immunol.* **5**, 306 (2014).
45. L. Cheng, J. Ma, J. Li, D. Li, G. Li, F. Li, Q. Zhang, H. Yu, F. Yasui, C. Ye, L. C. Tsao, Z. Hu, L. Su, L. Zhang, Blocking type I interferon signaling enhances T cell recovery and reduces HIV-1 reservoirs. *J. Clin. Invest.* **127**, 269–279 (2017).
46. S. G. Deeks, P. M. Odorizzi, R. P. Sekaly, The interferon paradox: Can inhibiting an antiviral mechanism advance an HIV cure? *J. Clin. Invest.* **127**, 103–105 (2017).
47. A. Zhen, V. Rezek, C. Youn, B. Lam, N. Chang, J. Rick, M. Carrillo, H. Martin, S. Kasparian, P. Syed, N. Rice, D. G. Brooks, S. G. Kitchen, Targeting type I interferon-mediated activation restores immune function in chronic HIV infection. *J. Clin. Invest.* **127**, 260–268 (2017).
48. S. Luo, Y. Wang, M. Zhao, Q. Lu, The important roles of type I interferon and interferon-inducible genes in systemic lupus erythematosus. *Int. Immunopharmacol.* **40**, 542–549 (2016).
49. L. Bennett, A. K. Palucka, E. Arce, V. Cantrell, J. Borvak, J. Banchereau, V. Pascual, Interferon and granulopoiesis signatures in systemic lupus erythematosus blood. *J. Exp. Med.* **197**, 711–723 (2003).
50. V. Pascual, J. Banchereau, A. K. Palucka, The central role of dendritic cells and interferon-alpha in SLE. *Curr. Opin. Rheumatol.* **15**, 548–556 (2003).
51. R. Felten, E. Dervovic, F. Chasset, J. E. Gottenberg, J. Sibilia, F. Scher, L. Arnaud, The 2018 pipeline of targeted therapies under clinical development for systemic lupus erythematosus: A systematic review of trials. *Autoimmun. Rev.* **17**, 781–790 (2018).
52. S. L. Rowland, J. M. Riggs, S. Gilfillan, M. Bugatti, W. Vermi, R. Kolbeck, E. R. Unanue, M. A. Sanjuan, M. Colonna, Early, transient depletion of plasmacytoid dendritic cells ameliorates autoimmunity in a lupus model. *J. Exp. Med.* **211**, 1977–1991 (2014).
53. M. Hasan, N. Dobbs, S. Khan, M. A. White, E. K. Wakeland, Q.-Z. Li, N. Yan, Cutting edge: Inhibiting TBK1 by compound II ameliorates autoimmune disease in mice. *J. Immunol.* **195**, 4573–4577 (2015).
54. H. Zhuang, S. Han, Y. Xu, Y. Li, H. Wang, L.-J. Yang, W. H. Reeves, Toll-like receptor 7-stimulated tumor necrosis factor α causes bone marrow damage in systemic lupus erythematosus. *Arthritis Rheum.* **66**, 140–151 (2014).
55. P. Y. Lee, J. S. Weinstein, D. C. Nacionales, P. O. Scumpia, Y. Li, E. Butfiloski, N. van Rooijen, L. Moldawer, M. Satoh, W. H. Reeves, A novel type I IFN-producing cell subset in murine lupus. *J. Immunol.* **180**, 5101–5108 (2008).
56. B. Debnath, S. Xu, F. Grande, A. Garofalo, N. Neamati, Small molecule inhibitors of CXCR4. *Theranostics* **3**, 47–75 (2013).
57. R. K. Mishra, A. K. Shum, L. C. Platanias, R. J. Miller, G. E. Schiltz, Discovery and characterization of novel small-molecule CXCR4 receptor agonists and antagonists. *Sci. Rep.* **6**, 30155 (2016).
58. K. Nujić, M. Banjanac, V. Munić, D. Polančec, V. Eraković Haber, Impairment of lysosomal functions by azithromycin and chloroquine contributes to anti-inflammatory phenotype. *Cell. Immunol.* **279**, 78–86 (2012).
59. S. Meyer, M. Woodward, C. Hertel, P. Vlaicu, Y. Haque, J. Kärner, A. Macagno, S. C. Onuoha, D. Fishman, H. Peterson, K. Metsküla, R. Uibo, K. Jäntti, K. Hokynar, A. S. B. Wolff; APECED patient collaborative, K. Krohn, A. Ranki, P. Peterson, K. Kisand, A. Hayday, AIRE-deficient patients harbor unique high-affinity disease-ameliorating autoantibodies. *Cell* **166**, 582–595 (2016).
60. T. Sterling, J. J. Irwin, ZINC 15—Ligand discovery for everyone. *J. Chem. Inf. Model.* **55**, 2324–2337 (2015).
61. H. Zhao, A. Caflisch, Discovery of ZAP70 inhibitors by high-throughput docking into a conformation of its kinase domain generated by molecular dynamics. *Bioorg. Med. Chem. Lett.* **23**, 5721–5726 (2013).
62. J. C. Phillips, R. Braun, W. Wang, J. Gumbart, E. Tajkhorshid, E. Villa, C. Chipot, R. D. Skeel, L. Kalé, K. Schulten, Scalable molecular dynamics with NAMD. *J. Comput. Chem.* **26**, 1781–1802 (2005).
63. J. Huang, S. Rauscher, G. Nawrocki, T. Ran, M. Feig, B. L. de Groot, H. Grubmüller, A. D. MacKerell Jr., CHARMM36m: An improved force field for folded and intrinsically disordered proteins. *Nat. Methods* **14**, 71–73 (2017).
64. V. Zoete, M. A. Cuendet, A. L. Grosdidier, O. Michielin, SwissParam: A fast force field generation tool for small organic molecules. *J. Comput. Chem.* **32**, 2359–2368 (2011).
65. P. Mark, L. Nilsson, Structure and dynamics of the TIP3P, SPC, and SPC/E water models at 298 K. *J. Phys. Chem.* **105**, 9954–9960 (2001).
66. R. J. Shattock, B. F. Haynes, B. Pulendran, J. Flores, J. Esparza, Improving defences at the portal of HIV entry: Mucosal and innate immunity. *PLOS Med.* **5**, e81 (2008).
67. J. A. Izaguirre, D. P. Catarello, J. M. Wozniak, R. D. Skeel, Langevin stabilization of molecular dynamics. *J. Chem. Phys.* **114**, 2090–2098 (2001).
68. A. E. Shaw, J. Hughes, Q. Gu, A. Behdenna, J. B. Singer, T. Dennis, R. J. Orton, M. Varela, R. J. Gifford, S. J. Wilson, M. Palmarini, Fundamental properties of the mammalian innate immune system revealed by multispecies comparison of type I interferon responses. *PLOS Biol.* **15**, e2004086 (2017).
69. X. Xie, J. Lu, E. J. Kulbokas, T. R. Golub, V. Mootha, K. Lindblad-Toh, E. S. Lander, M. Kellis, Systematic discovery of regulatory motifs in human promoters and 3′ UTRs by comparison of several mammals. *Nature* **434**, 338–345 (2005).
70. A. Subramanian, P. Tamayo, V. K. Mootha, S. Mukherjee, B. L. Ebert, M. A. Gillette, A. Paulovich, S. L. Pomeroy, T. R. Golub, E. S. Lander, J. P. Mesirov, Gene set enrichment analysis: A knowledge-based approach for interpreting genome-wide expression profiles. *Proc. Natl. Acad. Sci. U.S.A.* **102**, 15545–15550 (2005).

Acknowledgments: We thank S. Dupuy from the Common Service of Flux Cytometry (S2C) of Paris Descartes University. We also thank N. Pietrancosta for providing us with some IT1t for the mice study. Furthermore, we thank J. Bess and J. Lifson for providing us with the inactivated purified HIV-1 viruses. **Funding:** This work was supported by the Agence National de la Recherche sur le SIDA et les Hépatites ANRS (to J.-P.H.) for the experiments and N.B. Fellowship (AAP 2017-166). N.S. acknowledges support from the ANRS for Fellowship (AAP 2016-1), the European Molecular Biology Organization (EMBO) for Fellowship (LT-834-2017), the start-up funding program "Baustein" of the Medical Faculty of Ulm University (LSBN.0147), and the Deutsche Forschungsgemeinschaft (DFG; SM 544/1-1). This work was also supported by SATT IDF Innov (www.idfinnov.com) through the project under grant no. 303. D.D. acknowledges support from the Agence National de Recherche ANR (CE17001002) and ImmunoQure for provision of mAbs for Simoa assays. J.M. acknowledges support from DFG (MU3115-8/1 and CRC1279). A.-S.K and Y.D. acknowledge support from the Société Nationale Française de Médecine Interne (SNFMI), from Hôpitaux Universitaires de Strasbourg (HUS), and from EU-funded (ERDF) project Interreg V "RARENET". A.-S.K. also acknowledges support from the French Ministry of Health (PHRC IR 2011). S.N. has benefited from support by the LABEX EpiGenMed, an "Investissements d'avenir" program (reference, ANR-10-LABX-12-01). B.J. acknowledges the BSD grant (Budgetantrag, 11225783). E.S.G. acknowledges the support of the German Research Foundation (DFG) under Germany's Excellence Strategy—EXC-2033—Projektnummer 390677874, the CRC1279, and the Boehringer-Ingelheim Foundation (Plus-3 Grant). These experiments used reagents provided by the AIDS and Cancer Virus Program, Biological Products Core Laboratory, Frederick National Laboratory for Cancer Research, supported with federal funds from the National Cancer Institute, National Institutes of Health, under contract HHSN261200800001E. **Author contributions:** N.S., M.P.R., D.D., and J.-P.H. designed research; N.S., N.B., S.N., M.P.R., M.H., and Y.R. performed the experiments; V.B. performed the SIMOA dosage; B.C. performed the nanostring experiments. Y.B.R.-B. and E.S.G. performed the molecular modeling and analysis. N.S., M.P.R., N.B., V.B., B.C., S.N., D.D., and J.-P.H. analyzed research; B.B-M., C.B., Y.R., V.B., P.Q., A.-S.K., and Y.D. gave access to patients' material; B.M. performed the statistical analysis; B.J. and N.L. gave access to tonsils and healthy donors' blood; F.K. and J.M. provided material and took part in scientific discussion; N.S., D.D., and J.M. contributed to writing the paper; and M.P.R. and J.-P.H. wrote the paper. **Competing interests:** N.S. and J.-P.H. are inventors on a patent related to this work filed by the Centre National de la Recherche Scientifique (CNRS) and the Université Paris Descartes (no. WO 2017/216368 Al, filed 16 June 2017, published 21 December 2017). The authors declare that they have no other competing interests. **Data and materials availability:** All data needed to evaluate the conclusions in the paper are present in the paper and/or the Supplementary Materials. The mAb for the Simoa IFN-α was obtained under a material transfer agreement. Requests for the mAb can be made to ImmunoQure AG directly. Additional data related to this paper may be requested from the authors.

Submitted 30 October 2018
Accepted 6 June 2019
Published 10 July 2019
10.1126/sciadv.aav9019

Citation: N. Smith, M. P. Rodero, N. Bekaddour, V. Bondet, Y. B. Ruiz-Blanco, M. Harms, B. Mayer, B. Bader-Meunier, P. Quartier, C. Bodemer, V. Baudouin, Y. Dieudonné, F. Kirchhoff, E. Sanchez Garcia, B. Charbit, N. Leboulanger, B. Jahrsdörfer, Y. Richard, A.-S. Korganow, J. Münch, S. Nisole, D. Duffy, J.-P. Herbeuval, Control of TLR7-mediated type I IFN signaling in pDCs through CXCR4 engagement—A new target for lupus treatment. *Sci. Adv.* **5**, eaav9019 (2019).

Article 2

jove

Isolation of Tonsillar Mononuclear Cells to Study Ex Vivo Innate Immune Responses in a Human Mucosal Lymphoid Tissue

Nikaïa Smith[1,2,3,4], **Nassima Bekaddour**[2,3,4], **Nicolas Leboulanger**[4,5], **Yolande Richard**[6], **Jean-Philippe Herbeuval**[2,3,4]

[1] Institute of Molecular Virology, Ulm University Medical Center [2] CNRS UMR-8601, Centre Interdisciplinaire Chimie Biologie [3] Team Chemistry & Biology, Modeling & Immunology for Therapy, Université Paris Descartes [4] Université Paris Descartes, Sorbonne Paris Cité [5] Pediatric Otolaryngology Department, Hôpital Necker-Enfants Malades, Assistance Publique Hôpitaux de Paris [6] Université de Paris, Institut Cochin

Corresponding Authors

Nikaïa Smith
nikaia.smith@pasteur.fr

Jean-Philippe Herbeuval
jean-philippe.herbeuval@parisdescartes.fr

Citation

Smith, N., Bekaddour, N., Leboulanger, N., Richard, Y., Herbeuval, J.P. Isolation of Tonsillar Mononuclear Cells to Study Ex Vivo Innate Immune Responses in a Human Mucosal Lymphoid Tissue. *J. Vis. Exp.* (160), e60914, doi:10.3791/60914 (2020).

Date Published

June 14, 2020

DOI

10.3791/60914

URL

jove.com/video/60914

Abstract

Studying isolated cells from mucosa-associated lymphoid tissues (MALT) allows understanding of immune cells response in pathologies involving mucosal immunity, because they can model host-pathogen interactions in the tissue. While isolated cells derived from tissues were the first cell culture model, their use has been neglected because tissue can be hard to obtain. In the present protocol, we explain how to easily process and culture tonsillar mononuclear cells (TMCs) from healthy human tonsils to study innate immune responses upon activation, mimicking viral infection in mucosal tissues. Isolation of TMCs from the tonsils is quick, because the tonsils barely have any epithelium and yield up to billions of all major immune cell types. This method allows detection of cytokine production using several techniques, including immunoassays, qPCR, microscopy, flow cytometry, etc., similar to the use of peripheral mononuclear cells (PBMCs) from blood. Furthermore, TMCs show a higher sensitivity to drug testing than PBMCs, which needs to be considered for future toxicity assays. Thus, ex vivo TMCs cultures are an easy and accessible mucosal model.

Introduction

Studies on human organs are restricted due to accessibility as well as obvious ethical reasons. However, they are essential to fully understand the complexity of human biology. Cultures of isolated cells (primary cultures or cell lines) are a standard system in cell biology studies due to their availability. While isolated cell cultures have allowed outstanding discoveries, the use of cell lines has come upon closer scrutiny because they do not fully mimic in vivo organ biology. However,

Copyright © 2020 JoVE Journal of Visualized Experiments

the culture of three-dimensional cells or tissue explants is highly complex[4,5,6]. Indeed, a piece of tissue or organ is highly heterogenous because its cell composition differs depending on the localization in the tissue. Thus, using tissue blocks requires the analysis of many technical and biological replicates, leading to the need of a large number of donors or patients.

The mucosa-associated lymphoid tissues (MALT) are structurally similar to the lymph nodes but have unique functions, because their main role is to regulate mucosal immunity[7]. Unlike the lymph nodes, which are usually located at some distance from the tissues, MALT are generally located immediately below the epithelium of the mucosal tissue. Histologically, they are mainly composed of high concentrations of B and T cells, but also antigen-presenting cells such as macrophages and dendritic cells. MALT constitute about 50% of the lymphoid tissue in the human body. MALT are subdivided into nine groups depending on their location: GALT (gut-), BALT (bronchus-), NALT (nasal-), CALT (conjunctival), LALT (larynx-), SALT (skin-), VALT (vulvo-), O-MALT (organized), and D-MALT (diffused). The O-MALT is mainly composed of the tonsils of Waldeyer's tonsillar ring and is the most accessible MALT[8,9]. Indeed, tonsils located in the oropharynx constitute the major barrier protecting the digestive and respiratory tracts from (potential) invasive microorganisms[10]. In addition, the tonsils are covered by a fine stratified squamous non-keratinizing epithelium, supported by a capsule of connective tissue containing blood vessels, nerves, and lymphatics, providing easy access to the immune cells[11,12]. Furthermore, tonsillectomy, the surgical act of removing tonsils, is a common procedure performed on children having sleep-disordered breathing, making tonsils an easily available tissue[13] in physiological settings.

Tonsils allow the study of immune cell response in pathologies involving mucosal immunity. Indeed, in HIV infection, because tonsils are composed of a high concentration of immune cells, they are the main target of viral replication but also produce a large amount of cytokines that are not detected in the circulation[14,15]. At steady states, rare populations of innate-like cells are present in various mucosal tissues, including the tonsils, but are essentially absent from blood.

Thus, mononuclear cells from tonsils (TMCs) are a more relevant and complex model than PBMCs and can answer more profound questions. On the other hand, the use of tissue explants can be complex and not always relevant to innate immune studies. Thus, we established a model to study mucosal immune activation using TMCs[16]. Here, we describe a method for efficient isolation of TMCs from fresh human tonsils. This method allows the recovery of a large number of immune cells while keeping their integrity for ex vivo studies.

Protocol

The specimens are not collected specifically for research purposes and the study is not considered invasive. However, human tonsils collection requires ethical approval by the local relevant authorities. In our case, it was approved by the Comité de Protection des Personnes (IDRCB/EUDRACT: 2018A0135847). Furthermore, consent of each patient or legal representative is requested to obtain donors' personal data (e.g., sex, age, history of ENT infections) that can help interpret experimental results.

Copyright © 2020 JoVE Journal of Visualized Experiments

1. Handling of the Human Tonsillar Tissue

1. Put tonsils from every donor in one sterile 50 mL vial containing 25 mL PBS 1x and transport at room temperature (RT) to the laboratory according to the authority's recommendations (use three levels of protection: vials, a safety box, and a bag).

   NOTE: The entire procedure should be carried out in a biological safety level 2 laboratory. All human specimens should be handled with care as they have not been previously qualified and may contain infectious agents.

2. **Clean all tools in between each use.**

   1. After use, disassemble the cell strainer and keep with all the other instruments (e.g., pestle, forceps) in a bath containing a detergent solution (1/10 volume detergent in H_2O) overnight.

   2. Brush each utensil to remove the tissue and wash with clear water.

   3. Dry all parts well, then prepare the cell strainer (85 mL, 37 mm diameter) by placing a 60 mesh steel grid on top of a 10 mesh steel grid and tightly close the ring.

   4. Place all the tools in sterile bags and autoclave.

2. Dissection of the Human Tonsillar Tissue and Isolation of the Tonsillar Mononuclear Cells (TMCs)

1. Place the cell strainer onto one 150 x 25 mm^2 (SPL150) cell culture dish and all the instruments in another SPL150 to keep them sterile.

2. Transfer the tonsils from the vial into the cell strainer using sterile forceps. Also pour in all of the PBS, which contains some cells that have egressed the tonsils. If necessary, add more PBS to immerse the grid.

   NOTE: The tissue should be immersed at all times to avoid desiccation.

3. Remove cauterized, bloody, and fibroid tissue using forceps and a scalpel.

   NOTE: Tonsils removed from children do not need this step.

4. Cut the tissues into small pieces of less than 0.5 cm in diameter using the scalpel and the curved tweezers. Cut all the tissue so that the small pieces can be immersed at all times.

5. Place a few pieces of tissue in the cell strainer and scrape them onto the grid with a glass pestle until only a really thin layer of white stroma remains. Remove and discard the stroma to avoid clogging the grid.

6. Once all the tissues have been squeezed through the grid, use a 10 mL pipette to transfer all the cell suspension onto the grid and scrape it one last time.

7. Transfer the cell suspension with a 10 mL pipette into a sterile vial. Wash the grid and the cell strainer with PBS 1x. Let the cell suspension rest for 5 min at RT on the bench. This step allows the precipitation and agglomeration of the leftover stroma, dead cells, and any released DNA, and will facilitate the next step.

8. Place a sterile 70 µm sieve on top of a new 50 mL vial (remove carefully from the envelope) and gently transfer the cell suspension onto it with a 10 mL pipette. Do not mix the suspension, because a pellet is frequently present. If the sieve is clogged, use the back of a sterile 1 mL pipette tip to scratch the cells trough the sieve. Change the sieve as often as necessary.

9. Centrifuge the cells at 250 x *g* for 10 min at 4 °C.

Copyright © 2020 JoVE Journal of Visualized Experiments

10. Discard the supernatant and resuspend the pellet by gently mixing the vial, then resuspend the cells in 35 mL of PBS.
11. In a new vial, place a new 70 µm sieve on top and transfer the cell suspension onto it with a 10 mL pipette. If the sieve is clogged, use the technique detailed in step 2.7.

3. Isolation of the TMCs by Cell Density Gradient

NOTE: The TMCs can be used after step 2.10. However, to obtain a clearer cell solution and to remove other cell debris and any red cells, it is advised to perform a cell density gradient isolation of the mononuclear cells.

1. Add 15 mL of the density gradient medium (d = 1.076 g/mL) in a new 50 mL vial. Pour the TMCs solution on top of the density gradient medium, being careful to minimize mixing of the suspension with the density gradient medium.
2. Centrifuge the solution at 1,000 x *g* for 30 min at RT with acceleration and break off.
3. Remove with a 10 mL pipette and discard the upper layer (containing mostly PBS 1x) without disturbing the interface between the TMCs and the density gradient medium.

   NOTE: The TMCs contains a low number of erythrocytes, therefore the solution is clear. Thus, the interface between the solution of TMCs in PBS and the density gradient medium can be difficult to visualize. Accordingly, cells can be resuspended in RPMI 1640 supplemented with 20 mM HEPES (without FBS) before the density gradient is performed.
4. Remove the TMCs with a sterile 1 mL pipette tip and place in a new 50 mL vial.
5. Wash the cells by adding 50 mL of PBS containing 2% of fetal bovine serum (FBS) and 2 mM EDTA and centrifuge the tube at 250 x *g* for 10 min at 4 °C to remove the remaining platelets.
6. Repeat step 3.5, but centrifuge the tube at 400 x *g* for 10 min at 4 °C.
7. Prepare culture medium (R10) by supplementing RPMI 1640 with 10% heat inactivated FBS, 2 mM L-glutamine, and the antibiotic solution (100 U/mL penicillium and 100 µg/mL streptomycin).
8. Resuspend the TMCs in 10 mL of R10 and count the cells. On average, this technique yields 5 x 10^8-2 x 10^9 TMCs per pair of tonsils. The cells can now be used for investigations like PBMCs from whole blood (e.g., purification of specific cell type, cell culture, flow cytometry, RT-qPCR, freezing, etc.).
9. **If needed, freeze the cells for further use using standard techniques for primary cell freezing.**
   1. Count the number of cells.
   2. Centrifuge the cells and remove the supernatant. Dissolve the pellet in enough 100% FBS for a final concentration of 1 x 10^8 cells/mL, then add the same volume of an 80% FBS + 20% DMSO solution. The cells will then be at 5 x 10^7 cells/mL. This step should be done at 4 °C and the FBS and DMSO solution should be kept at 4 °C before using.
   3. Distribute 1 mL of the cell solution into cryotubes and put them in a slow freezing container that has been at 4 °C overnight to control the rate of cell freezing. Place it at -80 °C.
   4. To thaw the cells, place the cryovials in a warm bath at 37 °C for a few seconds with constant agitation. As

Copyright © 2020 JoVE Journal of Visualized Experiments

soon as the cells start to thaw, transfer them to 49 mL of R10 and centrifuge to remove the DMSO. Count the cells and use them as PBMCs.

NOTE: Although freezing and thawing the TMCs will remove debris, it will also damage some rare cell types. If clumps or debris are present after thawing, it is best to pass the cell suspension through a sterile 70 µm sieve before using it.

4. Phenotyping of TMCs by Flow Cytometry

1. Retrieve 5 x 10^6 cells from the previous solution for each antibody mixture panel that needs to be tested and place in a 5 mL cytometry tube. Retrieve 1 x 10^6 cells for the unstained control.
2. Wash the cells in PBS and centrifuge at 400 x *g* for 5 min at 4 °C. Resuspend them in 500 µL of PBS (1 x 10^6 cells/mL) and incubate with a viability stain for 30 min at 4 °C in the dark.
3. Add 5 µL heat inactivated human AB serum per 100 µL of cell suspension and incubate for 15 min at 4 °C in the dark.
4. Wash the cells in PBS + 2% FBS + 2 mM EDTA (Wash Buffer) and centrifuge at 400 x *g* for 5 min at 4 °C.
5. Resuspend the TMCs in 500 µL of Wash Buffer containing the antibodies as detailed in **Table 1**. Incubate the cells for 30 min at 4 °C in the dark.
6. Wash the cells in Wash Buffer and centrifuge at 400 x *g* for 5 min at 4 °C. Resuspend the TMCs in 500 µL of PBS containing 0.5% of paraformaldehyde (PFA). Keep in the dark at 4 °C until acquisition by flow cytometry.

   NOTE: PFA is hazardous. Use a commercial ready-to-use solution to prepare the 0.5% PFA solution.

Antibody	Clone	Fluorochrome	Company
Live-Dead		BV405	ThermoFisher Scientific
CD3	SP34-2	V500	BD Pharmingen
CD8	SK1	Amcyan	BD Pharmingen
CD8	BW135/80	VioBlue	Miltenyi Biotec
CD4	RPA-T4	PE-Cy7	BD Pharmingen
CD45	HI30	PerCP-cy5.5	BD
CD19	HD237	ECD	Beckman Coulter
CD20	2H7	Alexa Fluor 700	BD Pharmingen
CD14	M5E2	PE-cy7	BD Pharmingen
CD14	M5E2	APC	BD Pharmingen
CD16	3G8	APC-H7	BD Pharmingen
CD56	MEM188	PE	BD Pharmingen
CD123	7G3	PE	BD Pharmingen

Copyright © 2020 JoVE Journal of Visualized Experiments

BDCA-1	L161	Pacific Blue	BD Pharmingen
BDCA-3	AD5-14H12	FITC	Miltenyi Biotec
BDCA-4	AD5-17F6	APC	Miltenyi Biotec
HLA-DR	G646-6	PerCP-cy5.5	BD Pharmingen
CD11c	3.9	Alexa Fluor 700	ebiosciences

Table 1: List of antibodies for cell characterization by flow cytometry.

5. Example of Activation of TMCs and Measurement of Cytokine Production

1. Dilute the TMCs in R10 medium to get a concentration of 2 x 10^6 cells/mL.
2. Distribute 400,000 TMCs in 200 µL of R10 in a 96 well round bottom plate.
3. To activate the cells, add 5 µg/mL of the TLR7/8 agonist resiquimod (R848) overnight.
4. Centrifuge the plates and retrieve the TMCs' supernatant and freeze it for further analysis. Cytokine production will be assessed using bead-based immunoassays to quantify multiple soluble cytokines simultaneously using a flow cytometer following the manufacturer's protocol.
5. Assess the viability of the cells using a luminescent cell viability assay following the manufacturer's protocol. Briefly, add 60 µL of cell viability solution to the wells and measure luminescence within 10 min (acquisition for 1 s/well).

Representative Results

We first characterized the immune profile of cells present in the culture and analyzed the amount of TMCs. We phenotyped the TMCs from tonsils with flow cytometry. As shown in **Figure 1**, all major immune cell types present in PBMCs from blood were represent in the TMCs from tonsils. However, in TMCs the frequency of all cell types, except B cells, were lower than in PBMCs.

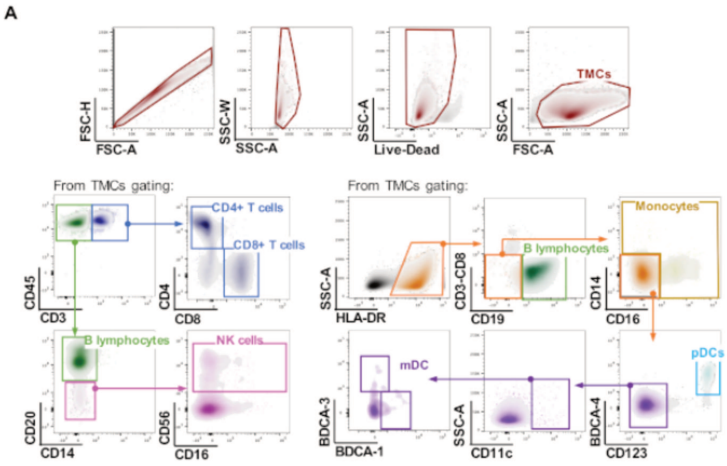

B

Cell type	% of live TMCs in tonsils	% of PBMCs in blood
B lymphocytes	57.44 ± 10.9	12.5 ± 10
CD4+ T cells	20.45 ± 5.87	42.5 ± 35
CD8+ T cells	3.22 ± 1.83	12.5 ± 25
NK cells	0.48 ± 0.39	10 ± 10
Monocytes	1.25 ± 1.34	7.5 ± 5
pDCs	0.064 ± 0.048	0.3 ± 0.13
BDCA-1+ DCs	0.0009 ± 0.0010	0.27 ± 0.26
BDCA-3+ DCs	0.008 ± 0.0080	0.13 ± 0.14

Figure 1: Phenotyping of TMCs in tonsils. TMCs from healthy donors were obtained after dissection of human tonsillar tissue and isolation of cells. (**A**) Cells were stained, and data were acquired by flow cytometry. Data represent a representative experiment. (**B**) The table summarizes the percentage of each cell type in live TMCs in tonsils from six different healthy donors and compares each to the percentage of each cell type in PBMCs from blood, as defined in the literature[18, 19]. Data are shown as the percentage of live cells SD. Please click here to view a larger version of this figure.

We then tested the immunological responses of the TMCs. One way to reproduce a cell's activation against a pathogen is to stimulate the innate immune sensors from the Toll-Like Receptors (TLRs) family. TLRs are mainly present in monocytes/macrophages, all dendritic cell (DC) subtypes, plasmacytoid dendritic cells (pDCs), and also in B cells. In this example, we studied TLR7 and TLR8, because they specialize in antiviral responses and most cases of tonsillitis (i.e., tonsil infections) are caused by a viral infection. Thus, TMCs from tonsils (graph in blue) from seven healthy donors were stimulated overnight with the TLR7/8 ligand resiquimod (R848). As in PBMCs (graph in green), activation through TLR7/8 signaling triggered production of type I interferons (IFN) and pro-inflammatory cytokines. In fact, the cytokine most highly produced in TMCs upon activation was IFNα, a member of the type I IFN family that is mainly involved in innate immunity against viral infection and is mostly produced by the pDCs. All cytokines tested, except IFN2/3 and IL-8, were produced by TMCs, although at lower levels than in PBMCs. Interestingly, some cytokines (mainly IL-8, but also IL-6, IL-10, and TNFα) were present in larger amount at basal levels. Furthermore, we compared the cytokine produced

Copyright © 2020 JoVE Journal of Visualized Experiments

by isolated TMCs or by tonsillar tissue blocs prepared as described previously[6]. We measured all types of IFN produced in the supernatant of both cell cultures using the STING-37 cell line reporter assay as described previously[17] and showed that we could only measure IFN levels in the isolated TMCs.

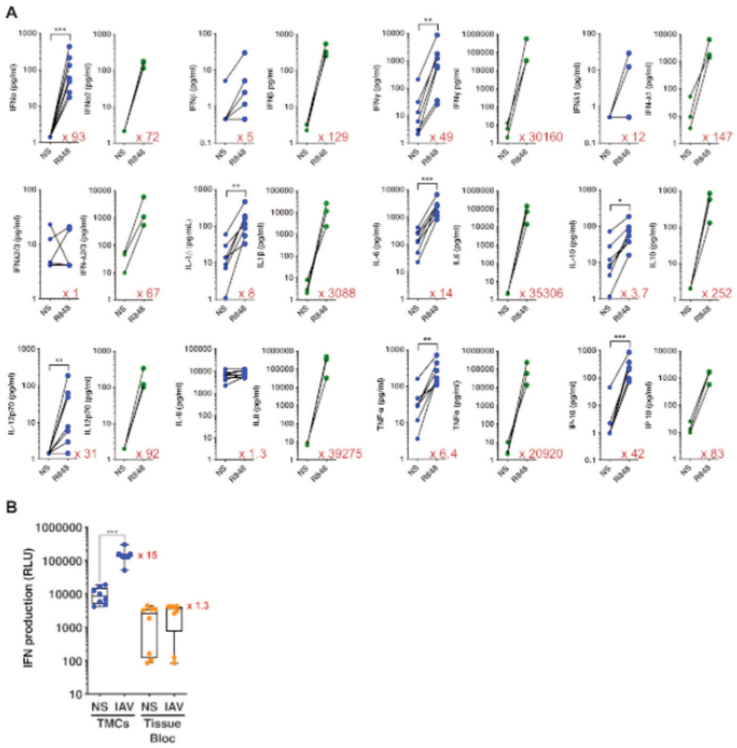

Figure 2: TMCs produced cytokines upon stimulation. (**A**) Purified and isolated TMCs (blue) and PBMCs (green) were stimulated overnight with R848 (5 µg/mL). Supernatants were retrieved and frozen until use. A bead-based immunoassay was performed to quantify multiple soluble cytokines simultaneously using a flow cytometer. The graphs represent the concentration in picograms per milliliter of each measured cytokine. The fold increases are annotated in red on the graphs. Mann-Whitney U test. (**B**) Purified and isolated TMCs from tonsils (blue) and tonsillar tissue blocs (orange) were stimulated for 24 h with Influenza A virus (IAV). A STING-37 reporter cell line assay was used to measure IFN production in the supernatant. Box and whisker plots with median ± minimum to maximum. Mann-Whitney U test. ***$P < 0.001$, **$P < 0.01$, *$P < 0.05$. NS = non-stimulated. Please click here to view a larger version of this figure.

Finally, we tested the viability of the TMCs. Several techniques are available to measure cell viability. Here, we used a luminescent cell viability assay, an easy and quick two-step assay. As shown in **Figure 3**, we clearly detected the cytotoxicity induced by compound 1 in TMCs, which was not toxic to PBMCs. Thus, TMCs showed a higher sensitivity to the drug tested.

Copyright © 2020 JoVE Journal of Visualized Experiments

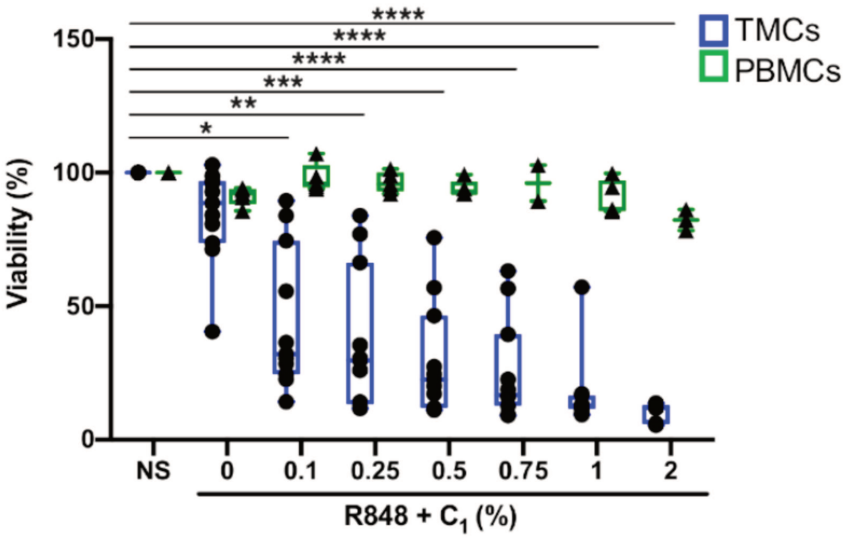

Figure 3: Compound 1 was toxic to TMCs. Purified and isolated TMCs and PBMCs were preincubated with compound 1 (C1) at various concentrations for 1 h and then stimulated overnight with R848 (5 µg/mL). Supernatants were retrieved, 60 µL of cell viability solution was added, and luminescence was measured. The * represents the statistical analysis comparing C1 to NS. Box and whisker plots with median ± minimum to maximum. Kruskal-Wallis test with Dunn's post hoc correction. ****$P < 0.0001$, ***$P < 0.001$, **$P < 0.01$, *$P < 0.05$. NS = non-stimulated. Please click here to view a larger version of this figure.

Discussion

Human tonsils represent an integrative and physiological ex vivo model to study innate immune responses at the mucosal interface, because they mimic the role of a secondary lymphoid organ. Interestingly, the cellular composition of the TMCs is similar to the PBMCs and includes all the major cell populations, although their percentage can be different from PBMCs from blood (**Figure 1**). Additional populations can also be found, as all immune responses are initiated in tissues (mucosa or secondary lymphoid organs) and not in blood.

The use of human tissue explants as well as the use of cell culture or blood cells each have their advantages. However, for the of study cytokine secretion and cell activation, tissue explants were not the best model. In fact, we could not detect any IFN production in the supernatant of tissue explants (**Figure 2B**). We speculate that it is directly consumed by the surrounding cells. On the other hand, stimulation of blood cells (PBMCs) can mimic the primary response to infection but do not mimic what is happening in the tissues, where most of the cytokines are produced and where viruses replicate. Therefore, we set up a protocol to isolate and purify cells arising out of a secondary lymphoid tissue, the tonsil. We purified TMCs from healthy human tonsils, which allows us to investigate immune cell activation upon stimulation. However, one of the limitations of this model is that TMCs do not produce as many pro-inflammatory cytokines as PBMCs ex

Copyright © 2020 JoVE Journal of Visualized Experiments

vivo upon TLR7/8 stimulation, although levels of IFNα, the major antiviral cytokine, is similar in both cultures.

The study of compound toxicity on TMCs versus PBMCs revealed that TMCs are more sensitive to a toxic drug (**Figure 3**). Thus, the toxicity of new drugs and future treatments should be tested in cells from tissues and not only on cell lines, PBMCs, or tissue explants. Therefore, the use of TMCs for drug testing seems to be a future application of the method described.

Tonsils from adults or children can be obtained and processed as described. However, we recommend obtaining tonsils from children for two main reasons: 1) Children's tonsils contain more cells than the adults'[20]. Indeed, tonsillar hypertrophy is particularly common in children, because they fight more childhood viruses. Thus, these large tonsils can become obstructive tonsils and need to be removed by a partial tonsillectomy to avoid complications like sleep apnea[13]; 2) Because adults' tonsils are usually removed after several episodes of ear-nose-throat (ENT) infections, these tonsils are less naïve and contain fewer cells.

It is critical to work on the tonsils as soon as possible after the removal surgery, ideally <3 h after collection. Indeed, right after removal and until dissection, the tonsils from each side are kept together in a 50 mL sterile vial containing around 20 mL of PBS, so that they are totally submerged.

Interdonor variability can represent a major issue for reproducibility. Indeed, variability in cellular composition between donors can be significant. Our protocol, using TMCs and not tissue explants, limits this variability because the cells from the whole tonsils are mixed before being plated and placed in culture, while tissue explants bring intradonor variability in cellular composition because the pieces come from different areas within the same specimen. Partial tonsillectomy can only be performed on noninflamed tonsils, which limits the inflammatory status variability between patients. We also recommend collecting tonsils surgically removed on different days. We have clearly noticed that inter-surgeon and inter-day variabilities are higher than interdonor variability (data not shown).

Disclosures

The authors have nothing to disclose.

Acknowledgments

This work was supported by the Agence National de la Recherche sur le SIDA et les Hépatites ANRS (J-P.H) for the experiments and N.B. fellowship (AAP 2017 166). N.S. acknowledges support from the ANRS for fellowship (AAP 2016 1), the European Molecular Biology Organization EMBO for Fellowship (LT 834 2017), the startup funding program "Baustein" of the Medical Faculty of Ulm University (LSBN.0147) and the Deutsche Forschungsgemeinschaft DFG (SM 544/1 1).

References

1. Taylor, M. W. A History of Cell Culture. *Viruses and Man: A History of Interactions.* 41-52 (2014).
2. Scherer, W. F., Syverton, J. T., Gey, G. O. Studies on the propagation in vitro of poliomyelitis viruses. IV. Viral multiplication in a stable strain of human malignant epithelial cells (strain HeLa) derived from an epidermoid carcinoma of the cervix. *The Journal of Experimental Medicine.* **97** (5), 695-710 (1953).
3. Jones, H. W. Record of the first physician to see Henrietta Lacks at the Johns Hopkins Hospital: History of the

Copyright © 2020 JoVE Journal of Visualized Experiments

beginning of the HeLa cell line. *American Journal of Obstetrics and Gynecology.* **176** (6), s227-s228 (1997).

4. Cummins, J. E. et al. Preclinical Testing of Candidate Topical Microbicides for Anti-Human Immunodeficiency Virus Type 1 Activity and Tissue Toxicity in a Human Cervical Explant Culture. *Antimicrobial Agents and Chemotherapy.* **51** (5), 1770-1779 (2007).
5. Abner, S. R. et al. A Human Colorectal Explant Culture to Evaluate Topical Microbicides for the Prevention of HIV Infection. *The Journal of Infectious Diseases.* **192** (9), 1545-1556 (2005).
6. Introini, A., Vanpouille, C., Fitzgerald, W., Broliden, K., Margolis, L. Ex Vivo Infection of Human Lymphoid Tissue and Female Genital Mucosa with Human Immunodeficiency Virus 1 and Histoculture. *Journal of Visualized Experiments.* (140), e57013 (2018).
7. Elmore, S. A. Enhanced Histopathology of Mucosa-Associated Lymphoid Tissue. *Toxicologic Pathology.* **34** (5), 687 (2006).
8. Strioga, M. M., Dobrovolskiene, N. T. Dendritic Cells as Targets of Vaccines and Adjuvants. *Immunopotentiators in Modern Vaccines.* 43-64 (2017).
9. Bachert, C., Möller, P. Die Tonsille als MALT (mucosa-associated lymphoid tissue) der Nasenschleimhaut. *Laryngo-Rhino-Otologie.* **69** (10), 515-520 (1990).
10. Perry, M., Whyte, A. Immunology of the tonsils. *Immunology Today.* **19** (9), 414-421 (1998).
11. Perry, M. E. The specialised structure of crypt epithelium in the human palatine tonsil and its functional significance. *Journal of Anatomy.* **185**, 111-127 (1994).
12. Cesta, M. F. Normal Structure, Function, and Histology of Mucosa-Associated Lymphoid Tissue. *Toxicologic Pathology.* **34** (5), 599-608 (2006).
13. Kaditis, A. G. et al. Obstructive sleep disordered breathing in 2-to 18-year-old children: diagnosis and management TASK FORCE REPORT ERS STATEMENT. *European Respiratory Journal.* **47**, 69-94 (2016).
14. Herbeuval, J. P. et al. HAART reduces death ligand but not death receptors in lymphoid tissue of HIV-infected patients and simian immunodeficiency virus-infected macaques. *AIDS.* **23** (1), 35-40 (2009).
15. Herbeuval, J. P. et al. Differential expression of IFN-alpha and TRAIL/DR5 in lymphoid tissue of progressor versus nonprogressor HIV-1-infected patients. *Proceedings of the National Academy of Sciences of the United States of America.* **103** (18), 7000-7005 (2006).
16. Smith, N. et al. Control of TLR7-mediated type I IFN signaling in pDCs through CXCR4 engagement-A new target for lupus treatment. *Science Advances.* **5** (7), eaav9019 (2019).
17. Lucas-Hourani, M. et al. Inhibition of pyrimidine biosynthesis pathway suppresses viral growth through innate immunity. *PLoS Pathogens.* **9** (10), e1003678 (2013).
18. Kleiveland, C. R. Peripheral Blood Mononuclear Cells. *The Impact of Food Bioactives on Health.* 161-167 (2015).
19. Ban, Y.-L., Kong, B.-H., Qu, X., Yang, Q.-F., Ma, Y.-Y. BDCA-1+, BDCA-2+ and BDCA-3+ dendritic cells in early human pregnancy decidua. *Clinical and Experimental Immunology.* **151** (3), 399-406 (2008).
20. Papaioannou, G. et al. Age-Dependent Changes in the Size of Adenotonsillar Tissue in Childhood:

Copyright © 2020 JoVE Journal of Visualized Experiments

Implications for Sleep-Disordered Breathing. *The Journal of Pediatrics.* **162** (2), 269-274.e4 (2013).

Copyright © 2020 JoVE Journal of Visualized Experiments

Article 3

Original Research

Identification of Primary Natural Killer Cell Modulators by Chemical Library Screening with a Luciferase-Based Functional Assay

SLAS Discovery
2019, Vol. 24(1) 25–37
© 2018 Society for Laboratory Automation and Screening
DOI: 10.1177/2472555218797078
slasdisc.sagepub.com
SAGE

Simon Hayek[1], Nassima Bekaddour[1], Laurie Besson[2,3], Rodolphe Alves de Sousa[1], Nicolas Pietrancosta[1], Sébastien Viel[2,3], Nikaia Smith[1], Yves Jacob[4], Sébastien Nisole[5], Rupasri Mandal[6], David S. Wishart[6], Thierry Walzer[2], Jean-Philippe Herbeuval[1], and Pierre-Olivier Vidalain[1]

Abstract

Natural killer (NK) cells are essential players of the innate immune response that secrete cytolytic factors and cytokines such as IFN-γ when contacting virus-infected or tumor cells. They represent prime targets in immunotherapy as defects in NK cell functions are hallmarks of many pathological conditions, such as cancer and chronic infections. The functional screening of chemical libraries or biologics would greatly help identify new modulators of NK cell activity, but commonly used methods such as flow cytometry are not easily scalable to high-throughput settings. Here we describe an efficient assay to measure the natural cytotoxicity of primary NK cells where the bioluminescent enzyme NanoLuc is constitutively expressed in the cytoplasm of target cells and is released in co-culture supernatants when lysis occurs. We fully characterized this assay using either purified NK cells or total peripheral blood mononuclear cells (PBMCs), including some patient samples, as effector cells. A pilot screen was also performed on a library of 782 metabolites, xenobiotics, and common drugs, which identified dextrometorphan and diphenhydramine as novel NK cell inhibitors. Finally, this assay was further improved by developing a dual-reporter cell line to simultaneously measure NK cell cytotoxicity and IFN-γ secretion in a single well, extending the potential of this system.

Keywords

natural killer cells, luciferase, screening, dextromethorphan, diphenhydramine

Introduction

Natural killer (NK) cells are essential players of the immune response against viruses and tumor cells.[1] As group 1 innate cytotoxic lymphoid cells, they are characterized by a potent cytotoxicity and the ability to secrete IFN-γ when activated. In humans, they represent 5%–20% of peripheral blood mononuclear cells (PBMCs). NK cells express a set of membrane receptors allowing them to discriminate normal cells from abnormal, virus-infected, or tumor cells. Tumorigenesis and viral infection are indeed often accompanied by the downregulation of NK cell inhibitory ligands and/or the upregulation of activator ligands at the cell surface, allowing target cell detection by NK cells. Once activated, NK cells release the pore-forming protein perforin[2] and pro-apoptotic factors including granzymes and death ligands (FasL, TRAIL, etc.). Besides, secreted IFN-γ contributes to the activation of other effector cells and the induction of an appropriate immune response. As such, NK cells are prime targets in

[1]Chimie & Biologie, Modélisation et Immunologie pour la Thérapie (CBMIT), Université Paris Descartes, CNRS, UMR8601, Paris, France
[2]Centre International de Recherche en Infectiologie, CIRI, Inserm, U1111, Université Claude Bernard Lyon 1, CNRS, UMR5308, École Normale Supérieure de Lyon, University of Lyon, Lyon, France
[3]Laboratoire d'Immunologie, Hospices Civils de Lyon, Centre Hospitalier Lyon Sud, Pierre-Bénite, France
[4]CNRS, UMR3569, Unité de Génétique Moléculaire des Virus à ARN, Institut Pasteur, Université Paris Diderot, Paris, France
[5]Institut de Recherche en Infectiologie de Montpellier, CNRS, UMR9004, Université de Montpellier, Montpellier, France
[6]Departments of Biological Sciences and Computing Science, University of Alberta, Edmonton, Alberta, Canada

Received May 12, 2018, and in revised form July 18, 2018. Accepted for publication Aug 6, 2018.

Corresponding Author:
Pierre-Olivier Vidalain, Chimie & Biologie, Modélisation et Immunologie pour la Thérapie (CBMIT), Université Paris Descartes, CNRS, UMR8601, 45 Rue des Saints Pères, Paris 75270, France.
Email: pierre-olivier.vidalain@parisdescartes.fr

immunotherapy and defects in their activation are hallmarks of pathological conditions, including cancers, genetic disorders, and viral chronic infections. Functional assays measuring NK cell cytotoxicity in vitro or ex vivo are therefore essential to evaluate the potential impact of small molecules, antibodies, or proteins on this immune cell population.

The reference method to measure the cytotoxic activity of NK cells ex vivo is based on the release of chromium 51 (^{51}Cr) by target cells preloaded with this radioactive isotope.[3] When target cells are co-incubated with NK cells, the permeabilization of their membrane is accompanied by the release of ^{51}Cr in culture supernatant, which reflects the cytolytic activity of NK cells. This method has been widely used for decades, but is progressively abandoned because of the risks and regulatory constraints associated with the manipulation of radioactive elements. A more recent and popular method is based on the use of multicolor flow cytometry to quantify the lysis of target cells in co-cultures.[4] Fluorescent dyes or specific membrane markers are used to discriminate NK cells from target cells at the time of analysis, while the fraction of dead target cells is calculated using viability dies. Alternatively, NK cell cytotoxicity can be indirectly quantified by surface immunostaining of the degranulation marker CD107a (LAMP1), which is correlated with NK cell-mediated lysis.[5] Although widely used, all methods based on flow cytometry require some expensive equipment and trained personal, and are time-consuming at both the acquisition and analysis steps. For these reasons, they are not well adapted to large-scale screening projects, and alternative strategies have been developed to measure NK cell activation in high-throughput settings.

Established strategies include the quantification of secreted IFN-γ by enzyme-linked immunosorbent assay (ELISA) in co-culture supernatants, which is tractable for high-throughput screening (HTS).[6,7] However, IFN-γ secretion is not always correlated with the cytotoxic activity, a limitation that adds to the significant cost and multistep protocol inherent to ELISA. Other described tests involve the co-culture of PBMCs or NK cells with adherent target cells.[8] After incubation, effector cells and dead target cells are washed out, and the number of living target cells still attached to culture wells is quantified by different methods. Alternatively, the number of adherent target cells in co-cultures, without the need for washing out NK cells, can be determined by electrical impedance measurements.[9] However, such assays are limited to adherent target cells and rely on the quantification of surviving cells in culture wells rather than a direct quantification of cell lysis. Finally, nonradioactive alternatives to ^{51}Cr have been developed, such as calcein, a fluorescent molecule, which can be loaded as a pro-form (Calcein-AM) in target cells.[10] However, calcein staining relies on endogenous cellular esterase for processing the pro-form of the dye and was criticized for its low signal-to-noise (S/N) ratio. Europium was also used as a nonradioactive substitute to ^{51}Cr, but it never became popular due to some high background observed in many target cell lines.[11] Other cytotoxicity assays are based on the release of endogenous cytosolic enzymes such as lactate dehydrogenase.[12] This enzyme can be detected in culture supernatants with synthetic substrates that are converted into colored or fluorescent products. The sensitivity of these methods has been a matter of debate, in particular in co-cultures, because when dying, not only target cells but also effector cells potentially release such endogenous enzymes in the medium. Therefore, there are still some unmet needs for a sensitive high-throughput assay to measure the cytotoxicity of NK cells.

Along with the development of *firefly* luciferase as a reporter in biological systems, bioluminescent assays have been engineered to measure NK cell cytotoxicity. Decarboxylation of the luciferase substrate luciferin by *firefly* luciferase leads to light emission that can be quantified. Interestingly, this reaction requires ATP that is essentially present in living but not dead cells. Thus, target cells were engineered to express *firefly* luciferase, and co-cultured with NK cells. When luciferin is added to culture wells, it penetrates all cells in the co-culture but is only processed by luciferase-expressing target cells that are alive and produce ATP.[13] This method was shown to outperform the standard ^{51}Cr cytotoxicity assay but is dependent on intracellular ATP levels, and the S/N ratio can be low in common target cell lines such as K562.[14] In parallel, other research groups tried to develop cytotoxicity assays based on the release of *firefly* luciferase in culture supernatants when lysis occurs.[15,16] However, this approach was hampered by the short half-life of *firefly* luciferase in culture medium at 37 °C. Recently, the development of high-performance luciferases derived from marine organisms has provided a new start to this approach.[17,18] The best example is NanoLuc, a synthetic luciferase of 19 kDa developed by Promega (Fitchburg, WI) from a luminescent enzyme of the sea shrimp *Oplophorus gracilirostris*.[19] This enzyme uses furimazine as a substrate, of which decarboxylation is ATP independent. NanoLuc is >150 times brighter than *firefly* luciferase and, more importantly, is stable for days in culture medium. We took advantage of this new generation of luciferase to develop a high-throughput functional assay to measure the natural cytotoxicity of primary NK cells (**Fig. 1**). Two clonal cell lines expressing high levels of NanoLuc in their cytoplasm, called K562-NL and twINNE, were engineered, and NanoLuc release in culture supernatant was determined in co-cultures with purified effector cells, including primary NK cells, total PBMCs from healthy donors, treated or not with cytokines or immunomodulatory compounds, and PBMCs from a perforin-deficient patient. We also established that NanoLuc release by target cells is robust enough to screen chemical libraries in high-throughput settings and to identify modulators of NK cell activity. Finally, we further improved this assay by developing the dual-reporter cell line

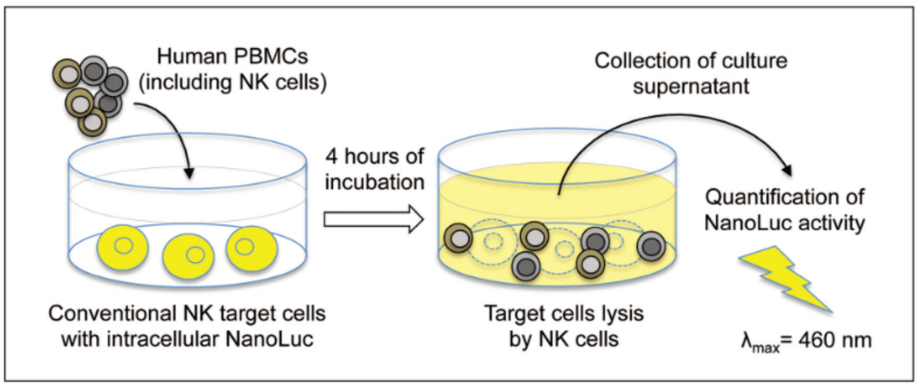

Figure 1. Principle of the luciferase-based cytotoxicity assay. PBMCs are co-cultured with target cells expressing high levels of NanoLuc in the intracellular compartment. After a few hours of incubation, NK cells from PBMCs mediate the lysis of target cells, thus releasing NanoLuc in culture supernatant. NanoLuc activity in culture supernatant reflects target cell lysis.

twINNE, where a *firefly* luciferase reporter gene is used to monitor interferon signaling in target cells while, in parallel, NanoLuc release is reporting their lysis.

Materials and Methods

Cells and Culture Conditions

Cells were cultured at 37 °C and 5% CO_2 in RPMI-1640 medium (Sigma-Aldrich, St. Louis, MO; R8758) containing 10% fetal calf serum (FCS). Human K562 cells were kindly provided by Dr. T. Walzer (CIRI, Lyon, France). The reporter cell line STING-37, corresponding to HEK-293 cells stably transfected with the interferon-stimulated response element (ISRE)-luciferase reporter gene, was previously described.[20] Blood from healthy blood bank donors was obtained from Etablissement Français du Sang (Convention 07/CABANEL/106; Paris, France). Human PBMCs were isolated by density centrifugation with Lymphoprep medium (StemCell Technologies, Vancouver, Canada) from total blood or leucocyte concentrates obtained when plateletpheresis is performed. NK cells were purified from PBMCs using the NK cell isolation kit from Miltenyi (Bergisch Gladbach, Germany). Recovered NK cells were pure at >94% as assessed by their CD3–/CD56+ phenotype. A patient with a confirmed homozygous missense mutation in *PRF1* was included in this study. A blood sample was obtained upon informed consent.

Cytokines, Small Compounds, and Reagents

Human IFN-γ from Roussel Uclaf (Romainville, France) was a kind gift of Dr. Mounira Chelbi-Alix. IL-2, IL-15, and TGF-β were obtained from Peprotech (Rocky Hill, NJ). R848 was obtained from Sigma-Aldrich, Torin2 was from Tocris (Bristol, UK), and rapamycin was from Calbiochem (San Diego, CA). Luciferase induction in twINNE cells was determined using the Bright-Glo (Promega, Fitchburg, WI) or Britelite plus reagents (PerkinElmer, Waltham, MA), according to the manufacturer's recommendations. Nanoluc expression was quantified in culture supernatants as previously described.[19] Cellular viability was determined by quantification of ATP in culture wells using the CellTiter-Glo assay (Promega). Bioluminescence was measured for 0.1 s with a luminometer (EnSpire; PerkinElmer). Tergitol NP9 was from Sigma-Aldrich.

Establishing K562-NanoLuc and twINNE Cell Lines

The NanoLuc gene was introduced in target cells by transduction with the pLVX-Puro lentiviral vector (Clontech, Mountain View, CA). First, the NanoLuc sequence was cloned in the pLVX-Puro vector using the Gateway cloning system (Thermo Fisher Scientific, Waltham, MA). Briefly, the pLVX-Puro plasmid was made compatible with the Gateway system by inserting the Gateway cassette C1 at the *Sma*I site to generate the new destination vector called pLVX-Puro-GW. A pDONR207 plasmid containing the coding sequence for the NanoLuc enzyme (Promega) was kindly provided by Dr. Y. Jacob (Institut Pasteur, Paris, France). The NanoLuc sequence was transferred by in vitro LR recombination from pDONR207 to pLVX-Puro-GW vector following the manufacturer's recommendations to obtain pLVX-Puro-NanoLuc. This vector was used to produce lentiviral particles by co-transfection with packaging plasmids pVSV-G and pGag-Pol (kindly provided by Dr. S. Nisole, IRIM, Montpellier, France) into HEK-293T cells. Culture supernatants containing lentiviral particles were collected 2 days later and stored at –80 °C.

K562 and STING-37 cells were transduced with the lentiviral vector expressing NanoLuc, and puromycin at 1 µg/mL was applied for 4 weeks to enrich the cellular pool for transduced cells. Using a cell sorter, 576 and 63 cells were cloned from the transduced populations of K562 and STING-37 cells, respectively. After 4 weeks, culture wells were tested for the expression of NanoLuc to identify best-growing clones expressing high levels of the enzyme. Top candidates were amplified for establishing the K562-NL and twINNE cell lines, which respectively correspond to K562 and STING-37 clones expressing high levels of NanoLuc.

Cell Cytotoxicity Assay. PBMCs from healthy donors were incubated overnight in the absence or presence of compounds to be tested. Unless specified otherwise, PBMCs were plated in 96-well, round-bottom plates at a concentration of 400,000 cells/well in a final volume of 100 µL. After 16 h, 16,000 K562-NanoLuc or 100,000 twINNE cells were added to culture wells (100 µL of a cell suspension at 160,000 cells/mL or 1×10^6 cells/mL, respectively). The total volume in culture wells was 200 µL, and plates were centrifuged briefly for 2 min at 1200 rpm. Unless specified otherwise, 20 µL of culture supernatants was collected after 4 or 7 h of co-culture for K562-NL or twINNE, respectively, and NanoLuc activity was determined by adding 40 µL of RPMI-1640 and 30 µL of NanoLuc reagent (as described in Hall et al.[19] Promega) in black, flat-bottom, 96½-well plates. Bioluminescence was measured for 0.1 s with a luminometer (Enspire; PerkinElmer).

To quantify the death of target cells by flow cytometry, K562-NL cells were labeled with the VDP450 dye at 1 µM in PBS (BD Biosciences, Franklin Lakes, NJ). After 10 min of incubation at 37 °C, cells were washed thoroughly in culture medium and co-cultured with PBMCs as described above. After 4 h, cells were collected and dead cells were labeled using the LIVE/DEAD fixable green stain reagent from Invitrogen (Waltham, MA) following the manufacturer's recommendations. Cells were analyzed by flow cytometry, and the percentage of dead K562-NL cells was determined by gating on the $VDP450^+$ cells.

Screening of the TMIC Human Metabolome Library. The TMIC Human Metabolome Library was obtained from The Metabolomics Innovation Center in Canada (TMIC; www.metabolomicscentre.ca). It is a comprehensive library of compounds representing a broad range of metabolites, xenobiotics, and drugs commonly found in body tissues. Briefly, 5 mg of each compound was dissolved in 2 mL of either pure water or a 50% mix of water and DMSO to achieve a final stock concentration of 2.5 mg/mL. Compounds were rearrayed in deep-well plates, and daughter plates were prepared by spotting 2 µL in round-bottom, 96-well plates for screening. Culture wells were filled with PBMCs at 400,000 cells/well in a final volume of 100 µL as described above, so that test compounds were at 50 µg/mL. For each screening plate, negative control wells were filled with culture medium alone, whereas positive control wells were filled with PBMCs plus 2 µL of a 50% water–DMSO mixture. After 16 h, 16,000 K562-NanoLuc cells were added to all culture wells (100 µL of a cell suspension at 160,000 cells/mL). NanoLuc activity in culture supernatants was determined after 4 h of co-culture as described above, and the results were expressed as a percentage relative to positive control wells. The Z′ factor that reflects the robustness and quality of the assay was calculated from means ($\mu+$ and $\mu-$) and standard deviations ($\sigma+$ and $\sigma-$) of negative and positive controls such as $Z' = 1 - 3*(\sigma+ + \sigma-)/(\mu+ - \mu-)$, as described by Zhang et al.[21] Very good assays have Z′ factors that are close or superior to 0.5. The signal-to-background (S/B) ratio corresponds to $\mu+/\mu-$, and the S/N ratio to $(\mu+ - \mu-)/\sigma-$, as previously defined.[21]

Results

Development and Assessment of the K562-NL Reporter Cell Line

Myeloid leukemia cells K562 were transduced with a lentiviral vector to express NanoLuc, and cell clones were carefully screened to select those expressing this bioluminescent enzyme at high levels. The best cellular clone was amplified to establish the K562-NL reporter cell line. First, we tested if NanoLuc is released in culture supernatants when membrane permeabilization occurs. K562-NL cells were treated with 1% Tergitol as a detergent to lyse cells, and culture supernatants were harvested at different time points. Cell lysis was confirmed by standard light microscopy (data not shown). As presented in **Figure 2A**, high levels of NanoLuc activity were detected in culture supernatants and were maximal after only 3 min. As expected, ATP in culture wells, which is a common biomarker of cellular metabolic activity and used to determine viability, was gradually degraded in the 0–30 min time window, showing that NanoLuc release is concomitant with cell death.

Since our goal was to determine whether K562-NL cells can be used as target cells to measure the cytotoxic activity of NK cells in PBMCs, we verified that NanoLuc activity in culture supernatants is not impaired by the addition of a large number of PBMCs in the culture wells. Increasing numbers of K562-NL cells—ranging from 2500 to 80,000 cells—were dispensed in culture wells of a 96-well plate and killed by freezing and thawing. Then, 400,000 PBMCs were added or not to culture wells, and after centrifugation, culture supernatants were immediately collected to quantify NanoLuc activity. As expected, the NanoLuc activity dramatically increased in culture supernatants when K562-NL cells were killed, and more importantly, the signal was not affected by the addition of PBMCs to culture wells (**Fig. 2B**). We also verified that the NanoLuc signal in culture supernatants of killed K562-NL cells mixed with PBMCs was stable in time, without any significant loss over 24 h (data not shown). Altogether, this demonstrated that NanoLuc release in culture supernatants of K562-NL cells is suitable to monitor their lysis by NK cells.

Measuring NK Cell Cytotoxicity with K562-NL Target Cells

A fixed number of K562-NL cells—herein referred as the target cells—were co-cultured with PBMCs, the effector

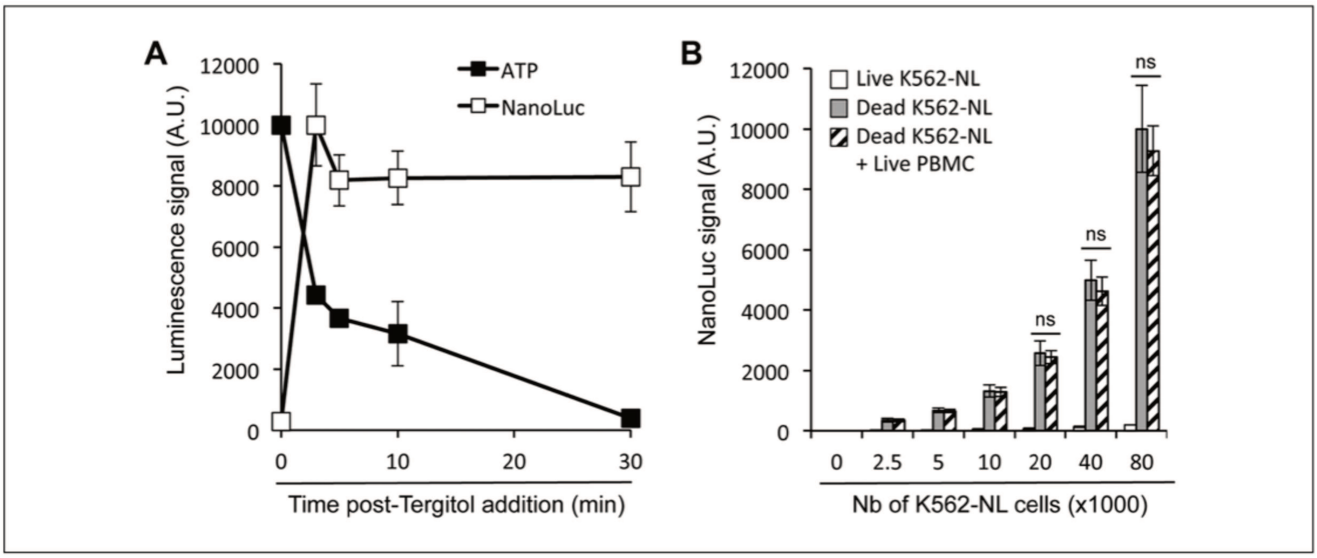

Figure 2. Nanoluc accumulates in culture supernatants of K562-NL cells when killed by chemical or physical treatments. (**A**) K562-NL cells were treated with 1% Tergitol, and NanoLuc released in culture supernatants was determined at different time points. Alternatively, ATP in culture wells was quantified as a measure of cellular viability. Raw luminescence values were normalized to the signal obtained with living K562-NL cells alone. (**B**) K562-NL cells were dispensed at different concentrations in culture wells and maintained alive or killed by freezing and thawing. When indicated, 400,000 PBMCs were added to culture wells containing dead K562-NL cells. Cell cultures were immediately centrifuged, and NanoLuc activity was quantified in culture supernatants. Raw luminescence values were normalized to the signal obtained with 80,000 living K562-NL cells alone. All data correspond to means ± SD of three independent experiments. ns = nonsignificant as determined by two-way ANOVA with Bonferroni post hoc test.

cells, at different effector-to-target (E/T) ratios ranging from 0.8 to 50. After 4 h of incubation, culture supernatants were harvested and tested for NanoLuc activity. Results were expressed as the percentage of NanoLuc released by K652-NL cells permeabilized with 1% Tergitol. As shown in **Figure 3A**, NanoLuc activity increased proportionally with E/T ratios. We also performed the same experiment quantifying the number of dead K562-NL cells in co-cultures by chemical staining (LIVE/DEAD reagent) and conventional flow cytometry analysis. NanoLuc accumulation in culture supernatants appeared to be more sensitive than flow cytometry, as the killing of K652-NL cells was detectable at lower E/T ratios (**Fig. 3A**). We also performed the same co-culture experiment at a 25/1 ratio and quantified NanoLuc in supernatants at different time points (**Fig. 3B**). As expected, the signal continuously increased over 8 h of co-culture. After 24 h of co-culture, 100% lysis was reached in these co-culture conditions (data not shown). However, 4 h was sufficient to obtain a strong signal that is statistically distinct from K562-NL cells alone. Finally, donor-to-donor variation was assessed by testing PBMCs from 13 different donors at an E/T ratio of 25/1 and measuring lysis of target cells after 4 h of co-culture (**Fig. 3C**). Altogether, this demonstrated the efficiency and robustness of this assay to detect the cytotoxic activity of PBMCs.

The percentage of NK cells in PBMCs varies from 5% to 20%. We thus performed the same assay with NK cells purified from PBMCs. As expected, NanoLuc activity increased in culture supernatants of K562-NL cells when co-cultured with purified NK cells (**Fig. 3D**) and reached high levels at lower E/T ratios than previously reported with total PBMCs. Furthermore, we showed that when PBMCs were depleted of NK cells, NanoLuc did not accumulate anymore in co-culture supernatants (**Fig. 3E**). Reconstitution with purified NK cells restored the cytotoxic activity of PBMCs and the accumulation of NanoLuc in culture supernatants. Altogether, these data demonstrated the key role of NK cells in the cytotoxicity of PBMCs toward K562-NL cells and the accumulation of NanoLuc in culture supernatants.

Testing the Effects of Known Modulators of NK Cell Cytotoxicity

We then tested in this assay the effect of small compounds or cytokines that are known to modulate NK cell cytotoxicity, either directly or indirectly. First, PBMCs were stimulated with R848 (or resiquimod), a small agonist of TLR7 and TLR8. R848 mimics the immunostimulatory effects of single-stranded viral RNA molecules and stimulates NK cell cytotoxicity through the activation of antigen-presenting

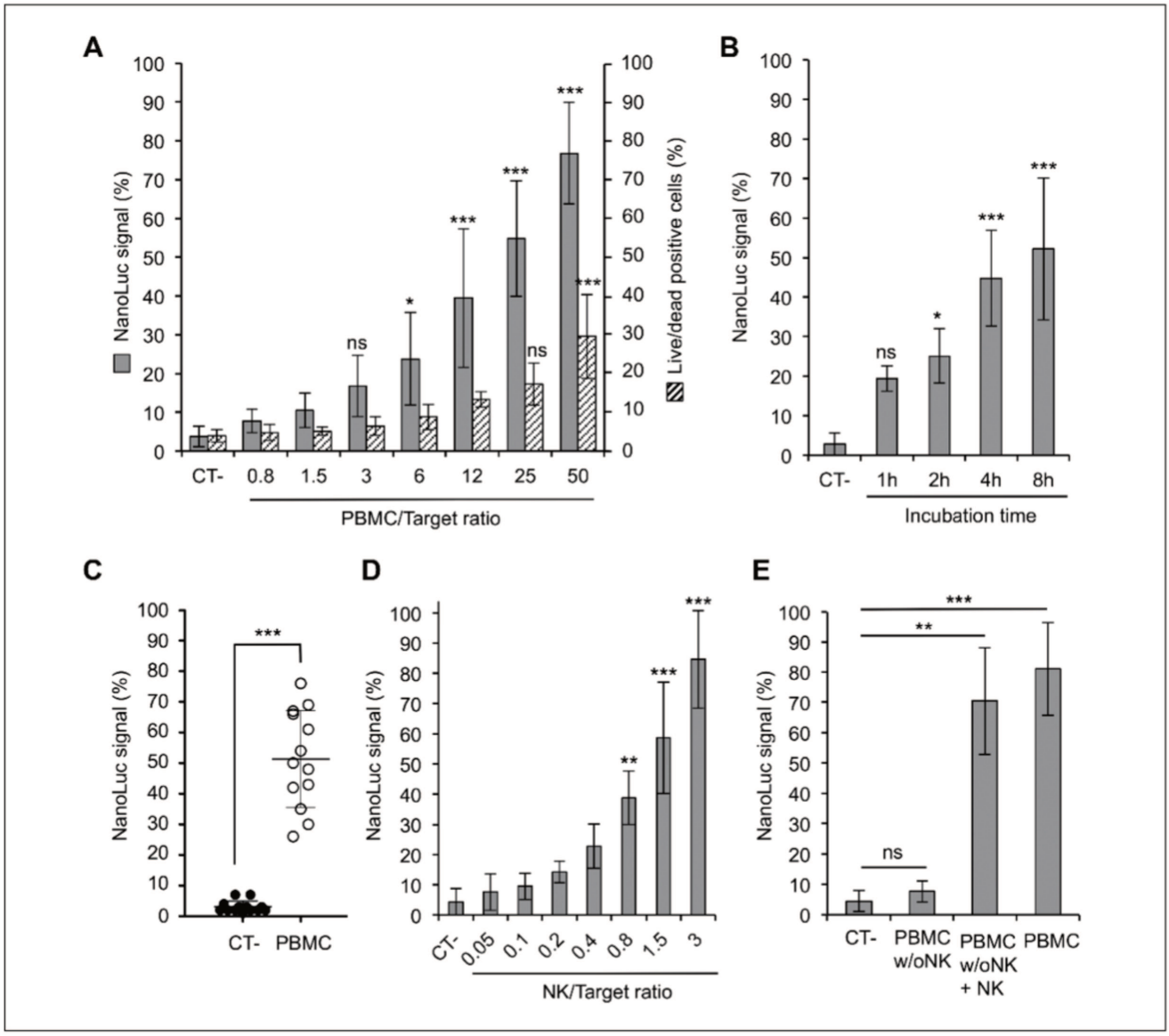

Figure 3. Measuring NK cell cytotoxicity with K562-NL target cells. (**A**) PBMCs were co-cultured with K562-NL cells at different E/T ratios. NanoLuc activity in culture supernatants was measured after 4 h of incubation. Results were expressed as a percentage of NanoLuc released by K652-NL cells permeabilized with 1% Tergitol. In parallel experiments, the number of dead K562-NL cells in co-cultures was determined by LIVE/DEAD viability staining and flow cytometry analysis. (**B**) PBMCs were co-cultured with K562-NL at a 25/1 ratio, and Nanoluc activity in culture supernatants was determined at different time points. (**C**) PBMCs from 13 different donors were co-cultured with K562-NL at a 25/1 ratio, and Nanoluc activity in culture supernatants was determined after 4 h of co-culture. Each circle corresponds to one specific donor, and the mean ± SD is represented. (**D**) NK cells were co-cultured with K562-NL cells at different E/T ratios, and NanoLuc activity in culture supernatants was determined after 4 h of incubation. (**E**) Total PBMCs or PBMCs depleted of NK cells (w/oNK) were co-cultured with K562-NL cells at a 25/1 ratio, and NanoLuc activity in supernatants was determined after 4 h of incubation. The w/oNK+NK condition corresponds to PBMCs depleted of NK cells that were reconstituted with 8% of purified NK cells. (**A–E**) Results were expressed as a percentage of NanoLuc released by K562-NL cells permeabilized with 1% Tergitol. All data correspond to means ± SD of at least three donors. *$p < 0.05$, **$p < 0.01$, and ***$p < 0.001$ as determined by one-way ANOVA with Bonferroni post hoc test (**A,B,D,E**) or Student's *t*-test (**C**). ns = nonsignificant.

cells. PBMCs were pretreated overnight with R848, and K562-NL target cells were added. After 4 h of co-culture, NanoLuc activity in culture supernatants was measured. As shown in **Figure 4A**, R848 increased NanoLuc levels in co-culture supernatants as a consequence of NK cell stimulation. Similar results were obtained when pretreating PBMCs

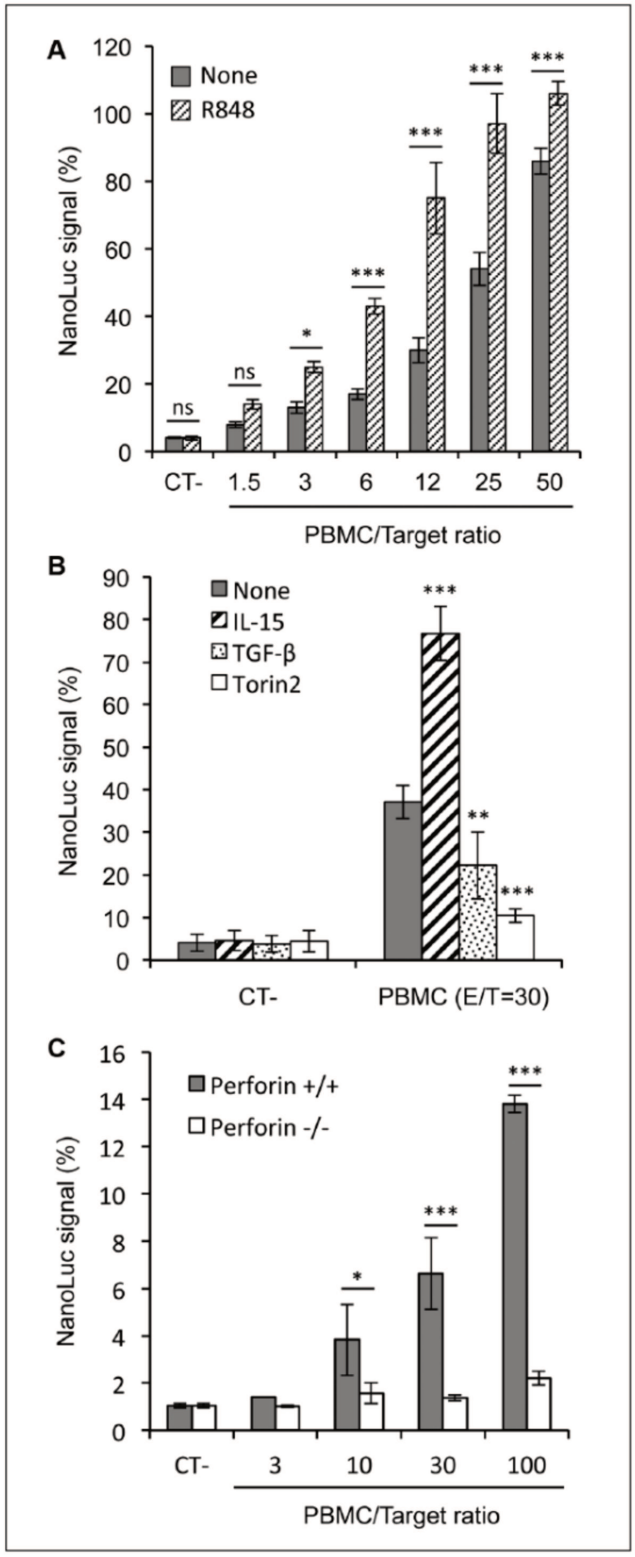

Figure 4. Testing the effects of known modulators of NK cell cytotoxicity. (**A**) PBMCs were pretreated overnight with R848 (15 µM) to stimulate the cytotoxicity of NK cells. K562-NL target cells were added, and NanoLuc activity in culture supernatants was determined after 4 h of co-culture. Data correspond to means ± SD of one representative experiment of three performed in triplicate. (**B**) PBMCs were pretreated overnight with IL-15 (100 ng/mL), TGF-β (10 ng/mL), or Torin2 (250 nM), and then K562-NL target cells were added. The experiment was performed at an E/T ratio of 30, and cells were co-cultured for 4 h at 37 °C before NanoLuc activity was determined in culture supernatants. Data correspond to means ± SD of three donors. (**C**) The cytotoxicity of PBMCs from a perforin –/– patient was compared with that of PBMCs from a healthy donor. PBMCs were co-cultured with K562-NL at different E/T ratios, and after 7 h at 37 °C, NanoLuc activity in culture supernatants was determined. Results were expressed as a percentage of NanoLuc released by K562-NL cells when permeabilized with 1% Tergitol (**A,C**) or co-cultured with IL2-stimulated PBMCs at a 100:1 E/T ratio (**B**). Data correspond to means ± SD of one experiment performed in duplicate. *$p < 0.05$, **$p < 0.01$, and ***$p < 0.001$ as determined by two-way ANOVA (**A,C**) or one-way ANOVA (**B**) with Bonferroni post hoc test. ns = nonsignificant.

(continued)

with IL-15, a cytokine known to increase the cytotoxicity of NK cells (**Fig. 4B**).[22] Alternatively, PBMCs were pretreated overnight with TGF-β, a cytokine known to inhibit NK cell functions.[23] As expected, NanoLuc accumulation in co-culture supernatants was reduced (**Fig. 4B**). Similar results were obtained with Torin2, a potent inhibitor of the mTOR pathway that is essential to NK cell cytotoxicity (**Fig. 4B**).[22] Altogether, these results demonstrated that our assay is suitable to screen small compounds or cytokines to identify new inhibitors or activators of NK cells.

Familial histiolymphocytosis (FHL) is a severe inflammatory condition characterized by abnormally activated macrophages infiltrating multiple tissues, hepatosplenomegaly, nonremitting high fever, cytopenia, hypertriglyceridemia, and hyperferritinemia. It is caused by gene mutations that impair NK and CD8 T-cell cytotoxic function. In this group of diseases, perforin (PRF1) deficiency is responsible for FHL type 2 (FHL2). Quick diagnosis of FHL and potent treatment are essential to prevent fatal evolution. To determine if our assay could help in the diagnosis of such a pathological condition, PBMCs from a perforin-deficient patient were tested. Because of technical constraints, PBMCs from this patient and the matching healthy control were conserved overnight at 4 °C before the assay could be performed. This probably accounts for the low cytotoxic activity detected with control PBMCs even at a high E/T ratio. Nevertheless, the results obtained clearly showed that PBMCs from the perforin-deficient patient completely lost their cytotoxic activity as assessed by the absence of NanoLuc accumulation in culture supernatants (**Fig. 4C**). Therefore, this assay can be used to monitor ex vivo the cytotoxic activity of NK cells from patients while starting from a blood sample of only a few milliliters and could be used as a screening test in the diagnosis of diseases caused by defects in lymphocyte cytotoxicity.

Screening a Chemical Library of Metabolites, Xenobiotics, and Common Drugs

Our next objective was to test if our NanoLuc-based functional assay was suitable to rapidly screen hundreds of molecules using fresh PBMCs. To establish a proof of concept, we selected a chemical library from TMIC that aggregates 782 metabolites, xenobiotics, and frequently used over-the-counter medications: the TMIC Human Metabolome Library. Our objective was to determine if some of these molecules might impact the function of NK cells, with potential consequences on the organism's ability to fight against virus infections or tumors.

PBMCs from two healthy donors were incubated overnight with compounds at 50 µg/mL, and K562-NL target cells were added to evaluate the cytotoxic activity of NK cells. Each screening plate included either four (donor 1) or seven (donor 2) positive and negative controls that corresponded to PBMCs + K562-NL cells or K562-NL cells alone, respectively. After 4 h of co-culture, NanoLuc activity was measured in culture supernatants. On average, the S/B ratio, which corresponds to the mean value of positive controls ($\mu+$) divided by the mean value of negative controls ($\mu-$), was 8.6 for donor 1 and 19.2 for donor 2. The S/N ratio, which corresponds to the difference of $\mu+$ minus $\mu-$ relative to the standard deviation of negative controls ($\sigma-$), was 22.2 for donor 1 and 66.5 for donor 2. The Z′ factor, which reflects the overall quality of the assay and is calculated with the formula $1 - 3*(\sigma+ + \sigma-)/(\mu+ - \mu-)$, was 0.49 for donor 1 and 0.61 for donor 2. Altogether, these statistical parameters qualify this assay for HTS.[21] In parallel, PBMCs were incubated in the same conditions with test compounds, and ATP levels in culture wells were determined to identify toxic molecules (**Fig. 5A**). Eighty compounds reduced ATP levels by more than 25%, thus supporting some significant impact on cellular metabolic activity and viability. Of the remaining 702 compounds, 12 compounds were found to inhibit the lysis of target cells by >75% in the two screens, supporting the inhibition of NK cell cytotoxicity toward target cells (**Fig. 5A**).

Interestingly, six of these compounds were previously reported to inhibit NK cells (**Fig. 5B**), thus confirming the robustness of our screening pipeline.[24–29] We also identified six compounds as new inhibitors, including three metabolites (7-dehydrocholesterol, oleanolic acid, tryptamine) and three medications (dextrometorphan, diphenhydramine, brompheniramine). These compounds were retested in dose–response experiments using PBMCs from at least three healthy donors to estimate the half-maximal inhibitory concentrations, which range from 10 to 126 µM (**Fig. 5C**). Dextrometorphan and diphenhydramine were particularly interesting because of the potent inhibition of target lysis, and a limited impact on the viability of PBMCs.

Development of a Dual-Reporter Assay to Measure Both Target Cell Lysis and IFN Secretion

NK cell activation is associated with the production of type II interferon (IFN-γ), which is released through vesicles and secretory pathways that are distinct from cytotoxic granules.[30] In order to further improve our screening assay, we developed new target cells for monitoring both the cytotoxic activity and the production of interferons by NK cells. We previously developed a HEK-293 cell line stably transfected with a *firefly* luciferase reporter gene controlled by ISREs in its promoter (STING-37 cell line).[20] These reporter cells not only respond to type I IFNs but also to IFN-γ, which efficiently induced the expression of *firefly* luciferase (**Fig. 6A**), making them suitable to detect the secretion of this cytokine by activated NK cells. Thus, STING-37 cells were engineered to express NanoLuc, so that NK cell cytotoxicity can be concomitantly monitored in the same culture wells. Best clones were amplified and carefully selected to establish a reporter cell line that we called twINNE because of its dual-reporter system based on *firefly* and NanoLuc luciferases. When these cells were co-cultured with PBMCs for 7 h at relatively low E/T ratios ranging from 0.5:1 to 4:1, NanoLuc expression in culture supernatants increased as a consequence of target cell lysis (**Fig. 6B**). In parallel, the cellular expression of *firefly* luciferase increased as the ISRE-luciferase reporter was induced in co-cultures (**Fig. 6B**). When the same experiment was performed at higher E/T ratios, the expression of *firefly* luciferase did not increase (data not shown), probably because target cells were lysed before the induction of the ISRE-luciferase reporter. Therefore, this dual-reporter system is allowing the quantification of both target cell lysis and interferon signaling from a single well, provided that experiments are performed at low E/T ratios. Finally, we tested Torin2, diphenhydramine, and dextromethorphan in this new assay. As expected, all three compounds were found to inhibit the lysis of target cells, but interestingly (**Fig. 6C**, upper panel), only Torin2 completely blocked the expression of the ISRE-luciferase reporter (**Fig. 6C**, lower panel). The situation was intermediate with dextromethorphan, while the ISRE-luciferase reporter was barely inhibited by diphenhydramine (**Fig. 6C**, lower panel). These profiles demonstrate the inhibitory properties of these drugs, but also support distinct modes of action for Torin2, dextromethorphan, and diphenhydramine and different consequences on NK cell functions. Altogether, this validates our assay and highlights the interest of such a dual-reporter system.

Discussion

NK cells play a central role in the innate immune response against intracellular pathogens and tumor cells and are

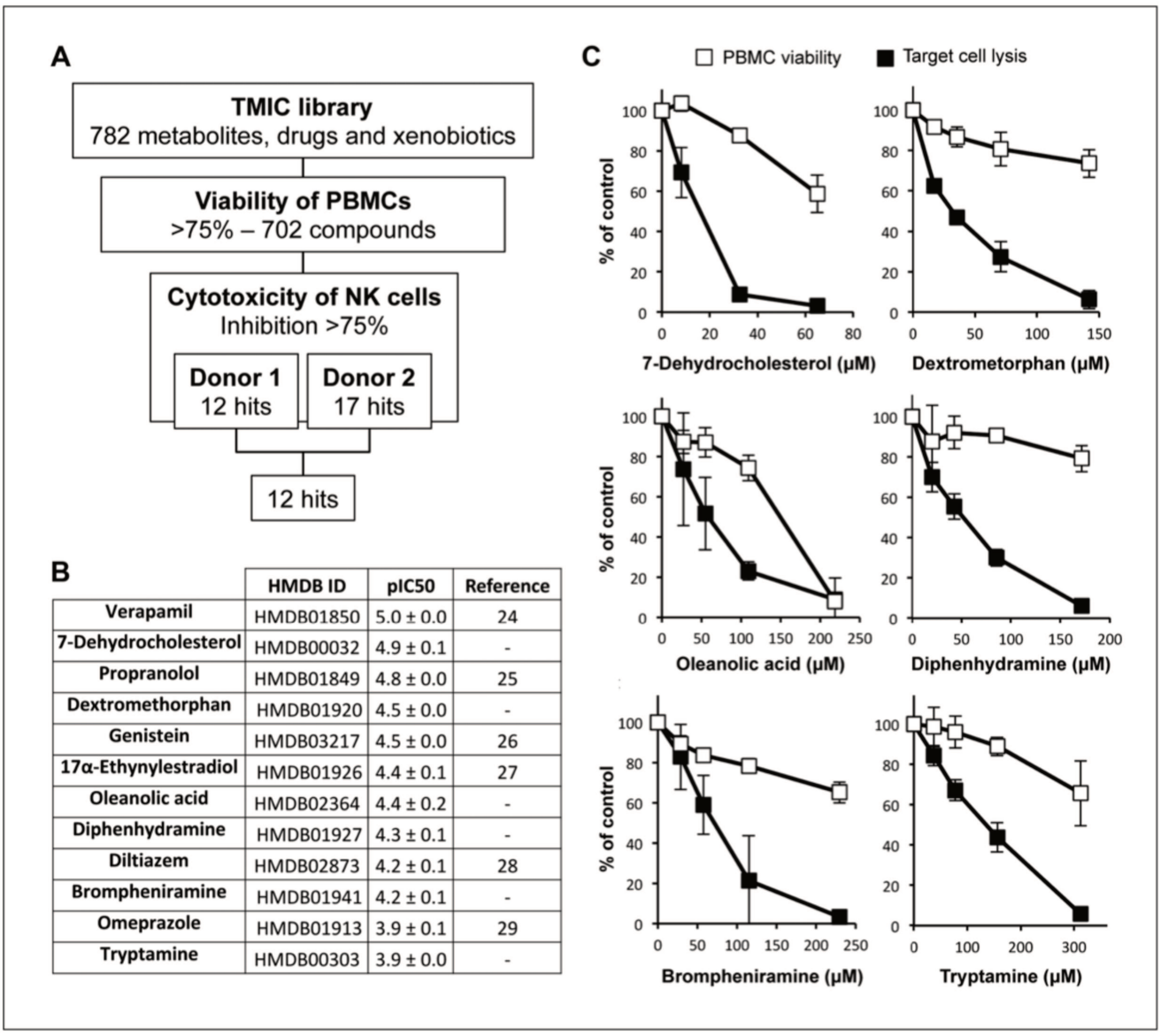

	HMDB ID	pIC50	Reference
Verapamil	HMDB01850	5.0 ± 0.0	24
7-Dehydrocholesterol	HMDB00032	4.9 ± 0.1	-
Propranolol	HMDB01849	4.8 ± 0.0	25
Dextromethorphan	HMDB01920	4.5 ± 0.0	-
Genistein	HMDB03217	4.5 ± 0.0	26
17α-Ethynylestradiol	HMDB01926	4.4 ± 0.1	27
Oleanolic acid	HMDB02364	4.4 ± 0.2	-
Diphenhydramine	HMDB01927	4.3 ± 0.1	-
Diltiazem	HMDB02873	4.2 ± 0.1	28
Brompheniramine	HMDB01941	4.2 ± 0.1	-
Omeprazole	HMDB01913	3.9 ± 0.1	29
Tryptamine	HMDB00303	3.9 ± 0.0	-

Figure 5. Screening a chemical library of metabolites, xenobiotics, and common drugs. PBMCs from two healthy donors were used to screen the TMIC Human Metabolome Library. (**A**) Screening pipeline showing the selection of nontoxic inhibitors of NK cell cytotoxicity. The viability of PBMCs was determined by ATP quantification in culture wells. By measuring NanoLuc levels in culture supernatants the inhibition of target cell lysis was assessed. (**B**) Twelve compounds were found to inhibit target cell lysis in two independent screens. pIC_{50} values correspond to $-\log_{10}$ values of the IC_{50} values as determined on PBMCs from ⩾3 healthy donors. References correspond to former studies already showing the inhibition of NK cells. (**C**) Dose–response experiments showing the viability of PBMCs and the inhibition of target cell lysis. (**A–C**) Results were expressed as a percentage of NanoLuc released by K562-NL cells when co-cultured with untreated PBMCs. Data correspond to means ± SD of ⩾3 healthy donors.

considered prime targets for innovative immunotherapies, and functional defects are associated with pathological conditions. Both natural and artificial molecules, including cytokines, drugs, and natural products, have been defined as modulators of NK cell activity, and some of them are developed for medical purposes. The identification of novel modulators requires both target-based approaches and functional screenings that are complementary. But the latter is complicated since current NK cell assays are not easily adapted to the HTS of large libraries of compounds. Besides, quick functional assays, ideally usable at the patient's bedside, are needed for the quick diagnosis of pathological conditions such as FHL where NK cell cytotoxicity is altered.

Luciferase-based functional assays have become increasingly popular because of the exceptional performances of this family of bioluminescent enzymes that emit a strong

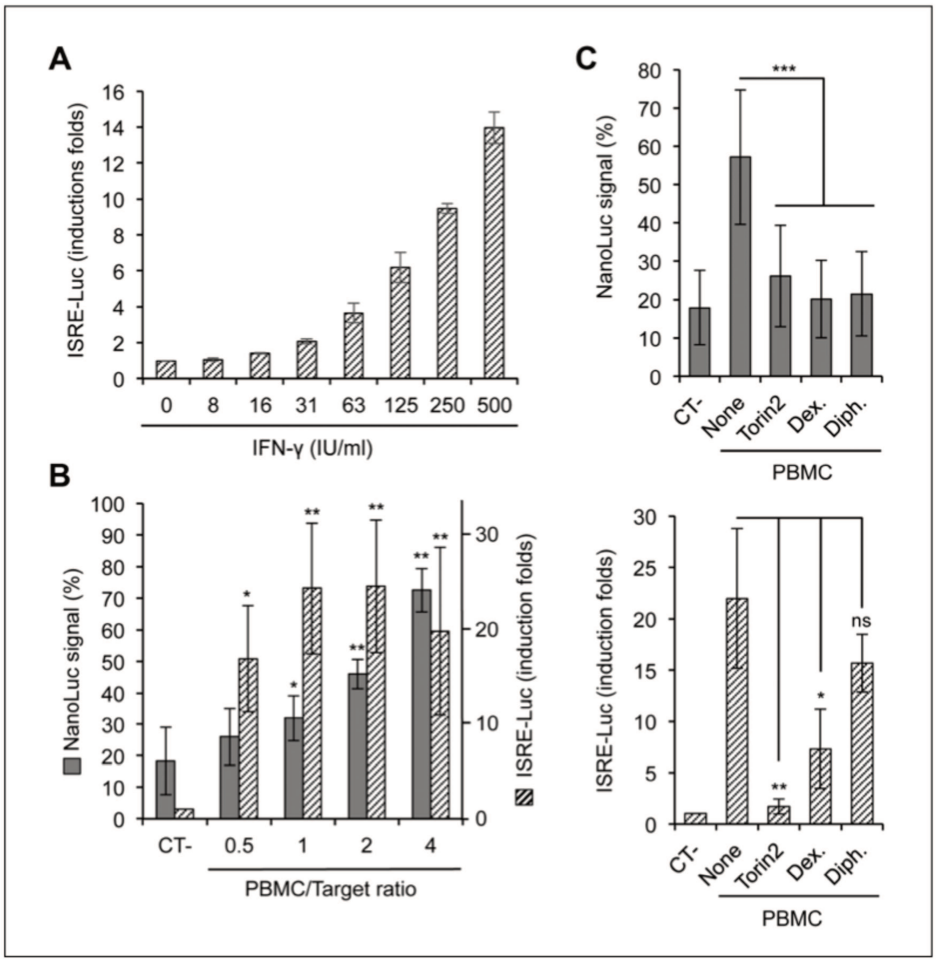

Figure 6. Measuring NK cell cytotoxicity and IFN secretion with dual-reporter cells. (**A**) Recombinant human IFN-γ is inducing the ISRE-luciferase reporter gene in twINNE cells. *Firefly* luciferase activity was determined after 24 h of incubation. (**B**) PBMCs were co-cultured with twINNE cells at different E/T ratios. NanoLuc activity in culture supernatants was measured after 7 h of incubation. The results were expressed as a percentage of NanoLuc released by twINNE cells permeabilized with 1% Tergitol. In parallel, ISRE-luciferase induction was determined in cell cultures at the same time point. (**C**) The same experiment as above at an E/T ratio of 4 with PBMCs pretreated overnight with Torin2 (500 nM), dextromethorphan (Dex; 140 µM), or diphenhydramine (Diph; 170 µM). Upper and lower panels correspond to NanoLuc activity in supernatants and ISRE-luciferase induction in co-cultures, respectively. (**A–C**) Data correspond to means ± SD of ⩾3 experiments performed in duplicate. $*p < 0.05$, $**p < 0.01$, and $***p < 0.001$ as determined by one-way ANOVA with Bonferroni post hoc test. ns = nonsignificant.

signal and are fully compatible with biological systems. Some attempts have been made to develop cell cytotoxicity assays based on *firefly* luciferase, but the poor stability of this enzyme after release in the extracellular medium greatly limited their performances.[15,16,31] This analytical issue was solved with the development of brighter, smaller, and much more stable luciferases of marine origins, such as NanoLuc, that use coelenterazine or its chemical analog furimazine as a substrate.[17–19] As we were developing our system, two research groups recently developed with success their own cytotoxicity assays by expressing these enzymes in target cells. They were used to measure antibody-dependent cellular cytotoxicity (ADCC), target cell lysis by chimeric antigen receptor (CAR) expressing T cells, and complement-dependent cytotoxicity.[32,33] Performances were found to be at least similar to ^{51}Cr release, which is considered the gold standard. Here, we established our own assay to measure the natural cytotoxicity of primary NK cells using appropriate targets, that is, K562 or HEK-293. Using PBMCs as a source of NK cells, this assay can be used to measure the inhibitory or stimulatory properties of small compounds or cytokines, but also to detect functional defects in PBMCs from patients (**Fig. 4C**). In the future, it will be interesting to further miniaturize this assay using 384-well plates as blood samples from patients, especially when testing babies, are limited in volume. Furthermore, we demonstrate the scalability of this assay as assessed by excellent statistical parameters. As proof of concept, we used the following settings to identify inhibitors of NK cells: 0.4×10^6 PBMCs/well at a 25/1 E/T ratio in a 96-well format. If we consider that 1×10^9 PBMCs are usually purified from one standard blood bag (500 mL), cells from a single donor are sufficient to screen 25 collection plates, including 80 compounds and control wells, which corresponds to 2000 different molecules. This makes possible the screening of medium-scale libraries on primary effector cells, a key point when looking for relevant cytotoxicity modulators.

From the screen of the TMIC Human Metabolome Library, we identified six molecules that were previously described in literature for their inhibitory properties on NK cells[24–29] and six molecules that were not reported for this

activity before. Interestingly, several of these molecules fall into pharmacological classes of drugs previously identified by Theorell et al.[34] as modulators of antibody-dependent NK cytotoxicity, including adrenergic receptor ligands (propranolol), Ca^{2+} channel blocker (verapamil, diltiazem), H1R-antagonist (diphenhydramine, brompheniramine), and serotonergic, dopaminergic, and muscarinergic antagonists (diphenhydramine, brompheniramine, dextrometorphan)—sometimes with opposite effects (17α-ethynylestradiol). However, all these drugs have multiple side targets, and mechanisms responsible for their biological activity toward PBMCs, and NK cells in particular, remain elusive without further investigations. Among the new NK cell inhibitors identified in the screen, dextromethorphan and diphenhydramine were the most interesting, showing some potent effects with a limited cytotoxicity on PBMCs. Dextrometorphan (*d*-3-methoxy-17-methylmorphinan) belongs to the morphinan family and is widely prescribed as a cough suppressant but is also used in the treatment of specific neurological disorders. It shows no affinity for the opioid receptor but was characterized as a nanomolar to low-micromolar-range antagonist of the NMDA receptor, an agonist of the σ1 receptor (σ1R), a serotonin–norepinephrine reuptake inhibitor, an antagonist of nicotinic receptors, and an inhibitor of voltage-gated calcium and potassium channels.[35] Interestingly, it was previously reported to have immunosuppressive properties at higher concentrations, for example, inhibiting the maturation of conventional dendritic cells,[36] but also disease progression in experimental mouse models of autoimmune disorders,[37,38] and inflammation and oxidative stress in heavy smokers.[39] Mechanisms involved are still poorly understood, but could also control the activation of NK cells. One hypothesis is that dextrometorphan, through interactions with σ1R or voltage-gated channels, perturbs Ca^{2+} mobilization that is essential for NK cell activation and degranulation. A second inhibitor of interest identified in the screen was diphenhydramine, a common first-generation H1-antihistamine, which is closely related to brompheniramine, which was also among selected hits. The IC_{50} of diphenhydramine for the H1 receptor is in the nanomolar range, which is incompatible with the higher concentrations required for inhibiting NK cells (**Fig. 5C**). Diphenhydramine has pharmacological interactions with multiple secondary targets, including muscarinic and α-adrenergic receptors, but also organic cation, serotonin, dopamine, and norepinephrine transporters.[40] Several of these receptors are expressed by immune cells and are potentially involved in the inhibitory effects of diphenhydramine on NK cells. This is supported by a report showing that diphenhydramine suppresses the innate immune response in a mouse model of septic peritonitis, and these effects are not mediated by H1R.[41] Altogether, our data suggest that diphenhydramine, dextrometorphan, and related drugs that are widely used to treat the symptoms of common cold may have unwanted effects on the innate immune response. This adds elements to the current debate on the low benefit/risk ratio of these molecules. Finally, it should be noted that we did not identify NK cell activators in the screen, probably because immunostimulatory molecules, which potentially induce inflammation, are relatively rare among prevalent metabolites or frequently used drugs.

Finally, we further improved our screening system by developing an original dual-reporter cell line to monitor both the secretion of IFN-γ by NK cells and their cytotoxic activity. Results obtained showed a good correlation between NK cell cytotoxicity and IFN-γ expression, as expected (**Fig. 6B**). Interestingly, when testing NK cell inhibitors in this dual-reporter system, we found that Torin2 efficiently blocked target cell lysis and the IFN response, whereas the effects of dextromethorphan and diphenhydramine were skewed for the inhibition of NK cell cytotoxicity (**Fig. 6C**). This suggests that these drugs have different modes of action. Cytotoxic granules with perforin/granzymes and vesicles containing IFN-γ are separate entities, which are delivered to the surface of NK cells through different secretory pathways.[30] While the secretion of IFN-γ vesicles is not polarized, cytotoxic granules are released at the contact interface with target cells, and this pathway could be selectively inhibited, in particular by diphenhydramine. Further experiments using purified NK cells and cellular imaging should be performed to test this hypothesis. Finally, it should be stressed that the dual-reporter assay we developed should be performed at a relatively low E/T ratio to let the expression of IFN-γ induce the ISRE-luc reporter before target cells are killed. Provided that this rule is properly followed, this dual-reporter system will provide much more complete functional data on the activation of NK cells when screening libraries of compounds or biologics in high-throughput settings. In the future, this should help identify modulators of NK cells of interest for developing innovative therapies.

Acknowledgments

We acknowledge the technical support of Stéphanie Dupuy from the Flow Cytometry Platform at Université Paris Descartes. Vincent Hervin, Eloi Coutant, and Yves L. Janin are acknowledged for a generous gift of furimazine. This work was supported by the Agence National de la Recherche (ChemInnate program to P.O.V. and S.N.), the Agence Nationale de Recherche sur le SIDA et les hepatitis virales (ANRS), Campus France (Programme CEDRE), SantImmune from the Fondation Paris Descartes, the Centre National de la Recherche Scientifique (CNRS; www.cnrs.fr), and the Institut National de la Santé et de la Recherche Médicale (INSERM; www.inserm.fr). S.H. was supported by the National Council for Scientific Research (Lebanon) and the Université Saint-Esprit de Kaslik (USEK).

Declaration of Conflicting Interests

The authors declared no potential conflicts of interest with respect to the research, authorship, and/or publication of this article.

Funding

The authors received no financial support for the research, authorship, and/or publication of this article.

ORCID iDs

Sébastien Viel http://orcid.org/0000-0002-5085-443X
Sébastien Nisole http://orcid.org/0000-0001-9793-419X
Pierre-Olivier Vidalain http://orcid.org/0000-0003-3082-7407

References

1. Vivier, E.; Tomasello, E.; Baratin, M.; et al. Functions of Natural Killer Cells. *Nat. Immunol.* **2008**, *9*, 503–510.
2. Voskoboinik, I.; Whisstock, J. C.; Trapani, J. A. Perforin and Granzymes: Function, Dysfunction and Human Pathology. *Nat. Rev. Immunol.* **2015**, *15*, 388–400.
3. Brunner, K. T.; Mauel, J.; Cerottini, J. C.; et al. Quantitative Assay of the Lytic Action of Immune Lymphoid Cells on 51-Cr-Labelled Allogeneic Target Cells In Vitro; Inhibition by Isoantibody and by Drugs. *Immunology* **1968**, *14*, 181–196.
4. Flieger, D.; Gruber, R.; Schlimok, G.; et al. A Novel Non-Radioactive Cellular Cytotoxicity Test Based on the Differential Assessment of Living and Killed Target and Effector Cells. *J. Immunol. Methods* **1995**, *180*, 1–13.
5. Alter, G.; Malenfant, J. M.; Altfeld, M. CD107a as a Functional Marker for the Identification of Natural Killer Cell Activity. *J. Immunol. Methods* **2004**, *294*, 15–22.
6. Lee, S. B.; Cha, J.; Kim, I. K.; et al. A High-Throughput Assay of NK Cell Activity in Whole Blood and Its Clinical Application. *Biochem. Biophys. Res. Commun.* **2014**, *445*, 584–590.
7. Gong, C.; Ni, Z.; Yao, C.; et al. A High-Throughput Assay for Screening of Natural Products That Enhanced Tumoricidal Activity of NK Cells. *Biol. Proced. Online* **2015**, *17*, 12.
8. Wahlberg, B. J.; Burholt, D. R.; Kornblith, P.; et al. Measurement of NK Activity by the Microcytotoxicity Assay (MCA): A New Application for an Old Assay. *J. Immunol. Methods* **2001**, *253*, 69–81.
9. Glamann, J.; Hansen, A. J. Dynamic Detection of Natural Killer Cell-Mediated Cytotoxicity and Cell Adhesion by Electrical Impedance Measurements. *Assay Drug Dev. Technol.* **2006**, *4*, 555–563.
10. Lichtenfels, R.; Biddison, W. E.; Schulz, H.; et al. CARE-LASS (Calcein-Release-Assay), an Improved Fluorescence-Based Test System to Measure Cytotoxic T Lymphocyte Activity. *J. Immunol. Methods* **1994**, *172*, 227–239.
11. von Zons, P.; Crowley-Nowick, P.; Friberg, D.; et al. Comparison of Europium and Chromium Release Assays: Cytotoxicity in Healthy Individuals and Patients with Cervical Carcinoma. *Clin. Diagn. Lab. Immunol.* **1997**, *4*, 202–207.
12. Decker, T.; Lohmann-Matthes, M. L. A Quick and Simple Method for the Quantitation of Lactate Dehydrogenase Release in Measurements of Cellular Cytotoxicity and Tumor Necrosis Factor (TNF) Activity. *J. Immunol. Methods* **1988**, *115*, 61–69.
13. McMillin, D. W.; Delmore, J.; Negri, J. M.; et al. Compartment-Specific Bioluminescence Imaging Platform for the High-Throughput Evaluation of Antitumor Immune Function. *Blood* **2012**, *119*, e131–e138.
14. Karimi, M. A.; Lee, E.; Bachmann, M. H.; et al. Measuring Cytotoxicity by Bioluminescence Imaging Outperforms the Standard Chromium-51 Release Assay. *PLoS One* **2014**, *9*, e89357.
15. Schafer, H.; Schafer, A.; Kiderlen, A. F.; et al. A Highly Sensitive Cytotoxicity Assay Based on the Release of Reporter Enzymes, from Stably Transfected Cell Lines. *J. Immunol. Methods* **1997**, *204*, 89–98.
16. Fu, X.; Tao, L.; Rivera, A.; et al. A Simple and Sensitive Method for Measuring Tumor-Specific T Cell Cytotoxicity. *PLoS One* **2010**, *5*, e11867.
17. Coutant, E. P.; Janin, Y. L. Synthetic Routes to Coelenterazine and Other Imidazo[1,2-a]pyrazin-3-one Luciferins: Essential Tools for Bioluminescence-Based Investigations. *Chemistry* **2015**, *21*, 17158–17171.
18. Tsuji, S.; Ohbayashi, T.; Yamakage, K.; et al. A Cytoplasmic Form of Gaussia Luciferase Provides a Highly Sensitive Test for Cytotoxicity. *PLoS One* **2016**, *11*, e0156202.
19. Hall, M. P.; Unch, J.; Binkowski, B. F.; et al. Engineered Luciferase Reporter from a Deep Sea Shrimp Utilizing a Novel Imidazopyrazinone Substrate. *ACS Chem. Biol.* **2012**, *7*, 1848–1857.
20. Lucas-Hourani, M.; Dauzonne, D.; Jorda, P.; et al. Inhibition of Pyrimidine Biosynthesis Pathway Suppresses Viral Growth through Innate Immunity. *PLoS Pathog.* **2013**, *9*, e1003678.
21. Zhang, J. H.; Chung, T. D.; Oldenburg, K. R. A Simple Statistical Parameter for Use in Evaluation and Validation of High Throughput Screening Assays. *J. Biomol. Screen.* **1999**, *4*, 67–73.
22. Marcais, A.; Cherfils-Vicini, J.; Viant, C.; et al. The Metabolic Checkpoint Kinase mTOR Is Essential for IL-15 Signaling During the Development and Activation of NK Cells. *Nat. Immunol.* **2014**, *15*, 749–757.
23. Viel, S.; Marcais, A.; Guimaraes, F. S.; et al. TGF-Beta Inhibits the Activation and Functions of NK Cells by Repressing the mTOR Pathway. *Sci. Signal* **2016**, *9*, ra19.
24. Schlichter, L.; Sidell, N.; Hagiwara, S. Potassium Channels Mediate Killing by Human Natural Killer Cells. *Proc. Natl. Acad. Sci. U.S.A.* **1986**, *83*, 451–455.
25. Hellstrand, K.; Hermodsson, S.; Strannegard, O. Evidence for a Beta-Adrenoceptor-Mediated Regulation of Human Natural Killer Cells. *J. Immunol.* **1985**, *134*, 4095–4099.
26. Whalen, M. M.; Doshi, R. N.; Homma, Y.; et al. Phospholipase C Activation in the Cytotoxic Response of Human Natural Killer Cells Requires Protein-Tyrosine Kinase Activity. *Immunology* **1993**, *79*, 542–547.
27. Baker, D. A.; Salvatore, W.; Milch, P. O. Effect of Low-Dose Oral Contraceptives on Natural Killer Cell Activity. *Contraception* **1989**, *39*, 119–124.
28. Ng, J.; Fredholm, B. B.; Jondal, M. Studies on the Calcium Dependence of Human NK Cell Killing. *Biochem. Pharmacol.* **1987**, *36*, 3943–3949.
29. Aybay, C.; Imir, T.; Okur, H. The Effect of Omeprazole on Human Natural Killer Cell Activity. *Gen. Pharmacol.* **1995**, *26*, 1413–1418.

30. Reefman, E.; Kay, J. G.; Wood, S. M.; et al. Cytokine Secretion Is Distinct from Secretion of Cytotoxic Granules in NK Cells. *J. Immunol.* **2010**, *184*, 4852–4862.
31. Alpert, M. D.; Heyer, L. N.; Williams, D. E.; et al. A Novel Assay for Antibody-Dependent Cell-Mediated Cytotoxicity against HIV-1- or SIV-Infected Cells Reveals Incomplete Overlap with Antibodies Measured by Neutralization and Binding Assays. *J. Virol*. **2012**, *86*, 12039–12052.
32. Rossignol, A.; Bonnaudet, V.; Clemenceau, B.; et al. A High-Performance, Non-Radioactive Potency Assay for Measuring Cytotoxicity: A Full Substitute of the Chromium-Release Assay Targeting the Regulatory-Compliance Objective. *MAbs* **2017**, *9*, 521–535.
33. Matta, H.; Gopalakrishnan, R.; Choi, S.; et al. Development and Characterization of a Novel Luciferase Based Cytotoxicity Assay. *Sci. Rep*. **2018**, *8*, 199.
34. Theorell, J.; Gustavsson, A. L.; Tesi, B.; et al. Immunomodulatory Activity of Commonly Used Drugs on Fc-Receptor-Mediated Human Natural Killer Cell Activation. *Cancer Immunol. Immunother*. **2014**, *63*, 627–641.
35. Nguyen, L.; Thomas, K. L.; Lucke-Wold, B. P.; et al. Dextromethorphan: An Update on Its Utility for Neurological and Neuropsychiatric Disorders. *Pharmacol. Ther*. **2016**, *159*, 1–22.
36. Chen, D. Y.; Song, P. S.; Hong, J. S.; et al. Dextromethorphan Inhibits Activations and Functions in Dendritic Cells. *Clin. Dev. Immunol*. **2013**, *2013*, 125643.
37. Chechneva, O. V.; Mayrhofer, F.; Daugherty, D. J.; et al. Low Dose Dextromethorphan Attenuates Moderate Experimental Autoimmune Encephalomyelitis by Inhibiting NOX2 and Reducing Peripheral Immune Cells Infiltration in the Spinal Cord. *Neurobiol. Dis*. **2011**, *44*, 63–72.
38. Chen, D. Y.; Lin, C. C.; Chen, Y. M.; et al. Dextromethorphan Exhibits Anti-Inflammatory and Immunomodulatory Effects in a Murine Model of Collagen-Induced Arthritis and in Human Rheumatoid Arthritis. *Sci. Rep*. **2017**, *7*, 11353.
39. Liu, P. Y.; Lin, C. C.; Tsai, W. C.; et al. Treatment with Dextromethorphan Improves Endothelial Function, Inflammation and Oxidative Stress in Male Heavy Smokers. *J. Thromb. Haemost*. **2008**, *6*, 1685–1692.
40. Krystal, A. D.; Richelson, E.; Roth, T. Review of the Histamine System and the Clinical Effects of H1 Antagonists: Basis for a New Model for Understanding the Effects of Insomnia Medications. *Sleep Med. Rev*. **2013**, *17*, 263–272.
41. Metz, M.; Doyle, E.; Bindslev-Jensen, C.; et al. Effects of Antihistamines on Innate Immune Responses to Severe Bacterial Infection in Mice. *Int. Arch Allergy Immunol*. **2011**, *155*, 355–360.

Article 4

frontiers in Immunology

MINI REVIEW
published: 02 July 2020
doi: 10.3389/fimmu.2020.01409

Check for updates

Beyond Anti-viral Effects of Chloroqui[https://www.frontiersin.org/articles/10.3389/fimmu.2020.01409/full]e

Vincent Gies[1,2,3]*, *Nassima Bekaddour*[4,5], *Yannick Dieudonné*[1,2,6], *Aurélien Guffroy*[1,2,6], *Quentin Frenger*[1,7], *Frédéric Gros*[1,7], *Mathieu Paul Rodero*[4,5], *Jean-Philippe Herbeuval*[4,5*†] and *Anne-Sophie Korganow*[1,2,6*†]

[1] Université de Strasbourg, INSERM UMR - S1109, Strasbourg, France, [2] Hôpitaux Universitaires de Strasbourg, Department of Clinical Immunology and Internal Medicine, National Reference Center for Systemic Autoimmune Diseases (CNR RESO), Tertiary Center for Primary Immunodeficiencies, Strasbourg, France, [3] Université de Strasbourg, Faculty of Pharmacy, Illkirch, France, [4] Université de Paris, CNRS UMR-8601, Paris, France, [5] Team Chemistry & Biology, Modeling & Immunology for Therapy, CBMIT, Paris, France, [6] Université de Strasbourg, Faculty of Medicine, Strasbourg, France, [7] Université de Strasbourg, Faculty of Life Sciences, Strasbourg, France

OPEN ACCESS

Edited by:
Massimo Gadina,
National Institute of Arthritis and Musculoskeletal and Skin Diseases (NIAMS), United States

Reviewed by:
Fabrizio Conti,
Sapienza University of Rome, Italy
Francesco Puppo,
University of Genoa, Italy
Tamer A. Gheita,
Cairo University, Egypt

***Correspondence:**
Vincent Gies
v.gies@unistra.fr
Jean-Philippe Herbeuval
jean-philippe.Herbeuval@parisdescartes.fr
Anne-Sophie Korganow
korganow@unistra.fr

†These authors have contributed equally to the work

Specialty section:
This article was submitted to Inflammation, a section of the journal Frontiers in Immunology

Received: 04 May 2020
Accepted: 02 June 2020
Published: 02 July 2020

Citation:
Gies V, Bekaddour N, Dieudonné Y, Guffroy A, Frenger Q, Gros F, Rodero MP, Herbeuval J-P and Korganow A-S (2020) Beyond Anti-viral Effects of Chloroquine/Hydroxychloroquine. Front. Immunol. 11:1409. doi: 10.3389/fimmu.2020.01409

As the world is severely affected by COVID-19 pandemic, the use of chloroquine and hydroxychloroquine in prevention or for the treatment of patients is allowed in multiple countries but remained at the center of much controversy in recent days. This review describes the properties of chloroquine and hydroxychloroquine, and highlights not only their anti-viral effects but also their important immune-modulatory properties and their well-known use in autoimmune diseases, including systemic lupus and arthritis. Chloroquine appears to inhibit *in vitro* SARS virus' replication and to interfere with SARS-CoV2 receptor (ACE2). Chloroquine and hydroxychloroquine impede lysosomal activity and autophagy, leading to a decrease of antigen processing and presentation. They are also known to interfere with endosomal Toll-like receptors signaling and cytosolic sensors of nucleic acids, which result in a decreased cellular activation and thereby a lower type I interferons and inflammatory cytokine secretion. Given the antiviral and anti-inflammatory properties of chloroquine and hydroxychloroquine, there is a rational to use them against SARS-CoV2 infection. However, the anti-interferon properties of these molecules might be detrimental, and impaired host immune responses against the virus. This duality could explain the discrepancy with the recently published studies on CQ/HCQ treatment efficacy in COVID-19 patients. Moreover, although these treatments could be an interesting potential strategy to limit progression toward uncontrolled inflammation, they do not appear *per se* sufficiently potent to control the whole inflammatory process in COVID-19, and more targeted and/or potent therapies should be required at least in add-on.

Keywords: chloroquine, hydroxychloroquine, COVID-19, SARS-CoV2, interferon, TLR, STING, RIG-I

INTRODUCTION

Chloroquine (CQ) and hydroxychloroquine (HCQ) are "old" drugs but are still widely used in very diverse situations, including infectious diseases (1–3), rheumatic/inflammatory diseases (4), or in clinical research protocols as add-on cancer therapy (5). Indeed, they are cheap and safe considering rare effective ocular toxicity (<2%) and acute cardiac toxicity. However, clinicians

should be warned that CQ/HCQ treatments, especially with high doses, can be complicated with heart failure, or non-reversible conduction disorders (6).

As the world is severely affected by COVID-19 pandemic, the use of CQ/HCQ in prevention or for the treatment of patients is at the center of much controversy in recent days. We thus believe appropriate to make a short review and discuss about their pharmacological properties and the ways CQ/HCQ are able to interfere with innate or adaptative immune system.

HISTORY OF HCQ/CQ

HCQ and CQ are weak bases with a common flat aromatic core structure. These decades-old drugs are in fact synthetic antimalarial drugs, although HCQ is above all a major treatment for systemic lupus (7). The story of antimalarials starts with the cinchona bark that was already used by the Incas for its antipyretic property rather than malaria treatment itself. It was only in 1820, that Pelletier and Caventou, french pharmacists, isolated the fundamental antimalarial alkaloid: quinine. During world war II, American soldiers who fought in the pacific region received antimalarials (quinacrine) in prophylaxis, showing a beneficial effect of this compound on lupus and rheumatoid arthritis. CQ was subsequently introduced in 1943, showing its beneficial effect in systemic lupus erythematosus in 1953 (8). CQ cardiac and retinal side effects led to the development, in 1955, of a hydroxylated derivative: HCQ, a little less active but above all less toxic molecule (9, 10). HCQ holds actually a major place in the treatment of autoimmune/ inflammatory rheumatic or dermatological diseases.

LYSOSOMAL ACTIVITY AND AUTOPHAGY

Autophagy is a catabolic homeostatic or induced process that involves the sequestration of cytoplasmic components in double-membraned autophagosomes. Autophagosomes ultimately fuse with lysosomes leading to the degradation of their content. Autophagy is a major player in immunity (11). It contributes to reduce inflammation by modulating type I interferon production and inflammasome activity. Autophagy is a countermeasure to infectious diseases clearing intracellular pathogens but autophagic membrane can conversely constitute hubs for viral replication. Autophagy also contributes to generate antigens processed on MHC class II (12).

An important mode of action of HCQ is the inhibition of lysosomal activity (**Figure 1** and **Table 1**). As weak bases (**Figure S1A**), CQ and HCQ accumulate in lysosomes (lysosomotropism) and inhibit their function. *In vitro*, CQ can disrupt the endolysosomal system and therefore destabilize the lysosomal membranes leading to intracellular release of lysosomal enzymes and impairment of autophagosome–lysosome fusion (13, 14). As a consequence LC3-II (microtubule-associated protein light chain 3-II), a lipidated protein normally associated with autophagosomes until degradation/recycling after fusion with lysosomes, accumulates under HCQ incubation (**Figure S1B**) (13, 25). Lysosomes are involved not only in the recycling of cellular substrates but also in the processing of antigens and their presentation on MHC class II proteins (4, 26–29). Thus, CQ/HCQ decrease, within 1 h *in vitro*, antigen processing and presentation by antigen presenting cells (4, 15, 16). Other mechanisms are invoked for the impact of HCQ or CQ on autophagy. Recently Rebecca et al. identified that inhibition of palmitoyl-protein thioesterase 1 (PPT1) is, at least in part, responsible for the observed anti-autophagy effect (30).

TOLL LIKE RECEPTORS

Perhaps the most important advance in our understanding of CQ/HCQ has been the discovery of their inhibiting effects on toll like receptors (TLRs), one of our first line of defense against bacterial and viral agents. HCQ and CQ inhibit some endosomal TLRs, mostly TLR7 and TLR9, which are able to recognize viral, bacterial and endogenous nucleic acids (**Figure 1** and **Table 1**) (4, 31). These TLRs are located in the intracellular compartments to minimize accidental exposure to self-nucleic material (31). TLR7 is activated by ssRNA compounds, while TLR9 is activated by unmethylated CpG DNA (32). Activation of these endosomal TLRs can significantly contribute to promoting inflammation and/or the development of autoimmune diseases, such as systemic lupus erythematosus (SLE) (33, 34). Therefore, inhibition of endosomal TLRs, and consequently type I interferons (IFN-I) production, holds great therapeutic potential for the treatment of autoimmune diseases (35). CQ/HCQ have shown their ability to inhibit, in mice and *in vitro*, the TLR9 stimulation induced by CpG and the underlying production of IL-6 and TNFα (36, 37). These drugs can also inhibits RNA-mediated activation of TLR7 signaling and the production of IFNα (38, 39). In addition to cytokines secretion, TLR7 and 9 inhibition will also impair costimulatory molecules expression, such as CD86 on B cells, contrary to stimulation with pokeweed mitogen (**Figure S1C**) (40). Two modes of action are currently suggested:

- Raising endosomal pH has been proposed as the explanation for defective maturation and antigen presentation as well as impaired responses to TLR activation. Indeed, acidic conditions are necessary for strong interactions of nucleic acids with TLR9 (17). In this way, blocking endosomal acidification hinders the signaling of TLR 3, 7, and 9 (18–20). Ewald et al. showed that cleavage of TLR9 does not take place in the absence of acidification of the endolysosomal compartments. However, the proteolysis of TLR9 is an essential step for the recognition of ligands (CpG for TLR9) and the recruitment of MyD88, and consequently the signaling of TLR9 (21).
- CQ/HCQ can also directly bind to nucleic acids and such interferences lead to structural changes in the TLR

Abbreviations: CQ, chloroquine; HCQ, hydroxychloroquine; IFN, interferon; IFN-I, type I interferons; NET, neutrophil extracellular trap; pDC, plasmacytoid dendritic cell; SARS, severe acute respiratory syndrome; SLE, systemic lupus erythematosus; TLR, toll like receptor.

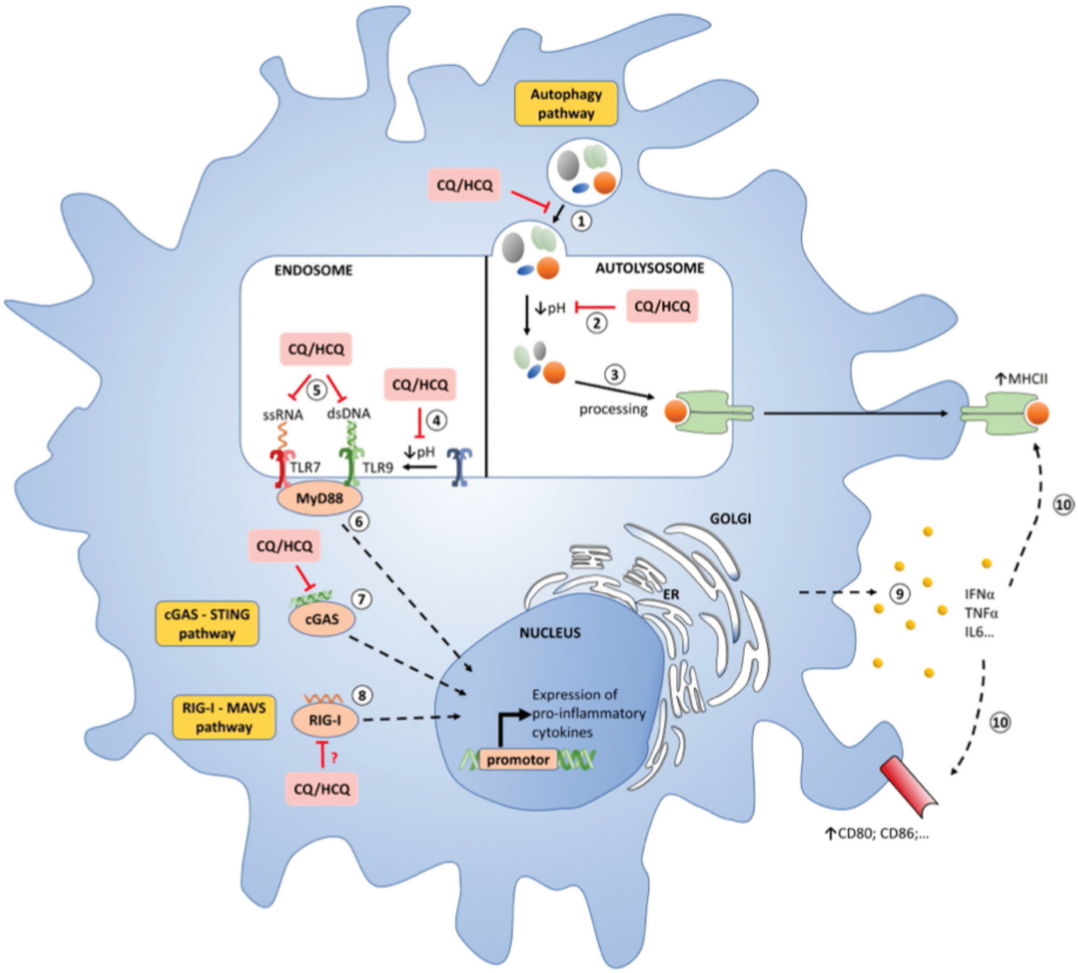

FIGURE 1 | Molecular mechanisms of chloroquine/hydroxychloroquine in pDCs. **(1)** Autophagosome-lysosome fusion. CQ/HCQ impair this step. **(2)** Degradation of cargo from autophagosome. CQ/HCQ accumulate in lysosomes (lysosomotropism) and inhibit their function by increasing the pH. **(3)** Antigens are processed on MHC class II. **(4)** Proteolysis of TLRs by acid-dependent proteases is an essential step for the recognition of ligands. CQ/HCQ inhibit acid-dependent proteases by increasing the pH. **(5)** TLRs interact with nucleic acids presented to endosomal compartments. HCQ and CQ can bind directly to nucleic acids, preventing their recognition and inhibiting TLR-ligand interactions. **(6)** TLRs activation lead to MyD88 recrutement with a subsequent synthesis of pro-inflammatory cytokines, especially IFN-I. **(7)** Cytosolic DNA binds to cGAS, which then synthesizes the second messenger cGAMP to mediate STING-dependent transcription of IFN-I. HCQ and CQ block the binding of dsDNA / cGAS, thus attenuating the underlying activation of the STING pathway mediated by cGAMP. **(8)** Cytosolic RNA is recognized by RIG-I, the signal is transferred to MAVS, then to subsequent interactors leading to expression of IFN-I. CQ/HCQ may impair this process. (**9** and **10**) The release of IFNα, among other cytokines, stimulates a feedback activation with notably MHCII and co-stimulatory molecules upregulation. CQ: chloroquine; dsDNA, double-stranded DNA; ER, endoplasmic reticulum; HCQ: hydroxychlroquine; IFN-I: type I interferons; MHC: major histocompatibily complex; pDC: plasmacytoid dendritic cell; TLR : toll like receptor.

ligands, preventing their recognition and inhibiting TLR-ligand interactions (18, 22).

PLASMACYTOID DENDRITIC CELLS

The capacity of plasmacytoid dendritic cells (pDCs) to produce massive quantities of type I IFN has driven our understanding about the biology of these cells and their major role in both immunity against virus and in inflammation/autoimmunity (41).

pDCs can be acutely activated through different cell surface receptors and cytosolic sensors but TLR7/9 are likely their dominant mode of activation for endogenous or exogenous nucleic acids, with respect to IFN-I production (41–45). When triggered, pDCs expressed costimulatory molecules, and are able to prime subsequently T cells. Within 10 h following the sensing of nucleic acids, more than 80% of genes expressed in pDCs are IFNs or driven by IFNs (41, 46, 47). In addition, pDCs secrete cytokines as IL-6, TNFα and IL-12 and control the expression of many inflammatory cytokines. Because of these properties, they are considered as one of the main cellular actor of anti-viral defense (45).

In parallel, pDCs and IFN-I, have been largely studied in chronic inflammatory/autoimmune diseases and systemic lupus

TABLE 1 | Main mechanisms of actions of CQ/HCQ.

Mode of actions	Molecular mechanisms	References
Impairment of lysosomal activity and autophagic process	CQ/HCQ accumulate in lysosomes (lysosomotropism) and inhibit their functions	(4, 13–16)
	CQ/HCQ Impair of autophagosome–lysosome fusion	
	CQ/HCQ decrease antigen processing and presentation, by antigen presenting cells	
Interference with TLR signaling	Accumulation of CQ/HCQ in lysosomes raises endosomal pH and hinders the signaling of TLR 3,7, and 9	(17–21)
	Direct binding of CQ/HCQ to nucleic acids prevents their recognition and inhibits TLR-ligand interactions	(18, 22)
Inhibition of cytosolic sensors of nucleic acids	CQ/HCQ reduce activation of STING pathway: CQ/HCQ block the binding of dsDNA to cGAS.	(23, 24)
	CQ/HCQ reduce activation of RIG-I, pathway? *(further investigations required)*	(24)

CQ, chloroquine; dsDNA, double-stranded DNA; HCQ, hydroxychlroquine.

(SLE) (48). IFN-I are involved in SLE physiopathology through multiple mechanisms, focusing recent therapeutic research and trials (49, 50). HCQ is essential in the treatment of the disease and in prevention of flares, and CQ/HCQ are able to decrease IFNs production by pDCs (**Figure S1D**) (22, 51). In addition, HCQ/CQ effects are not limited to pDCs and result in several other cytokines inhibition (**Figures S1E,F**) (22, 52–54).

CYTOSOLIC SENSORS OF NUCLEIC ACIDS

Apart from TLRs, HCQ/CQ interfere with other pattern recognition receptors (PRRs) essential to the anti-viral response namely the cGAS–STING and RIG-I–MAVS pathways (**Figure 1** and **Table 1**). These cytosolic PRRs recognize and respond to DNA and RNA, respectively (23, 55). Cytosolic DNA is recognized by the cGAS-STING signaling axis which stimulates antiviral immunity by inducing IFN-I (56, 57). More precisely, cytosolic DNA binds to cGAS, which then synthesizes the second messenger cGAMP to mediate STING-dependent transcription of IFN-I (57). CQ/HCQ block the binding of dsDNA to cGAS, thus attenuating the underlying activation of the STING pathway mediated by cGAMP (23, 24).

Cytosolic RNA is recognized by RIG-I, the signal is transferred to MAVS, then to subsequent interactors leading to expression of IFN-I (55). An et al. showed that CQ/HCQ may inhibit RIG-I–stimulated induction of IFNs (24). However, the potential impacts of CQ/HCQ on this pathway need further investigations.

OTHER EFFECTS OF CQ/HCQ

Considering CQ/HCQ and pathogens direct interactions, only the interference of CQ and *Plasmodium,* via hemozoin crystallization inhibition leading to parasite death, has been clearly documented (58). Immunity against infectious agents, including bacteria, virus or fungus, also involve vessels, and inflammation at the endothelium level (59). In this view, CQ/HCQ has been suggested to prevent prothrombotic state and endothelial dysfunction (60, 61). Finally, neutrophil extracellular traps (NETs) and the ability to mount NETosis is essential in innate immunity against pathogens. However, CQ is also effective as an early upstream inhibitor of NET formation in murine models of inflammation (62).

CQ/HCQ AND SARS-COV2 INFECTION

Considering SARS-CoV2, which is at the center of current concerns, some studies argue for lower nasopharyngeal carriage after 6 days (63) and an overall improvement of patients with CQ/HCQ (63–66), while more recent studies do not show rapid viral clearance or lower mortality (67–73).

Little is known about the mechanisms of action of CQ/HCQ during SARS-CoV2 infection. CQ has repeatedly demonstrated its ability, *in vitro* or in mouse models, to inhibit the replication of various strains of coronavirus, including those responsible for severe acute respiratory syndrome (SARS) in 2002 and 2003 (74–76). Additionally, *in vitro* studies carried out on SARS-CoV2 responsible for COVID-19 infection also confirm the potential interest of CQ/HCQ (77–79). Indeed, the increased endosomal pH due to CQ/HCQ may affect early stage of viral replication, via inhibition of virus-endosome fusion (80), and seem to stall the release of viral genome (77, 79). Although a direct interaction between HCQ/CQ and the virus has yet not been described, *in vitro* CQ interferes with terminal glycosylation of the SARS coronavirus receptor ACE2 (75, 81). Strikingly *ACE2* is an interferon stimulated gene (82, 83), as CQ/HCQ decrease IFN-I secretion, they may also hinder the expression of the viral receptor in the neighboring airway epithelial cells (83).

DISCUSSION

Thanks to its known capacity to inhibit both TLRs and cGAS-STING pathway, HCQ is a first line treatment in SLE and other autoimmune/inflammatory conditions. More than 70% of SLE patients around the world are under HCQ therapy which represents today indeed thousands of people. From its wide use, we know that HCQ efficiency takes a few weeks to impact clinical symptoms, as arthritis, or cutaneous manifestations (7). However, despite the first use of CQ and HCQ in immune related disease almost 70 years ago, their exact mechanisms of action are only beginning to be understood, whether considering pharmacokinetic or molecular mechanisms. In any case, *in vitro* CQ/HCQ inhibit the production of IFN-I and inflammatory cytokines by innate immune cells. However, considering cytokines profile in SLE patients under diverse immunosuppressive therapies compared to untreated patients (84), HCQ *per se* is far from being the most efficient.

Recently, a new coronavirus SARS-CoV2 infection (or COVID-19) has started to spread around world with the development of pneumonia and severe acute respiratory

syndrome (SARS). CQ/HCQ remain at the center of a therapy controversy as several publications describe an improvement of patients with CQ/HCQ (63–66), while others give results showing rather their ineffectiveness (67–73). Undoubtedly, several mechanistical arguments are in favor of HCQ/CQ interfering with coronavirus infection and virus spreading. However, we know that COVID-19 is not only an acute viral infection. Some patients experience a biphasic evolution/two-step disease progression. They are first infected, viremic, with flu-symptoms. At this stage, they may develop mild respiratory manifestations. Some days later, for yet unclear reasons, disease can dramatically worsen with an inflammatory procession leading to a subsequent "cytokine storm," a pro-thrombotic state and even a macrophage activation syndrome with heavy lung damage and/or multiorgan failure (85–87).

Looking back to SARS-CoV models, it has been suggested and documented in mice that the first phase of the disease could be accompanied by an initial virus mediated and adapted IFN-I response. The second phase of the disease would occur secondary to an inappropriate delayed IFN-I production in infected lungs. This leads to a subsequent and excessive innate immune response with pathogenic inflammatory monocyte-macrophages and sub-optimal T cell response, partly due to T cell apoptosis, which is not enough to dampen immune innate system overactivation (88). Accordingly, a recent study from Hadjadj et al. identified an impaired IFN-I activity, increased T cell apoptosis and exacerbated inflammatory responses in severe COVID-19 patients (89). Thus, like what has been suggested for SARS-CoV-1 infection (88), the driving clinical features of severe COVID-19 patients stem from a dysregulated immune response in patients with notably a delayed and abnormal production of IFN-I (82, 89).

Hence, what are our aims when we treat SARS-CoV2 infection with CQ/HCQ ? Do we wish to decrease a beginning viremia by endolysosomal pathway inhibition with CQ/HCQ, which may further delay the anti-viral IFN-I response? or do we wish to control the inflammatory storm by interfering with PRRs and endosomal TLRs signaling, leading to a decreased cellular activation and thereby cytokine secretion? Then, if we initiate the treatment in the second phase of the disease, when the disease becomes somehow an inflammatory disease, are we really in frame with CQ/HCQ already demonstrated properties?

It appears from our clinical experience and from national or international series of COVID19 infected patients, that men are more affected than women (69, 90) and patients with autoimmune diseases, including SLE who are under HCQ or other immunosuppressive drugs, are not drastically affected. This could have other explanations than HCQ efficiency: (i) most of patients with autoimmunity are women, (ii) some of them present an intrinsic IFN-I response which is not completely abolished by HCQ and remains more intense than healthy donors, (iii) immunosuppressive therapies could impact or prevent high auto-inflammatory conditions.

At this time, we do not have any definitive clue concerning CQ/HCQ impacts on the first anti-viral phase of COVID-19, and the use of CQ/HCQ must remain cautious as results from recent studies do not support these treatments (67, 69, 72). Considering published data on COVID-19 disease and older data about SARS physiopathology, and although CQ/HCQ remain an interesting potential strategy to limit progression toward uncontrolled inflammation, they do not appear *per se* to be sufficient to control the whole inflammatory process in COVID-19, and more targeted and/or potent therapies should be required at least in add-on.

AUTHOR CONTRIBUTIONS

VG, AG, MR, J-PH, and A-SK wrote the manuscript. VG, AG, YD, FG, J-PH, and A-SK performed the literature search. VG, YD, and NB designed the figures. NB, VG, AG, YD, and QF performed the experiments. NB, VG, YD, AG, QF, FG, MR, J-PH, and A-SK interpreted the data. All authors reviewed and approved the manuscript.

FUNDING

Publication fees were supported by Hôpitaux Universitaires de Strasbourg.

ACKNOWLEDGMENTS

We thank Benoit Beitz (BIOASTER, LYON, France) for expert technical assistance for the mass cytometry (CYTOF) analysis.

SUPPLEMENTARY MATERIAL

The Supplementary Material for this article can be found online at: https://www.frontiersin.org/articles/10.3389/fimmu.2020.01409/full#supplementary-material

REFERENCES

1. Raoult D, Houpikian P, Tissot Dupont H, Riss JM, Arditi-Djiane J, Brouqui P. Treatment of Q fever endocarditis: comparison of 2 regimens containing doxycycline and ofloxacin or hydroxychloroquine. *Arch Intern Med.* (1999) 159:167–73. doi: 10.1001/archinte.159.2.167
2. Lagier J-C, Raoult D. Whipple's disease and tropheryma whipplei infections: when to suspect them and how to diagnose and treat them. *Curr Opin Infect Dis.* (2018) 31:463–70. doi: 10.1097/QCO.0000000000000489
3. Tang Y-Q, Ye Q, Huang H, Zheng W-Y. An overview of available antimalarials: discovery, mode of action and drug resistance. *Curr Mol Med.* (2020). doi: 10.2174/1566524020666200207123253. [Epub ahead of print].
4. Schrezenmeier E, Dörner T. Mechanisms of action of hydroxychloroquine and chloroquine: implications for rheumatology. *Nat Rev Rheumatol.* (2020) 16:155–66. doi: 10.1038/s41584-020-0372-x
5. Xu R, Ji Z, Xu C, Zhu J. The clinical value of using chloroquine or hydroxychloroquine as autophagy inhibitors in the treatment of cancers: a systematic review and meta-analysis. *Medicine.* (2018) 97:e12912. doi: 10.1097/MD.0000000000012912

6. Chatre C, Roubille F, Vernhet H, Jorgensen C, Pers Y-M. cardiac complications attributed to chloroquine and hydroxychloroquine: a systematic review of the literature. *Drug Saf.* (2018) 41:919–31. doi: 10.1007/s40264-018-0689-4
7. Fanouriakis A, Kostopoulou M, Alunno A, Aringer M, Bajema I, Boletis JN, et al. 2019 update of the EULAR recommendations for the management of systemic lupus erythematosus. *Ann Rheum Dis.* (2019) 78:736–45. doi: 10.1136/annrheumdis-2019-215089
8. Shee JC. Lupus erythematosus treated with chloroquine. *Lancet.* (1953) 265:201–2. doi: 10.1016/S0140-6736(53)90138-X
9. Wallace DJ. The history of antimalarials. *Lupus.* (1996) 5(Suppl. 1):S2–3. doi: 10.1177/0961203396005001021
10. Lee S-J, Silverman E, Bargman JM. The role of antimalarial agents in the treatment of SLE and lupus nephritis. *Nat Rev Nephrol.* (2011) 7:718–29. doi: 10.1038/nrneph.2011.150
11. Arbogast F, Gros F. Lymphocyte autophagy in homeostasis, activation, and inflammatory diseases. *Front Immunol.* (2018) 9:1801. doi: 10.3389/fimmu.2018.02627
12. Choi AMK, Ryter SW, Levine B. Autophagy in human health and disease. *N Engl J Med.* (2013) 368:651–62. doi: 10.1056/NEJMra1205406
13. Mauthe M, Orhon I, Rocchi C, Zhou X, Luhr M, Hijlkema K-J, et al. Chloroquine inhibits autophagic flux by decreasing autophagosome-lysosome fusion. *Autophagy.* (2018) 14:1435–55. doi: 10.1080/15548627.2018.1474314
14. Circu M, Cardelli J, Barr MP, O'Byrne K, Mills G, El-Osta H. Modulating lysosomal function through lysosome membrane permeabilization or autophagy suppression restores sensitivity to cisplatin in refractory non-small-cell lung cancer cells. *PLoS ONE.* (2017) 12:e0184922. doi: 10.1371/journal.pone.0184922
15. Ziegler HK, Unanue ER. Decrease in macrophage antigen catabolism caused by ammonia and chloroquine is associated with inhibition of antigen presentation to T cells. *Proc Natl Acad Sci USA.* (1982) 79:175–8. doi: 10.1073/pnas.79.1.175
16. Fox RI. Mechanism of action of hydroxychloroquine as an antirheumatic drug. *Semin Arthritis Rheu.* (1993) 23:82–91. doi: 10.1016/S0049-0172(10)80012-5
17. Mellman I, Fuchs R, Helenius A. Acidification of the endocytic and exocytic pathways. *Annu Rev Biochem.* (1986) 55:663–700. doi: 10.1146/annurev.bi.55.070186.003311
18. Häcker H, Mischak H, Miethke T, Liptay S, Schmid R, Sparwasser T, et al. CpG-DNA-specific activation of antigen-presenting cells requires stress kinase activity and is preceded by non-specific endocytosis and endosomal maturation. *EMBO J.* (1998) 17:6230–40. doi: 10.1093/emboj/17.21.6230
19. Garcia-Cattaneo A, Gobert F-X, Müller M, Toscano F, Flores M, Lescure A, et al. Cleavage of Toll-like receptor 3 by cathepsins B and H is essential for signaling. *Proc Natl Acad Sci USA.* (2012) 109:9053–8. doi: 10.1073/pnas.1115091109
20. Ewald SE, Engel A, Lee J, Wang M, Bogyo M, Barton GM. Nucleic acid recognition by Toll-like receptors is coupled to stepwise processing by cathepsins and asparagine endopeptidase. *J Exp Med.* (2011) 208:643–51. doi: 10.1084/jem.20100682
21. Ewald SE, Lee BL, Lau L, Wickliffe KE, Shi G-P, Chapman HA, et al. The ectodomain of Toll-like receptor 9 is cleaved to generate a functional receptor. *Nature.* (2008) 456:658–62. doi: 10.1038/nature07405
22. Kužnik A, Benčina M, Švajger U, Jeras M, Rozman B, Jerala R. Mechanism of endosomal tlr inhibition by antimalarial drugs and imidazoquinolines. *J Immunol.* (2011) 186:4794–804. doi: 10.4049/jimmunol.1000702
23. Gaidt MM, Ebert TS, Chauhan D, Ramshorn K, Pinci F, Zuber S, et al. The DNA inflammasome in human myeloid cells is initiated by a STING-cell death program upstream of NLRP3. *Cell.* (2017) 171:1110–24.e18. doi: 10.1016/j.cell.2017.09.039
24. An J, Woodward JJ, Sasaki T, Minie M, Elkon KB. Cutting edge: antimalarial drugs inhibit IFN-β production through blockade of cyclic GMP-AMP synthase–DNA interaction. *J Immunol.* (2015) 194:4089–93. doi: 10.4049/jimmunol.1402793
25. Klionsky DJ, Abdelmohsen K, Abe A, Abedin MJ, Abeliovich H, Acevedo Arozena A, et al. Guidelines for the use and interpretation of assays for monitoring autophagy (3rd edition). *Autophagy.* (2016) 12:1–222. doi: 10.1080/15548627.2015.1100356
26. Lotteau V, Teyton L, Peleraux A, Nilsson T, Karlsson L, Schmid SL, et al. Intracellular transport of class II MHC molecules directed by invariant chain. *Nature.* (1990) 348:600–5. doi: 10.1038/348600a0
27. Ghislat G, Lawrence T. Autophagy in dendritic cells. *Cell Mol Immunol.* (2018) 15:944–52. doi: 10.1038/cmi.2018.2
28. Münz C. Autophagy beyond intracellular MHC class II antigen presentation. *Trends Immunol.* (2016) 37:755–63. doi: 10.1016/j.it.2016.08.017
29. Ballabio A, Bonifacino JS. Lysosomes as dynamic regulators of cell and organismal homeostasis. *Nat Rev Mol Cell Biol.* (2020) 21:101–18. doi: 10.1038/s41580-019-0185-4
30. Rebecca VW, Nicastri MC, Fennelly C, Chude CI, Barber-Rotenberg JS, Ronghe A, et al. PPT1 promotes tumor growth and is the molecular target of chloroquine derivatives in cancer. *Cancer Discov.* (2019) 9:220–9. doi: 10.1158/2159-8290.CD-18-0706
31. Wallace DJ, Gudsoorkar VS, Weisman MH, Venuturupalli SR. New insights into mechanisms of therapeutic effects of antimalarial agents in SLE. *Nat Rev Rheumatol.* (2012) 8:522–33. doi: 10.1038/nrrheum.2012.106
32. Barrat FJ, Elkon KB, Fitzgerald KA. Importance of nucleic acid recognition in inflammation and autoimmunity. *Annu Rev Med.* (2016) 67:323–36. doi: 10.1146/annurev-med-052814-023338
33. Barrat FJ, Meeker T, Gregorio J, Chan JH, Uematsu S, Akira S, et al. Nucleic acids of mammalian origin can act as endogenous ligands for Toll-like receptors and may promote systemic lupus erythematosus. *J Exp Med.* (2005) 202:1131–9. doi: 10.1084/jem.20050914
34. Marshak-Rothstein A. Toll-like receptors in systemic autoimmune disease. *Nat Rev Immunol.* (2006) 6:823–35. doi: 10.1038/nri1957
35. Hennessy EJ, Parker AE, O'Neill LAJ. Targeting Toll-like receptors: emerging therapeutics? *Nat Rev Drug Discov.* (2010) 9:293–307. doi: 10.1038/nrd3203
36. Hong Z, Jiang Z, Liangxi W, Guofu D, Ping L, Yongling L, et al. Chloroquine protects mice from challenge with CpG ODN and LPS by decreasing proinflammatory cytokine release. *Int Immunopharmacol.* (2004) 4:223–34. doi: 10.1016/j.intimp.2003.12.006
37. Macfarlane DE, Manzel L. Antagonism of immunostimulatory CpG-oligodeoxynucleotides by quinacrine, chloroquine, and structurally related compounds. *J Immunol.* (1998) 160:1122–31.
38. Lau CM, Broughton C, Tabor AS, Akira S, Flavell RA, Mamula MJ, et al. RNA-associated autoantigens activate B cells by combined B cell antigen receptor/Toll-like receptor 7 engagement. *J Exp Med.* (2005) 202:1171–7. doi: 10.1084/jem.20050630
39. Vollmer J, Tluk S, Schmitz C, Hamm S, Jurk M, Forsbach A, et al. Immune stimulation mediated by autoantigen binding sites within small nuclear RNAs involves Toll-like receptors 7 and 8. *J Exp Med.* (2005) 202:1575–85. doi: 10.1084/jem.20051696
40. Gies V, Schickel J-N, Jung S, Joublin A, Glauzy S, Knapp A-M, et al. Impaired TLR9 responses in B cells from patients with systemic lupus erythematosus. *JCI Insight.* (2018) 3:e96795. doi: 10.1172/jci.insight.96795
41. Barrat FJ, Su L. A pathogenic role of plasmacytoid dendritic cells in autoimmunity and chronic viral infection. *J Exp Med.* (2019) 216:1974–85. doi: 10.1084/jem.20181359
42. Liu Y-J. IPC: professional type 1 interferon-producing cells and plasmacytoid dendritic cell precursors. *Annu Rev Immunol.* (2005) 23:275–306. doi: 10.1146/annurev.immunol.23.021704.115633
43. Saitoh S-I, Abe F, Kanno A, Tanimura N, Saitoh YM, Fukui R, et al. TLR7 mediated viral recognition results in focal type I interferon secretion by dendritic cells. *Nat Commun.* (2017) 8:1–12. doi: 10.1038/s41467-017-01687-x
44. Swiecki M, Colonna M. The multifaceted biology of plasmacytoid dendritic cells. *Nat Rev Immunol.* (2015) 15:471–85. doi: 10.1038/nri3865
45. Reizis B. Plasmacytoid dendritic cells: development, regulation, and function. *Immunity.* (2019) 50:37–50. doi: 10.1016/j.immuni.2018.12.027
46. Duramad O, Fearon KL, Chan JH, Kanzler H, Marshall JD, Coffman RL, et al. IL-10 regulates plasmacytoid dendritic cell response to CpG-containing immunostimulatory sequences. *Blood.* (2003) 102:4487–92. doi: 10.1182/blood-2003-07-2465
47. Ito T, Kanzler H, Duramad O, Cao W, Liu Y-J. Specialization, kinetics, and repertoire of type 1 interferon responses by human plasmacytoid predendritic cells. *Blood.* (2006) 107:2423–31. doi: 10.1182/blood-2005-07-2709

48. Kaul A, Gordon C, Crow MK, Touma Z, Urowitz MB, van Vollenhoven R, et al. Systemic lupus erythematosus. *Nat Rev Dis Primers.* (2016) 2:16039. doi: 10.1038/nrdp.2016.39
49. Rönnblom L, Leonard D. Interferon pathway in SLE: one key to unlocking the mystery of the disease. *Lupus Sci Med.* (2019) 6:e000270. doi: 10.1136/lupus-2018-000270
50. Smith N, Rodero MP, Bekaddour N, Bondet V, Ruiz-Blanco YB, Harms M, et al. Control of TLR7-mediated type I IFN signaling in pDCs through CXCR4 engagement—a new target for lupus treatment. *Sci Adv.* (2019) 5:eaav9019. doi: 10.1126/sciadv.aav9019
51. Sacre K, Criswell LA, McCune JM. Hydroxychloroquine is associated with impaired interferon-alpha and tumor necrosis factor-alpha production by plasmacytoid dendritic cells in systemic lupus erythematosus. *Arthritis Res Ther.* (2012) 14:R155. doi: 10.1186/ar3895
52. Picot S, Peyron F, Vuillez JP, Polack B, Ambroise-Thomas P. Chloroquine inhibits tumor necrosis factor production by human macrophages *in vitro*. *J Infect Dis.* (1991) 164:830. doi: 10.1093/infdis/164.4.830
53. Jang C-H, Choi J-H, Byun M-S, Jue D-M. Chloroquine inhibits production of TNF-alpha, IL-1beta and IL-6 from lipopolysaccharide-stimulated human monocytes/macrophages by different modes. *Rheumatology.* (2006) 45:703–10. doi: 10.1093/rheumatology/kei282
54. van den Borne BE, Dijkmans BA, de Rooij HH, le Cessie S, Verweij CL. Chloroquine and hydroxychloroquine equally affect tumor necrosis factor-alpha, interleukin 6, and interferon-gamma production by peripheral blood mononuclear cells. *J Rheumatol.* (1997) 24:55–60.
55. Pichlmair A, Schulz O, Tan CP, Näslund TI, Liljeström P, Weber F, et al. RIG-I-mediated antiviral responses to single-stranded RNA bearing 5'-phosphates. *Science.* (2006) 314:997–1001. doi: 10.1126/science.1132998
56. Ishikawa H, Barber GN. STING is an endoplasmic reticulum adaptor that facilitates innate immune signalling. *Nature.* (2008) 455:674–8. doi: 10.1038/nature07317
57. Sun L, Wu J, Du F, Chen X, Chen ZJ. Cyclic GMP-AMP synthase is a cytosolic DNA sensor that activates the type I interferon pathway. *Science.* (2013) 339:786–91. doi: 10.1126/science.1232458
58. Kapishnikov S, Staalsø T, Yang Y, Lee J, Pérez-Berná AJ, Pereiro E, et al. Mode of action of quinoline antimalarial drugs in red blood cells infected by *Plasmodium* falciparum revealed *in vivo*. *Proc Natl Acad Sci USA.* (2019) 116:22946–52. doi: 10.1073/pnas.1910123116
59. Konradt C, Hunter CA. Pathogen interactions with endothelial cells and the induction of innate and adaptive immunity. *Eur J Immunol.* (2018) 48:1607–20. doi: 10.1002/eji.201646789
60. Espinola RG, Pierangeli SS, Gharavi AE, Harris EN, Ghara AE. Hydroxychloroquine reverses platelet activation induced by human IgG antiphospholipid antibodies. *Thromb Haemost.* (2002) 87:518–22. doi: 10.1055/s-0037-1613033
61. Rand JH, Wu X-X, Quinn AS, Ashton AW, Chen PP, Hathcock JJ, et al. Hydroxychloroquine protects the annexin A5 anticoagulant shield from disruption by antiphospholipid antibodies: evidence for a novel effect for an old antimalarial drug. *Blood.* (2010) 115:2292–9. doi: 10.1182/blood-2009-04-213520
62. Denning N-L, Aziz M, Gurien SD, Wang P. DAMPs and NETs in Sepsis. *Front Immunol.* (2019) 10:2536. doi: 10.3389/fimmu.2019.02536
63. Gautret P, Lagier J-C, Parola P, Hoang VT, Meddeb L, Mailhe M, et al. Hydroxychloroquine and azithromycin as a treatment of COVID-19: results of an open-label non-randomized clinical trial. *Int J Antimicrob Agents.* (2020) 105949. doi: 10.1016/j.ijantimicag.2020.105949. [Epub ahead of print].
64. Chen Z, Hu J, Zhang Z, Jiang S, Han S, Yan D, et al. Efficacy of hydroxychloroquine in patients with COVID-19: results of a randomized clinical trial. *medRxiv. [Preprint].* (2020). doi: 10.1101/2020.03.22.20040758. [Epub ahead of print].
65. Sarma P, Kaur H, Kumar H, Mahendru D, Avti P, Bhattacharyya A, et al. Virological and clinical cure in covid-19 patients treated with hydroxychloroquine: a systematic review and meta-analysis. *J Med Virol.* (2020). doi: 10.1002/jmv.25898
66. Yu B, Li C, Chen P, Zhou N, Wang L, Li J, et al. Low dose of hydroxychloroquine reduces fatality of critically ill patients with COVID-19. *Sci China Life Sci.* (2020). doi: 10.1007/s11427-020-1732-2. [Epub ahead of print].
67. Mahévas M, Tran V-T, Roumier M, Chabrol A, Paule R, Guillaud C, et al. Clinical efficacy of hydroxychloroquine in patients with covid-19 pneumonia who require oxygen: observational comparative study using routine care data. *BMJ.* (2020) 369:m1844. doi: 10.1136/bmj.m1844
68. Molina JM, Delaugerre C, Le Goff J, Mela-Lima B, Ponscarme D, Goldwirt L, et al. No evidence of rapid antiviral clearance or clinical benefit with the combination of hydroxychloroquine and azithromycin in patients with severe COVID-19 infection. *Med Mal Infect.* (2020) 50:384. doi: 10.1016/j.medmal.2020.03.006
69. Rosenberg ES, Dufort EM, Udo T, Wilberschied LA, Kumar J, Tesoriero J, et al. Association of treatment with hydroxychloroquine or azithromycin with in-hospital mortality in patients with COVID-19 in New York State. *JAMA.* (2020). doi: 10.1001/jama.2020.8630. [Epub ahead of print].
70. Tang W, Cao Z, Han M, Wang Z, Chen J, Sun W, et al. Hydroxychloroquine in patients with mainly mild to moderate coronavirus disease 2019: open label, randomised controlled trial. *BMJ.* (2020) 369:m1849. doi: 10.1136/bmj.m1849
71. Geleris J, Sun Y, Platt J, Zucker J, Baldwin M, Hripcsak G, et al. Observational study of hydroxychloroquine in hospitalized patients with covid-19. *N Engl J Med.* (2020) 382:2411–8. doi: 10.1056/NEJMoa2012410
72. Boulware DR, Pullen MF, Bangdiwala AS, Pastick KA, Lofgren SM, Okafor EC, et al. A randomized trial of hydroxychloroquine as postexposure prophylaxis for Covid-19. *N Engl J Med.* (2020). doi: 10.1056/NEJMoa2016638
73. Magagnoli J, Narendran S, Pereira F, Cummings T, Hardin JW, Sutton SS, et al. Outcomes of hydroxychloroquine usage in United States veterans hospitalized with Covid-19. *medRxiv.* (2020). doi: 10.1016/j.medj.2020.06.001
74. Keyaerts E, Vijgen L, Maes P, Neyts J, Van Ranst M. *In vitro* inhibition of severe acute respiratory syndrome coronavirus by chloroquine. *Biochem Biophys Res Commun.* (2004) 323:264–8. doi: 10.1016/j.bbrc.2004.08.085
75. Vincent MJ, Bergeron E, Benjannet S, Erickson BR, Rollin PE, Ksiazek TG, et al. Chloroquine is a potent inhibitor of SARS coronavirus infection and spread. *Virol J.* (2005) 2:69. doi: 10.1186/1743-422X-2-69
76. Barnard DL, Day CW, Bailey K, Heiner M, Montgomery R, Lauridsen L, et al. Evaluation of immunomodulators, interferons and known *in vitro* SARS-coV inhibitors for inhibition of SARS-coV replication in BALB/c mice. *Antivir Chem Chemother.* (2006) 17:275–84. doi: 10.1177/095632020601700505
77. Wang M, Cao R, Zhang L, Yang X, Liu J, Xu M, et al. Remdesivir and chloroquine effectively inhibit the recently emerged novel coronavirus (2019-nCoV) *in vitro*. *Cell Res.* (2020) 30:269–71. doi: 10.1038/s41422-020-0282-0
78. Yao X, Ye F, Zhang M, Cui C, Huang B, Niu P, et al. *In vitro* antiviral activity and projection of optimized dosing design of hydroxychloroquine for the treatment of severe acute respiratory syndrome coronavirus 2 (SARS-CoV-2). *Clin Infect Dis.* (2020) ciaa237. doi: 10.1093/cid/ciaa237
79. Liu J, Cao R, Xu M, Wang X, Zhang H, Hu H, et al. Hydroxychloroquine, a less toxic derivative of chloroquine, is effective in inhibiting SARS-CoV-2 infection *in vitro*. *Cell Discov.* (2020) 6:1–4. doi: 10.1038/s41421-020-0156-0
80. Yang Z-Y, Huang Y, Ganesh L, Leung K, Kong W-P, Schwartz O, et al. pH-dependent entry of severe acute respiratory syndrome coronavirus is mediated by the spike glycoprotein and enhanced by dendritic cell transfer through DC-SIGN. *J Virol.* (2004) 78:5642–50. doi: 10.1128/JVI.78.11.5642-5650.2004
81. Yan R, Zhang Y, Li Y, Xia L, Guo Y, Zhou Q. Structural basis for the recognition of SARS-CoV-2 by full-length human ACE2. *Science.* (2020) 367:1444–8. doi: 10.1126/science.abb2762
82. Blanco-Melo D, Nilsson-Payant BE, Liu W-C, Uhl S, Hoagland D, Møller R, et al. Imbalanced host response to SARS-CoV-2 drives development of COVID-19. *Cell.* (2020) 181:1036–45.e9. doi: 10.1016/j.cell.2020.04.026
83. Ziegler CGK, Allon SJ, Nyquist SK, Mbano IM, Miao VN, Tzouanas CN, et al. SARS-CoV-2 receptor ACE2 is an interferon-stimulated gene in human airway epithelial cells and is detected in specific cell

subsets across tissues. *Cell*. (2020) 181:1016–35.e19. doi: 10.1016/j.cell.2020.04.035

84. Banchereau R, Hong S, Cantarel B, Baldwin N, Baisch J, Edens M, et al. Personalized immunomonitoring uncovers molecular networks that stratify lupus patients. *Cell*. (2016) 165:551–65. doi: 10.1016/j.cell.2016.03.008
85. Lescure F-X, Bouadma L, Nguyen D, Parisey M, Wicky P-H, Behillil S, et al. Clinical and virological data of the first cases of COVID-19 in Europe: a case series. *Lancet Infect Dis*. (2020) 20:697–706. doi: 10.1016/S1473-3099(20)30200-0
86. Mehta P, McAuley DF, Brown M, Sanchez E, Tattersall RS, Manson JJ. COVID-19: consider cytokine storm syndromes and immunosuppression. *Lancet*. (2020) 395:1033–4. doi: 10.1016/S0140-6736(20)30628-0
87. Chen G, Wu D, Guo W, Cao Y, Huang D, Wang H, et al. Clinical and immunologic featsures in severe and moderate coronavirus disease (2019). *J Clin Invest*. (2020) 130:2620–9. doi: 10.1101/2020.02.16.20023903
88. Channappanavar R, Fehr AR, Vijay R, Mack M, Zhao J, Meyerholz DK, et al. Dysregulated type I interferon and inflammatory monocyte-macrophage responses cause lethal pneumonia in SARS-CoV-infected mice. *Cell Host Microbe*. (2016) 19:181–93. doi: 10.1016/j.chom.2016.01.007
89. Hadjadj J, Yatim N, Barnabei L, Corneau A, Boussier J, Pere H, et al. Impaired type I interferon activity and exacerbated inflammatory responses in severe Covid-19 patients. *medRxiv. [Preprint]*. (2020) 1. doi: 10.1101/2020.04.19.2008015
90. Guan W, Ni Z, Hu Y, Liang W, Ou C, He J, et al. Clinical characteristics of coronavirus disease 2019 in China. *N Engl J Med*. (2020) 382:1708–20. doi: 10.1101/2020.02.06.2000974

Conflict of Interest: AG received funding from Shire Takeda, outside the submitted work.

The remaining authors declare that the research was conducted in the absence of any commercial or financial relationships that could be construed as a potential conflict of interest.

Copyright © 2020 Gies, Bekaddour, Dieudonné, Guffroy, Frenger, Gros, Rodero, Herbeuval and Korganow. This is an open-access article distributed under the terms of the Creative Commons Attribution License (CC BY). The use, distribution or reproduction in other forums is permitted, provided the original author(s) and the copyright owner(s) are credited and that the original publication in this journal is cited, in accordance with accepted academic practice. No use, distribution or reproduction is permitted which does not comply with these terms.

Article 5

European Journal of Medicinal Chemistry xxx (xxxx) xxx

Contents lists available at ScienceDirect

European Journal of Medicinal Chemistry

journal homepage: http://www.elsevier.com/locate/ejmech

Research paper

Cerpegin-derived furo[3,4-*c*]pyridine-3,4(1*H*,5*H*)-diones enhance cellular response to interferons by *de novo* pyrimidine biosynthesis inhibition

Simon Hayek [a], Nicolas Pietrancosta [a, 1], Anna A. Hovhannisyan [b], Rodolphe Alves de Sousa [a], Nassima Bekaddour [a], Laura Ermellino [a, c], Enzo Tramontano [c], Stéphanie Arnould [d], Claude Sardet [d], Julien Dairou [e], Olivier Diaz [f], Vincent Lotteau [f], Sébastien Nisole [g], Gagik Melikyan [b, **], Jean-Philippe Herbeuval [a], Pierre-Olivier Vidalain [a, *]

[a] *Chimie et Biologie, Modélisation et Immunologie pour la Thérapie (CBMIT), Laboratoire de Chimie et Biochimie Pharmacologiques et Toxicologiques, Université Paris Descartes, CNRS UMR8601, Paris, France*
[b] *Department of Organic Chemistry, Yerevan State University, Yerevan, Armenia*
[c] *Laboratory of Molecular Virology, Department of Life and Environmental Sciences, University of Cagliari, Cagliari, Italy*
[d] *Institut de Recherche en Cancérologie de Montpellier, INSERM U1194, Université de Montpellier, Institut Régional du Cancer de Montpellier, Montpellier, France*
[e] *Chimie Bio-inorganique des Dérivés Soufrés et Pharmacochimie (CBDSP), Laboratoire de Chimie et Biochimie Pharmacologiques et Toxicologiques, Université Paris Descartes, CNRS UMR8601, Paris, France*
[f] *Centre International de Recherche en Infectiologie, INSERM U1111, CNRS UMR5308, Université Lyon 1, ENS de Lyon, Lyon, France*
[g] *Institut de Recherche en Infectiologie de Montpellier, CNRS UMR9004, Université de Montpellier, Montpellier, France*

ARTICLE INFO

Article history:
Received 9 September 2019
Received in revised form
2 November 2019
Accepted 4 November 2019
Available online xxx

Keywords:
Interferon
Pyrimidine biosynthesis
Cerpegin
DHODH
DNA damage response

ABSTRACT

There is an increasing interest in the field of cancer therapy for small compounds targeting pyrimidine biosynthesis, and in particular dihydroorotate dehydrogenase (DHODH), the fourth enzyme of this metabolic pathway. Three available DHODH structures, featuring three different known inhibitors, were used as templates to screen *in silico* an original chemical library from Erevan University. This process led to the identification of P1788, a compound chemically related to the alkaloid cerpegin, as a new class of pyrimidine biosynthesis inhibitors. In line with previous reports, we investigated the effect of P1788 on the cellular innate immune response. Here we show that pyrimidine depletion by P1788 amplifies cellular response to both type-I and type II interferons, but also induces DNA damage as assessed by γH2AX staining. Moreover, the addition of inhibitors of the DNA damage response led to the suppression of the P1788 stimulatory effects on the interferon pathway. This demonstrates that components of the DNA damage response are bridging the inhibition of pyrimidine biosynthesis by P1788 to the interferon signaling pathway. Altogether, these results provide new insights on the mode of action of novel pyrimidine biosynthesis inhibitors and their development for cancer therapies.

© 2019 Elsevier Masson SAS. All rights reserved.

1. Introduction

DNA and RNA syntheses require large amounts of purine and pyrimidine nucleosides as precursors. This makes quickly dividing cells highly dependent on *de novo* nucleoside biosynthesis, whereas quiescent and slowly growing cells essentially rely on intracellular recycling of nucleosides or their uptake from extracellular fluids. Consequently, cancer cells are particularly sensitive to nucleoside biosynthesis inhibitors such as 5-fluorouracil, methotrexate, or 6-

* Corresponding author. Current Address: Centre International de Recherche en Infectiologie (CIRI), INSERM U1111, CNRS UMR5308, Université Lyon 1, ENS de Lyon, 21 Avenue Tony Garnier, 69365, Lyon, Cedex 07, France.
** Corresponding author.
E-mail addresses: gagik.melikyan@yahoo.com (G. Melikyan), pierre-olivier.vidalain@inserm.fr (P.-O. Vidalain).
[1] Current Address: Sorbonne Université, INSERM, CNRS, Neurosciences Paris Seine - Institut de Biologie Paris Seine (NPS - IBPS), 75005 Paris, France. Sorbonne Université, CNRS, Laboratoire des Biomolécules (UMR7203), 75005 Paris, France.

https://doi.org/10.1016/j.ejmech.2019.111855
0223-5234/© 2019 Elsevier Masson SAS. All rights reserved.

Please cite this article as: S. Hayek et al., Cerpegin-derived furo[3,4-*c*]pyridine-3,4(1*H*,5*H*)-diones enhance cellular response to interferons by *de novo* pyrimidine biosynthesis inhibition, European Journal of Medicinal Chemistry, https://doi.org/10.1016/j.ejmech.2019.111855

mercaptopurine, which are extensively used in clinical practice. Among antimetabolites that are currently investigated for their antitumoral properties, molecules targeting dihydroorotate dehydrogenase (DHODH), the fourth enzyme of *de novo* pyrimidine biosynthesis, are the subject of intense research [1–3]. In this metabolic pathway, three enzymatic steps are required to convert glutamine, aspartate, and bicarbonate into dihydroorotate (DHO), which is the substrate for DHODH [3]. Its oxidation by DHODH leads to orotate, which is converted into uridine monophosphate (UMP) that serves as a precursor for cytidine and thymidine biosynthesis. This makes DHODH a rate-limiting enzyme in the biosynthesis of pyrimidine nucleosides, and a potential target for antimetabolite development.

In the 90s, brequinar, a potent DHODH inhibitor passed preclinical studies, and was evaluated for its antitumor properties in multiple phase-I and phase-II trials [1–3]. However, severe adverse effects and a lack of efficacy in patients with different types of solid tumors stopped its development. This setback also led to the disregard of DHODH inhibition as a valuable strategy for anticancer therapies. Concomitantly, teriflunomide, another DHODH inhibitor, and its related prodrug (leflunomide), were evaluated successfully and approved for the treatment of rheumatoid arthritis and later on for multiple sclerosis despite significant side effects [1–3]. This drug was shown to impair the proliferation of immune cells by inhibiting pyrimidine biosynthesis. It also interferes through tyrosine kinase inhibition and Aryl Hydrocarbon Receptor (AhR) activation, which altogether contribute to its immunosuppressive properties [4]. Despite the failure of brequinar in past clinical studies, recent publications renewed interest in DHODH as a target in cancer therapy and both old and recent series of DHODH inhibitors were shown to have promising antitumor properties. This was demonstrated in various *in vivo* models when administered alone or in combination with other drugs, in particular in acute myeloid leukemia (AML), neuroblastoma, PTEN (Phosphatase and TENsin homolog) mutant triple negative breast cancer cells, and KRAS (V-Ki-ras2 Kirsten rat sarcoma viral oncogene homolog) mutant pancreatic cancer cells [5–14]. Several DHODH inhibitors, including brequinar, leflunomide and new molecules such as BAY2402234 or PTC299, are currently being evaluated in clinical trials for cancer therapy [15,16]. Some pyrimidine biosynthesis inhibitors also exhibit broad-spectrum antiviral activity *in vitro* [1–3,17–19] and *in vivo* [20–22], opening new fields of application for this class of antimetabolites. In this context, the identification of novel DHODH inhibitors with original chemical and pharmacological properties has become a priority to overcome the limitations of existing molecules [23–27].

Beyond its cytostatic effects, DHODH inhibition is known to have a strong impact on gene expression, cell metabolism, and differentiation [5,12,14,15,28]. Our team is interested in the existing relationships between pyrimidine biosynthesis and the activation of innate immunity, with a specific focus on the interferon (IFN) response. IFN-α/β (or type I IFNs) are key antiviral and antitumoral cytokines that are produced by both immune and non-immune cells. They are released upon stimulation by viral PAMPs (Pathogen-Associated Molecular Patterns) such as double-stranded RNA molecules, or cellular DAMPs (Damage-Associated Molecular Patterns) including DNA breaks. Once bound to their target receptors, IFN-α/β mobilize the JAK (Janus Kinase) and STAT (Signal Transducers and Activators of Transcription) signaling cascade to induce a large panel of target genes, the ISGs (Interferon-Stimulated Genes), which encode numerous antiviral and antitumoral factors. IFNs and ISGs are therefore essential for the innate immune response against viruses and for the control of carcinogenesis [29,30]. Most interestingly, it is now well documented that pyrimidine biosynthesis inhibitors (i) induce some ISGs by a non-canonical and IFN-independent pathway, and (ii) enhance the expression of IFNs and ISGs when induced by viruses or viral PAMPs such as double-stranded RNA molecules [22,31–41]. Data from the literature suggest that DHODH inhibitors amplify the cellular response to type I IFNs, but this was only shown using a reporter gene containing Interferon-Stimulated Response Elements (ISRE) driving transcription of luciferase and never explored in detail [32,34]. The mechanism by which the inhibition of pyrimidine biosynthesis promotes the expression of IFNs and ISGs remains poorly understood and thus needs to be further documented [22,32,36,40,41]. The positive interaction between the inhibition of pyrimidine biosynthesis and the innate immune response likely contributes to the antiviral activity of DHODH inhibitors and it is tempting to speculate that it could also participate to the antitumor effect of these molecules as well.

DHODH, anchored by its N-terminal extremity to the internal mitochondrial membrane, uses flavin mononucleotide (FMN) and ubiquinone (or coenzyme Q_{10}) as cofactors in a two-step redox reaction. Ubiquinone is usually located in the mitochondrial membrane. Close contact between DHODH and the membrane allows ubiquinone to shuttle into a hydrophobic channel of this enzyme in order to contact FMN as recently modelled [42]. A majority of DHODH inhibitors that have been described in the literature compete with ubiquinone for binding to this channel, and interact with a limited number of well-characterized residues [1–3]. Here, we took advantage of three high-definition structures available in the Protein Data Bank (PDB) for human DHODH bound to unrelated inhibitors to develop and benchmark a pipeline for *in silico* screening (4OQV, 3KVJ, 4RR4). This led to the identification of P1788, a compound featuring structural components of the plant alkaloid cerpegin [43,44], as a new class of pyrimidine biosynthesis inhibitors. We then used this compound to establish that cellular response to both type-I and II IFNs is amplified in cell cultures where pyrimidine biosynthesis is blocked. We provide evidence that pyrimidine biosynthesis inhibition by P1788 activates the DNA damage response to amplify the interferon response. Altogether, our results reinforce the link between this metabolic pathway and the innate immune response and its therapeutic potential in various acute and chronic diseases.

2. Materials and methods

2.1. Chemical syntheses

All solvents and chemicals were purchased from the Armenian Institute of Applied Chemistry (ARIAC). Dimethylformamide (DMF), dimethylacetal (DMA) and xylene were dried using standard procedure. ^{1}H NMR and ^{13}C NMR spectra were recorded in deuterated dimethyl sulfoxide (DMSO-d_6) at ambient temperature using a 500 MHz nuclear magnetic resonance (NMR) spectrometer equipped with a 5 mm cryogenically cooled probe $^{1}H/^{13}C/^{2}D$ optimized for carbon-13 detection with z-gradients. The chemical shifts were reported in ppm downfield from tetramethylsilane (TMS). For compounds P2702, P2703, P2705 and P2706, ^{1}H NMR and ^{13}C NMR spectra were recorded with a Varian Mercury 300 spectrometer operating at 300 MHz and 75 MHz with TMS as internal standard in DMSO-d_6/CCl_4 solution at 303 K. Electrospray ionization (ESI) and high resolution mass spectrometry (HRMS) analyses were conducted using a Thermo Scientific High Resolution Exactive Orbitrap Mass spectrometer. The measurements were performed on the NMR platform and Mass spectrometry platform of UMR8601 CNRS laboratory. Elemental analyses were carried out by the CNRS microanalysis service at Gif-sur-Yvette. Melting points were determined on a Kofler hot-stage microscope and are uncorrected.

Please cite this article as: S. Hayek et al., Cerpegin-derived furo[3,4-*c*]pyridine-3,4(1*H*,5*H*)-diones enhance cellular response to interferons by *de novo* pyrimidine biosynthesis inhibition, European Journal of Medicinal Chemistry, https://doi.org/10.1016/j.ejmech.2019.111855

2.1.1. Procedure for the synthesis of cerpegin N-Substituted derivatives

The general procedure used for the synthesis of substituted cerpegin analogs was described in our previous reports [43,45]. Initial (E)-ethyl 4-(2-(dimethylamino)vinyl)-5,5-disubstituted-2-oxo-2,5-dihydrofuran-3-carboxylates (**II**) were synthesized according to previously described methods [43–46]. Briefly, condensation of 2-oxo-2,5-dihydrofurans (**I**; 10 mmol) and DMF/DMA (1.44 ml; 12 mmol) was achieved in 3 h in boiling anhydrous xylene (10 ml) to give the corresponding compounds (**II**) in yields of up to 80–90% (Scheme 1). In a flask fitted with a reflux, compound (**II**) (10 mmol) and the corresponding amine (40 mmol) were mixed in anhydrous xylene (7 mL). In the case of amines with low boiling points (bp < 100 °C) the reaction was undertaken without xylene using an excess of amine. The mixture was boiled for 15 h (extra 2 h after cessation of dimethylamine evolution), cooled to room temperature, and 5 mL of light petroleum was added. The resulting precipitates were filtered, washed with ether and dried. Yields and physical data of the resulting compounds are provided in Supplementary Materials and Methods.

2.1.2. Synthesis of N-cyclopropyl-4-methyl-2-oxo-1-oxaspiro[4.5]dec-3-ene-3-carboxamide (P2708)

A mixture of ethyl 4-methyl-2-oxo-1-oxaspiro[4.5]dec-3-ene-3-carboxylate (2.38 g; 10 mmol) and cyclopropylamine (0.9 mL; 13 mmol) in ethanol (1 mL) was left at room temperature 20 h. The resulting precipitate was filtered, washed with cold ether and recrystallized from ethanol. Yields and physical data of the resulting compound are provided in Supplementary Materials and Methods.

2.1.3. In silico screening

The *in silico* docking was performed with Discovery Studio (Discovery Studio Modeling Environment, release 4.5; Dassault Systemes BIOVIA: San Diego, 2015) as an interface to LibDock, a docking algorithm developed by Diller and Merz [47]. LibDock uses protein site features called HotSpots which are tagged as polar or apolar. Prior to the docking procedure, the receptor HotSpot file was calculated. In parallel, ligands were prepared (*i.e.* tautomer generation, protonation depending of pKa, or stereoisomer generation), then random ligand conformations were generated for each ligand structure by high-temperature molecular dynamics using the BEST algorithm. The different conformations of ligands were placed into the active site and HotSpots were matched as triplets. After a manual optimization and curation step, the ligand poses were scored. Because ligand hydrogens were removed during the docking process, they were added back to the ligand poses and optimized by minimization. The ligand poses with the highest LibDock scores were retained and clustered according to their binding mode.

2.1.4. Cells and culture conditions

Cells were cultured at 37 °C and 5% CO_2 in Dulbecco's Modified Eagle's Medium (DMEM; Sigma-Aldrich; D6429) containing 10% fetal calf serum (FCS; Sigma-Aldrich; F0804), penicillin and streptomycin. Experiments were performed on HEK-293 cells stably transfected with the ISRE-Luciferase reporter gene (ISRE-Luc), with or without NanoLuc as an additional reporter gene [32,48]. ISRE-Luc and ISG expression levels were unaffected by the presence of this additional reporter gene, and data from cells with or without NanoLuc were treated indifferently. Human peripheral blood mononuclear cells (PBMC) from one healthy donor were isolated by density centrifugation with Lymphoprep medium (StemCell Technologies) from leucocytes concentrates obtained when plateletpheresis was performed (Etablissement Français du Sang; Paris; France). To activate PBMCs, cells were treated for 24 h with the TLR7/8 ligand R848 at 5 μg/ml (Sigma-Aldrich) and supernatants were harvested. Cytokine expression levels were assessed using the LEGENDplex Human Anti-Virus Response Panel (BioLegend). Results are presented in Supplementary Table I.

2.1.5. Reagents, cytokines and small compounds

Firefly luciferase expression in culture wells was measured using the Bright-Glo (Promega) or Britelite plus reagents (PerkinElmer), according to the manufacturer's recommendations. Cellular viability was determined by quantification of adenosine triphosphate (ATP) in culture wells using the CellTiter-Glo assay (Promega). Bioluminescence was measured for 0.1 s with a luminometer (EnSpire; PerkinElmer). Recombinant IFN-α was from Sigma-Aldrich or PBL Assay Science. Recombinant IFN-γ was from Roussel Uclaf (a kind gift of Dr. Mounira Chelbi-Alix) or Miltenyi Biotech. Uridine, orotate, dihydroorotate, PF477736 (Checkpoint

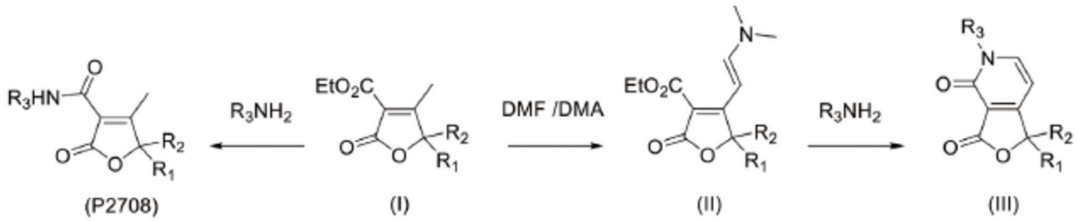

R_1, R_2, R_3	Norcerpegin	P2703	P1788	P2512	P1781	P2705	P2707	P1792	P1793	P2706	P2708	P2701	P2702	P2718	P2717
H	R_3			R_2											
Me	R_1, R_2	R_1			R_3							R_1, R_2	R_1		
ethyl													R_2	R_1, R_2	
isopropyl						R_3									
cyclopropyl		R_3	R_3								R_3	R_3	R_3	R_3	R_3
cyclobutyl							R_3								
cyclopentyl								R_3							R_1, R_2
cyclohexyl			R_1, R_2	R_1, R_2	R_1, R_2	R_1, R_2	R_1, R_2	R_1, R_2	R_1, R_2, R_3	R_1, R_2	R_1, R_2				
cyclopropylmethyl										R_3					
benzyl		R_2													

Scheme 1. Synthesis of cerpegin derivatives.

Kinase 1 inhibitor), mirin (MRE11 inhibitor), C646 (P300/CREB-Binding Protein inhibitor), teriflunomide, brequinar, and mitoxantrone were all from Sigma-Aldrich. Vidofludimus was from Selleckchem. AZD6738 (Ataxia telangiectasia and Rad3-related kinase inhibitor) was from Euromedex.

2.1.6. Metabolite analysis

Nucleoside/nucleotide quantification in HEK-293 cells was performed by high-performance liquid chromatography (HPLC)-coupled spectrophotometry as previously described in Ref. [38]. Experimental details are provided in the "Supplementary Materials and Methods".

2.1.7. Gene expression analysis by RT-qPCR

ISG expression levels were determined by Reverse Transcription and quantitative Polymerase Chain Reaction (RT-qPCR) as follows. Total RNAs were extracted from 2×10^5 cells using the RNeasy Micro kit including DNase (Qiagen). Reverse transcription of cellular RNA into cDNA was achieved using the RevertAid H Minus first-strand cDNA synthesis kit (Thermo Scientific). Real-time PCRs were performed in duplicate using the Takyon ROX SYBR MasterMix dTTP blue kit (Eurogentec) and a 7900HT Fast RT-PCR system (Applied Biosystems). Transcripts were quantified using the following program: 3 min at 95 °C, followed by 35 cycles of 15 s at 95 °C, 25 s at 60 °C, and 25 s at 72 °C. For each transcript, CT values were normalized both to the expression levels of RPL13A (60S ribosomal protein L13a) and unstimulated control samples using the $2^{-\Delta\Delta CT}$ method. The primers used for the quantification of transcripts are presented in Supplementary Table II.

2.1.8. γH2AX immunostaining

Cells were harvested after 24 h of culture, washed with PBS, trypsinized and fixed for 30 min in paraformaldehyde (PFA 4%). Cells were washed and permeabilized with Perm Buffer III (BD Biosciences) for 5 min. After one washing step, cells were stained with a mouse monoclonal anti-γH2AX antibody (1/400 dilution, 3F2 Clone, ThermoFisher) or a matching isotypic control in phosphate-buffered saline (PBS) + 2% bovine serum albumin (BSA). After 45 min at 4 °C, cells were washed again and incubated with a secondary Alexa Fluor 488-conjugated goat anti-mouse antibody (1/500, A21121, ThermoFisher). Cells were washed after 45 min at 4 °C of incubation, and analyzed by flow cytometry using a FACSCanto II (BD Biosciences).

3. Results

3.1. In silico identification of DHODH inhibitors

Ubiquinone is a rather large cofactor made of a 1,4-benzoquinone and a tail of 10 isoprenyl chemical subunits (Fig. 1A). The structure of human DHODH bound to ubiquinone, or its reduced form ubiquinol, has not been resolved yet. However, more than 50 co-structures of human DHODH featuring chemical inhibitors are available in the PDB. The vast majority of these inhibitors were found to bind a hydrophobic funnel localized at the contact interface of DHODH with the mitochondrial membrane. This lipophilic pocket was considered as the binding site for ubiquinone allowing a direct contact with FMN at its extremity as recently modelized by Costeira-Paulo J. et al. [42]. As shown in Fig. 1A, our molecular docking protocol confirmed that ubiquinone perfectly fits within this binding pocket. We also validated that Arg136, which is essential for DHODH activity and mutated in patients with Miller syndrome, interacts with one of the keto groups of ubiquinone as reported in Ref. [42]. To perform the molecular docking-based screening, we selected in PDB three available high-resolution structures of DHODH binding chemically-unrelated inhibitors: 4OQV, 3KVJ and 4RR4 [49,50]. These structures were not selected on the basis of the activity of the compounds, but because the compounds display different binding modes to human DHODH. Indeed, all three compounds are interacting with Arg136 and FMN in the hydrophobic funnel but the rest of the interactions with DHODH are highly diverse (Fig. 1B). This provided three slightly different DHODH structures to undertake an *in silico* screening. To benchmark our screening protocol, we showed that algorithm-based docking of each inhibitor perfectly matched the corresponding X-ray derived DHODH structure as assessed by a low Root-Mean-Square Deviation (RMSD) comparison (Fig. 1B).

The virtual high-throughput screening (vHTS) was performed on a set of 1,587 compounds from Yerevan State University, a chemical library that encompasses a large diversity of original structures. To ensure a time/precision ratio compatible with vHTS, we used a protocol in which amino acid side chains of the protein are left flexible only around the binding site, and we tested 10 random conformers for each ligand. The resulting ligand poses were further filtered to select compounds expected to bind Arg136 and FMN, and then ranked according to their docking scores as described in the Material and Methods section. The entire library was screened against the three selected DHODH structures. Finally, a total of 26, 49, and 55 compounds respectively fulfilled our criteria when using the 4OQV, 3KVJ and 4RR4 structures (Fig. 1C). To further increase the stringency of our screening, we selected the 11 compounds identified with at least two of the three above-mentioned structures. Interestingly, this subset included two molecules, P2703 and P1788 (Fig. 1D), which featured a 1,1,5-trimethylfuro[3,4-*c*]pyridine-3,4(1*H*,5*H*)-dione component similar to one seen in the alkaloid cerpegin. To our knowledge, such double-ringed structure with two adjacent keto groups contacting Arg136 was new for DHODH inhibitors and thus deserved further investigations.

3.2. Functional validation of selected hits

Since our main interest in DHODH inhibitors is their capacity to boost the cellular innate immune response, we used a reporter cell line expressing luciferase under the control of five interferon-stimulated response elements (ISRE-Luc) to assess the biological activity of the selected compounds. We and other groups have previously shown that in such a reporter system, cellular response to IFN-α/β is amplified by DHODH inhibitors [32,34]. Cells were incubated with increasing concentrations of selected compounds in the presence of recombinant IFN-α, and luciferase activity was quantified 24 h later. Of the 11 compounds tested, 9 were inactive but the two related compounds P2703 and P1788 efficiently increased cellular response to IFN-α (Fig. 2A). To further confirm the inhibition properties of this chemical series, we tested the capacity of P1788 to block cellular proliferation, a phenotype that is also associated with DHODH inhibition. P1788 efficiently inhibited the proliferation of HEK-293 cells when monitored over three days (Fig. 2B).

3.3. Structure activity relationships

To determine some structure activity relationship for this chemical series, and confront them with the docking model determined for P2703 and P1788 (Fig. 1D), we prepared the array of chemical analogs of cerpegin depicted in Fig. 3. Each compound was tested for its ability to boost cellular response to IFN-α using ISRE-Luc reporter cells as shown in Fig. 2A. A dose-response ranging from 0.8 to 150 μM was obtained for each molecule, and the corresponding pEC50s were calculated to compare their

Please cite this article as: S. Hayek et al., Cerpegin-derived furo[3,4-*c*]pyridine-3,4(1*H*,5*H*)-diones enhance cellular response to interferons by *de novo* pyrimidine biosynthesis inhibition, European Journal of Medicinal Chemistry, https://doi.org/10.1016/j.ejmech.2019.111855

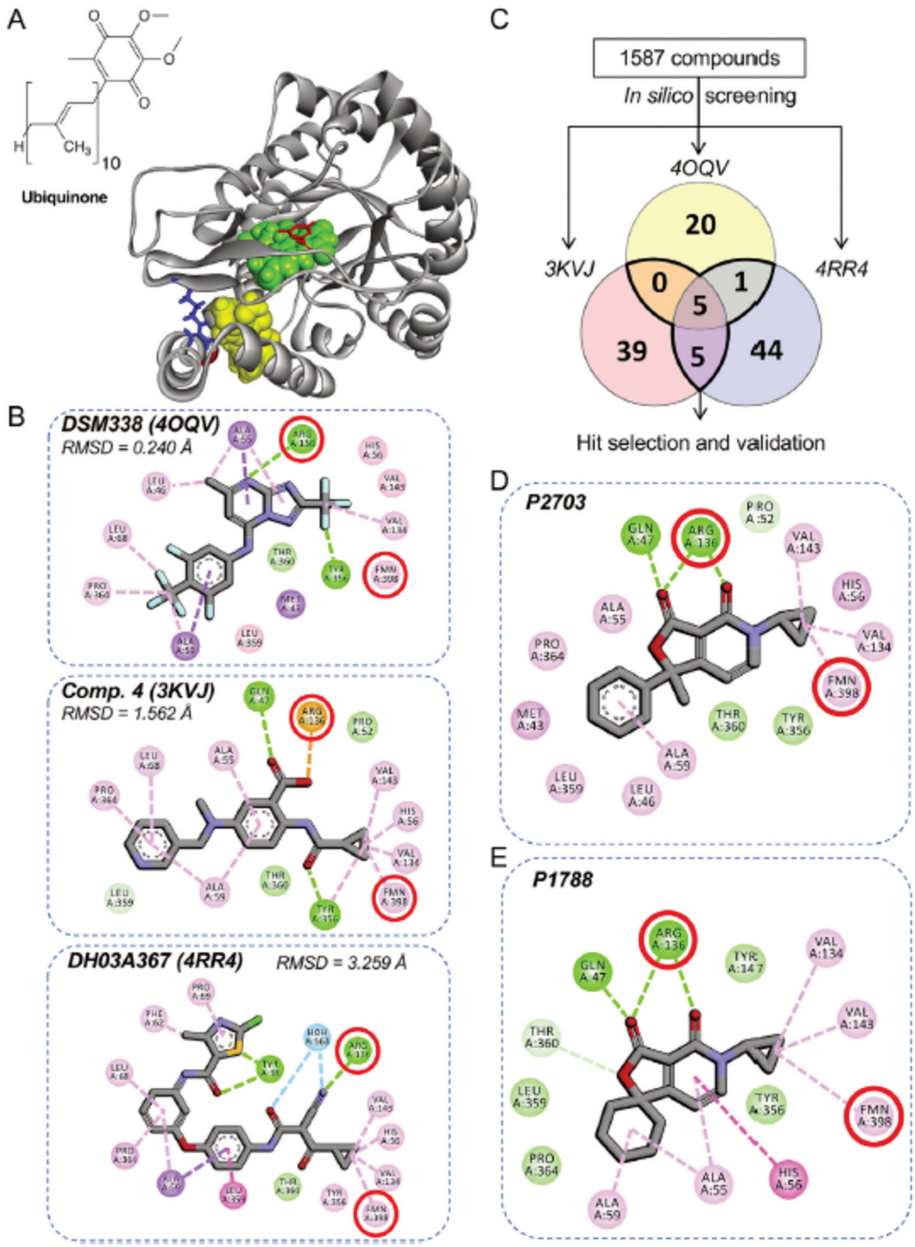

Fig. 1. ***In silico*** **screening procedure for the identification of novel DHODH inhibitors. (A)** DHODH structure was retrieved from PDB (3KVJ), showing orotate (red), FMN (green), and Arg136 (blue). The DHODH inhibitor present in the ubiquinone-binding site of the structure was removed and replaced by a ubiquinone analog without the hydrophobic tail to facilitate the *in silico* docking (yellow). Ubiquinone structure is shown in the upper left panel as a reference. **(B)** Schematic 2-D diagrams of small molecule inhibitors as bound to DHODH in PDB structures 4OQV, 3KVJ and 4RR4. For each inhibitor, the RMSD value estimates the position overlap between structural data and results of the *in silico* docking. **(C)** Venn diagram showing the results of the screenings performed on DHODH structures from 4OQV, 3KVJ, and 4RR4. We selected the 11 hit compounds identified in more than one screen for further evaluation. **(D–E)** Schematic 2-D diagrams of P2703 and P1788 bound to DHODH as determined by *in silico* docking. (For interpretation of the references to colour in this figure legend, the reader is referred to the Web version of this article.)

biological effect (Fig. 3). Norcerpegin (1,1-dimethylfuro[3,4-*c*]pyridine-3,4(1*H*,5*H*)-dione), the original scaffold of this chemical series, was inactive. The difference of effect seen between P1788 and compounds P2512, P1781 or P2705 demonstrated that a cyclopropyl substituent on the nitrogen was essential. Furthermore, compounds with the larger N-cyclobutyl (P2707), N-cyclopentyl (P1792), or N-cyclohexyl (P1793) groups were also inactive. Similarly, P2706 exhibiting an extended cyclopropylmethyl group showed no activity at tested concentrations. Altogether, these results support our docking model in which this cyclopropyl group fully occupies the DHODH hydrophobic pocket made of FMN, Val134 and Val143 (Fig. 1D). We also found that a double hydrophobic substitution on position 1 of the furopyridine scaffold was essential as seen for compounds featuring a spirocyclopentane (P2717), a spirocyclohexane (P1788) or a phenyl and a methyl group (P2703). This is consistent with our docking model where such substituents interact with Ala59 or Ala55 at the entry side of the hydrophobic pocket (Fig. 1D). Finally, opening the pyridine group as in P2708 also impaired the biological activity of the molecule. This last result is in line with a structuring role for the furopyridine

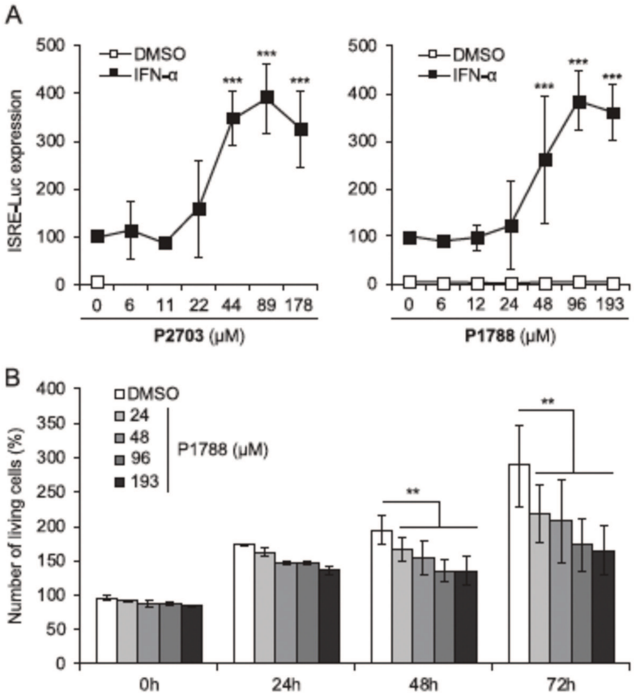

Fig. 2. Cellular response to IFN-α is amplified by P1788 and P2703. (A) HEK-293 cells with the ISRE-Luc reporter gene were treated with P1788, P2703 or DMSO alone in the absence or presence of IFN-α (150 IU/ml). Expression of the ISRE-Luc reporter gene was determined 24 h later, and results were normalized using cells treated with IFN-α alone as reference. **(B)** Cells were treated with DMSO or P1788 at different concentrations, and the number of viable cells was determined using the CellTiter-Glo reagent after 24, 48 and 72 h of culture. Results were expressed as a percentage relative to untreated cells at t = 0 h. Data represent means±SD of three (A) or two (B) independent experiments. $^{**}p < 0.01$; $^{***}p < 0.001$ as calculated by one-way analysis of variance (ANOVA) with Bonferroni's *post hoc* test.

scaffold. Altogether, these results validate our docking model for P2703 and P1788 in the ubiquinone binding pocket of DHODH.

To compare the activity of P2703 and P1788 with well-characterized inhibitors of DHODH, teriflunomide, vidofludimus and brequinar were evaluated in the same cellular assay (Fig. 3). Teriflunomide and vidofludimus were significantly more active than P2703 and P1788 (EC50 = 8.9 and 2.8 μM *vs* 27 and 44 μM, respectively), but all four molecules showed EC50s within the micromolar range. Only brequinar was much more active with an EC50 equal to 56 nM. Because P2703 and P1788 were within a range of activity close to fully optimized molecules like teriflunomide or vidofludimus, we decided to further investigate the properties of these molecules. Although P2703 was slightly more active, P1788 was selected as the prototype of this chemical series because a larger batch had been produced and was readily available.

3.4. P1788 targets the pyrimidine biosynthesis pathway

To demonstrate that P1788 is indeed targeting the pyrimidine metabolism, we treated cells with this molecule and quantified nucleoside levels by liquid chromatography coupled with spectrophotometry. As shown in Fig. 4A, pyrimidine levels collapsed in P1788-treated cells (U and C), whereas purine levels were unaffected (G and A). This shows that P1788 interferes with pyrimidine homeostasis as expected. We then determined if the amplification of IFN-α/β signaling by P1788 is a consequence of pyrimidine depletion in treated cells. To address this question, cells with the ISRE-Luc reporter gene were treated with recombinant IFN-α and P1788 in the absence or presence of uridine. The addition of uridine completely reverted the effect of P1788, thus demonstrating that pyrimidine depletion is indeed responsible for the amplified response to IFN-α as shown in Fig. 4B. In order to determine more precisely which step of pyrimidine biosynthesis is inhibited by P1788, the same experiment was performed using a culture medium supplemented with either DHO or orotate (Fig. 4C). While DHO showed no effect on cellular response to IFN-α, orotate completely reverted the effect of P1788. As DHO and orotate are respectively the substrate and product of DHODH, these results confirmed that P1788 is inhibiting this critical step of the pyrimidine biosynthesis pathway.

3.5. P1788 amplifies cellular response to both type I and type II IFNs

As stated above, it has previously been shown that DHODH inhibition amplifies cellular response to IFN-α/β [32,34]. However, this was only documented using an ISRE-Luc reported gene and never validated by the actual monitoring of cellular ISGs. We took advantage of P1788 as a novel inhibitor to address this question. Cells were treated with increasing concentrations of IFN-α in the absence or presence of P1788, and expression levels of 12 ISGs were determined by RT-qPCR. ISGs were induced by IFN-α alone, but P1788 further enhanced their expression (Fig. 5A). For example, a 4 to 5-fold increase in Mx2 expression level was observed when cells stimulated with IFN-α were co-treated with P1788 (Fig. 5B). Altogether, this confirmed that P1788 can boost the cellular response to IFN-α.

To our knowledge, it is still unknown if pyrimidine biosynthesis inhibitors are also able to amplify the cellular response to IFN-γ. This is particularly interesting because this cytokine, which is massively produced by Natural Killer (NK) cells and $CD8^+$ T lymphocytes, plays a key role in antitumoral immune responses and adaptive immunity in general. We thus investigated the effects of P1788 on this pathway. Cells with the ISRE-Luc reporter gene were stimulated with recombinant IFN-γ in the absence or presence of P1788. As shown in Fig. 6A, the reporter gene was induced by IFN-γ, and P1788 further increased its expression. To further validate this observation, we collected supernatants of human PBMCs stimulated with R848, a synthetic ligand for TLR7. Such conditioned supernatants contain IFN-γ as shown in Supplementary Table I and were used to stimulate cells with the ISRE-Luc reporter gene. P1788 strongly increased the cellular response to conditioned supernatants from PBMCs (Fig. 6B). Our results demonstrate that P1788 is able to amplify cellular response to both type I and type II interferons.

3.6. Key factors of the DNA damage response link P1788 to the IFN signaling pathway

Pyrimidine depletion by DHODH inhibitors has been shown to block DNA replication, leading to S phase accumulation and the activation of DNA damage response [9] (Fig. 7A). It is also well known that DNA damage are able to prime or induce the IFN response to prevent infections or tumor formation, depending on the cellular system [29,51]. The DNA damage response could therefore functionally link the inhibition of DHODH to the innate immunity as recently documented by Luthra P. et al. [40]. To address this question in our cellular system, we first determined if P1788 treatment induced the DNA damage response by measuring γH2AX, the phosphorylated form of H2AX (H2A histone family member X) on serine 139. As shown in Fig. 7B, P1788 induced a significant increase in γH2AX staining as determined by flow cytometry. Similar γH2AX levels were achieved with the reference DHODH inhibitor teriflunomide but the signal was much higher

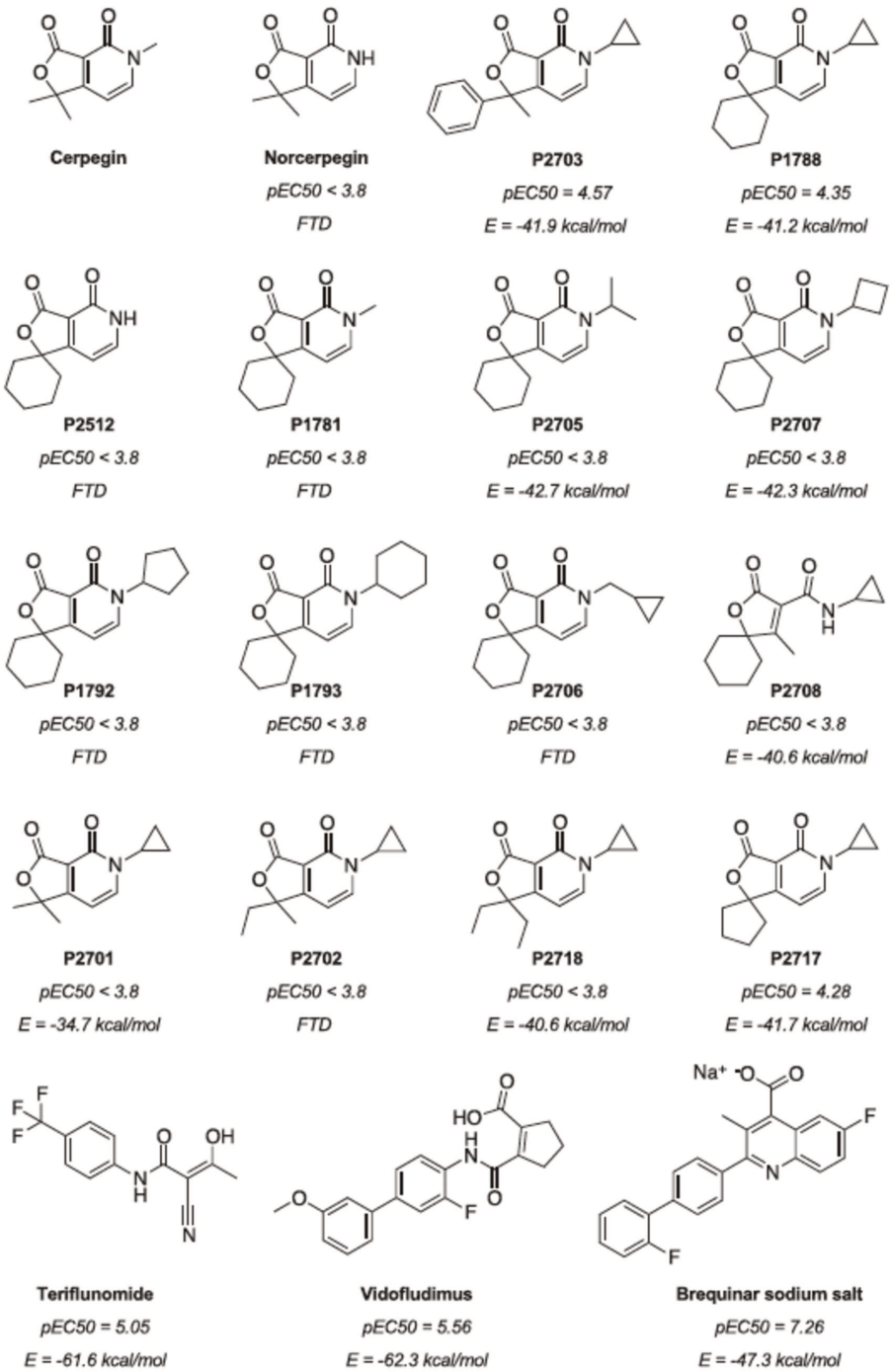

Fig. 3. Structure/activity relationships. Chemical analogs of P1788 and P2703 were tested for their ability to boost cellular response to IFN-α in HEK-293 cells with the ISRE-Luc reporter gene. Teriflunomide, vidofludimus and brequinar were tested as reference DHODH inhibitors in the same cellular assay. pEC50s, corresponding to $-\log_{10}$ of the half maximal effective molar concentrations, were computed from a four-parameter fitting curve using Prism software (GraphPad). Binding energies were also computed by *in silico* docking for comparison with pEC50s. FTD ("failed to determine") is indicated when binding energies could not be computed. The chemical structure of cerpegin is shown as a reference.

with mitoxantrone, a potent topoisomerase II inhibitor that induces massive DNA damage. Furthermore, P1788 effect was neutralized by the addition of uridine, thus implicating pyrimidine depletion in this effect. The inhibition of *de novo* pyrimidine biosynthesis by P1788 is therefore associated to the induction of a mild DNA damage response which probably reflects the accumulation of stalled DNA forks in S phase.

The exonuclease activity of the double-strand break repair protein MRE11, which is part of the MRE11/RAD50/NBS1 (MRN) complex, plays an important role in the stabilization, resection, and restart of stalled DNA forks (Fig. 7A). MRE11 also exhibits some endonuclease activity involved in the cleavage and release of single-stranded DNA from the resection site which contributes to IFN activation [52]. We tested the effect of mirin, an inhibitor of the

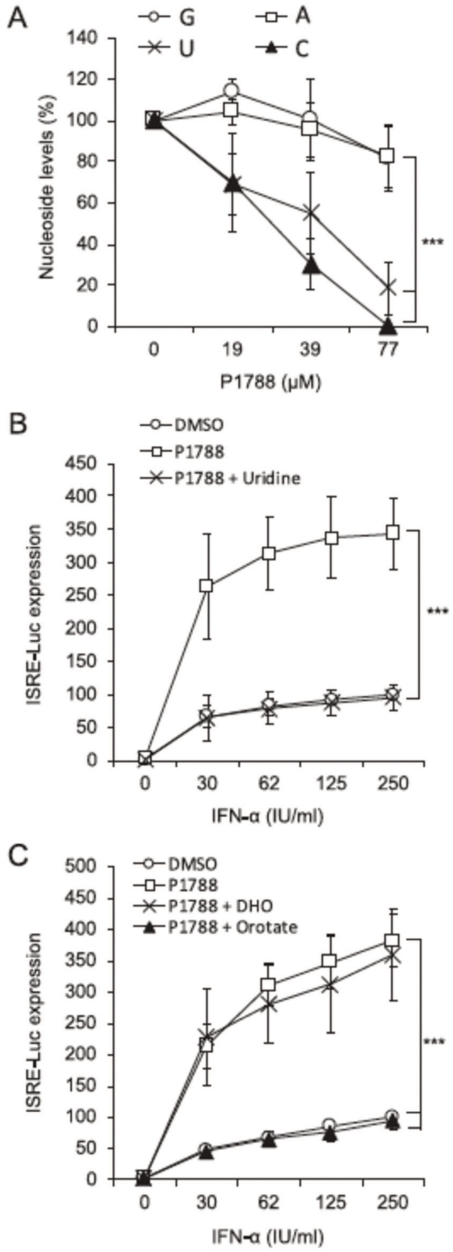

Fig. 4. P1788 is inhibiting pyrimidine biosynthesis. (A) Cells were treated with DMSO or increasing concentrations of P1788. 24 h later, cells were harvested and intracellular levels of purine (G/A) and pyrimidine (C/U) were determined by HPLC-coupled spectrophotometry. Results were normalized using DMSO-treated cells as a reference. **(B)** Cells were treated with increasing concentrations of IFN-α with DMSO, P1788 (80 µM) or P1788 (80 µM) and uridine (125 µM). 24 h later, expression of the ISRE-Luc reporter gene was determined. Results were normalized using cells treated with DMSO + IFN-α at 250 IU/ml as a reference. **(C)** Same experiment as in (A), but culture medium was supplemented with 3 mM of orotate or DHO instead of uridine. Data represent means±SD of three independent experiments. ***$p < 0.001$ as calculated by two-way ANOVA.

MRE11 nuclease activity, on the cellular response to IFN-α in the absence or presence of P1788. As shown in Fig. 7C, mirin completely abolished the booster effect of P1788 on ISRE-Luc induction by IFN-α. Cellular viability was not affected by this treatment as shown in Supp. Fig. 1A. The Ataxia telangiectasia and Rad3-related kinase (ATR) are co-activated with the MRN complex by single-stranded DNA breaks and then phosphorylate CHK1 (Checkpoint Kinase 1) to block cell cycle progression upon DNA damage [53]. We tested potent inhibitors of either ATR (AZD6738) or CHK1 (PF477736) in our system. ATR or CHK1 inhibitors abolished the effects of P1788 on the IFN-α response, further supporting a role of the DNA damage response as shown in Fig. 7D and E. Interestingly, ATR or CHK1 inhibition also showed significant effects on the cellular response to IFN-α in the absence of P1788. This suggests that a steady-state activation of ATR and CHK1 in these cells somehow contributes to the IFN response. As stated, these treatments showed limited (AZD6738) or no effect (PF477736) on cellular viability (Supp. Fig. 1B). Finally, we evaluated the contribution of P300 and CBP (CREB-Binding protein), two related histone acetyltransferases that are activated downstream of the DNA damage response but also regulate the expression of ISGs. We thus treated cells with C636, a small compound inhibiting both P300 and CBP, and induced the ISRE-Luc reporter gene with IFN-α with or without P1788. As shown in Fig. 7F, the inhibition of P300/CBP slightly decreased cellular response to IFN-α, but most importantly abolished the effect of P1788. These results confirm the functional link between the DNA damage response and the IFN-potentiating effect of P1788.

4. Discussion

De novo pyrimidine biosynthesis is essential to fulfill the metabolic needs of quickly proliferating cells. As such, there is an increased interest in the field of cancer for molecules blocking critical steps of this enzymatic pathway. Here, we detailed the identification of P1788 and related molecules as a new series of pyrimidine biosynthesis inhibitors. These compounds were selected by virtual screening using three structures of DHODH co-crystallized with chemically distinct inhibitors bound to the ubiquinone/ubiquinol pocket. This approach was previously used by other teams and our results confirm its efficacy [54–57]. We then established the inhibition of pyrimidine biosynthesis pathway in P1788-treated cells by measuring nucleoside levels and using cellular response to IFN-α as a functional readout. The fact that orotate but not DHO nullified the effects of P1788 in this test supports the inhibition of DHODH by this molecule. It is of interest that P1788 and related molecules of this chemical series feature the unique chemical scaffold found in the alkaloid cerpegin (Fig. 3) [43,44]. Cerpegin is found in the Indian plant *Ceropegia juncea*, which has been used for centuries in folk medicine as a tranquilizer, anti-inflammatory, analgesic, and anti-ulcer therapy. Modern studies showed that compounds with the cerpegin scaffold inhibit the 20S subunit of the proteasome [43,45]. The results described here show that compounds also based on the cerpegin scaffold but with different additional chemical groups inhibit pyrimidine biosynthesis. The two-edged fused polycyclic moieties of this chemical series are actually reminiscent of known DHODH inhibitors, including brequinar, dicoumarol, and DD778 that we recently described [38]. Brequinar interacts with Arg136 of DHODH through its carboxylic acid group whereas in dicoumarol, the lactone oxygen atom was suggested to play this role [58]. According to our *in silico* model, the interaction of P1788 with Arg136 is mediated by the diketone motif. To our knowledge, this mode of interaction was not previously reporter for DHODH inhibitors and clearly distinguishes the P1788 series from known DHODH inhibitors.

We took advantage of our lead molecule P1788 to characterize in details the impact of pyrimidine biosynthesis inhibition on cellular response to IFNs. It is well known that DHODH inhibition can (i) induce ISGs independently of IFN production or JAK/STAT signaling and (ii) amplify the expression of both ISGs and IFN genes in response to double-stranded RNA molecules, a viral PAMP that

Please cite this article as: S. Hayek et al., Cerpegin-derived furo[3,4-*c*]pyridine-3,4(1*H*,5*H*)-diones enhance cellular response to interferons by *de novo* pyrimidine biosynthesis inhibition, European Journal of Medicinal Chemistry, https://doi.org/10.1016/j.ejmech.2019.111855

A

	DMSO					P1788				
IFN-α (IU/ml)	0	30	60	125	250	0	30	60	125	250
ISG15	1	49	66	70	76	2	123	163	200	226
IFIT3	1	21	44	56	69	2	39	69	99	129
IFIT1	1	24	37	49	65	1	51	85	115	145
IFIT2	1	6	15	28	45	2	26	61	112	165
IFI6	1	4	18	25	33	2	47	64	80	91
IFI27	1	2	14	23	33	3	44	83	117	143
IFITM3	1	2	11	13	16	1	6	12	14	15
DDX58	1	2	8	11	14	2	16	23	31	38
Mx2	1	1	2	4	7	2	7	13	20	28
IFIT5	1	2	3	3	3	1	3	3	4	5
PKR	1	1	2	3	3	1	2	3	3	4
PML	1	1	2	2	3	1	3	4	5	5

B

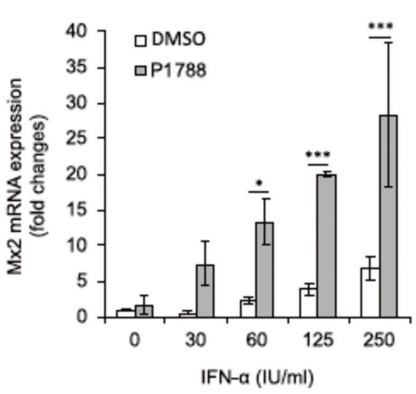

Fig. 5. ISG induction by IFN-α is enhanced in the presence of P1788. (A) HEK cells with the ISRE-Luc reporter gene were cultured with increasing concentrations of IFN-α and co-treated with DMSO or P1788 (80 μM). 16 h later, induction levels of indicated ISGs were determined by RT-qPCR, and expressed as fold changes relative to control cells (DMSO alone). Results highlighted in bold correspond to statistically significant values when comparing untreated to P1788-treated cells from three independent experiments ($p < 0.05$ determined by two-way ANOVA with Bonferroni's post hoc test). **(B)** Corresponding data for Mx2 mRNA expression were displayed as a bar chart showing mean values±SD. *$p < 0.05$; ***$p < 0.001$ as calculated by two-way ANOVA with Bonferroni's *post hoc* test.

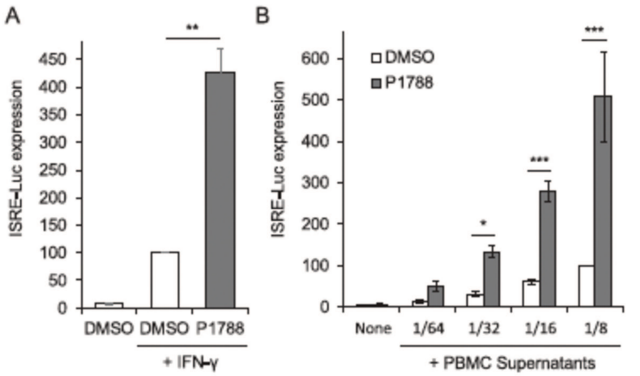

Fig. 6. Cellular response to IFN-γ is amplified by P1788. (A) HEK-293 cells with the ISRE-Luc reporter gene were treated with DMSO or P1788 (80 μM) in the absence or presence of recombinant IFN-γ (150 IU/ml). Luciferase activity in culture wells was determined 24 h later. Results were normalized using cells treated with DMSO + IFN-γ as reference. **$p < 0.01$ as calculated by two-tailed *t*-test. **(B)** Same experiment as in (A), but cells were stimulated with different dilutions ranging from 1/8 to 1/64 of conditioned supernatants from activated PBMCs. Results were normalized using cells treated with 1/8 diluted supernatants as reference. Data represent means±SD of three independent experiments. *$p < 0.05$; ***$p < 0.001$ determined by two-way ANOVA with Bonferroni's *post hoc* test.

binds and activates RIG-like receptors (RLRs). Literature also suggested that cellular response to type I IFNs is amplified when DHODH is inhibited as assessed with an ISRE-Luc reporter gene [32,34]. Here, we have analyzed a dozen of ISGs by RT-qPCR, and found that their induction by recombinant IFN-α is, as expected, enhanced in the presence of P1788. This illustrates that the cellular stress associated to pyrimidine deprivation is acting at multiple steps of the innate immune response. Most interestingly, we also found that P1788 amplifies cellular response to IFN-γ. This was shown using purified recombinant IFN-γ or conditioned supernatants from activated PBMCs. IFN-γ activates a signaling cascade that significantly differs from IFN-α/β as it binds a specific receptor (IFNGR1/2) and mobilizes Jak1/Jak2 kinases — as opposed to Jak1/Tyk2 for IFN-α/β — to phosphorylate STAT1. STAT2 is not involved in the signaling cascade induced by IFN-γ. Our results and the literature suggest that a common mechanism triggered by pyrimidine deprivation amplifies cellular response to both IFN-α/β, IFN-γ, and RLR ligands. IFNs rely on STAT1/2 for gene transcription, whereas RLRs activate Interferon Regulatory Factors 3 (IRF3). It is therefore tempting to speculate that a common costimulatory factor associates to these transcription factors when pyrimidine biosynthesis is impaired. Discovering this mechanism remains a major challenge in our understanding of the mechanisms linking pyrimidine metabolism to innate immunity.

Here, we showed that P1788 treatment was associated to the induction of a DNA damage response as assessed by γH2AX staining. Furthermore, the enhanced response to IFN-α was dependent on MRE11, ATR, CHK1, and P300/CBP. MRE11, ATR, and CHK1 are all activated by single-stranded genomic DNA, in particular at stalled

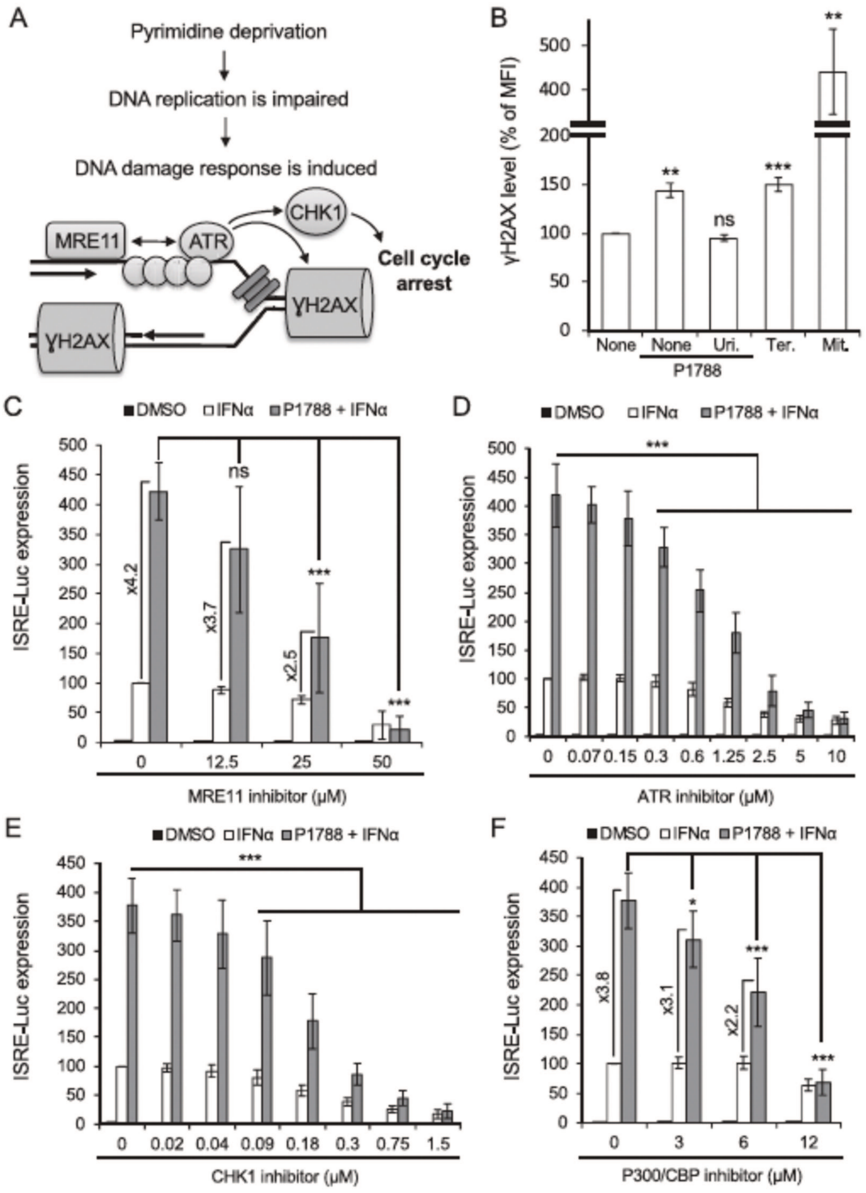

Fig. 7. Immunostimulatory properties of P1788 is linked to DNA damage response. (A) Simplified model of the DNA damage response induced by pyrimidine deprivation at stalled DNA replication forks. (B) Cells were treated with DMSO, P1788 (80 μM), P1788 + uridine (Uri.; 125 μM), teriflunomide (Ter.; 50 μM) or mitoxantrone (Mit.; 50 nM). 24 h later, cells were harvested and γH2AX level was determined by immunostaining and flow cytometry analysis. Data represent means±SD of three independent experiments. $^{**}p < 0.01$; $^{***}p < 0.001$ as calculated by two-tailed *t*-test. **(C–F)** HEK-293 cells with the ISRE-Luc reporter gene were treated with DMSO, IFN-α (150 IU/ml) or IFN-α + P1788 (80 μM), in the absence or presence of mirin (C), AZD6738 (D), PF477736 (E) or C636 (F) to inhibit MRE11, ATR, CHK1 and P300/CBP, respectively. Luciferase activity in culture wells was determined 24 h later, and results were normalized using cells treated with IFN-α alone as reference. Data represent means±SD of at least three independent experiments (B–F). $^{*}p < 0.05$; $^{**}p < 0.01$; $^{***}p < 0.001$ as calculated by standard Student's t-test (B) or one-way ANOVA with Bonferroni's *post hoc* test (C–F).

DNA replication forks which likely accumulate when intracellular pyrimidine concentration drops below a certain threshold [52]. This further supports the idea that the DNA damage response represents the functional link between the inhibition of pyrimidine biosynthesis and the innate immune response. Most interestingly, we and others have previously shown that Interferon Regulatory Factor 1 (IRF1) is essential to ISG induction in cells treated with pyrimidine biosynthesis inhibitors alone, double-stranded RNA, or both [32,40]. IRF1 is a transcription factor that is upregulated by the DNA damage response and promotes the expression of ISGs, either alone or in association with STATs and IRFs [59,60]. In addition, it was shown that IRF1-mediated transcription relies on P300/CBP, two related histone acetyltransferases that we implicated in the signaling cascade downstream of P1788 [61]. In a recent report by Luthra et al., it has been shown that DNA damage associated with the inhibition of pyrimidine biosynthesis activate ATM (Ataxia Telangiectasia Mutated), a kinase activated by double-stranded DNA breaks, which was essential to the induction of ISGs by pyrimidine biosynthesis inhibitors [40]. In line with this work, we conclude from our observations that the DNA damage response links pyrimidine deprivation to the innate immune response and to IRF1, and show that P300/CBP is also involved in this phenomenon.

In conclusion, we have identified and characterized a new series of compounds inhibiting pyrimidine biosynthesis. Future work will

Please cite this article as: S. Hayek et al., Cerpegin-derived furo[3,4-*c*]pyridine-3,4(1*H*,5*H*)-diones enhance cellular response to interferons by *de novo* pyrimidine biosynthesis inhibition, European Journal of Medicinal Chemistry, https://doi.org/10.1016/j.ejmech.2019.111855

aim at improving these compounds to obtain more potent inhibitors with optimized pharmacological properties. These molecules enhance cellular response to IFN-α/β, and DNA damage response plays a key role in this mechanism. Most importantly, we showed that cellular response to IFN-γ is also enhanced in the presence of P1788. This latter finding is opening exciting perspectives in cancer therapy as IFN-γ contributes to the antitumoral activity of both NK cells and $CD8^+$ T lymphocytes [62]. This suggests that the benefit of DHODH inhibitors relies not only on their cytostatic effects but also on their capacity to boost an antitumoral response. If confirmed *in vivo* this would represent a significant step toward the development of this new category of antitumoral drugs.

Declaration of competing interest

Structures and DHODH-inhibitory activities of the original compounds described in this manuscript have been patented.

Acknowledgments

We acknowledge the technical support of Stéphanie Dupuy from the Flow Cytometry Platform at Université Paris Descartes. We thank the chemical library of UMR8601 of Paris Descartes University for preparing and providing access to Yerevan's complete database for virtual and physical screening. We thank Dr. Farah Hodeib and Dr. Yves Janin for proofreading the manuscript. This work was supported by the Agence Nationale de la Recherche (ChemInnate program to POV and SN), Campus France (Programme CEDRE), SantImmune from the Fondation Paris Descartes, the Centre National de la Recherche Scientifique (CNRS; www.cnrs.fr), and the Institut National de la Santé Et de la Recherche Médicale (INSERM). SH was supported by the National Council for Scientific Research (Lebanon) and the Université Saint-Esprit de Kaslik (USEK).

Appendix A. Supplementary data

Supplementary data to this article can be found online at https://doi.org/10.1016/j.ejmech.2019.111855.

References

[1] H. Munier-Lehmann, P.-O. Vidalain, F. Tangy, Y.L. Janin, On dihydroorotate dehydrogenases and their inhibitors and uses, J. Med. Chem. 56 (2013) 3148–3167, https://doi.org/10.1021/jm301848w.

[2] M.L. Lolli, S. Sainas, A.C. Pippione, M. Giorgis, D. Boschi, F. Dosio, Use of human dihydroorotate dehydrogenase (hDHODH) inhibitors in autoimmune diseases and new perspectives in cancer therapy, Recent Patents Anticancer Drug Discov 13 (2018) 86–105, https://doi.org/10.2174/1574892812666171108124218.

[3] J.T. Madak, A. Bankhead, C.R. Cuthbertson, H.D. Showalter, N. Neamati, Revisiting the role of dihydroorotate dehydrogenase as a therapeutic target for cancer, Pharmacol. Ther. 195 (2018) 111–131, https://doi.org/10.1016/j.pharmthera.2018.10.012.

[4] E.F. O'Donnell, K.S. Saili, D.C. Koch, P.R. Kopparapu, D. Farrer, W.H. Bisson, L.K. Mathew, S. Sengupta, N.I. Kerkvliet, R.L. Tanguay, S.K. Kolluri, The anti-inflammatory drug leflunomide is an agonist of the aryl hydrocarbon receptor, PLoS One 5 (2010), https://doi.org/10.1371/journal.pone.0013128.

[5] D.B. Sykes, Y.S. Kfoury, F.E. Mercier, M.J. Wawer, J.M. Law, M.K. Haynes, T.A. Lewis, A. Schajnovitz, E. Jain, D. Lee, H. Meyer, K.A. Pierce, N.J. Tolliday, A. Waller, S.J. Ferrara, A.L. Eheim, D. Stoeckigt, K.L. Maxcy, J.M. Cobert, J. Bachand, B.A. Szekely, S. Mukherjee, L.A. Sklar, J.D. Kotz, C.B. Clish, R.I. Sadreyev, P.A. Clemons, A. Janzer, S.L. Schreiber, D.T. Scadden, Inhibition of dihydroorotate dehydrogenase overcomes differentiation blockade in acute myeloid leukemia, Cell 167 (2016) 171–186, https://doi.org/10.1016/j.cell.2016.08.057, e15.

[6] T.A. Lewis, D.B. Sykes, J.M. Law, B. Muñoz, J.K. Rustiguel, M.C. Nonato, D.T. Scadden, S.L. Schreiber, Development of ML390: a human DHODH inhibitor that induces differentiation in acute myeloid leukemia, ACS Med. Chem. Lett. 7 (2016) 1112–1117, https://doi.org/10.1021/acsmedchemlett.6b00316.

[7] D. Mathur, E. Stratikopoulos, S. Ozturk, N. Steinbach, S. Pegno, S. Schoenfeld, R. Yong, V.V. Murty, J.M. Asara, L.C. Cantley, R. Parsons, PTEN regulates glutamine flux to pyrimidine synthesis and sensitivity to dihydroorotate dehydrogenase inhibition, Cancer Discov. 7 (2017) 380–390, https://doi.org/10.1158/2159-8290.CD-16-0612.

[8] S. Zhu, X. Yan, Z. Xiang, H.-F. Ding, H. Cui, Leflunomide reduces proliferation and induces apoptosis in neuroblastoma cells in vitro and in vivo, PLoS One 8 (2013), e71555, https://doi.org/10.1371/journal.pone.0071555.

[9] S. Arnould, G. Rodier, G. Matar, C. Vincent, N. Pirot, Y. Delorme, C. Berthet, Y. Buscail, J.Y. Noël, S. Lachambre, M. Jarlier, F. Bernex, H. Delpech, P.O. Vidalain, Y.L. Janin, C. Theillet, C. Sardet, Checkpoint kinase 1 inhibition sensitises transformed cells to dihydroorotate dehydrogenase inhibition, Oncotarget 8 (2017) 95206–95222, https://doi.org/10.18632/oncotarget.19199.

[10] M.J.G.W. Ladds, I.M.M. van Leeuwen, C.J. Drummond, S. Chu, A.R. Healy, G. Popova, A. Pastor Fernández, T. Mollick, S. Darekar, S.K. Sedimbi, M. Nekulova, M.C.C. Sachweh, J. Campbell, M. Higgins, C. Tuck, M. Popa, M.M. Safont, P. Gelebart, Z. Fandalyuk, A.M. Thompson, R. Svensson, A.-L. Gustavsson, L. Johansson, K. Färnegårdh, U. Yngve, A. Saleh, M. Haraldsson, A.C.A. D'Hollander, M. Franco, Y. Zhao, M. Håkansson, B. Walse, K. Larsson, E.M. Peat, V. Pelechano, J. Lunec, B. Vojtesek, M. Carmena, W.C. Earnshaw, A.R. McCarthy, N.J. Westwood, M. Arsenian-Henriksson, D.P. Lane, R. Bhatia, E. McCormack, S. Laín, A DHODH inhibitor increases p53 synthesis and enhances tumor cell killing by p53 degradation blockage, Nat. Commun. 9 (2018) 1107, https://doi.org/10.1038/s41467-018-03441-3.

[11] M. Koundinya, J. Sudhalter, A. Courjaud, B. Lionne, G. Touyer, L. Bonnet, I. Menguy, I. Schreiber, C. Perrault, S. Vougier, B. Benhamou, B. Zhang, T. He, Q. Gao, P. Gee, D. Simard, M.P. Castaldi, R. Tomlinson, S. Reiling, M. Barrague, R. Newcombe, H. Cao, Y. Wang, F. Sun, J. Murtie, M. Munson, E. Yang, D. Harper, M. Bouaboula, J. Pollard, C. Grepin, C. Garcia-Echeverria, H. Cheng, F. Adrian, C. Winter, S. Licht, I. Cornella-Taracido, R. Arrebola, A. Morris, Dependence on the pyrimidine biosynthetic enzyme DHODH is a synthetic lethal vulnerability in mutant KRAS-driven cancers, Cell Chem. Biol. 25 (2018) 705–717, https://doi.org/10.1016/j.chembiol.2018.03.005, e11.

[12] M. Bajzikova, J. Kovarova, A.R. Coelho, S. Boukalova, S. Oh, K. Rohlenova, D. Svec, S. Hubackova, B. Endaya, K. Judasova, A. Bezawork-Geleta, K. Kluckova, L. Chatre, R. Zobalova, A. Novakova, K. Vanova, Z. Ezrova, G.J. Maghzal, S. Magalhaes Novais, M. Olsinova, L. Krobova, Y.J. An, E. Davidova, Z. Nahacka, M. Sobol, T. Cunha-Oliveira, C. Sandoval-Acuña, H. Strnad, T. Zhang, T. Huynh, T.L. Serafim, P. Hozak, V.A. Sardao, W.J.H. Koopman, M. Ricchetti, P.J. Oliveira, F. Kolar, M. Kubista, J. Truksa, K. Dvorakova-Hortova, K. Pacak, R. Gurlich, R. Stocker, Y. Zhou, M.V. Berridge, S. Park, L. Dong, J. Rohlena, J. Neuzil, Reactivation of dihydroorotate dehydrogenase-driven pyrimidine biosynthesis restores tumor growth of respiration-deficient cancer cells, Cell Metabol. 29 (2019) 399–416, https://doi.org/10.1016/j.cmet.2018.10.014, e10.

[13] X. Wang, K. Yang, Q. Wu, L.J.Y. Kim, A.R. Morton, R.C. Gimple, B.C. Prager, Y. Shi, W. Zhou, S. Bhargava, Z. Zhu, L. Jiang, W. Tao, Z. Qiu, L. Zhao, G. Zhang, X. Li, S. Agnihotri, P.S. Mischel, S.C. Mack, S. Bao, J.N. Rich, Targeting pyrimidine synthesis accentuates molecular therapy response in glioblastoma stem cells, Sci. Transl. Med. 11 (2019), https://doi.org/10.1126/scitranslmed.aau4972.

[14] M. Hosseini, L. Dousset, P. Michon, W. Mahfouf, E. Muzotte, V. Bergeron, D. Bortolotto, R. Rossignol, F. Moisan, A. Taieb, A.-K. Bouzier-Sore, H.R. Rezvani, UVB-induced DHODH upregulation, which is driven by STAT3, is a promising target for chemoprevention and combination therapy of photocarcinogenesis, Oncogenesis 8 (2019) 52, https://doi.org/10.1038/s41389-019-0161-z.

[15] S. Christian, C. Merz, L. Evans, S. Gradl, H. Seidel, A. Friberg, A. Eheim, P. Lejeune, K. Brzezinka, K. Zimmermann, S. Ferrara, H. Meyer, R. Lesche, D. Stoeckigt, M. Bauser, A. Haegebarth, D.B. Sykes, D.T. Scadden, J.-A. Losman, A. Janzer, The novel dihydroorotate dehydrogenase (DHODH) inhibitor BAY 2402234 triggers differentiation and is effective in the treatment of myeloid malignancies, Leukemia 33 (10) (2019) 2403–2415, https://doi.org/10.1038/s41375-019-0461-5.

[16] L. Cao, M. Weetall, C. Trotta, K. Cintron, J. Ma, M.J. Kim, B. Furia, C. Romfo, J.D. Graci, W. Li, J. Du, J. Sheedy, J. Hedrick, N. Risher, S. Yeh, H. Qi, T. Arasu, S. Hwang, W. Lennox, R. Kong, J. Petruska, Y.-C. Moon, J. Babiak, T.W. Davis, A. Jacobson, N.G. Almstead, A. Branstrom, J.M. Colacino, S.W. Peltz, Targeting of hematologic malignancies with PTC299, A novel potent inhibitor of dihydroorotate dehydrogenase with favorable pharmaceutical properties, Mol. Cancer Ther. 18 (2019) 3–16, https://doi.org/10.1158/1535-7163.MCT-18-0863.

[17] A. Bonavia, M. Franti, E. Pusateri Keaney, K. Kuhen, M. Seepersaud, B. Radetich, J. Shao, A. Honda, J. Dewhurst, K. Balabanis, J. Monroe, K. Wolff, C. Osborne, L. Lanieri, K. Hoffmaster, J. Amin, J. Markovits, M. Broome, E. Skuba, I. Cornella-Taracido, G. Joberty, T. Bouwmeester, L. Hamann, J.A. Tallarico, R. Tommasi, T. Compton, S.M. Bushell, Identification of broad-spectrum antiviral compounds and assessment of the druggability of their target for efficacy against respiratory syncytial virus (RSV), Proc. Natl. Acad. Sci. U.S.A. 108 (2011) 6739–6744, https://doi.org/10.1073/pnas.1017142108.

[18] Q.-Y. Wang, S. Bushell, M. Qing, H.Y. Xu, A. Bonavia, S. Nunes, J. Zhou, M.K. Poh, P. Florez de Sessions, P. Niyomrattanakit, H. Dong, K. Hoffmaster, A. Goh, S. Nilar, W. Schul, S. Jones, L. Kramer, T. Compton, P.-Y. Shi, Inhibition of

dengue virus through suppression of host pyrimidine biosynthesis, J. Virol. 85 (2011) 6548–6556, https://doi.org/10.1128/JVI.02510-10.
[19] H.-H. Hoffmann, A. Kunz, V.A. Simon, P. Palese, M.L. Shaw, Broad-spectrum antiviral that interferes with de novo pyrimidine biosynthesis, Proc. Natl. Acad. Sci. U.S.A. 108 (2011) 5777–5782, https://doi.org/10.1073/pnas.1101143108.
[20] M. Marschall, I. Niemann, K. Kosulin, A. Bootz, S. Wagner, T. Dobner, T. Herz, B. Kramer, J. Leban, D. Vitt, T. Stamminger, C. Hutterer, S. Strobl, Assessment of drug candidates for broad-spectrum antiviral therapy targeting cellular pyrimidine biosynthesis, Antivir. Res. 100 (2013) 640–648, https://doi.org/10.1016/j.antiviral.2013.10.003.
[21] C.-F. Yang, B. Gopula, J.-J. Liang, J.-K. Li, S.-Y. Chen, Y.-L. Lee, C.S. Chen, Y.-L. Lin, Novel AR-12 derivatives, P12-23 and P12-34, inhibit flavivirus replication by blocking host de novo pyrimidine biosynthesis, Emerg. Microb. Infect. 7 (2018) 187, https://doi.org/10.1038/s41426-018-0191-1.
[22] N.N. Cheung, K.K. Lai, J. Dai, K.H. Kok, H. Chen, K.-H. Chan, K.-Y. Yuen, R.Y.T. Kao, Broad-spectrum inhibition of common respiratory RNA viruses by a pyrimidine synthesis inhibitor with involvement of the host antiviral response, J. Gen. Virol. 98 (2017) 946–954, https://doi.org/10.1099/jgv.0.000758.
[23] F. Zeng, L. Quan, G. Yang, T. Qi, L. Zhang, S. Li, H. Li, L. Zhu, X. Xu, Structural optimization and structure-activity relationship of 4-thiazolidinone derivatives as novel inhibitors of human dihydroorotate dehydrogenase, Mol. Basel Switz. 24 (2019), https://doi.org/10.3390/molecules24152780.
[24] T. Zeng, Z. Zuo, Y. Luo, Y. Zhao, Y. Yu, Q. Chen, A novel series of human dihydroorotate dehydrogenase inhibitors discovered by in vitro screening: inhibition activity and crystallographic binding mode, FEBS Open Bio 9 (2019) 1348–1354, https://doi.org/10.1002/2211-5463.12658.
[25] V.K. Vyas, G. Qureshi, D. Oza, H. Patel, K. Parmar, P. Patel, M.D. Ghate, Synthesis of 2-,4,-6-, and/or 7-substituted quinoline derivatives as human dihydroorotate dehydrogenase (hDHODH) inhibitors and anticancer agents: 3D QSAR-assisted design, Bioorg. Med. Chem. Lett 29 (2019) 917–922, https://doi.org/10.1016/j.bmcl.2019.01.038.
[26] S. Sainas, A.C. Pippione, E. Lupino, M. Giorgis, P. Circosta, V. Gaidano, P. Goyal, D. Bonanni, B. Rolando, A. Cignetti, A. Ducime, M. Andersson, M. Järvå, R. Friemann, M. Piccinini, C. Ramondetti, B. Buccinnà, S. Al-Karadaghi, D. Boschi, G. Saglio, M.L. Lolli, Targeting myeloid differentiation using potent 2-hydroxypyrazolo[1,5- a]pyridine scaffold-based human dihydroorotate dehydrogenase inhibitors, J. Med. Chem. 61 (2018) 6034–6055, https://doi.org/10.1021/acs.jmedchem.8b00373.
[27] J.T. Madak, C.R. Cuthbertson, Y. Miyata, S. Tamura, E.M. Petrunak, J.A. Stuckey, Y. Han, M. He, D. Sun, H.D. Showalter, N. Neamati, Design, synthesis, and biological evaluation of 4-quinoline carboxylic acids as inhibitors of dihydroorotate dehydrogenase, J. Med. Chem. 61 (2018) 5162–5186, https://doi.org/10.1021/acs.jmedchem.7b01862.
[28] M. Hosseini, L. Dousset, W. Mahfouf, M. Serrano-Sanchez, I. Redonnet-Vernhet, S. Mesli, Z. Kasraian, E. Obre, M. Bonneu, S. Claverol, M. Vlaski, Z. Ivanovic, W. Rachidi, T. Douki, A. Taieb, A.-K. Bouzier-Sore, R. Rossignol, H.R. Rezvani, Energy metabolism rewiring precedes UVB-induced primary skin tumor formation, Cell Rep. 23 (2018) 3621–3634, https://doi.org/10.1016/j.celrep.2018.05.060.
[29] T. Li, Z.J. Chen, The cGAS-cGAMP-STING pathway connects DNA damage to inflammation, senescence, and cancer, J. Exp. Med. 215 (2018) 1287–1299, https://doi.org/10.1084/jem.20180139.
[30] B.S. Parker, J. Rautela, P.J. Hertzog, Antitumour actions of interferons: implications for cancer therapy, Nat. Rev. Cancer 16 (2016) 131–144, https://doi.org/10.1038/nrc.2016.14.
[31] R. Harvey, K. Brown, Q. Zhang, M. Gartland, L. Walton, C. Talarico, W. Lawrence, D. Selleseth, N. Coffield, J. Leary, K. Moniri, S. Singer, J. Strum, K. Gudmundsson, K. Biron, K.R. Romines, P. Sethna, GSK983: a novel compound with broad-spectrum antiviral activity, Antivir. Res. 82 (2009) 1–11, https://doi.org/10.1016/j.antiviral.2008.12.015.
[32] M. Lucas-Hourani, D. Dauzonne, P. Jorda, G. Cousin, A. Lupan, O. Helynck, G. Caignard, G. Janvier, G. André-Leroux, S. Khiar, N. Escriou, P. Desprès, Y. Jacob, H. Munier-Lehmann, F. Tangy, P.-O. Vidalain, Inhibition of pyrimidine biosynthesis pathway suppresses viral growth through innate immunity, PLoS Pathog. 9 (2013), e1003678, https://doi.org/10.1371/journal.ppat.1003678.
[33] M. Lucas-Hourani, H. Munier-Lehmann, F. El Mazouni, N.A. Malmquist, J. Harpon, E.P. Coutant, S. Guillou, O. Helynck, A. Noel, A. Scherf, M.A. Phillips, F. Tangy, P.-O. Vidalain, Y.L. Janin, Original 2-(3-alkoxy-1H-pyrazol-1-yl) azines inhibitors of human dihydroorotate dehydrogenase (DHODH), J. Med. Chem. 58 (2015) 5579–5598, https://doi.org/10.1021/acs.jmedchem.5b00606.
[34] K.L. Yeo, Y.-L. Chen, H.Y. Xu, H. Dong, Q.-Y. Wang, F. Yokokawa, P.-Y. Shi, Synergistic suppression of dengue virus replication using a combination of nucleoside analogs and nucleoside synthesis inhibitors, Antimicrob. Agents Chemother. 59 (2015) 2086–2093, https://doi.org/10.1128/AAC.04779-14.
[35] Y. Wang, W. Wang, L. Xu, X. Zhou, E. Shokrollahi, K. Felczak, L.J.W. van der Laan, K.W. Pankiewicz, D. Sprengers, N.J.H. Raat, H.J. Metselaar, M.P. Peppelenbosch, Q. Pan, Cross talk between nucleotide synthesis pathways with cellular immunity in constraining hepatitis E virus replication, Antimicrob. Agents Chemother. 60 (2016) 2834–2848, https://doi.org/10.1128/AAC.02700-15.
[36] D.-H. Chung, J.E. Golden, R.S. Adcock, C.E. Schroeder, Y.-K. Chu, J.B. Sotsky, D.E. Cramer, P.M. Chilton, C. Song, M. Anantpadma, R.A. Davey, A.I. Prodhan, X. Yin, X. Zhang, Discovery of a broad-spectrum antiviral compound that inhibits pyrimidine biosynthesis and establishes a type 1 interferon-independent antiviral state, Antimicrob. Agents Chemother. 60 (2016) 4552–4562, https://doi.org/10.1128/AAC.00282-16.
[37] E. Pery, A. Sheehy, N. Miranda Nebane, V. Misra, M.K. Mankowski, L. Rasmussen, E. Lucile White, R.G. Ptak, D. Gabuzda, Redoxal, an inhibitor of de novo pyrimidine biosynthesis, augments APOBEC3G antiviral activity against human immunodeficiency virus type 1, Virology 484 (2015) 276–287, https://doi.org/10.1016/j.virol.2015.06.014.
[38] M. Lucas-Hourani, D. Dauzonne, H. Munier-Lehmann, S. Khiar, S. Nisole, J. Dairou, O. Helynck, P.V. Afonso, F. Tangy, P.-O. Vidalain, Original chemical series of pyrimidine biosynthesis inhibitors that boost the antiviral interferon response, Antimicrob. Agents Chemother. 61 (2017), https://doi.org/10.1128/AAC.00383-17.
[39] K. Lee, D.-E. Kim, K.-S. Jang, S.-J. Kim, S. Cho, C. Kim, Gemcitabine, a broad-spectrum antiviral drug, suppresses enterovirus infections through innate immunity induced by the inhibition of pyrimidine biosynthesis and nucleotide depletion, Oncotarget 8 (2017) 115315–115325, https://doi.org/10.18632/oncotarget.23258.
[40] P. Luthra, J. Naidoo, C.A. Pietzsch, S. De, S. Khadka, M. Anantpadma, C.G. Williams, M.R. Edwards, R.A. Davey, A. Bukreyev, J.M. Ready, C.F. Basler, Inhibiting pyrimidine biosynthesis impairs Ebola virus replication through depletion of nucleoside pools and activation of innate immune responses, Antivir. Res. 158 (2018) 288–302, https://doi.org/10.1016/j.antiviral.2018.08.012.
[41] J. Zhou, D. Wang, B.H.-Y. Wong, C. Li, V.K.-M. Poon, L. Wen, X. Zhao, M.C. Chiu, X. Liu, Z. Ye, S. Yuan, K.-H. Sze, J.F.-W. Chan, H. Chu, K.K.-W. To, K.Y. Yuen, Identification and characterization of GLDC as host susceptibility gene to severe influenza, EMBO Mol. Med. 11 (2019), https://doi.org/10.15252/emmm.201809528.
[42] J. Costeira-Paulo, J. Gault, G. Popova, M.J.G.W. Ladds, I.M.M. van Leeuwen, M. Sarr, A. Olsson, D.P. Lane, S. Laín, E.G. Marklund, M. Landreh, Lipids shape the electron acceptor-binding site of the peripheral membrane protein dihydroorotate dehydrogenase, Cell Chem. Biol. 25 (2018) 309–317, https://doi.org/10.1016/j.chembiol.2017.12.012, e4.
[43] A. Hovhannisyan, T.H. Pham, D. Bouvier, L. Qin, G. Melikyan, M. Reboud-Ravaux, M. Bouvier-Durand, C1 and N5 derivatives of cerpegin: synthesis of a new series based on structure-activity relationships to optimize their inhibitory effect on 20S proteasome, Bioorg. Med. Chem. Lett 23 (2013) 2696–2703, https://doi.org/10.1016/j.bmcl.2013.02.079.
[44] A. Hovhannisyan, T.H. Pham, D. Bouvier, A. Piroyan, L. Dufau, L. Qin, Y. Cheng, G. Melikyan, M. Reboud-Ravaux, M. Bouvier-Durand, New C(4)- and C(1)-derivatives of furo[3,4-c]pyridine-3-ones and related compounds: evidence for site-specific inhibition of the constitutive proteasome and its immunoisoform, Bioorg. Med. Chem. Lett 24 (2014) 1571–1580, https://doi.org/10.1016/j.bmcl.2014.01.072.
[45] T.H. Pham, A. Hovhannisyan, D. Bouvier, L. Tian, M. Reboud-Ravaux, G. Melikyan, M. Bouvier-Durand, A new series of N5 derivatives of the 1,1,5-trimethyl furo[3,4-c]pyridine-3,4-dione (cerpegin) selectively inhibits the post-acid activity of mammalian 20S proteasomes, Bioorg. Med. Chem. Lett 22 (2012) 3822–3827, https://doi.org/10.1016/j.bmcl.2012.03.105.
[46] D. Villemin, N. Cheikh, L. Liao, N. Bar, J.-F. Lohier, J. Sopkova, N. Choukchou-Braham, B. Mostefa-Kara, Two versatile routes towards Cerpegin and analogues: applications of a one pot reaction to new analogues of Cerpegin, Tetrahedron 68 (2012) 4906–4918, https://doi.org/10.1016/j.tet.2012.03.057.
[47] D.J. Diller, K.M. Merz, High throughput docking for library design and library prioritization, Proteins 43 (2001) 113–124.
[48] S. Hayek, N. Bekaddour, L. Besson, R. Alves de Sousa, N. Pietrancosta, S. Viel, N. Smith, Y. Jacob, S. Nisole, R. Mandal, D.S. Wishart, T. Walzer, J.-P. Herbeuval, P.-O. Vidalain, Identification of primary natural killer cell modulators by chemical library screening with a luciferase-based functional assay, SLAS Discov. Adv. Life Sci. R D. 24 (2019) 25–37, https://doi.org/10.1177/2472555218797078.
[49] X. Deng, S. Kokkonda, F. El Mazouni, J. White, J.N. Burrows, W. Kaminsky, S.A. Charman, D. Matthews, P.K. Rathod, M.A. Phillips, Fluorine modulates species selectivity in the triazolopyrimidine class of Plasmodium falciparum dihydroorotate dehydrogenase inhibitors, J. Med. Chem. 57 (2014) 5381–5394, https://doi.org/10.1021/jm500481t.
[50] L.R. McLean, Y. Zhang, W. Degnen, J. Peppard, D. Cabel, C. Zou, J.T. Tsay, A. Subramaniam, R.J. Vaz, Y. Li, Discovery of novel inhibitors for DHODH via virtual screening and X-ray crystallographic structures, Bioorg. Med. Chem. Lett 20 (2010) 1981–1984, https://doi.org/10.1016/j.bmcl.2010.01.115.
[51] F. Coquel, C. Neumayer, Y.-L. Lin, P. Pasero, SAMHD1 and the innate immune response to cytosolic DNA during DNA replication, Curr. Opin. Immunol. 56 (2018) 24–30, https://doi.org/10.1016/j.coi.2018.09.017.
[52] F. Coquel, M.-J. Silva, H. Técher, K. Zadorozhny, S. Sharma, J. Nieminuszczy, C. Mettling, E. Dardillac, A. Barthe, A.-L. Schmitz, A. Promonet, A. Cribier, A. Sarrazin, W. Niedzwiedz, B. Lopez, V. Costanzo, L. Krejci, A. Chabes, M. Benkirane, Y.-L. Lin, P. Pasero, SAMHD1 acts at stalled replication forks to prevent interferon induction, Nature 557 (2018) 57–61, https://doi.org/10.1038/s41586-018-0050-1.
[53] J. Lee, W.G. Dunphy, The Mre11-Rad50-Nbs1 (MRN) complex has a specific role in the activation of Chk1 in response to stalled replication forks, Mol. Biol. Cell 24 (2013) 1343–1353, https://doi.org/10.1091/mbc.E13-01-0025.
[54] T. Herz, K. Wolf, J. Kraus, B. Kramer, 4SCan/vADME: intelligent library screening as a shortcut from hits to lead compounds, Expert Opin. Drug

Please cite this article as: S. Hayek et al., Cerpegin-derived furo[3,4-*c*]pyridine-3,4(1*H*,5*H*)-diones enhance cellular response to interferons by *de novo* pyrimidine biosynthesis inhibition, European Journal of Medicinal Chemistry, https://doi.org/10.1016/j.ejmech.2019.111855

Metabol. Toxicol. 2 (2006) 471–484, https://doi.org/10.1517/17425255.2.3.471.
[55] Y. Diao, W. Lu, H. Jin, J. Zhu, L. Han, M. Xu, R. Gao, X. Shen, Z. Zhao, X. Liu, Y. Xu, J. Huang, H. Li, Discovery of diverse human dihydroorotate dehydrogenase inhibitors as immunosuppressive agents by structure-based virtual screening, J. Med. Chem. 55 (2012) 8341–8349, https://doi.org/10.1021/jm300630p.
[56] V.K. Vyas, M. Ghate, Development of docking-based 3D QSAR models for the design of substituted quinoline derivatives as human dihydroorotate dehydrogenase (hDHODH) inhibitors, SAR QSAR, Environ. Res. 24 (2013) 625–645, https://doi.org/10.1080/1062936X.2013.792871.
[57] M. Sucharita, B. Poorani, P. Swaminathan, An insilico workflow that yields experimentally comparable inhibitors for human DiHydroOrotate DeHydrogenase, Curr. Comput. Aided Drug Des. (2019), https://doi.org/10.2174/1573409915666190528114703.
[58] I. Fritzson, B. Svensson, S. Al-Karadaghi, B. Walse, U. Wellmar, U.J. Nilsson, D. da Graça Thrige, S. Jönsson, Inhibition of human DHODH by 4-hydroxycoumarins, fenamic acids, and N-(alkylcarbonyl)anthranilic acids identified by structure-guided fragment selection, ChemMedChem 5 (2010) 608–617, https://doi.org/10.1002/cmdc.200900454.
[59] M. Frontini, M. Vijayakumar, A. Garvin, N. Clarke, A ChIP-chip approach reveals a novel role for transcription factor IRF1 in the DNA damage response, Nucleic Acids Res. 37 (2009) 1073–1085, https://doi.org/10.1093/nar/gkn1051.
[60] M. Abou El Hassan, K. Huang, Z. Xu, T. Yu, R. Bremner, Frequent interferon regulatory factor 1 (IRF1) binding at remote elements without histone modification, J. Biol. Chem. 293 (2018) 10353–10362, https://doi.org/10.1074/jbc.RA118.002889.
[61] D. Dornan, M. Eckert, M. Wallace, H. Shimizu, E. Ramsay, T.R. Hupp, K.L. Ball, Interferon regulatory factor 1 binding to p300 stimulates DNA-dependent acetylation of p53, Mol. Cell. Biol. 24 (2004) 10083–10098, https://doi.org/10.1128/MCB.24.22.10083-10098.2004.
[62] M.R. Zaidi, G. Merlino, The two faces of interferon-γ in cancer, Clin. Cancer Res. Off. J. Am. Assoc. Cancer Res. 17 (2011) 6118–6124, https://doi.org/10.1158/1078-0432.CCR-11-0482.

Please cite this article as: S. Hayek et al., Cerpegin-derived furo[3,4-*c*]pyridine-3,4(1*H*,5*H*)-diones enhance cellular response to interferons by *de novo* pyrimidine biosynthesis inhibition, European Journal of Medicinal Chemistry, https://doi.org/10.1016/j.ejmech.2019.111855

Article 6

Cytokine 144 (2021) 155533

Contents lists available at ScienceDirect

Cytokine

journal homepage: www.elsevier.com/locate/cytokine

Differential levels of IFNα subtypes in autoimmunity and viral infection

Vincent Bondet [a], Mathieu P. Rodero [b], Céline Posseme [a,c], Pierre Bost [d,e], Jérémie Decalf [a], Liis Haljasmägi [f], Nassima Bekaddour [b], Gillian I. Rice [l,m], Vinit Upasani [h], Jean-Philippe Herbeuval [b], John A. Reynolds [g,i,j,k], Tracy A. Briggs [l,m], Ian N. Bruce [g,i], Claudia Mauri [n], David Isenberg [n], Madhvi Menon [n,t], David Hunt [o], Benno Schwikowski [d,e], Xavier Mariette [p], Stanislas Pol [q], Flore Rozenberg [r], Tineke Cantaert [h], J. Eric Gottenberg [s], Kai Kisand [f], Darragh Duffy [a,*]

[a] Translational Immunology Lab, Institut Pasteur, Paris, France
[b] Chimie & Biologie, Modélisation et Immunologie pour la Thérapie (CBMIT), Université de Paris, CNRS, UMR8601, Paris, France
[c] Frontiers of Innovation in Research and Education PhD program, CRI doctoral school, Université de Paris, Paris 75005, France
[d] Systems Biology Group, Department of Computational Biology and USR 3756, Institut Pasteur and CNRS, Paris 75015, France
[e] Sorbonne Universite, Complexite du vivant, Paris 75005, France
[f] Molecular Pathology, Institute of Biomedicine and Translational Medicine, University of Tartu, Tartu, Estonia
[g] Centre for Musculoskeletal Research, Division of Musculoskeletal and Dermatological Sciences, School of Biological Sciences, University of Manchester, Manchester, UK
[h] Immunology Unit, Institut Pasteur du Cambodge, Institut Pasteur International Network, Phnom Penh, Cambodia
[i] NIHR Manchester Biomedical Research Centre, Manchester University NHS Foundation Trust, Manchester Academic Health Science Centre, The University of Manchester, Manchester, UK
[j] Rheumatology Research Group, Institute of Inflammation and Ageing, College of Medical and Dental Sciences, University of Birmingham, Birmingham, UK
[k] Rheumatology Department, Sandwell and West Birmingham NHS Trust, Birmingham, UK
[l] Division of Evolution and Genomic Sciences, School of Biological Sciences, University of Manchester, Manchester, UK
[m] Manchester Centre for Genomic Medicine, St Mary's Hospital, Manchester University Hospitals NHS Foundation Trust, Manchester, UK
[n] Centre for Rheumatology Research, Division of Medicine, University College of London, London WC1E 6JF, UK
[o] Centre for Genomic and Experimental Medicine, Medical Research Council Institute of Genetics and Molecular Medicine, The University of Edinburgh, Edinburgh, UK
[p] Rheumatology, Université Paris-Saclay, Assistance Publique–Hôpitaux de Paris (AP-HP), Hôpital Bicêtre, INSERM UMR1184, Le Kremlin-Bicetre, France
[q] Unite d'Hépatologie, Assistance Publique–Hopitaux de Paris (AP-HP), Hopital Cochin, Paris, France
[r] Department of Virology, APHP-CUP, Université de Paris, Paris, France
[s] Faculté de Médecine de l'Université de Strasbourg, Strasbourg, France
[t] Lydia Becker Institute of Immunology and Inflammation, Division of Infection, Immunity & Respiratory Medicine, School of Biological Sciences, University of Manchester, UK

ARTICLE INFO

Keywords:
IFNα subtypes
TLR activation
IFN function
Anti-IFNα autoantibodies
Viral infection
Autoimmunity

ABSTRACT

Type I interferons are essential for host response to viral infections, while dysregulation of their response can result in autoinflammation or autoimmunity. Among IFNα (alpha) responses, 13 subtypes exist that signal through the same receptor, but have been reported to have different effector functions. However, the lack of available tools for discriminating these closely related subtypes, in particular at the protein level, has restricted the study of their differential roles in disease. We developed a digital ELISA with specificity and high sensitivity for the IFNα2 subtype. Application of this assay, in parallel with our previously described pan-IFNα assay, allowed us to study different IFNα protein responses following cellular stimulation and in diverse patient cohorts. We observed different ratios of IFNα protein responses between viral infection and autoimmune patients. This analysis also revealed a small percentage of autoimmune patients with high IFNα2 protein measurements but low pan-IFNα measurements. Correlation with an ISG score and functional activity showed that in this small sub group of patients, IFNα2 protein measurements did not reflect its biological activity. This unusual phenotype was partly explained by the presence of anti-IFNα auto-antibodies in a subset of autoimmune patients. This study reports ultrasensitive assays for the study of IFNα proteins in patient samples and highlights the insights that can be obtained from the use of multiple phenotypic readouts in translational and clinical studies.

* Corresponding author at: Translational Immunology Lab, Institut Pasteur, 25, rue du Dr. Roux, 75724 Paris Cedex 15, France.
E-mail address: darragh.duffy@pasteur.fr (D. Duffy).

https://doi.org/10.1016/j.cyto.2021.155533
Received 3 February 2021; Received in revised form 30 March 2021; Accepted 31 March 2021
Available online 30 April 2021
1043-4666/© 2021 The Author(s). Published by Elsevier Ltd. This is an open access article under the CC BY license (http://creativecommons.org/licenses/by/4.0/).

1. Introduction

Type I interferons are essential for host responses to viral infections [1]. Their dysregulation is also implicated in many autoimmune diseases, such as systemic lupus erythematosus (SLE) and primary Sjögren's syndrome (pSS) [2], while their exact role in bacterial infection remains unclear [3]. Within the type I interferon class there are 9 types; IFNα (alpha), IFNβ (beta), IFNκ (kappa), IFNω (omega), IFNδ (delta), IFNε (epsilon), IFNτ (tau), IFNζ (zeta) and IFNν (nu) (IFNδ/τ/ζ/ν not found in humans) that all signal through the IFNAR receptor complex [4]. Furthermore, within the IFNα types there are 13 subtypes that exhibit marked evolutionary differences in terms of selective conservation, suggesting different immunological relevance [5].

Some studies have reported differential functions, at least in terms of anti-viral responses [6–9], but much remains unknown in terms of broader differential activity between the different IFNα subtypes. Furthermore, in autoimmunity, the potential role of different IFNα subtypes is even less clear, despite their strong implication in the pathogenesis of many such diseases [10]. Such studies have been restricted by the high level of sequence homology among the different subtypes, as well as the lack of tools to study them, in particular at the protein level. Indeed, until recently, IFNα protein was challenging to directly measure in human samples, with interferon stimulated genes (ISG) or functional activity used as proxy readouts. This limitation was overcome with the application of Simoa digital ELISA [11], and the use of unique monoclonal antibodies isolated from APECED patients [12] that enabled the detection of all IFNα protein subtypes with more or less equivalent and high sensitivity [13]. Direct measurement of the protein allowed us to identify the cellular sources of pathological IFNα in patients with STING mutations and juvenile dermatomyositis, to be circulating monocytes and pDCs [13] and tissue myoblasts [14], respectively. In contrast in active TB infection, we demonstrated an absence of plasma IFN-I [15], suggesting that the widely reported blood ISG signature most likely reflects signaling in the infected tissue [3].

In this study we adapted the digital ELISA using commercial antibodies specific for IFNα2 and used both assays to study autoimmune and infected patient cohorts. While both assays correlated well in the majority of patients, discrepancies between the two were observed which revealed interesting clinical observations. In particular, the balance between the results obtained using the two assays was modified by the presence of autoantibodies in some patients and the nature of the TLR that was activated. This provides a starting point for beginning to dissect potential different roles of IFNα subtypes in human disease.

2. Materials and methods

2.1. Patient cohorts

Patients were not specifically enrolled for this study, all quantifications were done on samples from existing clinical cohorts that were previously described: Rodero *et al.* [13], Reynolds *et al.* (LEAP cohort) [16], Bost *et al.* (In review) (ASSESS cohort), Menon *et al.* (In preparation), Sultanik *et al.* [17] (C10-08 cohort) and Upasani *et al.* [18].

The Rodero *et al.* (2017) cohort includes patients with systemic lupus erythematosus (SLE), juvenile SLE (JSLE), connective tissue disease (CTD), retinal vasculopathy with cerebral leukodystrophy (RVCL), juvenile dermatomyositis (JDM), monogenic interferonopathies (MI), and central nervous system (CNS) infections. All samples were collected with informed consent. The study was approved by the Leeds (East) Research Ethics Committee (reference number 10/H1307/132), by the Comité de Protection des Personnes (ID-RCB/EUD RACT:2014-A01017-40), and by the South-East Scotland Research Ethics Committee (0114/SS/0003).

The Lupus Extended Autoimmune Phenotype (LEAP) cohort includes patients with systemic lupus erythematosus (SLE), primary Sjögren's syndrome (pSS), undifferentiated connective tissue disease (UCTD), mixed connective tissue disease (MCTD), systemic sclerosis (SSc) and idiopathic inflammatory myopathies (IIM). Patients were recruited from Manchester University NHS Foundation Trust and Salford Royal NHS Foundation Trust. Ethical approval was obtained from the Greater Manchester East Research Ethics Committee (13/NW/0564).

The ASSESS national multi-center prospective cohort (Assessment of Systemic complications and Evolution in Sjögren's Syndrome) was set up in 2006 thanks to a grant from the French Ministry of Health. Fifteen centers for autoimmune disease were established to recruit consecutive patients with primary Sjögren's syndrome fulfilling American-European Consensus Criteria (AECG) between 2006 and 2009. The study was approved by the Ethics Committee of Bichat Hospital in 2006. All patients gave their informed written consent. This study was followed for 5 years with the grant of the French Ministry of Health and this study will be extended for 20 years by the French Society of Rheumatology (SFR).

The Menon *et al.* (in preparation) cohort consists of serum samples from 476 SLE patients (mean age 46 ± 15 years, 40 male) recruited at the University College of London. 11 patients with high autoantibody values were studied longitudinally. The ethics committee of the University College London Hospitals National Health Service Trust approved this study. Patients were recruited after obtaining informed consent.

The C10-08 cHCV cohort (n = 88) were sampled as part of a prospective study (C10-08) sponsored by the Institut National de la Sante et de la Recherche Medicale (Inserm) and by the Agence Nationale de Recherche sur le Sida et les Hepatites Virales (ANRS-C10-08). Approval of the study was obtained from the French Comité de protection des personnes (CPP IDF II) in 2010, August 2nd, and all patients gave written informed consent. This cohort includes patients with chronic hepatitis C virus infection (genotype is 1 and 4) prior to treatment with either pegylated-IFNα and ribavirin or a direct acting anti-viral (boceprevir or telaprevir).

The Upasani *et al.* [18] cohort includes 115 children (≥2 years) who presented with dengue-like symptoms at the Kanta Bopha Hospital in Phnom Penh, Cambodia. Blood samples were obtained within 96 h of fever onset at hospital admittance. Plasmas were tested for presence of dengue virus using a nested RT-qPCR at the Institut Pasteur du Cambodge. Patients were classified according to the WHO 1997 severity criteria upon hospital discharge as dengue fever (DF), dengue haemorrhagic fever (DHF) and dengue shock syndrome (DSS). Ethical approval for the study was obtained from the National Ethics Committee of Health Research of Cambodia. Patients were recruited after obtaining written informed consent. The dengue cohort of this paper includes 56 of these 115 patients, randomly selected. The dengue cohort and the Upasani *et al.* [18] cohort are not statistically different in terms of age (median 10, IQR 6–12 vs median 9, IQR 5–11) and pan-alpha interferon concentrations (p = 0.536, Mann-Whitney test), and these two cohorts show similar percentages of female (48% vs 53), DF (82% vs 72), DHF (13% vs 17), DSS (5% vs 9), primary infection (25% vs 17) or secondary infection (75% vs 71) patients.

The viral CNS infection cohort (n = 18) includes all Rodero *et al.* [13] related patients whose diagnosis was mainly viral meningitis or viral encephalitis. Details are shown on Table S1.

For this study, samples were categorized based on clinical diagnosis and are summarized in Table 1. All SLE and JSLE samples from Rodero *et al.* [13] (n = 56) and LEAP cohorts (n = 39) were combined here to form the SLE cohort. All anti-IFNα positive and a randomly selected group of anti-IFNα negative SLE patients with a similar size (n = 111) were added from Menon *et al.* (in preparation) cohort to this SLE cohort (n = 206). All CTD samples from Rodero *et al.* [13] cohort (n = 19) and UCTD and MCTD samples from LEAP cohort (n = 33) were merged here to form the CTD cohort (n = 52). All pSS samples from LEAP cohort (n = 12) and all samples from ASSESS cohort (n = 380) were merged to form the pSS cohort (n = 392). Longitudinal SLE samples (n = 11) from Menon *et al.* (in preparation) study were studied in a different part. Patient numbers, gender and age are shown in Table 1 for each cohort.

Table 1
Demographic characteristics of each cohort. Patient number, gender, age and diagnosis for each cohort. Data are shown as the n (%) or median (IRQ). LEAP (lupus extended autoimmune phenotype) cohort: see Reynolds et al. [16]. Rodero et al. cohort: see reference 13. ASSESS (assessment of systemic complications (signs) and evolution in Sjögren's syndrome) cohort: see Bost et al. (In review). Menon et al. cohort: paper in preparation. C10-08 cohort: see Sultanik et al. [17]. Upasani et al. cohort: see reference 18. MCTD: mixed CTD. UCDT: undifferentiated CTD. pSS: primary Sjögren's syndrome. SLE: systemic lupus erythematosus. CTD: connective tissue disease. JSLE : juvenile SLE. CNS: central nervous system. cHCV: chronic hepatitis C virus infection. DF: dengue fever. DHF: dengue haemorrhagic fever. DSS: dengue shock syndrome.

Cohorts used in this study (patients included only):

Cohort	Patient number	Gender, female	Age	Diagnosis
LEAP	84	79 (94%)	49 (36–57)	MCTD: 6 (7%) UCTD: 27 (32%) pSS: 12 (14%) SLE: 39 (46%)
Rodero *et al.* (2017)	93	76 (82%)	42 (26–54)	CTD: 19 (20%) JSLE: 6 (6%) SLE: 50 (54%) Viral CNS infection: 18 (19%)
ASSESS	380	353 (93%)	59 (51–67)	pSS: 380 (100%)
Menon *et al.* (in preparation)	111	100 (90%)	53 (40–63)	SLE: 111 (100%)
C10-08	88	41 (47%)	58 (50–65)	cHCV: 88 (100%)
Upasani *et al.* (2020)	56	27 (48%)	10 (6–12)	DF: 46 (82%) DHF: 7 (13%) DSS : 3 (5%)

Clinical diagnosis cohorts:

Cohort	Patient number	Gender, female	Age
CTD	52	48 (92%)	48 (33–53)
pSS	392	365 (93%)	58 (51–67)
SLE	206	189 (92%)	50 (38–60)
cHCV	88	41 (47%)	58 (50–65)
Dengue	56	27 (48%)	10 (6–12)
Viral CNS infection	18	6 (33%)	2 (<1–31)

2.2. Healthy donors

Fresh whole blood was collected into sodium heparin tubes from healthy French volunteers enrolled at the Clinical Investigation and Access to BioResources (ICAReB) platform (Center for Translational Research, Institut Pasteur, Paris, France). These donors were part of the CoSImmGEn cohort (NCT03925272). The biobank activity of this platform is certified ISO 9001 and NFS 96–900. Written informed consent was obtained from all study participants. Fresh whole blood was diluted 1:3 with RPMI medium 1640 (1X) + GlutaMAX into 5 mL Polystyrene round-bottom tube. Diluted whole blood was either left without any stimulant to mimic the Null condition or stimulated with LPS (LPS-EB ultrapure InvivoGen) at the final concentration of 10 ng/mL, Poly(I:C) (HMW VacciGrade InvivoGen) at the final concentration of 20 μg/mL, R848 (Vaccigrade InvivoGen) at the final concentration of 1uM. Tubes were vortexed and incubated at 37 °C, 5% CO2 for 22 h. Supernatants were collected and stored at −20 °C until use.

2.3. pDC isolation and stimulation

Blood from healthy donors was obtained from "Etablissement Français du Sang" (convention # 07/CABANEL/106; Paris, France). Experimental procedures with human blood were done according to the European Union guidelines and the Declaration of Helsinki. Human peripheral blood mononuclear cells (PBMCs) were isolated by density centrifugation from peripheral blood leukocyte separation medium (STEMCELL Technologies). *In vitro* experiments were performed using human plasmacytoid dendritic cells (pDCs) purified from PBMCs by negative selection with the EasySep Human Plasmacytoid DC enrichment kit (STEMCELL Technologies). pDCs were cultured in RPMI 1640 (Invitrogen, Gaithersburg, MD) containing 10% heat-inactivated fetal bovine serum and 1 mM glutamine (Hyclone, Logan, UT). For stimulation experiments purified pDCs were seeded at 1×10^5/100 μL. Cells were stimulated for 16 h with the TLR7/TLR8 agonist Resiquimod (R848; Invivogen) at 5 μg/mL or the TLR4 agonist lipopolysaccharide (LPS; Invivogen) at 100 ng/mL or the TLR9 agonist class A CpG ODNs (CpG-A; Invivogen) at 5 μM or the STING agonist cGAMP (Invivogen) or the TLR3 agonist polyinosinic-polycytidylic acid (poly(I:C); Invivogen) at 5 ug/mL. Supernatants were then collected for IFNα detection.

2.4. Sample preparation for digital-ELISA assays

All serum and plasma samples were thawed and centrifugated at 10,000*g*, +4°C for 10 min. Supernatants were diluted in the Detector / Sample Diluent (Quanterix) for pan-IFNα or IFNα2 quantification, then incubated one hour at room temperature before analysis. Biological samples were diluted from 1/3 to 1/300 depending on the amount of material available and to avoid saturation. NP40 was added in the Detector / Sample Diluent used for cHCV, dengue or viral CNS infection samples at a final concentration of 0.5% (v/v) to inactivate viruses.

2.5. Calibrators and pure recombinant IFNα subtypes

Recombinant IFNα1, IFNα1(Val114), IFNα4a, IFNα4b, IFNα5, IFNα6, IFNα7, IFNα8, IFNα10, IFNα14, IFNα16, IFNα17, and IFNα21 were purchased from PBL Assay Science. Recombinant IFNα2c was purchased from eBioscience. Recombinant IFNβ, IFNλ1, IFNλ2, IFNω and IFNγ were purchased from PeproTech.

2.6. Pan-IFNα digital ELISA assay

The Simoa pan-IFNα assay was developed using the Quanterix Homebrew kit according to the manufacturer's instructions and using two autoantibodies specific for IFNα isolated and cloned from two APS1/APECED patients. The 8H1 antibody clone was used as a capture antibody after coating on paramagnetic beads (0.3 mg/mL), and the 12H5 was biotinylated (biotin/antibody ratio = 30/1) and used as the detector at a concentration of 0.3ug/mL. The SBG revelation enzyme concentration was 150 pM. Recombinant IFNα17 was used as calibrator. The limit of detection was calculated by the mean value of all blank runs + 2SD after log conversion. The assay is fully described in Rodero *et al.* [13] and a video presenting all the steps is shown in Llibre *et al* [19].

2.7. IFNα2 digital ELISA assay

The Simoa IFNα2 assay was also developed using the Quanterix Homebrew kit. The BMS216C (eBioscience) antibody clone was used as a capture antibody after coating on paramagnetic beads (0.3 mg/mL), and the BMS216BK already biotinylated antibody clone was used as the detector at a concentration of 0.3ug/mL. The SBG revelation enzyme concentration was 150 pM. Recombinant IFNα2c was used as calibrator. The limit of detection was calculated by the mean value of all blank runs + 2SD after log conversion.

2.8. ISG score determination

For SLE and CTD patients ISG score was calculated by qPCR as previously described using six ISG genes (Rice *et al.* [20]). Blood was collected in PAXgene tubes (PreAnalytix), and total RNA was extracted

using a PAXgene (PreAnalytix) RNA isolation kit. RNA concentration was assessed by fluorimetric analysis. After DNAse treatment, RNA was converted into cDNA with the High Capacity cDNA reverse transcriptase kit (Qiagen). Quantitative reverse transcription polymerase chain reaction (RT-qPCR) analysis was performed using the TaqMan Universal PCR Master Mix (Applied Biosystems) and cDNA derived from 40 ng total RNA. Using TaqMan probes for IFI27 (Hs01086370_m1), IFI44L (Hs00199115_m1), IFIT1 (Hs00356631_g1), ISG15 (Hs00192713_m1), RSAD2 (Hs01057264_m1), and SIG LEC1 (Hs00988063_m1), the relative abundance of each target transcript was normalized to the expression level of HPRT1 (Hs03929096_g1) and 18S (Hs999999001_s1) and assessed with the Applied Biosystems StepOne Software v2.1 and DataAssist Software v.3.01. For each of the six probes, individual (patient and control) data were expressed relative to a single calibrator (control C25). The median fold change of the six ISGs, when compared with the median of the combined 29 healthy controls, was used to create an IFN score for each patient. RQ is equal to $2^{-\Delta Ct}$ (i.e., the normalized fold change relative to a control). All patients were selected for this analysis, except the ASSESS ones for which the protocol was different.

For pSS patients the ISG-score was determined from microarray data. After validation of the RNA quality with Bioanalyzer 2100 (using Agilent RNA6000 nano chip kit), 75 ng of total RNA was reverse transcripted using the GeneChip® WT Plus Reagent Kit (Affymetrix) without globin mRNA reduction. Briefly, the resulting double-stranded cDNA was used for *in vitro* transcription with T7 RNA polymerase (all these steps are included in the WT cDNA synthesis and amplification kit of Affymetrix). After purification according to Affymetrix's protocol, 5.5 μg of Sens Target DNA were fragmented and biotin-labelled. After control of fragmentation using Bioanalyzer 2100, cDNA was then hybridized to GeneChip® Clariom S Human (Affymetrix) at 45 °C for 17 h. After overnight hybridization, chips were washed on the GeneChip Fluidics Station 450 following specific protocols (Affymetrix) and scanned using the GCS3000 7G. The scanned images were then analyzed with Expression Console software (Affymetrix) to obtain raw data (.cel files) and Quality Control metrics. Computational analyses were performed on R 3.4.3. Microarray data were loaded and normalised using the oligo package. Briefly .cel files were loaded using the read.celfiles() functions and normalised using the Robust Multi Array algorithm implemented in the rma() function with default parameters. Quality of data normalization was checked through visual inspection of intensity distribution across chips. Microarrays probes were annotated using the clariomshumanhttranscriptcluster.db package and if several probes were mapped to the same gene, the probe with the highest coefficient of variation was selected. Then, the ISG score for each patient was calculated as the median of normalized data available for the same genes, i.e. IFI27, IFI44L, IFIT1, ISG15, RSAD2 and SIG LEC1 as previously defined (Rice *et al.* [20]).

2.9. IFN-activity determination

Type I IFN activity was measured by determining the cytopathic reduction (i.e., protection of Madin–Darby bovine kidney (MDBK) cells against cell death after infection with vesicular stomatitis virus) afforded by patient serum. A reference of human IFNα, standardized against the National Institutes of Health reference Ga 023–902–530, was included with each titration. IFNα activity in normal healthy serum is < 2 IU/mL. Patients were selected randomly from the SLE, CTD and pSS cohorts to equilibrate the number of results in each cohort and at each IFNα17/α2c protein ratio (n = 113).

2.10. Competition assays

SLE patient plasma samples or pure recombinant IFNα subtypes were diluted with Detector / Sample Diluent (Quanterix) and preincubated with 50 μg/mL of the IFNα capture antibody 8H1 or BMS216C (eBioscience) for 30 min at room temperature before Simoa analysis.

2.11. Anti-IFNα autoantibodies quantification

Anti-IFNα (1,2,8,21) and anti-IFNα (4,5,6,7) quantifications were done in each LEAP SLE, LEAP CTD and ASSESS Sjögren's patients cohorts from a similar restricted number of samples, randomly selected (n = 113). Autoantibodies against IFNα were measured with luciferase based immunoprecipitation assay (LIPS) as described previously (Meyer *et al.*[12]). IFNA subtype sequences were cloned into modified pPK-CMV-F4 fusion vector (PromoCell GmbH, Germany) where Firefly luciferase was substituted in the plasmid for NanoLuc luciferase (Promega, USA), transfected to HEK293 cells and IFNα-luciferase fusion proteins collected with tissue culture supernatant. $1x10^6$ luminescence units (LU) of IFNα1, IFNα2, IFNα8 and IFNα21 fusion proteins were combined to one IP reaction (pool 1), and IFNα4, IFNα5, IFNα6 and IFNα7 fusion proteins to another (pool 2). Serum samples were incubated with Protein G Agarose beads (Exalpha Biologicals, USA) at room temperature for 1 h in 96-well microfilter plate (Merck Millipore, Germany) before the antigen mix was added for another hour. After washing the plate with vacuum system, Nano-Glo® Luciferase Assay Reagent was added (Promega, USA). Luminescence intensity was measured by VICTOR X Multilabel Plate Reader (PerkinElmer Life Sciences, USA). The results were expressed in arbitrary units (AU) representing fold over the mean of the negative control samples. The cut-off was set at 2.0 AU. Anti-IFNα8 and anti-IFNα2 quantifications were done for five patients with high autoantibody values studied longitudinally. The previous protocol was employed using only the IFNα8 and IFNα2 fusion proteins. Serial dilutions from serum samples were co-incubated with fixed concentrations of these antigens. IC50 was calculated based on the dose–response curve. This is the dilution factor that halves the signal or reduces IFN activity 50% from its maximum.

2.12. Statistical analyses

GraphPad Prism was used for statistical analysis. A Mann-Whitney test was used to test for differences induced by the two buffers used to treat samples. ANOVA tests (Kruskal–Wallis) with Dunn's post testing for multiple comparisons were used to test for differences between patients groups, or stimulation groups. *p < 0.05; **p < 0.01; ***p < 0.001; ****p < 0.0001. A Chi square test was used to characterize the differences between two distributions of results. For all analyses, p values<0.05 were considered statistically significant. Median and 95% confidence interval were reported. Spearman correlations are used to compare the two IFNα assays.

2.13. Data availability

All available patient data is shown in Supplementary Table S1.

3. Results

3.1. Comparison of IFNα2 and pan-IFNα digital ELISA assays

To enable the study of IFNα protein subtypes we developed a Simoa digital ELISA utilizing a monoclonal antibody (mAb) pair specific for IFNα2. This assay had a limit of detection (LOD) of 1 fg/mL and no cross-reactivity for IFNβ, IFNλ1, IFNλ2, IFNω, and IFNγ (Fig. 1a). This level of sensitivity, and lack of cross-reactivity, were similar to our previously described pan-IFNα Simoa assay that utilized mAbs isolated from APECED patients (Fig. 1b). We also tested the reactivity of the new IFNα2 assay for all 13 (and the natural variant IFNα1/Val114) IFNα subtypes which revealed differing levels of specificity, with the highest specificity for IFNα2 and IFNα6 (Fig. 1c). This was in contrast to pan-IFNα assay which has equally high specificity for all IFNα subtypes, with the exception of IFNα2 (Fig. 1d).

To explore this differential specificity between the two assays for the IFNα subtypes, we tested each of the 13 (and the natural variant IFNα1/

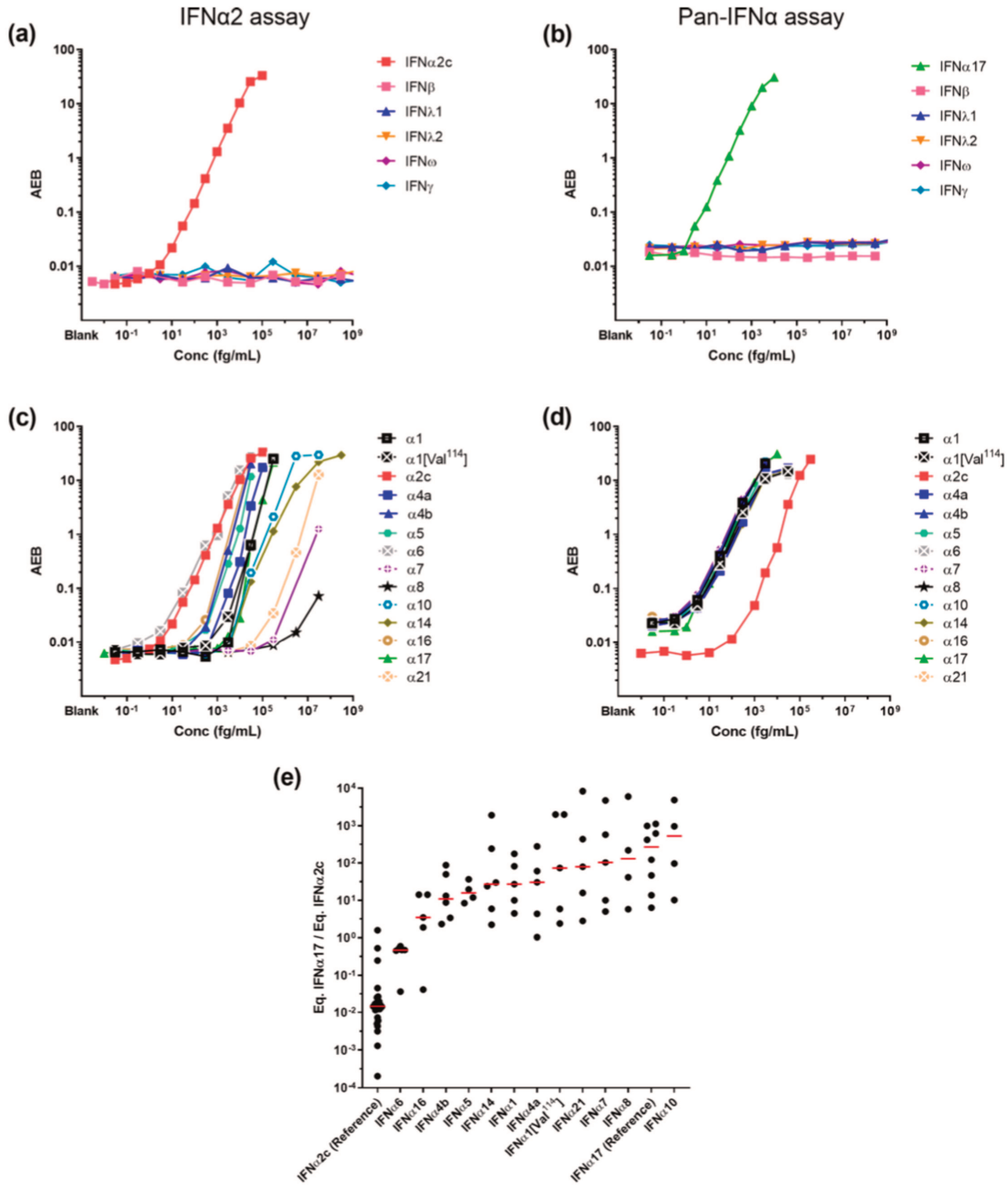

Fig. 1. Digital ELISAs to study IFNα subtypes. Response (Average Enzyme per Bead) of the IFNα2 assay (a) and pan-IFNα (b) at different concentrations for the recombinant proteins IFNβ, IFNλ, IFNω and IFNγ. Response (Average Enzyme per Bead) of the IFNα2 assay (c) and pan-IFNα (d) at different concentrations for recombinant IFNα subtypes and the natural variant IFNα1(Val114). (e) The IFNα17/IFNα2c ratio for different concentrations of recombinant IFNα subtypes and the natural variant IFNα1(Val114) as measured by both the IFNα2 assay and pan-IFNα assays.

Val114) IFNα subtypes at different concentrations, from no response to saturation, and plotted the ratio of the results obtained in the two assays (Fig. 1e). Results are expressed as concentrations after calibration, to IFNα17 for the pan-IFNα assay and IFNα2 for the IFNα2 assay. This range of values therefore captures the possible biological distributions of IFNα17/α2, with ratios ranging from 10^4 to $2x10^{-4}$. Recombinant IFNα2 presented a low ratio as it was recognized with high specificity by the IFNα2 assay, but with low specificity by the pan-IFNα assay. IFNα6 had an intermediate ratio as it was recognized equally well by both assays, and all other subtypes presented a ratio higher than 1 due to greater specificity with the pan-IFNα assay.

3.2. *TLR activation can modify the balance of IFNα protein subtypes.*

To test the potential biological relevance of these observations we tested the hypothesis that different TLR stimulation could modify the balance of IFNα subtypes. To do this, we stimulated whole blood and purified plasmacytoid Dendritic Cells (pDCs) (the main IFNα producing

cell type) with different TLR ligands and quantified IFNα in the supernatant with both assays. Whole blood from healthy donors was stimulated with LPS (TLR4), Poly(I:C) (TLR3), and R848 (TLR7/8) plus a Null control for 22 h using concentrations previously defined to be within the linear range of response [21]. Response with both assays correlated extremely well as expected (Rs = 0.96, $p < 0.0001$ Spearman test), with R848 showing the strongest induction followed by equivalent responses for LPS and Poly(I:C) (Fig. 2a). Purified pDCs from healthy donors were stimulated with relevant ligands for TLR9, their main innate sensor, namely CpG-A and cGAMP, as well as LPS (TLR4), Poly(I:C) (TLR3), and R848 (TLR7/8). Strong responses were observed after stimulation with all TLR9 agonists and R848, with a good positive correlation between both assays (Rs = 0.79, $p < 0.0001$ Spearman test) (Fig. 2b). A high background (10^4 fg/mL) is observed using the IFNα2 assay, probably due to non-specific cell activation due to experimental manipulation. Because this non-specific activation could modify the results, we next calculated the IFNα17/α2 ratio between the different stimulation conditions for samples that were effectively stimulated by our molecules (significant difference and fold-induction compared to non-stimulated condition). For whole blood we observed a significantly lower ratio ($p = 0.0008$) between TLR7/8 ligands and TLR4 and TLR3 ligands (Fig. 2c). For pDCs we observed a significantly ($p = 0.0229$) higher ratio between TLR9 and TLR7/8 ligands (Fig. 2d). Therefore, in both whole blood and pDC responses to stimulation our assays could detect differential induction of IFNα protein subtypes depending on the TLR pathway targeted validating the biological relevance of this approach.

3.3. Comparison of IFNα subtype protein ratios in autoimmune and infection.

To test the potential clinical relevance of the IFNα17/α2 ratio in disease we applied both IFNα2 and pan-IFNα assays to plasma from patients with acute (dengue and viral central nervous system infection) or chronic (HCV) viral infection, as well as autoimmune conditions; systemic lupus erythematosus (SLE), connective tissue disease (CTD), and primary Sjögren's Syndrome (pSS), all pathologies previously shown to be associated with increased IFN signaling. Both assays showed an overall strong and positive correlation (Rs = 0.6198 $p < 0.0001$, Spearman test), however there were certain patients from both chronic viral infection and autoimmune groups whose IFNα results did not correlate well between the two assays (Fig. 3a). To explore this further we examined the IFNα ratio as previously described. Patients with acute viral diseases – dengue or CNS infections – showed the narrowest distribution range of IFNα17/α2 ratios with intermediate medians at 0.6 and 1.0 respectively (Fig. 3b). In contrast, patients chronically infected with HCV showed a wider distribution range of IFNα17/α2 ratios from 2×10^{-4} to 10^2 and a median of 2.6 suggesting the presence of multiple IFNα subtypes. Strikingly the three autoimmune

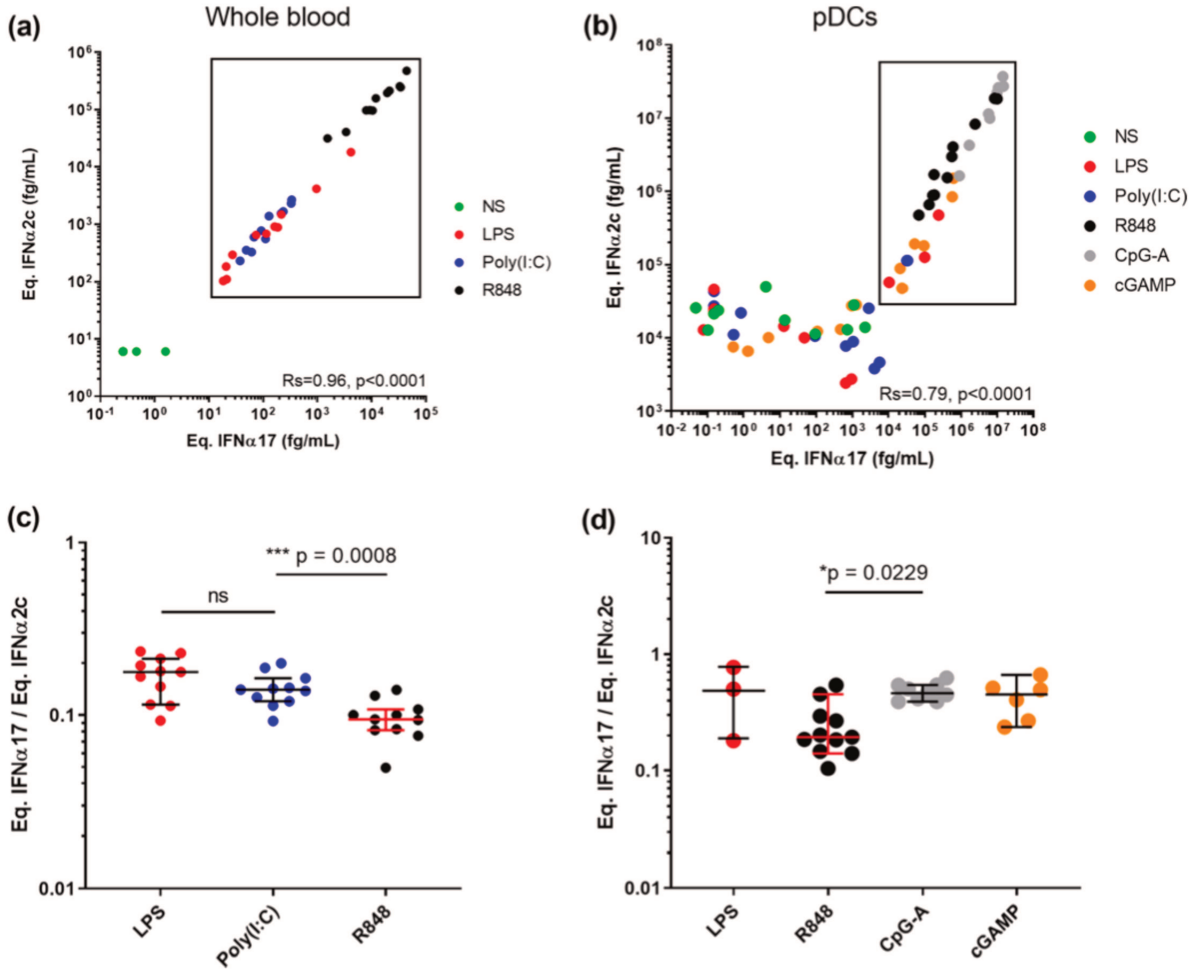

Fig. 2. TLR activation can modify the IFNα subtype balance. IFNα concentrations obtained using the IFNα2 and pan-IFNα assays after (a) whole blood stimulation with LPS (TLR4), Poly(I:C) (TLR3) or R848 (TLR7/8) and (b) pDC stimulation with LPS, Poly(I:C), R848, CpG-A (TLR9) or cGAMP (TLR9). Comparison of the IFNα17/α2 protein ratios obtained from (c) whole blood and (d) pDC stimulation with different agonists. Kruskal-Wallis test with Dunn's correction for multiple comparisons and Spearman correlations are reported.

cohorts all showed a similar wide distribution range with median values from 0.46 to 0.82. Intriguingly the autoimmune cohorts also revealed interesting sub-groups of outlier individuals with extremely low IFNα17/α2 ratios below 2×10^{-4}. These represented 3% of the total patients tested. A Kruskal–Wallis test with Dunn's post testing for multiple comparisons revealed significant differences between the SLE patients and pSS and cHCV patients, with a greater presence of low values in patients with autoimmune diseases suggesting a higher proportion of IFNα2 protein. These results collectively suggest that the level of disease complexity could explain the scale of the ratio distribution.

3.4. Patients with extremely low IFNα17/α2 protein ratio display reduced IFN signaling and function

The identification of SLE, CTD and pSS patients with an IFNα17/α2 ratio below $2x10^{-4}$ was intriguing, as results with recombinant molecules showed the extreme low probability of this phenotype occurring (Fig. 1e). Our SLE, CTD and pSS patient cohorts contained respectively 12/206 (5.8%), 6/52 (12%) and 6/392 (1.5%) samples with this phenotype (Fig. 4a, d, g). To examine a potential functional relevance for this abnormal ratio we plotted an interferon stimulated gene (ISG) score calculated by qPCR or microarray (previously described) against

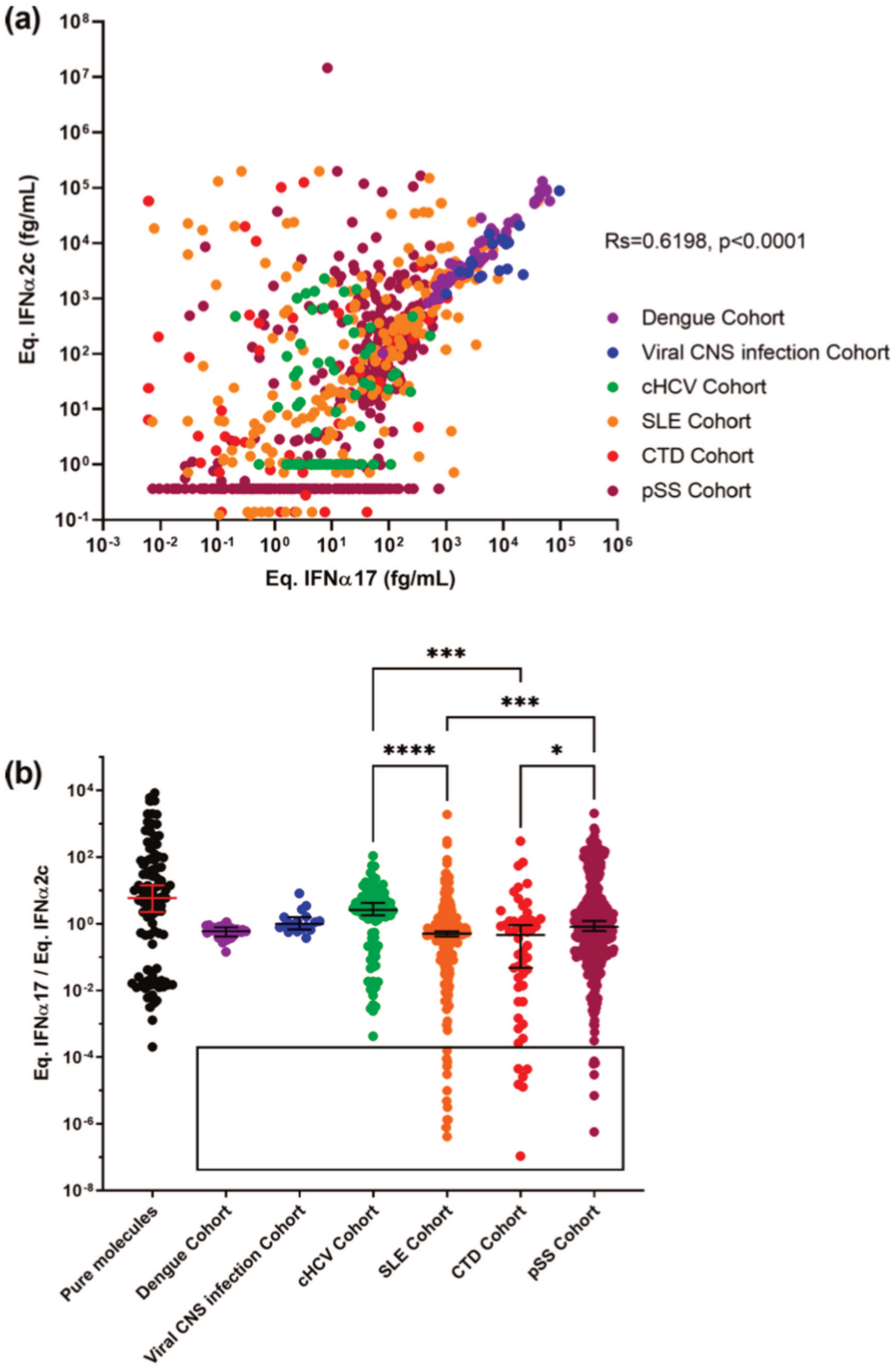

Fig. 3. IFNα subtype protein ratios in autoimmune and infection. IFNα concentrations obtained using the IFNα2 and pan-IFNα assays in plasma samples from patients with acute dengue infection, chronic HCV infection (cHCV), systemic lupus erythematosus (SLE), connective tissue disease (CTD), and primary Sjögren's syndrome (pSS). Values for viral central nervous system (CNS) infections are obtained from cerebrospinal fluid samples (a). The IFNα17/IFNα2c ratio as measured by both the IFNα2 and pan-IFNα assays for different concentrations of recombinant IFNα subtypes (left) and for the same patient samples (b). Kruskal-Wallis test with Dunn's correction for multiple comparisons and Spearman correlations are reported.

the individual equivalent IFNα17 (Fig. 4b, e and h) and IFNα2c (Fig. 4c, f, i) concentrations. This analysis revealed that for patients with low IFNα17/α2 ratios (red dots), the pan-IFNα value positively correlated as expected with the ISG score, and in line with other patients (blue dots). In contrast, these patients showed abnormally low ISG scores in regard to their IFNα2 results (orange dots). This suggested that in certain patients the IFNα2 protein value did not well reflect *in vivo* activity. To further test this hypothesis, we performed an IFN cytopathic assay on a subset of samples selected randomly from each cohort and at each IFNα17/α2c protein ratio. This revealed that patients with extremely low IFNα17/α2 ratios, also had low IFN activity (Fig. 4j and 4 k), despite these samples having apparent high IFNα2 protein concentrations.

3.5. Extremely low IFNα17/α2 protein ratio is not due to non-specific effects

A possible technical explanation for these unusual observations was non-specific binding within the assays. To test this hypothesis, we re-analyzed a series of 32 SLE samples in which the proportion of samples showing extremely low IFNα17/α2 ratios was increased in an assay buffer (Buffer B, Quanterix) specifically developed for low background. We have previously shown that this buffer successfully suppresses non-specific binding in an IFNβ assay [15]. This revealed identical results (no difference between the buffer groups, $p = 0.1103$, Fig S1), and moreover samples with a low IFNα17/α2 protein ratio maintained this phenotype irrespective of the buffer used (surrounded points), indicating that the phenotype was not due to non-specific binding.

3.6. Auto-antibodies against IFNα can explain the abnormal IFNα subtype ratios

A potential explanation for the extreme IFNα17/α2 ratio is the presence of auto-antibodies, which have been reported to develop against cytokines in autoimmune patients. To test this possibility, we performed a series of *in vitro* experiments. The addition of the 8H1 pan-alpha capture antibody in pure IFNα17 solutions at different concentrations reduces the IFNα17/α2 ratio (Fig. 5a). The anti-IFNα2c capture antibody produces no effect in these solutions but, added into IFNα2c solutions, the antibody increases the ratio (Fig. 5b). The addition of 8H1 in a selection of five SLE samples reduces the IFNα17/α2 ratio (Fig. 5c). This demonstrates that the presence of anti-IFNα auto-antibodies in biological samples could modify the ratio.

Therefore, we tested SLE patients for auto-antibodies against IFNα (subtypes 1,2,4,5,6,7,8 and 21) in their serum. A comparison of the auto-antibody negative and positive patients using the Chi square test revealed a higher proportion of extremely low IFNα17/α2 ratios in the anti-IFNα positive group supporting this hypothesis (Fig. 5d). We next examined SLE patients for whom longitudinal sampling was available over multiple years, which revealed interesting inter-patient variability. Strongly supporting our hypothesis for the role of anti-IFNα autoantibodies, certain patients showed continuous high levels of IFNα2 and initial high levels of pan-IFNα that suddenly dropped to undetectable concentrations. Strikingly these sudden undetectable pan-IFNα concentrations occur in parallel to detectable presence of auto-antibodies against IFNα2 and IFNα8. Two patients (Fig. 5e and f) out of 11 patients examined showed this pattern of high IFNα2, and low pan-IFNα, in the presence of anti-IFNα autoantibodies. One other patient with high longitudinal anti-IFNα auto-antibodies did not have elevated levels of IFNα protein at any time point examined (Fig S2). The other eight patients showed lower anti-IFNα auto-antibodies concentrations. Finally, we tested the LEAP SLE, the LEAP CTD and the ASSESS pSS cohorts for anti-IFNα (1,2,8,21) and anti-IFNα (4,5,6,7) autoantibodies to estimate the frequency of this phenotype. 12% of the SLE and CTD patients, and 6.3% of the pSS patients produce anti-IFNα auto-antibodies (Fig. 5g).

4. Discussion

Type I interferons are essential for anti-viral immunity as recently highlighted in studies of severe COVID-19 disease [22–23]. These studies and others have highlighted the need to directly quantify the cytokine protein in patient samples, which has been made possible by the recent development of digital ELISA [11]. However new tools to differentiate the diverse IFNα subtypes are required to further our understanding of their potential differential functions. We illustrate here how two complementary anti-IFNα assays can be used in tandem to reveal differences in IFNα subtype biology. This included subtle but significant differences in subtype expression between acute and chronic viral infection, and autoimmune diseases, and also after TLR stimulation of whole blood and isolated pDCs. However, our results also reveal discrepancies that can occur depending on the specificity of the monoclonal antibodies used.

In our originally described Simoa pan-IFNα assay [13], 8H1 and 12H5 antibody clones were selected because of their ability to quantify all IFN alpha subtypes. Isolated from APECED patients [12], these mAbs also have extremely high affinity and neutralizing capacity making them good candidates for therapeutic use. These attributes help to explain the good correlations observed between results with this assay and ISG scores and IFN-activity across all patient groups. In contrast, the BMS216C and BMS216BK antibody clones used in the IFNα2 assay were developed in mice for ELISA applications. As such they recognize human-characteristic epitopes on IFNα molecules, that are likely distinct from the functional binding sites. As a result, we observed lower correlations between IFNα2c concentrations measured with this assay and ISG score or IFN-activity. In support of these hypotheses, we compared the amino acid sequences and three-dimensional structures published online in the PDB database (www.rcsb.org) with the reactivity of all IFN molecules we tested in our two assays. From this, we estimated the pan-alpha assay epitope to be the ^{100}MQEVGV sequence in the IFNα17 molecule, and the IFNα2 assay epitope to be the ^{110}LMKED sequence in the IFNα2 molecule. Akabayov *et al.* [24] previously determined the IFNα2 amino-acids implicated in binding with the IFNAR1 receptor. From this, our estimated pan-IFNα epitope, but not the predicted IFNα2 epitope, includes a high concentration of IFNAR1 receptor binding amino-acids. These observations are consistent with the fact that the pan-IFNα assay uses neutralizing antibodies, but not the IFNα2 assay. An alternative explanation for the weaker correlation between ISG and the IFNα2 assay could be lower ISG induction by IFNα2 compared to the other subtypes but existing literature does not support such strong differences [25]. Alternative explanations could include potential inter-individual differences due to *in vivo* kinetics of response, leukocyte composition, or unidentified post-translational modifications. However, the epitope considerations could also explain the results observed in longitudinal patients, where autoantibodies against IFNα8 may compete with the pan-IFNα antibodies for the functional epitopes to reduce the IFNα concentrations measured. In contrast, the autoantibodies may not block the epitopes recognized by the IFNα2 assay resulting in no modification of the IFNα2 concentrations measured. This implicates that autoantibodies have a neutralizing efficiency, a hypothesis that could be verified measuring ISG score or IFN-activity in these longitudinal samples.

Autoimmune disorders are well known to induce production of autoantibodies [26]. Nevertheless, their presence can be detrimental in cases of acute viral infection where type I interferon responses are crucial for host protection, as recently demonstrated for COVID-19 [23]. We observed anti-IFNα autoantibody positivity in 12% of SLE and CTD groups, and 6% in the pSS group. Gupta *et al.* [27] previously quantified 11% in SLE patients and 9% in pSS patients which is in line with our results. Questions remain on differential and overlapping specificities of the IFNα auto-antibodies for the 13 IFNα subtypes, which are also likely to be heterogenous between individuals. Additional studies with well characterized assays will be required to address this relevant question.

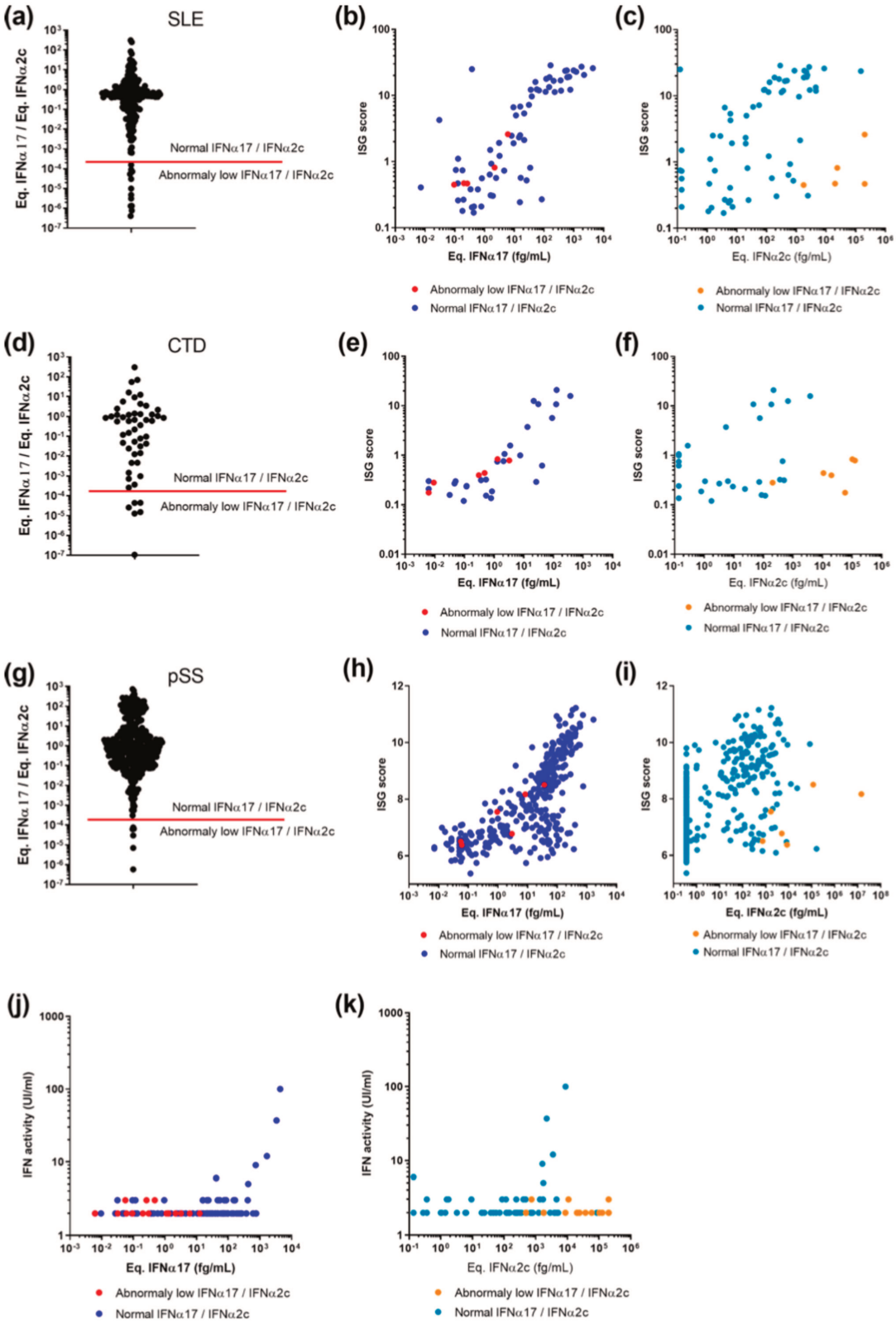

Fig. 4. Integration of IFNα17/α2 protein ratios with ISG score and functional activity. IFNα17/α2 protein ratios obtained from samples of patients with (a) SLE, (d) CTD and (g) pSS. The red bar indicates the lower IFNα17/α2 protein ratio using pure molecules. Correlation of ISG score with pan-IFNα assay (b, e, h) or IFNα2 assay results (c, f, i) for same patients. Correlation of IFN functional activity with pan-IFNα assay (j) or IFNα2 assay results (k) for same patients. Patients with an IFNα17/α2 protein ratio threshold above the $2 \cdot 10^{-4}$ cut off are in blue, those below in red.

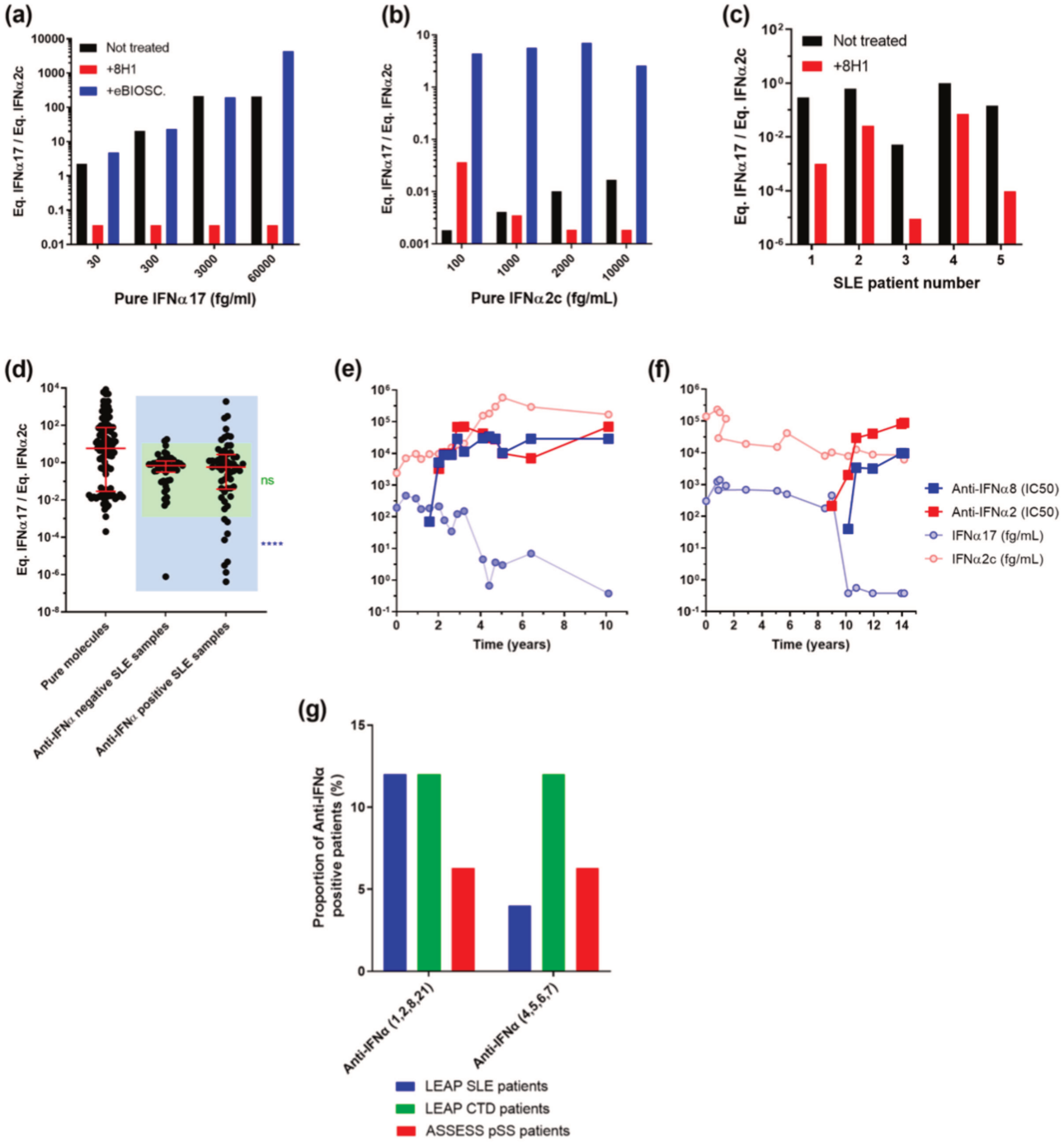

Fig. 5. Association of anti-IFNα auto-antibodies and the abnormal IFNα subtype ratios. (a) Competition assays after addition of the 8H1 clone anti-IFNα antibody in pure IFNα17 solutions at different concentrations reduces the ratio. (b) Addition of the anti-IFNα2 antibody in pure IFNα2c solutions at different concentrations increases the ratio. (c) Addition of 8H1 in five SLE patient samples reduces the IFNα17/α2 ratio. (d) IFNα17/α2 protein ratios for SLE patient samples characterized positive for anti-IFNα antibodies in comparison with negative SLE patient samples and pure molecules. (e-f) Longitudinal analysis of anti-IFNα8 and anti-IFNα2 antibody concentrations, pan-IFNα and IFNα2 assays results over time (years) in two SLE patients. (g) Proportion of anti-IFNα auto-antibodies positive samples in LEAP SLE, LEAP CTD and ASSESS pSS patients.

We also observed extremely low IFNα ratios for autoimmune patients, which were absent in the cHCV, the dengue or the viral CNS infection patients. The proportion of these low ratio patients was 3%, lower than that observed for overall anti-IFNα autoantibody positivity. These differences may be due to autoantibodies targeting multiple distinct IFNα epitopes, or that extremely low ratios are only one possible consequence of autoantibody production, and explains why only two longitudinal patients out of 11 showed this phenotype.

Finally, this work highlights the additional information that can be obtained from using two different ELISA assays to quantify a single cytokine. The presence of autoantibodies, or enzymatic cleavage as previously described [28], could potentially decrease protein activity without decreasing the overall protein concentration. Autoantibodies could also reduce an ELISA measurement without decreasing the actual

protein concentration, e.g. if the protein is captured to circulating immune complexes. Real or active concentrations in the presence of autoantibodies are not accessible using a single ELISA, depending on the epitope recognized by the mAbs. The use of a second ELISA assay may be required, or alternatively a functional activity assay for confirmation. Additional approaches such as proximity extension assays may also potential overcome these issues through the use of two complementary Abs for double target recognition [29]. The relevance of these issues is increased for cytokines that show multiple subtypes quantified using ELISA assays that show a particular response for each subtype. It becomes impossible to compare two results without the verification that the subtype balance is the same in the two related samples. However, across the multiple patient cohorts we examined the frequency of this phenotype was relatively low, at only 3% of total patient samples examined. Therefore, once mAbs are verified for specificity and cross-reactivity such challenges may only be encountered when testing large patient cohorts.

CRediT authorship contribution statement

Vincent Bondet: Conceptualization, Methodology, Validation, Formal analysis, Investigation, Data curation, Writing - original draft, Writing - review & editing, Visualization. **Mathieu P. Rodero:** Conceptualization, Validation, Resources, Writing - review & editing. **Céline Posseme:** Investigation, Writing - review & editing. **Pierre Bost:** Investigation, Writing - review & editing. **Jérémie Decalf:** Investigation, Writing - review & editing. **Liis Haljasmägi:** Investigation, Writing - review & editing. **Nassima Bekaddour:** Investigation, Writing - review & editing. **Gillian I. Rice:** Investigation, Writing - review & editing. **Vinit Upasani:** Investigation, Writing - review & editing. **Jean-Philippe Herbeuval:** Resources, Validation, Investigation, Writing - review & editing. **John A. Reynolds:** Resources, Validation, Investigation, Writing - review & editing. **Tracy A. Briggs:** Resources, Validation, Investigation, Writing - review & editing. **Ian N. Bruce:** Resources, Validation, Investigation, Writing - review & editing. **Claudia Mauri:** Resources, Validation, Investigation, Writing - review & editing. **David Isenberg:** Resources, Validation, Investigation, Writing - review & editing. **Madhvi Menon:** Resources, Validation, Investigation, Writing - review & editing. **David Hunt:** Resources, Validation, Investigation, Writing - review & editing. **Benno Schwikowski:** Resources, Validation, Investigation, Writing - review & editing. **Xavier Mariette:** Resources, Validation, Investigation, Writing - review & editing. **Stanislas Pol:** Resources, Validation, Investigation, Writing - review & editing. **Flore Rozenberg:** Resources, Validation, Investigation, Writing - review & editing. **Tineke Cantaert:** Resources, Validation, Investigation, Writing - review & editing. **J. Eric Gottenberg:** Resources, Validation, Investigation, Writing - review & editing. **Kai Kisand:** Conceptualization, Validation, Investigation, Resources, Writing - review & editing. **Darragh Duffy:** Conceptualization, Methodology, Validation, Investigation, Writing - original draft, Writing - review & editing, Supervision, Project administration, Funding acquisition.

Declaration of Competing Interest

The authors declare that they have no known competing financial interests or personal relationships that could have appeared to influence the work reported in this paper.

Acknowledgements

We thank all patients and healthy donors who provided samples used in this study, as well as the clinical support teams that enabled their collection. We thank Immunoqure for provision of mAbs for the pan-IFNα assay. We acknowledge support from the ANR (CE17001002) awarded to DD.

Appendix A. Supplementary material

Supplementary data to this article can be found online at https://doi.org/10.1016/j.cyto.2021.155533.

References

[1] W.M. Schneider, et al., Interferon-stimulated genes: a complex web of host defenses, Annu. Rev. Immunol. 32 (2014) 513–545, https://doi.org/10.1146/annurev-immunol-032713-120231.
[2] G.E. Thorlacius, et al., An update on the role of type I interferons in systemic lupus erythematosus and Sjögren's syndrome, Curr. Opin. Rheumatol. 30 (2018) 471–481, https://doi.org/10.1097/BOR.0000000000000524.
[3] L. Moreira-Teixeira, et al., Type I interferons in tuberculosis: Foe and occasionally friend, J. Exp. Med. 215 (2018) 1273–1285, https://doi.org/10.1084/jem.20180325.
[4] G. Schreiber, The molecular basis for differential type I interferon signaling, J. Biol. Chem. 292 (2017) 7285–7294, https://doi.org/10.1074/jbc.R116.774562.
[5] J. Manry, et al., Evolutionary genetic dissection of human interferons, J. Exp. Med. 208 (2011) 2747–2759, https://doi.org/10.1084/jem.20111680.
[6] K. Guo, et al., Qualitative differences between the IFNα subtypes and IFNβ influence chronic mucosal HIV-1 pathogenesis, PLoS Pathog. 16 (2020) 1008986, https://doi.org/10.1371/journal.ppat.1008986.
[7] K.J. Hasenkrug, et al., Different biological activities of specific interferon alpha subtypes, mSphere 4 (2019) e00127–19, https://doi.org/10.1128/mSphere.00127-19.
[8] E. Schlaepfer, et al., Reply to Hasenkrug *et al.*, "Different Biological Activities of Specific Interferon Alpha Subtypes", mSphere 4 (2019) e00275–19, https://doi.org/10.1128/mSphere.00275-19.
[9] N. Gerlach, et al., Anti-retroviral effects of type I IFN subtypes in vivo, Eur. J. Immunol. 39 (2009) 136–146, https://doi.org/10.1002/eji.200838311.
[10] C. Uggenti, et al., Self-awareness: nucleic acid-driven inflammation and the Type I interferonopathies, Annu. Rev. Immunol. 37 (2019) 247–267, https://doi.org/10.1146/annurev-immunol-042718-041257.
[11] D.M. Rissin, et al., Single-molecule enzyme-linked immunosorbent assay detects serum proteins at subfemtomolar concentrations, Nat. Biotechnol. 28 (2010) 595–599, https://doi.org/10.1038/nbt.1641.
[12] S. Meyer, et al., AIRE-Deficient Patients Harbor Unique High-Affinity Disease-Ameliorating Autoantibodies, Cell 166 (2016) 582–595, https://doi.org/10.1016/j.cell.2016.06.024.
[13] M.P. Rodero, et al., Detection of interferon alpha protein reveals differential levels and cellular sources in disease, J. Exp. Med. 214 (2017) 1547–1555, https://doi.org/10.1084/jem.20161451.
[14] C. Gitiaux, et al., Myogenic progenitor cells exhibit Type I interferon-driven proangiogenic properties and molecular signature during juvenile dermatomyositis, Arthritis Rheumatol. 70 (2018) 134–145, https://doi.org/10.1002/art.40328.
[15] A. Llibre, et al., Plasma Type I IFN protein concentrations in human tuberculosis, Front. Cell. Infect. Microbiol. 9 (2019) 296, https://doi.org/10.3389/fcimb.2019.00296.
[16] J.A. Reynolds, et al., Type I interferon in patients with systemic autoimmune rheumatic disease is associated with haematological abnormalities and specific autoantibody profiles, Arthritis Res. Ther. 21 (2019) 147, https://doi.org/10.1186/s13075-019-1929-4.
[17] A. Sultanik, et al., Baseline phospho-stat1 level in PBMC is a non-invasive biomarker of early virological response to triple therapy in chronic HCV infection – ANRS C10–08 Study, J. Hepatol. 58 (2013) S478, https://doi.org/10.1016/S0168-8278(13)61178-2.
[18] V. Upasani, et al., Decreased Type I interferon production by plasmacytoid dendritic cells contributes to severe dengue, Front. Immunol. 11 (2020), 605087, https://doi.org/10.3389/fimmu.2020.605087.
[19] A. Llibre, et al., Development and validation of an ultrasensitive single molecule array digital enzyme-linked immunosorbent assay for human interferon-α, J. Vis. Exp. (2018) https://doi.org/10.3791/57421.
[20] G.I. Rice, et al., Assessment of interferon-related biomarkers in Aicardi-Goutières syndrome associated with mutations in TREX1, RNASEH2A, RNASEH2B, RNASEH2C, SAMHD1, and ADAR: a case-control study, Lancet Neurol. 12 (2013) 1159–1169, https://doi.org/10.1016/S1474-4422(13)70258-8.
[21] D. Duffy, et al., Functional analysis via standardized whole-blood stimulation systems defines the boundaries of a healthy immune response to complex stimuli, Immunity 40 (2014) 436–450, https://doi.org/10.1016/j.immuni.2014.03.002.
[22] J. Hadjadj, et al., Impaired type I interferon activity and inflammatory responses in severe COVID-19 patients, Science 369 (2020) 718–724, https://doi.org/10.1126/science.abc6027.
[23] P. Bastard, et al., Auto-antibodies against type I IFNs in patients with life-threatening COVID-19, Science 2020 Sep 24:eabd4585. doi: 10.1126/science.abd4585.
[24] S.R. Akabayov, et al., NMR Mapping of the IFNAR1-EC binding site on IFNα2 reveals allosteric changes in the IFNAR2-EC binding site, Biochemistry 49 (2010) 687–695, https://doi.org/10.1021/bi901313x.
[25] P. Hillyer, et al., Expression profiles of human interferon-alpha and interferon-lambda subtypes are ligand- and cell-dependent, Immunol. Cell Biol. 90 (2012) 774–783, https://doi.org/10.1038/icb.2011.109.

[26] K. Elkon, et al., Nature and functions of autoantibodies, Nat. Rev. Rheumatol. 4 (2008) 491–498, https://doi.org/10.1038/ncprheum0895.
[27] S. Gupta, et al., Distinct functions of autoantibodies against interferon in systemic Lupus Erythematosus: A comprehensive analysis of anticytokine autoantibodies in common rheumatic diseases, Arthritis Rheumatol. 68 (2016) 1677–1687, https://doi.org/10.1002/art.39607.
[28] J. Decalf, et al., Inhibition of DPP4 activity in humans establishes its in vivo role in CXCL10 post-translational modification: prospective placebo-controlled clinical studies, EMBO Mol. Med. 8 (2016) 679–683, https://doi.org/10.15252/emmm.201506145.
[29] S. Fredriksson, et al., Protein detection using proximity-dependent DNA ligation assays, Nat. Biotechnol. 20 (2002) 473–477, https://doi.org/10.1038/nbt0502-473.

REFERENCES BIBLIOGRAPHIQUES

A

Activation of the NLRP3 Inflammasome [WWW Document], 2017. InvivoGen. URL https://www.invivogen.com/review-nlrp3-inflammasome (accessed 2.18.21).

Agarwal, S., Misra, R., Aggarwal, A., 2008. Interleukin 17 levels are increased in juvenile idiopathic arthritis synovial fluid and induce synovial fibroblasts to produce proinflammatory cytokines and matrix metalloproteinases. J Rheumatol 35, 515–519.

Ait Yahia, S., Wallaert, B., Tsicopoulos, A., 2013. Rôle des récepteurs de type NOD dans les maladies allergiques. Revue Française d'Allergologie 53, 411–418. https://doi.org/10.1016/j.reval.2013.02.18

Albee, L.J., Eby, J.M., Tripathi, A., LaPorte, H.M., Gao, X., Volkman, B.F., Gaponenko, V., Majetschak, M., 2017. α1-Adrenergic Receptors Function Within Hetero-Oligomeric Complexes With Atypical Chemokine Receptor 3 and Chemokine (C-X-C motif) Receptor 4 in Vascular Smooth Muscle Cells. J Am Heart Assoc 6, e006575. https://doi.org/10.1161/JAHA.117.006575

Alexopoulou, L., Desnues, B., Demaria, O., 2012. [Toll-like receptor 8: the awkward TLR]. Medecine sciences : M/S. https://doi.org/10.1051/medsci/2012281023
Alonso-Ruiz, A., Pijoan, J.I., Ansuategui, E., Urkaregi, A., Calabozo, M., Quintana, A., 2008. Tumor necrosis factor alpha drugs in rheumatoid arthritis: systematic review and metaanalysis of efficacy and safety. BMC Musculoskelet Disord 9, 52. https://doi.org/10.1186/1471-2474-9-52

Alonso-Ruiz, A., Pijoan, J.I., Ansuategui, E., Urkaregi, A., Calabozo, M., Quintana, A., 2008. Tumor necrosis factor alpha drugs in rheumatoid arthritis: systematic review and metaanalysis of efficacy and safety. BMC Musculoskelet Disord 9, 52. https://doi.org/10.1186/1471-2474-9-52

Aringer, Martin, Karen Costenbader, David Daikh, Ralph Brinks, Marta Mosca, Rosalind Ramsey-Goldman, Josef S. Smolen, et al. « 2019 European League Against Rheumatism/American College of Rheumatology Classification Criteria for Systemic Lupus Erythematosus ». *Arthritis & Rheumatology (Hoboken, N.J.)* 71, nº 9 (septembre 2019): 1400-1412. https://doi.org/10.1002/art.40930.

B

Bach, E.A., Aguet, M., Schreiber, R.D., 1997. The IFN gamma receptor: a paradigm for cytokine receptor signaling. Annu Rev Immunol 15, 563–591. https://doi.org/10.1146/annurev.immunol.15.1.563

Baggiolini, M., Dewald, B., Moser, B., 1997. Human chemokines: an update. Annu Rev Immunol 15, 675–705. https://doi.org/10.1146/annurev.immunol.15.1.675

Balan, S., Arnold-Schrauf, C., Abbas, A., Couespel, N., Savoret, J., Imperatore, F., Villani, A.-C., Vu Manh, T.-P., Bhardwaj, N., Dalod, M., 2018. Large-Scale Human Dendritic Cell Differentiation Revealing Notch-Dependent Lineage Bifurcation and Heterogeneity. Cell Rep 24, 1902-1915.e6. https://doi.org/10.1016/j.celrep.2018.07.033

Banchereau, R., Hong, S., Cantarel, B., Baldwin, N., Baisch, J., Edens, M., Cepika, A.-M., Acs, P., Turner, J., Anguiano, E., Vinod, P., Khan, S., Obermoser, G., Blankenship, D., Wakeland, E., Nassi, L., Gotte, A., Punaro, M., Liu, Y.-J., Banchereau, J., Rossello-Urgell, J., Wright, T., Pascual, V., 2016. Personalized Immunomonitoring Uncovers Molecular Networks that Stratify Lupus Patients. Cell 165, 1548–1550. https://doi.org/10.1016/j.cell.2016.05.057

Bauernfeind, F.G., Horvath, G., Stutz, A., Alnemri, E.S., MacDonald, K., Speert, D., Fernandes-Alnemri, T., Wu, J., Monks, B.G., Fitzgerald, K.A., Hornung, V., Latz, E., 2009. Cutting edge: NF-kappaB activating pattern recognition and cytokine receptors license NLRP3 inflammasome activation by regulating NLRP3 expression. J Immunol 183, 787–791. https://doi.org/10.4049/jimmunol.0901363

Bazan, J.F., Bacon, K.B., Hardiman, G., Wang, W., Soo, K., Rossi, D., Greaves, D.R., Zlotnik, A., Schall, T.J., 1997. A new class of membrane-bound chemokine with a CX3C motif. Nature 385, 640–644. https://doi.org/10.1038/385640a0

Bengtsson, A.A., Sturfelt, G., Truedsson, L., Blomberg, J., Alm, G., Vallin, H., Rönnblom, L., 2000. Activation of type I interferon system in systemic lupus erythematosus correlates with disease activity but not with antiretroviral antibodies. Lupus 9, 664–671. https://doi.org/10.1191/096120300674499064

Berger, E.A., Murphy, P.M., Farber, J.M., 1999. Chemokine receptors as HIV-1 coreceptors: roles in viral entry, tropism, and disease. Annu Rev Immunol 17, 657–700. https://doi.org/10.1146/annurev.immunol.17.1.657

Berntson, L., Fasth, A., Andersson-Gäre, B., Kristinsson, J., Lahdenne, P., Marhaug, G., Nielsen, S., Pelkonen, P., Svensson, E., Nordic Study Group, 2001. Construct validity of ILAR and EULAR criteria in juvenile idiopathic arthritis: a population based incidence study from the Nordic countries. International League of Associations for Rheumatology. European League Against Rheumatism. J Rheumatol 28, 2737–2743.

Beukelman, T., Patkar, N.M., Saag, K.G., Tolleson-Rinehart, S., Cron, R.Q., DeWitt, E.M., Ilowite, N.T., Kimura, Y., Laxer, R.M., Lovell, D.J., Martini, A., Rabinovich, C.E., Ruperto, N., 2011. 2011 American College of Rheumatology recommendations for the treatment of juvenile idiopathic arthritis: initiation and safety monitoring of therapeutic agents for the treatment of arthritis and systemic features. Arthritis Care Res (Hoboken) 63, 465–482. https://doi.org/10.1002/acr.20460

Blanco, P., Palucka, A.K., Gill, M., Pascual, V., Banchereau, J., 2001. Induction of dendritic cell differentiation by IFN-alpha in systemic lupus erythematosus. Science 294, 1540–1543. https://doi.org/10.1126/science.1064890

Blanco, P., Pitard, V., Viallard, J.-F., Taupin, J.-L., Pellegrin, J.-L., Moreau, J.-F., 2005. Increase in activated CD8+ T lymphocytes expressing perforin and granzyme B correlates with

disease activity in patients with systemic lupus erythematosus. Arthritis Rheum 52, 201–211. https://doi.org/10.1002/art.20745

Blanco-Melo, D., Nilsson-Payant, B.E., Liu, W.-C., Uhl, S., Hoagland, D., Møller, R., Jordan, T.X., Oishi, K., Panis, M., Sachs, D., Wang, T.T., Schwartz, R.E., Lim, J.K., Albrecht, R.A., tenOever, B.R., 2020. Imbalanced Host Response to SARS-CoV-2 Drives Development of COVID-19. Cell 181, 1036-1045.e9. https://doi.org/10.1016/j.cell.2020.04.026

Bonham, K.S., Orzalli, M.H., Hayashi, K., Wolf, A.I., Glanemann, C., Weninger, W., Iwasaki, A., Knipe, D.M., Kagan, J.C., 2014. A promiscuous lipid-binding protein diversifies the subcellular sites of toll-like receptor signal transduction. Cell 156, 705–716. https://doi.org/10.1016/j.cell.2014.01.019

Brocker, C., Thompson, D., Matsumoto, A., Nebert, D.W., Vasiliou, V., 2010. Evolutionary divergence and functions of the human interleukin (IL) gene family. Hum Genomics 5, 30–55. https://doi.org/10.1186/1479-7364-5-1-30

Brown, G.D., Taylor, P.R., Reid, D.M., Willment, J.A., Williams, D.L., Martinez-Pomares, L., Wong, S.Y.C., Gordon, S., 2002. Dectin-1 is a major beta-glucan receptor on macrophages. J Exp Med 196, 407–412. https://doi.org/10.1084/jem.20020470

Broxmeyer, H.E., Orschell, C.M., Clapp, D.W., Hangoc, G., Cooper, S., Plett, P.A., Liles, W.C., Li, X., Graham-Evans, B., Campbell, T.B., Calandra, G., Bridger, G., Dale, D.C., Srour, E.F., 2005. Rapid mobilization of murine and human hematopoietic stem and progenitor cells with AMD3100, a CXCR4 antagonist. J Exp Med 201, 1307–1318. https://doi.org/10.1084/jem.20041385

Bruchard, M., Mignot, G., Derangère, V., Chalmin, F., Chevriaux, A., Végran, F., Boireau, W., Simon, B., Ryffel, B., Connat, J.L., Kanellopoulos, J., Martin, F., Rébé, C., Apetoh, L., Ghiringhelli, F., 2013. Chemotherapy-triggered cathepsin B release in myeloid-derived suppressor cells activates the Nlrp3 inflammasome and promotes tumor growth. Nat Med 19, 57–64. https://doi.org/10.1038/nm.2999

C

Capobianchi, M.R., Uleri, E., Caglioti, C., Dolei, A., 2015. Type I IFN family members: similarity, differences and interaction. Cytokine Growth Factor Rev 26, 103–111. https://doi.org/10.1016/j.cytogfr.2014.10.011

Caux, C., Dezutter-Dambuyant, C., Schmitt, D., Banchereau, J., 1992. GM-CSF and TNF-α cooperate in the generation of dendritic Langerhans cells. Nature 360, 258–261. https://doi.org/10.1038/360258a0

Cederblad, B., Blomberg, S., Vallin, H., Perers, A., Alm, G.V., Rönnblom, L., 1998. Patients with systemic lupus erythematosus have reduced numbers of circulating natural interferon-alpha- producing cells. J Autoimmun 11, 465–470. https://doi.org/10.1006/jaut.1998.0215
Chang, J.J., Altfeld, M., 2009. TLR-mediated immune activation in HIV. Blood 113, 269–270. https://doi.org/10.1182/blood-2008-10-184598

Cella, M., Jarrossay, D., Facchetti, F., Alebardi, O., Nakajima, H., Lanzavecchia, A., Colonna,

M., 1999. Plasmacytoid monocytes migrate to inflamed lymph nodes and produce large amounts of type I interferon. Nat Med 5, 919–923. https://doi.org/10.1038/11360

Chen, X., Cui, R., Li, R., Lin, H., Huang, Z., Lin, L., 2016. Development of pristane induced mice model for lupus with atherosclerosis and analysis of TLR expression. Clin Exp Rheumatol 34, 600–608.

Choi, W.-T., Duggineni, S., Xu, Y., Huang, Z., An, J., 2012. Drug discovery research targeting the CXC chemokine receptor 4 (CXCR4). J Med Chem 55, 977–994. https://doi.org/10.1021/jm200568c

Chow, K.V., Sutherland, R.M., Zhan, Y., Lew, A.M., 2017. Heterogeneity, functional specialization and differentiation of monocyte-derived dendritic cells. Immunol Cell Biol 95, 244–251. https://doi.org/10.1038/icb.2016.104

Cohn, L., Chatterjee, B., Esselborn, F., Smed-Sörensen, A., Nakamura, N., Chalouni, C., Lee, B.-C., Vandlen, R., Keler, T., Lauer, P., Brockstedt, D., Mellman, I., Delamarre, L., 2013. Antigen delivery to early endosomes eliminates the superiority of human blood BDCA3+ dendritic cells at cross presentation. Journal of Experimental Medicine 210, 1049–1063. https://doi.org/10.1084/jem.20121251

Cole, K.E., Strick, C.A., Paradis, T.J., Ogborne, K.T., Loetscher, M., Gladue, R.P., Lin, W., Boyd, J.G., Moser, B., Wood, D.E., Sahagan, B.G., Neote, K., 1998. Interferon-inducible T cell alpha chemoattractant (I-TAC): a novel non-ELR CXC chemokine with potent activity on activated T cells through selective high affinity binding to CXCR3. J Exp Med 187, 2009–2021. https://doi.org/10.1084/jem.187.12.2009

Collison, L.W., Workman, C.J., Kuo, T.T., Boyd, K., Wang, Y., Vignali, K.M., Cross, R., Sehy, D., Blumberg, R.S., Vignali, D.A.A., 2007. The inhibitory cytokine IL-35 contributes to regulatory T-cell function. Nature 450, 566–569. https://doi.org/10.1038/nature06306

Conti, P., Ronconi, G., Caraffa, A., Gallenga, C., Ross, R., Frydas, I., Kritas, S., 2020. Induction of pro-inflammatory cytokines (IL-1 and IL-6) and lung inflammation by Coronavirus-19 (COVI-19 or SARS-CoV-2): anti-inflammatory strategies. J Biol Regul Homeost Agents 34, 327–331. https://doi.org/10.23812/CONTI-E

Crisafulli, S., Pandya, Y., Moolchan, K., Lavoie, T., 2008. Interferon gamma: activity and ELISA detection comparisons. Biotechniques 45, 101–102. https://doi.org/10.2144/000112943

Crozat, K., Vivier, E., Dalod, M., 2009. Crosstalk between components of the innate immune system: promoting anti-microbial defenses and avoiding immunopathologies. Immunological Reviews 227, 129–149. https://doi.org/10.1111/j.1600-065X.2008.00736.x

Cucak, H., Yrlid, U., Reizis, B., Kalinke, U., Johansson-Lindbom, B., 2009. Type I interferon signaling in dendritic cells stimulates the development of lymph-node-resident T follicular helper cells. Immunity 31, 491–501. https://doi.org/10.1016/j.immuni.2009.07.005

D

De Clercq, E., 2015. AMD3100/CXCR4 Inhibitor. Front Immunol 6, 276. https://doi.org/10.3389/fimmu.2015.00276

de Jager, W., Hoppenreijs, E.P.A.H., Wulffraat, N.M., Wedderburn, L.R., Kuis, W., Prakken, B.J., 2007. Blood and synovial fluid cytokine signatures in patients with juvenile idiopathic arthritis: a cross-sectional study. Ann. Rheum. Dis. 66, 589–598. https://doi.org/10.1136/ard.2006.061853

Deng, H., Liu, R., Ellmeier, W., Choe, S., Unutmaz, D., Burkhart, M., Di Marzio, P., Marmon, S., Sutton, R.E., Hill, C.M., Davis, C.B., Peiper, S.C., Schall, T.J., Littman, D.R., Landau, N.R., 1996. Identification of a major co-receptor for primary isolates of HIV-1. Nature 381, 661–666. https://doi.org/10.1038/381661a0

Dinarello, C., Arend, W., Sims, J., Smith, D., Blumberg, H., O'Neill, L., Goldbach-Mansky, R., Pizarro, T., Hoffman, H., Bufler, P., Nold, M., Ghezzi, P., Mantovani, A., Garlanda, C., Boraschi, D., Rubartelli, A., Netea, M., van der Meer, J., Joosten, L., Mandrup-Poulsen, T., Donath, M., Lewis, E., Pfeilschifter, J., Martin, M., Kracht, M., Muehl, H., Novick, D., Lukic, M., Conti, B., Solinger, A., Kelk, P., Peyman, K., van de Veerdonk, F., Gabel, C., 2010. IL-1 family nomenclature. Nat Immunol 11, 973. https://doi.org/10.1038/ni1110-973

Dzionek, A., Fuchs, A., Schmidt, P., Cremer, S., Zysk, M., Miltenyi, S., Buck, D.W., Schmitz, J., 2000. BDCA-2, BDCA-3, and BDCA-4: Three Markers for Distinct Subsets of Dendritic Cells in Human Peripheral Blood. The Journal of Immunology 165, 6037–6046. https://doi.org/10.4049/jimmunol.165.11.6037

Dzionek, A., Sohma, Y., Nagafune, J., Cella, M., Colonna, M., Facchetti, F., Günther, G., Johnston, I., Lanzavecchia, A., Nagasaka, T., Okada, T., Vermi, W., Winkels, G., Yamamoto, T., Zysk, M., Yamaguchi, Y., Schmitz, J., 2001. BDCA-2, a novel plasmacytoid dendritic cell-specific type II C-type lectin, mediates antigen capture and is a potent inhibitor of interferon alpha/beta induction. J Exp Med 194, 1823–1834. https://doi.org/10.1084/jem.194.12.1823

E

Evinger, M., Maeda, S., Pestka, S., 1981. Recombinant human leukocyte interferon produced in bacteria has antiproliferative activity. J Biol Chem 256, 2113–2114.

F

Farkas, L., Beiske, K., Lund-Johansen, F., Brandtzaeg, P., Jahnsen, F.L., 2001. Plasmacytoid dendritic cells (natural interferon- alpha/beta-producing cells) accumulate in cutaneous lupus erythematosus lesions. Am J Pathol 159, 237–243. https://doi.org/10.1016/s0002-9440(10)61689-6

Ferrari, D., Pizzirani, C., Adinolfi, E., Lemoli, R.M., Curti, A., Idzko, M., Panther, E., Di Virgilio, F., 2006. The P2X7 receptor: a key player in IL-1 processing and release. J Immunol 176, 3877–3883. https://doi.org/10.4049/jimmunol.176.7.3877

Fitzgerald, K.A., McWhirter, S.M., Faia, K.L., Rowe, D.C., Latz, E., Golenbock, D.T., Coyle, A.J., Liao, S.-M., Maniatis, T., 2003. IKKepsilon and TBK1 are essential components of the IRF3 signaling pathway. Nat Immunol 4, 491–496. https://doi.org/10.1038/ni921

Fore, F., Budipranama, M., Destiawan, R.A., 2022. TLR10 and Its Role in Immunity. Handb Exp Pharmacol 276, 161–174. https://doi.org/10.1007/164_2021_541Franchi, L., Warner, N.,

Viani, K., Nuñez, G., 2009. Function of Nod-like receptors in microbial recognition and host defense. Immunol Rev 227, 106–128. https://doi.org/10.1111/j.1600-065X.2008.00734.x

Forero, A., Ozarkar, S., Li, H., Lee, C.H., Hemann, E.A., Nadjsombati, M.S., Hendricks, M.R., So, L., Green, R., Roy, C.N., Sarkar, S.N., von Moltke, J., Anderson, S.K., Gale, M., Savan, R., 2019. Differential Activation of the Transcription Factor IRF1 Underlies the Distinct Immune Responses Elicited by Type I and Type III Interferons. Immunity 51, 451-464.e6. https://doi.org/10.1016/j.immuni.2019.07.007

Frucht, D.M., Fukao, T., Bogdan, C., Schindler, H., O'Shea, J.J., Koyasu, S., 2001. IFN-gamma production by antigen-presenting cells: mechanisms emerge. Trends Immunol 22, 556–560. https://doi.org/10.1016/s1471-4906(01)02005-1

Fujisawa, J., Iwakura, Y., Kawade, Y., 1978. Nonglycosylated mouse L cell interferon produced by the action of tunicamycin. Journal of Biological Chemistry 253, 8677–8679.

Fung, K.Y., Mangan, N.E., Cumming, H., Horvat, J.C., Mayall, J.R., Stifter, S.A., De Weerd, N., Roisman, L.C., Rossjohn, J., Robertson, S.A., Schjenken, J.E., Parker, B., Gargett, C.E., Nguyen, H.P.T., Carr, D.J., Hansbro, P.M., Hertzog, P.J., 2013. Interferon-ε protects the female reproductive tract from viral and bacterial infection. Science 339, 1088–1092. https://doi.org/10.1126/science.1233321

Furusato, B., Mohamed, A., Uhlén, M., Rhim, J.S., 2010. CXCR4 and cancer. Pathol Int 60, 497–505. https://doi.org/10.1111/j.1440-1827.2010.02548.x

G

Ganju, R.K., Brubaker, S.A., Meyer, J., Dutt, P., Yang, Y., Qin, S., Newman, W., Groopman, J.E., 1998. The alpha-chemokine, stromal cell-derived factor-1alpha, binds to the transmembrane G-protein-coupled CXCR-4 receptor and activates multiple signal transduction pathways. J Biol Chem 273, 23169–23175. https://doi.org/10.1074/jbc.273.36.23169

Garcia-Minambres, A., Eid, S.G., Mangan, N.E., Pade, C., Lim, S.S., Matthews, A.Y., de Weerd, N.A., Hertzog, P.J., Mak, J., 2017. Interferon epsilon promotes HIV restriction at multiple steps of viral replication. Immunol Cell Biol 95, 478–483. https://doi.org/10.1038/icb.2016.123

Garcia-Romo, G.S., Caielli, S., Vega, B., Connolly, J., Allantaz, F., Xu, Z., Punaro, M., Baisch, J., Guiducci, C., Coffman, R.L., Barrat, F.J., Banchereau, J., Pascual, V., 2011. Netting neutrophils are major inducers of type I IFN production in pediatric systemic lupus erythematosus. Sci Transl Med 3, 73ra20. https://doi.org/10.1126/scitranslmed.3001201

Gattorno, M., Chicha, L., Gregorio, A., Ferlito, F., Rossi, F., Jarrossay, D., Lanzavecchia, A., Martini, A., Manz, M.G., 2007. Distinct expression pattern of IFN-alpha and TNF-alpha in juvenile idiopathic arthritis synovial tissue. Rheumatology (Oxford) 46, 657–665. https://doi.org/10.1093/rheumatology/kel346

Gattorno, M., Prigione, I., Morandi, F., Gregorio, A., Chiesa, S., Ferlito, F., Favre, A., Uccelli, A., Gambini, C., Martini, A., Pistoia, V., 2005. Phenotypic and functional characterisation of CCR7+ and CCR7- CD4+ memory T cells homing to the joints in juvenile idiopathic arthritis.

Arthritis Res Ther 7, R256-267. https://doi.org/10.1186/ar1485

Gaur, P., Myles, A., Misra, R., Aggarwal, A., 2017. Intermediate monocytes are increased in enthesitis-related arthritis, a category of juvenile idiopathic arthritis. Clin Exp Immunol 187, 234–241. https://doi.org/10.1111/cei.12880

Geijtenbeek, T.B.H., Gringhuis, S.I., 2009. Signalling through C-type lectin receptors: shaping immune responses. Nat Rev Immunol 9, 465–479. https://doi.org/10.1038/nri2569

Giancane, G., Consolaro, A., Lanni, S., Davì, S., Schiappapietra, B., Ravelli, A., 2016. Juvenile Idiopathic Arthritis: Diagnosis and Treatment. Rheumatol Ther 3, 187–207. https://doi.org/10.1007/s40744-016-0040-4

Gibbert, K., Schlaak, J.F., Yang, D., Dittmer, U., 2013. IFN-α subtypes: distinct biological activities in anti-viral therapy. Br J Pharmacol 168, 1048–1058. https://doi.org/10.1111/bph.12010

Ginhoux, F., Jung, S., 2014. Monocytes and macrophages: developmental pathways and tissue homeostasis. Nat Rev Immunol 14, 392–404. https://doi.org/10.1038/nri3671

Gomariz, R.P., Gutiérrez-Cañas, I., Arranz, A., Carrión, M., Juarranz, Y., Leceta, J., Martínez, C., 2010. Peptides targeting Toll-like receptor signalling pathways for novel immune therapeutics. Curr Pharm Des 16, 1063–1080. https://doi.org/10.2174/138161210790963841
Gordon, S., Taylor, P.R., 2005. Monocyte and macrophage heterogeneity. Nat Rev Immunol 5, 953–964. https://doi.org/10.1038/nri1733

Gorman, J.D., Criswell, L.A., 2002. The shared epitope and severity of rheumatoid arthritis. Rheum Dis Clin North Am 28, 59–78. https://doi.org/10.1016/s0889-857x(03)00069-3
Goubau, D., Deddouche, S., Reis e Sousa, C., 2013. Cytosolic sensing of viruses. Immunity 38, 855–869. https://doi.org/10.1016/j.immuni.2013.05.007

Gualtierotti, R., Ingegnoli, F., Griffini, S., Grovetti, E., Meroni, P.L., Cugno, M., 2016. Prothrombotic biomarkers in patients with rheumatoid arthritis: the beneficial effect of IL-6 receptor blockade. Clin. Exp. Rheumatol. 34, 451–458.

Guiducci, C., Gong, M., Xu, Z., Gill, M., Chaussabel, D., Meeker, T., Chan, J.H., Wright, T., Punaro, M., Bolland, S., Soumelis, V., Banchereau, J., Coffman, R.L., Pascual, V., Barrat, F.J., 2010. TLR recognition of self nucleic acids hampers glucocorticoid activity in lupus. Nature 465, 937–941. https://doi.org/10.1038/nature09102

Gulino, A.V., Moratto, D., Sozzani, S., Cavadini, P., Otero, K., Tassone, L., Imberti, L., Pirovano, S., Notarangelo, Lucia D., Soresina, R., Mazzolari, E., Nelson, D.L., Notarangelo, Luigi D., Badolato, R., 2004. Altered leukocyte response to CXCL12 in patients with warts hypogammaglobulinemia, infections, myelokathexis (WHIM) syndrome. Blood 104, 444–452. https://doi.org/10.1182/blood-2003-10-3532

H

Hadjadj, J., Yatim, N., Barnabei, L., Corneau, A., Boussier, J., Smith, N., Péré, H., Charbit, B., Bondet, V., Chenevier-Gobeaux, C., Breillat, P., Carlier, N., Gauzit, R., Morbieu, C., Pène, F., Marin, N., Roche, N., Szwebel, T.-A., Merkling, S.H., Treluyer, J.-M., Veyer, D., Mouthon, L.,

Blanc, C., Tharaux, P.-L., Rozenberg, F., Fischer, A., Duffy, D., Rieux-Laucat, F., Kernéis, S., Terrier, B., 2020. Impaired type I interferon activity and inflammatory responses in severe COVID-19 patients. Science 369, 718–724. https://doi.org/10.1126/science.abc6027

Hardy, M.P., Owczarek, C.M., Jermiin, L.S., Ejdebäck, M., Hertzog, P.J., 2004. Characterization of the type I interferon locus and identification of novel genes. Genomics 84, 331–345. https://doi.org/10.1016/j.ygeno.2004.03.003

Harris, J.G., Kessler, E.A., Verbsky, J.W., 2013. Update on the treatment of juvenile idiopathic arthritis. Curr Allergy Asthma Rep 13, 337–346. https://doi.org/10.1007/s11882-013-0351-2

Hatse, S., Princen, K., Bridger, G., De Clercq, E., Schols, D., 2002. Chemokine receptor inhibition by AMD3100 is strictly confined to CXCR4. FEBS Lett 527, 255–262. https://doi.org/10.1016/s0014-5793(02)03143-5

Hegen, M., Keith, J.C., Collins, M., Nickerson-Nutter, C.L., 2008. Utility of animal models for identification of potential therapeutics for rheumatoid arthritis. Ann. Rheum. Dis. 67, 1505–1515. https://doi.org/10.1136/ard.2007.076430

Hernandez, P.A., Gorlin, R.J., Lukens, J.N., Taniuchi, S., Bohinjec, J., Francois, F., Klotman, M.E., Diaz, G.A., 2003. Mutations in the chemokine receptor gene CXCR4 are associated with WHIM syndrome, a combined immunodeficiency disease. Nat Genet 34, 70–74. https://doi.org/10.1038/ng1149

Hillyer, P., Mane, V.P., Schramm, L.M., Puig, M., Verthelyi, D., Chen, A., Zhao, Z., Navarro, M.B., Kirschman, K.D., Bykadi, S., Jubin, R.G., Rabin, R.L., 2012. Expression profiles of human interferon-alpha and interferon-lambda subtypes are ligand- and cell-dependent. Immunol Cell Biol 90, 774–783. https://doi.org/10.1038/icb.2011.109

Hooks, J.J., Moutsopoulos, H.M., Geis, S.A., Stahl, N.I., Decker, J.L., Notkins, A.L., 1979. Immune interferon in the circulation of patients with autoimmune disease. N Engl J Med 301, 5–8. https://doi.org/10.1056/NEJM197907053010102

Hornung, V., Bauernfeind, F., Halle, A., Samstad, E.O., Kono, H., Rock, K.L., Fitzgerald, K.A., Latz, E., 2008. Silica crystals and aluminum salts activate the NALP3 inflammasome through phagosomal destabilization. Nat Immunol 9, 847–856. https://doi.org/10.1038/ni.1631

Huang, D.W., Sherman, B.T., Lempicki, R.A., 2009a. Systematic and integrative analysis of large gene lists using DAVID bioinformatics resources. Nat Protoc 4, 44–57. https://doi.org/10.1038/nprot.2008.211

Huang, D.W., Sherman, B.T., Lempicki, R.A., 2009b. Bioinformatics enrichment tools: paths toward the comprehensive functional analysis of large gene lists. Nucleic Acids Res 37, 1–13. https://doi.org/10.1093/nar/gkn923

Huang, H., Xiang, J., 2004. Synergistic effect of lymphotactin and interferon gamma-inducible protein-10 transgene expression in T-cell localization and adoptive T-cell therapy of tumors. Int J Cancer 109, 817–825. https://doi.org/10.1002/ijc.20043

Huang, X., Dorta-Estremera, S., Yao, Y., Shen, N., Cao, W., 2015. Predominant Role of

Plasmacytoid Dendritic Cells in Stimulating Systemic Autoimmunity. Frontiers in Immunology 6, 526. https://doi.org/10.3389/fimmu.2015.00526

Hung, W.T., Chen, Y.M., Lan, J.L., Chen, H.H., Chen, Y.H., Chen, D.Y., Hsieh, C.W., Wen, M.C., 2011. Antinucleosome antibodies as a potential biomarker for the evaluation of renal pathological activity in patients with proliferative lupus nephritis. Lupus 20, 1404–1410. https://doi.org/10.1177/0961203311417033

I

IL-35-producing B cells are critical regulators of immunity during autoimmune and infectious diseases - PubMed [WWW Document], n.d. URL https://pubmed.ncbi.nlm.nih.gov/24572363/ (accessed 11.6.21).

Imai, T., Yoshida, T., Baba, M., Nishimura, M., Kakizaki, M., Yoshie, O., 1996. Molecular cloning of a novel T cell-directed CC chemokine expressed in thymus by signal sequence trap using Epstein-Barr virus vector. J Biol Chem 271, 21514–21521. https://doi.org/10.1074/jbc.271.35.21514

Inngjerdingen, M., Damaj, B., Maghazachi, A.A., 2000. Human NK cells express CC chemokine receptors 4 and 8 and respond to thymus and activation-regulated chemokine, macrophage-derived chemokine, and I-309. J Immunol 164, 4048–4054. https://doi.org/10.4049/jimmunol.164.8.4048

Inohara, N., Koseki, T., Lin, J., del Peso, L., Lucas, P.C., Chen, F.F., Ogura, Y., Núñez, G., 2000. An induced proximity model for NF-kappa B activation in the Nod1/RICK and RIP signaling pathways. J Biol Chem 275, 27823–27831. https://doi.org/10.1074/jbc.M003415200

Inohara, N., Koseki, T., Peso, L. del, Hu, Y., Yee, C., Chen, S., Carrio, R., Merino, J., Liu, D., Ni, J., Núñez, G., 1999. Nod1, an Apaf-1-like Activator of Caspase-9 and Nuclear Factor-κB *. Journal of Biological Chemistry 274, 14560–14567. https://doi.org/10.1074/jbc.274.21.14560

Inohara, N., Nuñez, G., 2003. NODs: intracellular proteins involved in inflammation and apoptosis. Nat Rev Immunol 3, 371–382. https://doi.org/10.1038/nri1086

Isaacs, A., Lindenmann, J., 1957. Virus interference. I. The interferon. Proc R Soc Lond B Biol Sci 147, 258–267. https://doi.org/10.1098/rspb.1957.0048

Ito, T., Kanzler, H., Duramad, O., Cao, W., Liu, Y.-J., 2006. Specialization, kinetics, and repertoire of type 1 interferon responses by human plasmacytoid predendritic cells. Blood 107, 2423–2431. https://doi.org/10.1182/blood-2005-07-2709

J

Jakubzick, C., Gautier, E.L., Gibbings, S.L., Sojka, D.K., Schlitzer, A., Johnson, T.E., Ivanov, S., Duan, Q., Bala, S., Condon, T., van Rooijen, N., Grainger, J.R., Belkaid, Y., Ma'ayan, A., Riches, D.W.H., Yokoyama, W.M., Ginhoux, F., Henson, P.M., Randolph, G.J., 2013. Minimal differentiation of classical monocytes as they survey steady-state tissues and transport antigen

to lymph nodes. Immunity 39, 599–610. https://doi.org/10.1016/j.immuni.2013.08.007

Jin, J.-O., Zhang, W., Du, J., Yu, Q., 2014. BDCA1-Positive Dendritic Cells (DCs) Represent a Unique Human Myeloid DC Subset That Induces Innate and Adaptive Immune Responses to Staphylococcus aureus Infection. Infection and Immunity 82, 4466–4476. https://doi.org/10.1128/IAI.01851-14

K

Kagan, J.C., Su, T., Horng, T., Chow, A., Akira, S., Medzhitov, R., 2008. TRAM couples endocytosis of Toll-like receptor 4 to the induction of interferon-beta. Nat Immunol 9, 361–368. https://doi.org/10.1038/ni1569

Kamphuis, S., Hrafnkelsdóttir, K., Klein, M.R., de Jager, W., Haverkamp, M.H., van Bilsen, J.H.M., Albani, S., Kuis, W., Wauben, M.H.M., Prakken, B.J., 2006. Novel self-epitopes derived from aggrecan, fibrillin, and matrix metalloproteinase-3 drive distinct autoreactive T-cell responses in juvenile idiopathic arthritis and in health. Arthritis Res Ther 8, R178. https://doi.org/10.1186/ar2088

Kankkunen, P., Teirilä, L., Rintahaka, J., Alenius, H., Wolff, H., Matikainen, S., 2010. (1,3)-beta-glucans activate both dectin-1 and NLRP3 inflammasome in human macrophages. J Immunol 184, 6335–6342. https://doi.org/10.4049/jimmunol.0903019

Kaul, A., Gordon, C., Crow, M.K., Touma, Z., Urowitz, M.B., van Vollenhoven, R., Ruiz-Irastorza, G., Hughes, G., 2016. Systemic lupus erythematosus. Nat Rev Dis Primers 2, 16039. https://doi.org/10.1038/nrdp.2016.39

Kawai, T., Akira, S., 2006. Innate immune recognition of viral infection. Nat Immunol 7, 131–137. https://doi.org/10.1038/ni1303

Kirkling, M.E., Cytlak, U., Lau, C.M., Lewis, K.L., Resteu, A., Khodadadi-Jamayran, A., Siebel, C.W., Salmon, H., Merad, M., Tsirigos, A., Collin, M., Bigley, V., Reizis, B., 2018. Notch Signaling Facilitates In Vitro Generation of Cross-Presenting Classical Dendritic Cells. Cell Rep 23, 3658-3672.e6. https://doi.org/10.1016/j.celrep.2018.05.068

Kirou, K.A., Mavragani, C.P., Crow, M.K., 2007. Activation of type I interferon in systemic lupus erythematosus. Expert Rev Clin Immunol 3, 579–588. https://doi.org/10.1586/1744666X.3.4.579

Kirou, K.A., Vakkalanka, R.K., Butler, M.J., Crow, M.K., 2000. Induction of Fas ligand-mediated apoptosis by interferon-alpha. Clin Immunol 95, 218–226. https://doi.org/10.1006/clim.2000.4866

Km, P., M, J., B, P., P, L., 2015. Collagen-Induced Arthritis: A model for Murine Autoimmune Arthritis. Bio Protoc 5. https://doi.org/10.21769/bioprotoc.1626

Koenderman, L., Tesselaar, K., Vrisekoop, N., 2022. Human neutrophil kinetics: a call to revisit old evidence. Trends Immunol S1471-4906(22)00189–2. https://doi.org/10.1016/j.it.2022.09.008

L

LaFleur, D.W., Nardelli, B., Tsareva, T., Mather, D., Feng, P., Semenuk, M., Taylor, K., Buergin, M., Chinchilla, D., Roshke, V., Chen, G., Ruben, S.M., Pitha, P.M., Coleman, T.A., Moore, P.A., 2001. Interferon-kappa, a novel type I interferon expressed in human keratinocytes. J Biol Chem 276, 39765–39771. https://doi.org/10.1074/jbc.M102502200

Lam, A.R., Bhattacharya, S., Patel, K., Hall, S.E., Mao, A., Vaidehi, N., 2011. Importance of receptor flexibility in binding of cyclam compounds to the chemokine receptor CXCR4. J Chem Inf Model 51, 139–147. https://doi.org/10.1021/ci1003027

Lande, R., Ganguly, D., Facchinetti, V., Frasca, L., Conrad, C., Gregorio, J., Meller, S., Chamilos, G., Sebasigari, R., Riccieri, V., Bassett, R., Amuro, H., Fukuhara, S., Ito, T., Liu, Y.-J., Gilliet, M., 2011. Neutrophils Activate Plasmacytoid Dendritic Cells by Releasing Self-DNA–Peptide Complexes in Systemic Lupus Erythematosus. Sci Transl Med 3, 73ra19. https://doi.org/10.1126/scitranslmed.3001180

Lande, R., Giacomini, E., Serafini, B., Rosicarelli, B., Sebastiani, G.D., Minisola, G., Tarantino, U., Riccieri, V., Valesini, G., Coccia, E.M., 2004. Characterization and recruitment of plasmacytoid dendritic cells in synovial fluid and tissue of patients with chronic inflammatory arthritis. J Immunol 173, 2815–2824. https://doi.org/10.4049/jimmunol.173.4.2815

Lapidot, T., 2001. Mechanism of human stem cell migration and repopulation of NOD/SCID and B2mnull NOD/SCID mice. The role of SDF-1/CXCR4 interactions. Ann N Y Acad Sci 938, 83–95. https://doi.org/10.1111/j.1749-6632.2001.tb03577.x

Le Bon, A., Thompson, C., Kamphuis, E., Durand, V., Rossmann, C., Kalinke, U., Tough, D.F., 2006. Cutting edge: enhancement of antibody responses through direct stimulation of B and T cells by type I IFN. J Immunol 176, 2074–2078. https://doi.org/10.4049/jimmunol.176.4.2074

Li, S.-F., Zhao, F.-R., Shao, J.-J., Xie, Y.-L., Chang, H.-Y., Zhang, Y.-G., 2017. Interferon-omega: Current status in clinical applications. Int Immunopharmacol 52, 253–260. https://doi.org/10.1016/j.intimp.2017.08.028

Li, T., Prokopec, S.D., Morrison, S., Lou, W., Reich, H., Gladman, D., Urowitz, M., Scholey, J., Fortin, P.R., Boutros, P.C., Wither, J., Landolt-Marticorena, C., 2015. Anti-nucleosome antibodies outperform traditional biomarkers as longitudinal indicators of disease activity in systemic lupus erythematosus. Rheumatology (Oxford) 54, 449–457. https://doi.org/10.1093/rheumatology/keu326

Liang, X., 2008. CXCR4, inhibitors and mechanisms of action. Chem Biol Drug Des 72, 97–110. https://doi.org/10.1111/j.1747-0285.2008.00681.x

Lipsky, P.E., 2006. Interleukin-6 and rheumatic diseases. Arthritis Res. Ther. 8 Suppl 2, S4. https://doi.org/10.1186/ar1918

Lotito, A.P.N., Campa, A., Silva, C.A.A., Kiss, M.H.B., Mello, S.B.V., 2007. Interleukin 18 as a marker of disease activity and severity in patients with juvenile idiopathic arthritis. J

Rheumatol 34, 823–830.

Lund, J.M., Alexopoulou, L., Sato, A., Karow, M., Adams, N.C., Gale, N.W., Iwasaki, A., Flavell, R.A., 2004. Recognition of single-stranded RNA viruses by Toll-like receptor 7. PNAS 101, 5598–5603. https://doi.org/10.1073/pnas.0400937101

Luster, A.D., Rothenberg, M.E., 1997. Role of the monocyte chemoattractant protein and eotaxin subfamily of chemokines in allergic inflammation. J Leukoc Biol 62, 620–633. https://doi.org/10.1002/jlb.62.5.620

M

Macaubas, C., Nguyen, K., Milojevic, D., Park, J.L., Mellins, E.D., 2009. Oligoarticular and polyarticular JIA: epidemiology and pathogenesis. Nat Rev Rheumatol 5, 616–626. https://doi.org/10.1038/nrrheum.2009.209

MacDonald, K.P.A., Munster, D.J., Clark, G.J., Dzionek, A., Schmitz, J., Hart, D.N.J., 2002. Characterization of human blood dendritic cell subsets. Blood 100, 4512–4520. https://doi.org/10.1182/blood-2001-11-0097

Mackay, C.R., 1997. Chemokines: what chemokine is that? Curr Biol 7, R384-386. https://doi.org/10.1016/s0960-9822(06)00181-3

Mangge, H., Kenzian, H., Gallistl, S., Neuwirth, G., Liebmann, P., Kaulfersch, W., Beaufort, F., Muntean, W., Schauenstein, K., 1995. Serum cytokines in juvenile rheumatoid arthritis. Correlation with conventional inflammation parameters and clinical subtypes. Arthritis Rheum. 38, 211–220. https://doi.org/10.1002/art.1780380209

Mantovani, A., Cassatella, M.A., Costantini, C., Jaillon, S., 2011. Neutrophils in the activation and regulation of innate and adaptive immunity. Nat Rev Immunol 11, 519–531. https://doi.org/10.1038/nri3024

Marié, I., Durbin, J.E., Levy, D.E., 1998. Differential viral induction of distinct interferon-alpha genes by positive feedback through interferon regulatory factor-7. EMBO J 17, 6660–6669. https://doi.org/10.1093/emboj/17.22.6660

Martinon, F., Burns, K., Tschopp, J., 2002. The inflammasome: a molecular platform triggering activation of inflammatory caspases and processing of proIL-beta. Mol Cell 10, 417–426. https://doi.org/10.1016/s1097-2765(02)00599-3

Martinon, F., Pétrilli, V., Mayor, A., Tardivel, A., Tschopp, J., 2006. Gout-associated uric acid crystals activate the NALP3 inflammasome. Nature 440, 237–241. https://doi.org/10.1038/nature04516

Martinon, F., Tschopp, J., 2005. NLRs join TLRs as innate sensors of pathogens. Trends Immunol 26, 447–454. https://doi.org/10.1016/j.it.2005.06.004

Matzinger, P., 1994. Tolerance, danger, and the extended family. Annu Rev Immunol 12, 991–1045. https://doi.org/10.1146/annurev.iy.12.040194.005015

McGreal, E.P., Rosas, M., Brown, G.D., Zamze, S., Wong, S.Y.C., Gordon, S., Martinez-Pomares, L., Taylor, P.R., 2006. The carbohydrate-recognition domain of Dectin-2 is a C-type lectin with specificity for high mannose. Glycobiology 16, 422–430. https://doi.org/10.1093/glycob/cwj077

Medzhitov, R., Preston-Hurlburt, P., Janeway, C.A., 1997. A human homologue of the Drosophila Toll protein signals activation of adaptive immunity. Nature 388, 394–397. https://doi.org/10.1038/41131

Merad, M., Martin, J.C., 2020. Pathological inflammation in patients with COVID-19: a key role for monocytes and macrophages. Nat Rev Immunol 20, 355–362. https://doi.org/10.1038/s41577-020-0331-4

Michalska, A., Blaszczyk, K., Wesoly, J., Bluyssen, H.A.R., 2018. A Positive Feedback Amplifier Circuit That Regulates Interferon (IFN)-Stimulated Gene Expression and Controls Type I and Type II IFN Responses. Front Immunol 9, 1135. https://doi.org/10.3389/fimmu.2018.01135

Mogensen, T.H., 2009. Pathogen recognition and inflammatory signaling in innate immune defenses. Clin Microbiol Rev 22, 240–273, Table of Contents. https://doi.org/10.1128/CMR.00046-08

Monceaux, V., Chiche-Lapierre, C., Chaput, C., Witko-Sarsat, V., Prevost, M.-C., Taylor, C.T., Ungeheuer, M.-N., Sansonetti, P.J., Marteyn, B.S., 2016. Anoxia and glucose supplementation preserve neutrophil viability and function. Blood 128, 993–1002. https://doi.org/10.1182/blood-2015-11-680918

Murphy, P.M., 2001. Chemokines and the molecular basis of cancer metastasis. N Engl J Med 345, 833–835. https://doi.org/10.1056/NEJM200109133451113

Murphy, P.M., Baggiolini, M., Charo, I.F., Hébert, C.A., Horuk, R., Matsushima, K., Miller, L.H., Oppenheim, J.J., Power, C.A., 2000. International union of pharmacology. XXII. Nomenclature for chemokine receptors. Pharmacol Rev 52, 145–176.

Murray, K.J., Luyrink, L., Grom, A.A., Passo, M.H., Emery, H., Witte, D., Glass, D.N., 1996. Immunohistological characteristics of T cell infiltrates in different forms of childhood onset chronic arthritis. J Rheumatol 23, 2116–2124.

N

Nehar-Belaid, D., Hong, S., Marches, R., Chen, G., Bolisetty, M., Baisch, J., Walters, L., Punaro, M., Rossi, R.J., Chung, C.H., Huynh, R.P., Singh, P., Flynn, W.F., Tabanor-Gayle, J.A., Kuchipudi, N., Mejias, A., Collet, M.A., Lucido, A.L., Palucka, K., Robson, P., Lakshminarayanan, S., Ramilo, O., Wright, T., Pascual, V., Banchereau, J.F., 2020. Mapping systemic lupus erythematosus heterogeneity at the single-cell level. Nature Immunology 21, 1094–1106. https://doi.org/10.1038/s41590-020-0743-0

Nielen, M.M.J., van Schaardenburg, D., Reesink, H.W., van de Stadt, R.J., van der Horst-Bruinsma, I.E., de Koning, M.H.M.T., Habibuw, M.R., Vandenbroucke, J.P., Dijkmans, B.A.C., 2004. Specific autoantibodies precede the symptoms of rheumatoid arthritis: a study of

serial measurements in blood donors. Arthritis Rheum 50, 380–386. https://doi.org/10.1002/art.20018

Nistala, K., Moncrieffe, H., Newton, K.R., Varsani, H., Hunter, P., Wedderburn, L.R., 2008. Interleukin-17-producing T cells are enriched in the joints of children with arthritis, but have a reciprocal relationship to regulatory T cell numbers. Arthritis Rheum 58, 875–887. https://doi.org/10.1002/art.23291

O

Oberlin, E., Amara, A., Bachelerie, F., Bessia, C., Virelizier, J.L., Arenzana-Seisdedos, F., Schwartz, O., Heard, J.M., Clark-Lewis, I., Legler, D.F., Loetscher, M., Baggiolini, M., Moser, B., 1996. The CXC chemokine SDF-1 is the ligand for LESTR/fusin and prevents infection by T-cell-line-adapted HIV-1. Nature 382, 833–835. https://doi.org/10.1038/382833a0

Oen, K.G., Cheang, M., 1996. Epidemiology of chronic arthritis in childhood. Semin Arthritis Rheum 26, 575–591. https://doi.org/10.1016/s0049-0172(96)80009-6

Ogura, Y., Inohara, N., Benito, A., Chen, F.F., Yamaoka, S., Nunez, G., 2001. Nod2, a Nod1/Apaf-1 family member that is restricted to monocytes and activates NF-kappaB. J Biol Chem 276, 4812–4818. https://doi.org/10.1074/jbc.M008072200

Ooi, K.G.-J., Galatowicz, G., Towler, H.M.A., Lightman, S.L., Calder, V.L., 2006. Multiplex cytokine detection versus ELISA for aqueous humor: IL-5, IL-10, and IFNgamma profiles in uveitis. Invest Ophthalmol Vis Sci 47, 272–277. https://doi.org/10.1167/iovs.05-0790

Oppenheim, J.J., Tewary, P., de la Rosa, G., Yang, D., 2007. Alarmins initiate host defense. Adv Exp Med Biol 601, 185–194. https://doi.org/10.1007/978-0-387-72005-0_19

Ozinsky, A., Underhill, D.M., Fontenot, J.D., Hajjar, A.M., Smith, K.D., Wilson, C.B., Schroeder, L., Aderem, A., 2000. The repertoire for pattern recognition of pathogens by the innate immune system is defined by cooperation between toll-like receptors. Proc Natl Acad Sci U S A 97, 13766–13771. https://doi.org/10.1073/pnas.250476497

P

Pawig, L., Klasen, C., Weber, C., Bernhagen, J., Noels, H., 2015. Diversity and Inter-Connections in the CXCR4 Chemokine Receptor/Ligand Family: Molecular Perspectives. Front Immunol 6, 429. https://doi.org/10.3389/fimmu.2015.00429

Pestka, S., Krause, C.D., Walter, M.R., 2004. Interferons, interferon-like cytokines, and their receptors. Immunol Rev 202, 8–32. https://doi.org/10.1111/j.0105-2896.2004.00204.x

Pétrilli, V., Papin, S., Dostert, C., Mayor, A., Martinon, F., Tschopp, J., 2007. Activation of the NALP3 inflammasome is triggered by low intracellular potassium concentration. Cell Death Differ 14, 1583–1589. https://doi.org/10.1038/sj.cdd.4402195

Petty, R.E., Southwood, T.R., Manners, P., Baum, J., Glass, D.N., Goldenberg, J., He, X., Maldonado-Cocco, J., Orozco-Alcala, J., Prieur, A.-M., Suarez-Almazor, M.E., Woo, P., International League of Associations for Rheumatology, 2004. International League of Associations for Rheumatology classification of juvenile idiopathic arthritis: second revision,

Edmonton, 2001. J. Rheumatol. 31, 390–392.

Prakken, B., Albani, S., Martini, A., 2011. Juvenile idiopathic arthritis. Lancet 377, 2138–2149. https://doi.org/10.1016/S0140-6736(11)60244-4

Preble, O.T., Rothko, K., Klippel, J.H., Friedman, R.M., Johnston, M.I., 1983. Interferon-induced 2'-5' adenylate synthetase in vivo and interferon production in vitro by lymphocytes from systemic lupus erythematosus patients with and without circulating interferon. J Exp Med 157, 2140–2146. https://doi.org/10.1084/jem.157.6.2140

Prutki, M., Tambic Bukovac, L., Jelusic, M., Potocki, K., Kralik, M., Malcic, I., 2008. Retrospective study of juvenile spondylarthropathies in Croatia over the last 11 years. Clin Exp Rheumatol 26, 693–699.

R

Ravelli, A., Migliavacca, D., Viola, S., Ruperto, N., Pistorio, A., Martini, A., 1999. Efficacy of folinic acid in reducing methotrexate toxicity in juvenile idiopathic arthritis. Clin Exp Rheumatol 17, 625–627.

Revised nomenclature for antigen-nonspecific T cell proliferation and helper factors, 1979. . J Immunol 123, 2928–2929.

Rimaniol, A.-C., Till, S.J., Garcia, G., Capel, F., Godot, V., Balabanian, K., Durand-Gasselin, I., Varga, E.M., Simonneau, G., Emilie, D., Durham, S.R., Humbert, M., 2003. The CX3C chemokine fractalkine in allergic asthma and rhinitis. J Allergy Clin Immunol 112, 1139–1146. https://doi.org/10.1016/j.jaci.2003.09.041

Robertson, M., Ritz, J., 1990. Biology and clinical relevance of human natural killer cells. Blood 76, 2421–2438. https://doi.org/10.1182/blood.V76.12.2421.2421

Rodero, M.P., Decalf, J., Bondet, V., Hunt, D., Rice, G.I., Werneke, S., McGlasson, S.L., Alyanakian, M.-A., Bader-Meunier, B., Barnerias, C., Bellon, N., Belot, A., Bodemer, C., Briggs, T.A., Desguerre, I., Frémond, M.-L., Hully, M., van den Maagdenberg, A.M.J.M., Melki, I., Meyts, I., Musset, L., Pelzer, N., Quartier, P., Terwindt, G.M., Wardlaw, J., Wiseman, S., Rieux-Laucat, F., Rose, Y., Neven, B., Hertel, C., Hayday, A., Albert, M.L., Rozenberg, F., Crow, Y.J., Duffy, D., 2017. Detection of interferon alpha protein reveals differential levels and cellular sources in disease. J Exp Med 214, 1547–1555. https://doi.org/10.1084/jem.20161451

Romani, N., Gruner, S., Brang, D., Kämpgen, E., Lenz, A., Trockenbacher, B., Konwalinka, G., Fritsch, P.O., Steinman, R.M., Schuler, G., 1994. Proliferating dendritic cell progenitors in human blood. Journal of Experimental Medicine 180, 83–93. https://doi.org/10.1084/jem.180.1.83

Rönnblom, L., Alm, G.V., 2002. The natural interferon-alpha producing cells in systemic lupus erythematosus. Hum Immunol 63, 1181–1193. https://doi.org/10.1016/s0198-8859(02)00757-7

Rose-John, S., 2018. Interleukin-6 Family Cytokines. Cold Spring Harb Perspect Biol 10, a028415. https://doi.org/10.1101/cshperspect.a028415

Ruperto, N., Murray, K.J., Gerloni, V., Wulffraat, N., de Oliveira, S.K.F., Falcini, F., Dolezalova, P., Alessio, M., Burgos-Vargas, R., Corona, F., Vesely, R., Foster, H., Davidson, J., Zulian, F., Asplin, L., Baildam, E., Consuegra, J.G., Ozdogan, H., Saurenmann, R., Joos, R., Pistorio, A., Woo, P., Martini, A., Pediatric Rheumatology International Trials Organization, 2004. A randomized trial of parenteral methotrexate comparing an intermediate dose with a higher dose in children with juvenile idiopathic arthritis who failed to respond to standard doses of methotrexate. Arthritis Rheum 50, 2191–2201. https://doi.org/10.1002/art.20288
Salanga, C.L., O'Hayre, M., Handel, T., 2009. Modulation of chemokine receptor activity through dimerization and crosstalk. Cell Mol Life Sci 66, 1370–1386. https://doi.org/10.1007/s00018-008-8666-1

S

Sallusto, F., Lanzavecchia, A., 1994. Efficient presentation of soluble antigen by cultured human dendritic cells is maintained by granulocyte/macrophage colony-stimulating factor plus interleukin 4 and downregulated by tumor necrosis factor alpha. J Exp Med 179, 1109–1118. https://doi.org/10.1084/jem.179.4.1109

Savarese, E., Steinberg, C., Pawar, R.D., Reindl, W., Akira, S., Anders, H.-J., Krug, A., 2008. Requirement of Toll-like receptor 7 for pristane-induced production of autoantibodies and development of murine lupus nephritis. Arthritis Rheum 58, 1107–1115. https://doi.org/10.1002/art.23407

Sedlackova, L., Velek, J., Vavrincova, P., Hromadnikova, I., 2006. Peripheral blood mononuclear cell responses to heat shock proteins and their derived synthetic peptides in juvenile idiopathic arthritis patients. Inflamm Res 55, 153–159. https://doi.org/10.1007/s00011-006-0065-1

Segal, A.W., 2005. How neutrophils kill microbes. Annu Rev Immunol 23, 197–223. https://doi.org/10.1146/annurev.immunol.23.021704.115653

Segura, E., Durand, M., Amigorena, S., 2013. Similar antigen cross-presentation capacity and phagocytic functions in all freshly isolated human lymphoid organ–resident dendritic cells. Journal of Experimental Medicine 210, 1035–1047. https://doi.org/10.1084/jem.20121103

Shen, P., Roch, T., Lampropoulou, V., O'Connor, R.A., Stervbo, U., Hilgenberg, E., Ries, S., Dang, V.D., Jaimes, Y., Daridon, C., Li, R., Jouneau, L., Boudinot, P., Wilantri, S., Sakwa, I., Miyazaki, Y., Leech, M.D., McPherson, R.C., Wirtz, S., Neurath, M., Hoehlig, K., Meinl, E., Grützkau, A., Grün, J.R., Horn, K., Kühl, A.A., Dörner, T., Bar-Or, A., Kaufmann, S.H.E., Anderton, S.M., Fillatreau, S., 2014. IL-35-producing B cells are critical regulators of immunity during autoimmune and infectious diseases. Nature 507, 366–370. https://doi.org/10.1038/nature12979

Shenoi, S., Wallace, C.A., 2010. Tumor necrosis factor inhibitors in the management of juvenile idiopathic arthritis: an evidence-based review. Paediatr Drugs 12, 367–377. https://doi.org/10.2165/11532610-000000000-00000

Shimada, K., Crother, T.R., Karlin, J., Dagvadorj, J., Chiba, N., Chen, S., Ramanujan, V.K., Wolf, A.J., Vergnes, L., Ojcius, D.M., Rentsendorj, A., Vargas, M., Guerrero, C., Wang, Y., Fitzgerald, K.A., Underhill, D.M., Town, T., Arditi, M., 2012. Oxidized mitochondrial DNA activates the NLRP3 inflammasome during apoptosis. Immunity 36, 401–414.

https://doi.org/10.1016/j.immuni.2012.01.009

Siegal, F.P., Kadowaki, N., Shodell, M., Fitzgerald-Bocarsly, P.A., Shah, K., Ho, S., Antonenko, S., Liu, Y.-J., 1999. The Nature of the Principal Type 1 Interferon-Producing Cells in Human Blood. Science 284, 1835–1837. https://doi.org/10.1126/science.284.5421.1835

Sittig, S.P., Bakdash, G., Weiden, J., Sköld, A.E., Tel, J., Figdor, C.G., de Vries, I.J.M., Schreibelt, G., 2016. A Comparative Study of the T Cell Stimulatory and Polarizing Capacity of Human Primary Blood Dendritic Cell Subsets [WWW Document]. Mediators of Inflammation. https://doi.org/10.1155/2016/3605643

Sleeman, M.A., Fraser, J.K., Murison, J.G., Kelly, S.L., Prestidge, R.L., Palmer, D.J., Watson, J.D., Kumble, K.D., 2000. B cell- and monocyte-activating chemokine (BMAC), a novel non-ELR alpha-chemokine. Int Immunol 12, 677–689. https://doi.org/10.1093/intimm/12.5.677

Smiljanovic, B., Radzikowska, A., Kuca-Warnawin, E., Kurowska, W., Grün, J.R., Stuhlmüller, B., Bonin, M., Schulte-Wrede, U., Sörensen, T., Kyogoku, C., Bruns, A., Hermann, S., Ohrndorf, S., Aupperle, K., Backhaus, M., Burmester, G.R., Radbruch, A., Grützkau, A., Maslinski, W., Häupl, T., 2018. Monocyte alterations in rheumatoid arthritis are dominated by preterm release from bone marrow and prominent triggering in the joint. Ann Rheum Dis 77, 300–308. https://doi.org/10.1136/annrheumdis-2017-211649

Smith, N., Pietrancosta, N., Davidson, S., Dutrieux, J., Chauveau, L., Cutolo, P., Dy, M., Scott-Algara, D., Manoury, B., Zirafi, O., McCort-Tranchepain, I., Durroux, T., Bachelerie, F., Schwartz, O., Münch, J., Wack, A., Nisole, S., Herbeuval, J.-P., 2017. Natural amines inhibit activation of human plasmacytoid dendritic cells through CXCR4 engagement. Nat Commun 8, 14253. https://doi.org/10.1038/ncomms14253

Smith, N., Rodero, M.P., Bekaddour, N., Bondet, V., Ruiz-Blanco, Y.B., Harms, M., Mayer, B., Bader-Meunier, B., Quartier, P., Bodemer, C., Baudouin, V., Dieudonné, Y., Kirchhoff, F., Sanchez Garcia, E., Charbit, B., Leboulanger, N., Jahrsdörfer, B., Richard, Y., Korganow, A.-S., Münch, J., Nisole, S., Duffy, D., Herbeuval, J.-P., 2019. Control of TLR7-mediated type I IFN signaling in pDCs through CXCR4 engagement-A new target for lupus treatment. Sci Adv 5, eaav9019. https://doi.org/10.1126/sciadv.aav9019

Smolewska, E., Stańczyk, J., Brózik, H., Biernacka-Zielińska, M., Cebula, B., Robak, T., Smolewski, P., 2008. Distribution and clinical significance of blood dendritic cells in children with juvenile idiopathic arthritis. Ann Rheum Dis 67, 762–768. https://doi.org/10.1136/ard.2007.077669

Steinman, R.M., 2006. Linking innate to adaptive immunity through dendritic cells. Novartis Found Symp 279, 101–109; discussion 109-113, 216–219.

Steinman, R.M., Cohn, Z.A., 1974. IDENTIFICATION OF A NOVEL CELL TYPE IN PERIPHERAL LYMPHOID ORGANS OF MICE : II. FUNCTIONAL PROPERTIES IN VITRO. Journal of Experimental Medicine 139, 380–397. https://doi.org/10.1084/jem.139.2.380

Steinman, R.M., Cohn, Z.A., 1973. IDENTIFICATION OF A NOVEL CELL TYPE IN PERIPHERAL LYMPHOID ORGANS OF MICE : I. MORPHOLOGY, QUANTITATION,

TISSUE DISTRIBUTION. Journal of Experimental Medicine 137, 1142–1162. https://doi.org/10.1084/jem.137.5.1142

Strieter, R.M., Polverini, P.J., Kunkel, S.L., Arenberg, D.A., Burdick, M.D., Kasper, J., Dzuiba, J., Van Damme, J., Walz, A., Marriott, D., 1995. The functional role of the ELR motif in CXC chemokine-mediated angiogenesis. J Biol Chem 270, 27348–27357. https://doi.org/10.1074/jbc.270.45.27348

Sun, L., He, C., Nair, L., Yeung, J., Egwuagu, C.E., 2015. Interleukin 12 (IL-12) Family Cytokines: Role in Immune Pathogenesis and Treatment of CNS Autoimmune Disease. Cytokine 75, 249–255. https://doi.org/10.1016/j.cyto.2015.01.030

Syedbasha, M., Egli, A., 2017. Interferon Lambda: Modulating Immunity in Infectious Diseases. Frontiers in Immunology 8, 119. https://doi.org/10.3389/fimmu.2017.00119

Tabarkiewicz, J., Postępski, J., Olesińska, E., Roliński, J., Tuszkiewicz-Misztal, E., 2011. Identification of dendritic cells in the blood and synovial fluid of children with Juvenile Idiopathic Arthritis. Folia Histochem Cytobiol 49, 188–199. https://doi.org/10.5603/fhc.2011.0026

T

Tada, H., Aiba, S., Shibata, K.-I., Ohteki, T., Takada, H., 2005. Synergistic effect of Nod1 and Nod2 agonists with toll-like receptor agonists on human dendritic cells to generate interleukin-12 and T helper type 1 cells. Infect Immun 73, 7967–7976. https://doi.org/10.1128/IAI.73.12.7967-7976.2005

Takeuchi, O., Akira, S., 2010. Pattern recognition receptors and inflammation. Cell 140, 805–820. https://doi.org/10.1016/j.cell.2010.01.022

Tan, E.M., Cohen, A.S., Fries, J.F., Masi, A.T., McShane, D.J., Rothfield, N.F., Schaller, J.G., Talal, N., Winchester, R.J., 1982. The 1982 revised criteria for the classification of systemic lupus erythematosus. Arthritis Rheum 25, 1271–1277. https://doi.org/10.1002/art.1780251101

Tasker, C., Subbian, S., Gao, P., Couret, J., Levine, C., Ghanny, S., Soteropoulos, P., Zhao, X., Landau, N., Lu, W., Chang, T.L., 2016. IFN-ε protects primary macrophages against HIV infection. JCI Insight 1, e88255. https://doi.org/10.1172/jci.insight.88255

Tattoli, I., Carneiro, L.A., Jéhanno, M., Magalhaes, J.G., Shu, Y., Philpott, D.J., Arnoult, D., Girardin, S.E., 2008. NLRX1 is a mitochondrial NOD-like receptor that amplifies NF-κB and JNK pathways by inducing reactive oxygen species production. EMBO Rep 9, 293–300. https://doi.org/10.1038/sj.embor.7401161

Teicher, B.A., Fricker, S.P., 2010. CXCL12 (SDF-1)/CXCR4 pathway in cancer. Clin Cancer Res 16, 2927–2931. https://doi.org/10.1158/1078-0432.CCR-09-2329

Ting, J.P.-Y., Lovering, R.C., Alnemri, E.S.Ph.D., Bertin, J., Boss, J.M., Davis, B., Flavell, R.A., Girardin, S.E., Godzik, A., Harton, J.A., Hoffman, H.M., Hugot, J.-P., Inohara, N., MacKenzie, A., Maltais, L.J., Nunez, G., Ogura, Y., Otten, L., Reed, J.C., Reith, W., Schreiber, S., Steimle, V., Ward, P.A., 2008. The NLR gene family: An official nomenclature. Immunity 28, 285–287. https://doi.org/10.1016/j.immuni.2008.02.005

Tomasello, E., Pollet, E., Vu Manh, T.-P., Uzé, G., Dalod, M., 2014. Harnessing Mechanistic Knowledge on Beneficial Versus Deleterious IFN-I Effects to Design Innovative Immunotherapies Targeting Cytokine Activity to Specific Cell Types. Front Immunol 5, 526. https://doi.org/10.3389/fimmu.2014.00526

Townson, D.H., Liptak, A.R., 2003. Chemokines in the corpus luteum: implications of leukocyte chemotaxis. Reprod Biol Endocrinol 1, 94. https://doi.org/10.1186/1477-7827-1-94
Tucci, M., Quatraro, C., Lombardi, L., Pellegrino, C., Dammacco, F., Silvestris, F., 2008. Glomerular accumulation of plasmacytoid dendritic cells in active lupus nephritis: role of interleukin-18. Arthritis Rheum 58, 251–262. https://doi.org/10.1002/art.23186

V

Vannucci, G., Cantarini, L., Giani, T., Marrani, E., Moretti, D., Pagnini, I., Simonini, G., Cimaz, R., 2013. Glucocorticoids in the management of systemic juvenile idiopathic arthritis. Paediatr Drugs 15, 343–349. https://doi.org/10.1007/s40272-013-0038-0

Vicari, A.P., Figueroa, D.J., Hedrick, J.A., Foster, J.S., Singh, K.P., Menon, S., Copeland, N.G., Gilbert, D.J., Jenkins, N.A., Bacon, K.B., Zlotnik, A., 1997. TECK: a novel CC chemokine specifically expressed by thymic dendritic cells and potentially involved in T cell development. Immunity 7, 291–301. https://doi.org/10.1016/s1074-7613(00)80531-2

von Andrian, U.H., Mempel, T.R., 2003. Homing and cellular traffic in lymph nodes. Nat Rev Immunol 3, 867–878. https://doi.org/10.1038/nri1222

von Wussow, P., Jakschies, D., Hochkeppel, H., Horisberger, M., Hartung, K., Deicher, H., 1989. MX homologous protein in mononuclear cells from patients with systemic lupus erythematosus. Arthritis Rheum 32, 914–918.

W

Wallace, C.A., Huang, B., Bandeira, M., Ravelli, A., Giannini, E.H., 2005. Patterns of clinical remission in select categories of juvenile idiopathic arthritis. Arthritis Rheum 52, 3554–3562. https://doi.org/10.1002/art.21389

Wang, R.-X., Yu, C.-R., Dambuza, I.M., Mahdi, R.M., Dolinska, M.B., Sergeev, Y.V., Wingfield, P.T., Kim, S.-H., Egwuagu, C.E., 2014. Interleukin-35 induces regulatory B cells that suppress autoimmune disease. Nat Med 20, 633–641. https://doi.org/10.1038/nm.3554

Wei, H., Li, B., Sun, A., Guo, F., 2019. Interleukin-10 Family Cytokines Immunobiology and Structure. Adv Exp Med Biol 1172, 79–96. https://doi.org/10.1007/978-981-13-9367-9_4

Weiss, P.F., Beukelman, T., Schanberg, L.E., Kimura, Y., Colbert, R.A., CARRA Registry Investigators, 2012. Enthesitis-related arthritis is associated with higher pain intensity and poorer health status in comparison with other categories of juvenile idiopathic arthritis: the Childhood Arthritis and Rheumatology Research Alliance Registry. J Rheumatol 39, 2341–2351. https://doi.org/10.3899/jrheum.120642

Wheelock, E.F., 1965. Interferon-Like Virus-Inhibitor Induced in Human Leukocytes by Phytohemagglutinin. Science 149, 310–311. https://doi.org/10.1126/science.149.3681.310
Williams, R.O., Marinova-Mutafchieva, L., Feldmann, M., Maini, R.N., 2000. Evaluation of TNF-α and IL-1 Blockade in Collagen-Induced Arthritis and Comparison with Combined Anti-

TNF-α/Anti-CD4 Therapy. The Journal of Immunology 165, 7240–7245. https://doi.org/10.4049/jimmunol.165.12.7240

Wu, J., Chen, Z.J., 2014. Innate immune sensing and signaling of cytosolic nucleic acids. Annu Rev Immunol 32, 461–488. https://doi.org/10.1146/annurev-immunol-032713-120156

Y

Yang, Junling, Leslie Wise, et Ken-Ichiro Fukuchi. « TLR4 Cross-Talk With NLRP3 Inflammasome and Complement Signaling Pathways in Alzheimer's Disease ». *Frontiers in Immunology* 11 (2020): 724. https://doi.org/10.3389/fimmu.2020.00724.

Yamamoto, M., Sato, S., Hemmi, H., Hoshino, K., Kaisho, T., Sanjo, H., Takeuchi, O., Sugiyama, M., Okabe, M., Takeda, K., Akira, S., 2003. Role of adaptor TRIF in the MyD88-independent toll-like receptor signaling pathway. Science 301, 640–643. https://doi.org/10.1126/science.1087262

Yan, B., Ye, S., Chen, G., Kuang, M., Shen, N., Chen, S., 2008. Dysfunctional CD4+,CD25+ regulatory T cells in untreated active systemic lupus erythematosus secondary to interferon-alpha-producing antigen-presenting cells. Arthritis Rheum 58, 801–812. https://doi.org/10.1002/art.23268

Yang, D., Han, Z., Oppenheim, J.J., 2017. ALARMINS AND IMMUNITY. Immunol Rev 280, 41–56. https://doi.org/10.1111/imr.12577

Yin, Z., Dai, J., Deng, J., Sheikh, F., Natalia, M., Shih, T., Lewis-Antes, A., Amrute, S.B., Garrigues, U., Doyle, S., Donnelly, R.P., Kotenko, S.V., Fitzgerald-Bocarsly, P., 2012. Type III IFNs are produced by and stimulate human plasmacytoid dendritic cells. J Immunol 189, 2735–2745. https://doi.org/10.4049/jimmunol.1102038

Ytterberg, S.R., Schnitzer, T.J., 1982. Serum interferon levels in patients with systemic lupus erythematosus. Arthritis Rheum 25, 401–406. https://doi.org/10.1002/art.1780250407

Z

Zavala-Flores, L.M., Villatoro-Hernandez, J., Gamez-Escobedo, A., Franco-Molina, M., Rangel-Colmenero, B.R., Villanueva-Olivo, A., Gutierrez-Puente, Y., de Oca-Luna, R.M., Valdés-Flores, J., Saucedo-Cardenas, O., 2009. Production of biologically active human lymphotactin (XCL1) by Lactococcus lactis. Biotechnol Lett 31, 215–220. https://doi.org/10.1007/s10529-008-9855-6

Zhao, Q., Jung, L.K., 2018. Frequency of CD19+CD24hiCD38hi regulatory B cells is decreased in peripheral blood and synovial fluid of patients with juvenile idiopathic arthritis: a preliminary study. Pediatr Rheumatol Online J 16, 44. https://doi.org/10.1186/s12969-018-0262-9

Zhou, R., Tardivel, A., Thorens, B., Choi, I., Tschopp, J., 2010. Thioredoxin-interacting protein links oxidative stress to inflammasome activation. Nat Immunol 11, 136–140. https://doi.org/10.1038/ni.1831

Zhuang, H., Szeto, C., Han, S., Yang, L., Reeves, W.H., 2015. Animal Models of Interferon

Signature Positive Lupus. Front Immunol 6, 291. https://doi.org/10.3389/fimmu.2015.00291

Zlotnik, A., Yoshie, O., 2000. Chemokines: a new classification system and their role in immunity. Immunity 12, 121–127. https://doi.org/10.1016/s1074-7613(00)80165-x

Zulian, F., Martini, G., Gobber, D., Plebani, M., Zacchello, F., Manners, P., 2004. Triamcinolone acetonide and hexacetonide intra-articular treatment of symmetrical joints in juvenile idiopathic arthritis: a double-blind trial. Rheumatology (Oxford) 43, 1288–1291. https://doi.org/10.1093/rheumatology/keh313